THE DEVELOPMENT OF *LEGIONELLA PNEUMOPHILA* REACHES DIFFERENT END POINTS IN AMOEBAE, MACROPHAGES AND CILIATES

by

Hany A. M. Abdelhady

Submitted in partial fulfilment of the requirements
for the degree of Doctor of Philosophy

at

Dalhousie University
Halifax, Nova Scotia
December 2013

DEDICATION

To the spirit of my father, who I wish was alive to share this moment with me, and to my mother, who always listened to my complaints and granted me her unlimited support over the years.

TABLE OF CONTENTS

LIST OF TABLES

LIST OF FIGURES

ABSTRACT

The intracellular pathogen *Legionella pneumophila* thrives in both natural and man-made water habitats where it replicates inside freshwater amoebae. *L. pneumophila* follows a developmental cycle as it grows in amoebae. The actively-multiplying intracellular replicative forms (RFs) differentiate into highly virulent mature infectious forms (MIFs) late in the amoeba infection, and are then released extracellularly. *L. pneumophila* accidentally infects susceptible humans causing the non-communicable Legionnaires' disease (LD). MIFs play a central role in the life cycle of *L. pneumophila* and are thought to be responsible for the transmission of LD. Early reports demonstrated that MIFs were poorly produced inside human macrophages, suggesting that the *L. pneumophila* progeny from human macrophages has fitness and infectivity disadvantages. Direct comparisons of the *L. pneumophila* progenies from amoebae and human macrophages have demonstrated that the progeny from amoebae is more morphologically differentiated, resistant to antibiotic challenges, and able to adhere to and initiate infections in host cells than the progeny from macrophages. Analysis of the transcriptomic and proteomic profiles of *L. pneumophila* inside different hosts has revealed a specific set of genes that are upregulated during differentiation of *L. pneumophila* into MIFs inside freshwater protozoa but not inside human macrophages, suggesting that these genes may be required for the full differentiation of *L. pneumophila* and, therefore, for the transmission of LD to susceptible humans. Since the expression of the gene *lpg1669*, which encodes a putative α-amylase, was upregulated in amoebae (highest level of upregulation among the tested genes) and inside *Tetrahymena* ciliates, but not inside human macrophages, the role of *lpg1669* in the differentiation of *L. pneumophila* into MIFs was investigated. An isogenic *lpg1669* deletion mutant did not display defects in morphological differentiation, *in vitro* (BYE broth) or *in vivo* (*A. castellanii* or U937 human macrophages) growth when compared to its parent strain, suggesting that the gene *lpg1669* is not essential for the intracellular differentiation of *L. pneumophila*. Collectively, these findings demonstrate that *L. pneumophila* can reach different developmental end points in different hosts and could also provide a clue for the lack of transmission of LD among humans.

LIST OF ABBREVIATIONS USED

Ab	antibody
ACES	(2-[2-amino-2-oxoethyl]-amino) ethanesulfonic acid
Amp^R	ampicillin resistant
ANOVA	Analysis of Variance
BCIP	5-bromo-4-chloro-3-indolylphosphate
BCYE	buffered charcoal yeast extract
BLAST	basic local alignment search tool
BSA	bovine serum albumin
BYE	buffered yeast extract
cAMP	3`, 5`-cyclic adenosine monophosphate
Cat	chloramphenicol acetyl transferase
c-di-GMP	bis-(3`, 5`)-cyclic dimeric guanosine monophosphate
CFU	colony forming unit
CLF	cyst-like form
Cm^R	chloramphenicol resistant
ddH_2O	distilled deionized water
dNTP	deoxyriboncleoside triphosphate
DTT	dithiothreitol
DMF	dimethylformamide
DMSO	dimethylsulfoxide
Dot	defect in organelle trafficking
ED	Entner-Doudoroff
EDTA	ethylenediaminetetraacetic acid
EP	exponential phase
EPF	exponential phase form
ER	endoplasmic reticulum
ERGIC	ER-Golgi intermediate compartment
FBS	fetal bovine serum
g	gram
g	gravity

GAP	GTPase activating protein
GDP	guanosine diphosphate
GEF	guanine nucleotide exchange factor
GFP	green fluorescent protein
Gm^R	gentamicin resistant
Icm	intracellular multiplication
IFN	interferon
IgG	immunoglobulin G
IL	interleukin
IPTG	isopropyl β-D-1-thiogalactopyranoside
Kan^R	kanamycin resistant
LAMP	lysosome-associated membrane protein
LB	Luria-Bertani
LCV	*Legionella*-containing vacuole
LD	legionnaires' disease
LLAPs	*Legionella*-like amoebal pathogens
LPS	lipopolysaccharide
MAb	monoclonal antibody
MEM	minimal essential medium
MIF	mature infectious form
min	minute
NBT	nitroblue tetrazolium
NCBI	National Center for Biotechnology Information
NCS	newborn calf serum
NEB	New England Biolabs
NF-κB	nuclear factor κB
OD	optical density
P	promoter
PBS	phosphate-buffered saline
PCB	plate count broth
PCR	polymerase chain reaction

PE	post-exponential
PHB	poly β-hydroxy butyrate
PMA	phorbol 12-myristate 13-acetate
ppGpp	guanosine 3`,5`-bipyrophosphate
ppm	part per million
RF	replicative form
ROS	reactive oxygen species
RPMI	Roswell Park Memorial Institute
SDS-PAGE	SDS-polyacrylamide gel electrophoresis
sec	second
Sm^R	streptomycin resistant
SP	stationary phase
SPF	stationary phase form
Std	standard deviation
Suc^R	sucrose resistant
T4SS	type IV secretion system
T4BSS	type IVB secretion system
TAE	tris acetate EDTA
TBOS	tris-Buffered Osterhout's solution
TBS	tris-buffered saline
TCA	trichloroacetic acid
TEM	transmission electron microscopy
Tet	tetracycline
TF	transmissive form
TTBS	tween 20-tris buffered saline

ACKNOWLEDGEMENTS

I would like to thank Dr. Rafael Garduño for accepting me into his laboratory and giving me the opportunity to pursue my PhD training. I am also grateful to Dr. Roy Duncan, Dr. Nikhil Thomas, and Dr. Ross Davidson for serving on my supervisory committee, for providing me with a second opinion on my work, and for their technical guidance over the PhD journey. I would like to thank Dr. Charles Dozois for agreeing to be the external examiner of my thesis defence.

I had the pleasure to work with a nice group of intelligent people at the Garduño lab. A big thank you goes to David Allan, Dr. Celia Lima, Dr. Gheyath Nasrallah (currently an assistant professor at Qatar University), Elizabeth Garduno, and Badii Al-Banna for helping me when I first came to the lab and doing the best they could to make my PhD adventure more manageable. I would like also to thank the undergraduate students that joined the lab for their summer / honors research projects; Eman Atwi, Julia Schümmelfeder (now Julia Wilhelms; Bonn Rhein-Sieg University of Applied Sciences), Sachiko Ito (Bonn Rhein-Sieg University of Applied Sciences), Erin Helson, Emma-Jean Slobodesky, Jungmin Kim, and Peter Robertson.

I am also grateful to the members of the Rohde's and the Thomas' labs. Thank you to Dr. Jeremy Benjamin, Julie Ryu, Saima Sidik, Erin Brouwers, Madhulika Prasad, and Daniel Arsenault and to Lauren Davey and Naif Jalal from Dr. Song Lee's lab for their technical expertise and their support and encouragement.

I would like to thank Dr. Gary Faulkner and Mary-Ann Trevors (the Electron Microscopy facility at Dalhousie University) for the technical assistance with my electron microscopy experiments. I would like to thank Dr. Alejandro Cohen (the Proteomics facility at Dalhousie University) for his assistance with the protein analysis by mass spectrometry.

I would also like to acknowledge the Canadian Institute of Health Research (CIHR), the Nova Scotia Health Research Foundation (NSHRF) for funding my research and the Egyptian Cultural Bureau in Montreal for granting me a scholarship to pursue my graduate studies.

Finally, I would like to thank the little boy inside me for not giving up too quickly and for being my last line of defense throughout all the hurdles I met until I was able to see the finish line.

CHAPTER 1: INTRODUCTION

1.1. *Legionella pneumophila* is an environmental human pathogen

Legionella pneumophila is a Gram-negative bacterium that inhabits freshwater environments, such as lakes and ponds, as an intracellular pathogen of freshwater amoebae (Rowbotham, 1986; Fields *et al.*, 2002). *L. pneumophila*, along with other bacteria, amoebae and protozoa can also colonize many anthropogenic (man-made) water systems, such as hot tubs, cooling towers, air conditioners, and spas. When aerosols from contaminated water sources are inhaled by susceptible humans, *L. pneumophila* can infect alveolar macrophages and cause an atypical pneumonia known as Legionnaires' disease (LD) (Fraser *et al.*, 1977; Horwitz, 1983; Horwitz, 1983). LD is acquired mainly by inhalation of *Legionella*-contaminated aerosols and not transmitted from person to person (i.e. not communicable); therefore *L. pneumophila* is considered an environmental pathogen (Fields *et al.*, 2002). The accidental human infection is a dead end for *L. pneumophila* replication. Human hosts act neither as a reservoir nor a viable vector for transmission of legionellae, rendering any infection futile. The lack of LD transmission among humans remains with no satisfactory explanation to date.

1.2. Legionellosis

Infections with *Legionella* result in legionellosis. Legionellosis can present clinically as a more severe atypical pneumonia known as Legionnaires' disease (LD) or as milder flu-like illness known as Pontiac fever, which is usually self-limited (Fraser *et al.*, 1977; McDade *et al.*, 1977; Glick *et al.*, 1978). Legionellosis has emerged in the second half of the 20th century as a result of the human alteration of the environment. Therefore, in its early stages after its discovery *L. pneumophila* fulfilled the definition of an emerging human pathogen. Legionellosis is mostly associated with man-made aquatic systems where water can reach higher temperatures, and accounts for 2-15% of community-acquired pneumonia cases that require hospitalization in the United States (Marston *et al.*, 1994).

LD is a severe multi-organ syndrome which develops within 2 to 10 days following exposure to legionellae. Symptoms of LD include fever, non-productive cough,

headache, myalgias, rigors, dyspnea, diarrhea, and delirium (Tsai *et al.*, 1979). LD was first recognized after the massive outbreak in Philadelphia, PA in 1976, where 182 cases and 29 deaths occurred among the participants of the Pennsylvania Division of The American Legion convention (Fraser *et al.*, 1977; Brenner *et al.*, 1979). Earlier reports suggested that person-to-person transmission was unlikely and demonstrated that the younger, more immunocompetent hotel employees were immune to the disease (Fraser *et al.*, 1977). A few months later, McDade *et al.* successfully isolated *L. pneumophila* and demonstrated its role as the causative agent of the outbreak (McDade *et al.*, 1977) . Pontiac fever is a mild flu-like, usually self-limiting form of legionellosis. It was first documented in 1968 in Pontiac, Michigan where employees of and visitors to the Health Department developed a self-limited febrile condition, which lasted for 2-5 days and resolved without further complications. *L. pneumophila* was retrospectively identified as the etiological agent for this condition ten years later (Glick *et al.*, 1978).

The factors which determine whether *Legionella* spp. will cause Legionnaires' disease (LD) or Pontiac fever remain unclear. Outbreaks of either LD or Pontiac fever are usually reported (Den Boer *et al.*, 1998; Luttichau *et al.*, 1998; Garcia-Fulgueiras *et al.*, 2003). However, simultaneous outbreaks of both Pontiac fever and LD are rarely seen (Girod *et al.*, 1982; Thomas *et al.*, 1993; Benin *et al.*, 2002). The same *Legionella* species can cause both diseases, although some species e.g. *L. micdadei* seem to be more often associated with mild clinical symptoms (Goldberg *et al.*, 1989; Fallon & Rowbotham, 1990; Fields *et al.*, 2001). Rowbotham has previously suggested that Pontiac fever may result from a hypersensitivity reaction to amoebae (Rowbotham, 1980; Rowbotham, 1986), which occurs when humans inhale vesicles from infected amoebae containing *Legionella* spp. He postulated that such reaction would activate macrophages and thereby inhibit the multiplication of legionellae in lung tissues (Rowbotham, 1980; Rowbotham, 1986). It has also been suggested that the competence of the host immune system may also play a role in determining the clinical outcome following exposure to *Legionella* spp (Girod *et al.*, 1982).

LD does not usually occur in healthy immunocompetent adults, but occurs mostly among immunocompromised individuals; therefore *L. pneumophila* is considered an opportunistic human pathogen. The typical risk factors for LD include age (with geriatric

individuals usually over 65 having increased susceptibility), smoking status, chronic obstructive pulmonary disease, alcohol intake, and immune suppression through immunocompromising diseases or immunosuppressive drugs (Stout & Yu, 1997; Fields *et al.*, 2002). The average mortality of LD has been confirmed to be about 15-20% of hospitalized cases (Edelstein & Meyer, 1984; Guerin, 1992; Roig & Rello, 2003). In the USA, the case-fatality rate was recorded as up to 40% in nosocomial cases, compared with 20% among people with community-acquired legionellosis (CDC, 1997).

Although 53 *Legionella* species containing 73 serogroups have been identified (Luck, 2010), 90% of the LD cases in North America and Europe are caused by *L. pneumophila*, with serogroup 1 responsible for over 84% of the cases worldwide (Marston *et al.*, 1997; Yu *et al.*, 2002; Muder & Yu, 2002). *Legionella bozemanaii* and *Legionella micdadei* are the next most common etiological agents of LD. Together; they account for ~ 2-7 % of *Legionella* infections worldwide (Muder & Yu, 2002). The rest of the cases (10%) are caused by other *L. pneumophila* serogroups and other *Legionella* species such as *L. longbeachae* (Yu *et al.*, 2002). *L. longbeachae*, the leading cause of legionellosis in Australia, has been found in potting soil, and is transmitted to susceptible humans through exposure to commercial potting soil (Steele *et al.*, 1990 a,b). *Legionella*-like amoebal pathogens (LLAPs) are obligate intracellular bacteria that are closely related to *Legionella* spp. and may also account for a number of respiratory diseases (Marrie *et al.*, 2001).

Legionnaires' disease (LD) has been associated with worldwide major outbreaks. In addition to the original outbreak that took place in Philadelphia, PA in 1976 (Fraser *et al.*, 1977; Brenner *et al.*, 1979), other major outbreaks took place in Melbourne Aquarium, Australia in 2000 (Greig *et al.*, 2004), Lens, France in 2003-2004(Nguyen *et al.*, 2006), and the Netherlands flower show in 1999 (Den Boer *et al.*, 2002; Lettinga *et al.*, 2002). The world's largest LD outbreak took place in Murcia, Spain in 2001 with 449 confirmed cases (Garcia-Fulgueiras *et al.*, 2003). A surveillance carried out by the European Legionnaires' Disease Surveillance Network (ELDSNet) and coordinated by the European Center for Disease Prevention and Control (ECDC) revealed that a total of 6296 cases of LD of which 438 deaths were reported in Europe in 2010 (Beaute *et al.*,

2013). In 2012, a severe cooling tower-associated outbreak of LD was reported in Edinburgh, Scotland with 50 confirmed cases and 3 deaths (McCormick *et al.*, 2012).

LD has a limited prevalence in Canada, with an average of 75 cases reported annually (Reimer *et al.*, 2010). A cross-Canada study has demonstrated that the rate of LD that requires hospital admission, based on urinary antigen testing, was higher in Halifax than the other tested sites (Marrie *et al.*, 2003). A major LD outbreak in Canada took place in Toronto in 2005 and resulted in 127 cases and 21fatalities (Gilmour *et al.*, 2007). Another major outbreak took place in Quebec City in 2012, resulting in 181 reported cases including 13 fatalities. (Levesque *et al.*, Conference abstract, Canadian journal of infectious diseases and medical microbiology, Spring 2013).

1.3. *L. pneumophila*, protozoa and human transmission

It has been hypothesized that *L. pneumophila* first became an intracellular parasite through its interaction with amoebae (Molmeret *et al.*, 2005), therefore understanding the interaction between amoebae and *L. pneumophila* in the natural environment is crucial to our understanding of *L. pneumophila* pathogenesis.

Protozoa provide the natural habitat for intracellular growth and multiplication of *L. pneumophila,* which increases the counts of legionellae into high levels and subsequently allows for the delivery of large infectious bacterial doses to susceptible humans resulting in the transmission of LD (Fields *et al.*, 1990).

Protozoa can also act as Trojan horses to provide protection for *L. pneumophila* against environmental stresses, which can protect *L. pneumophila* from eradication by chemical disinfectants (Barbaree *et al.*, 1986; King *et al.*, 1988). This may explain why elimination of legionellae from water systems is often difficult. For example, the resistance of amoebae to monochloramine could explain the high resistance of *L. pneumophila* to monochloramine in the presence of amoebae in water systems (Thomas *et al.*, 2004).

Intracellular growth of *L. pneumophila* inside protozoa also induces the virulence traits and primes the bacteria for infection of new hosts. Compared to *in vitro*-grown *L. pneumophila*, amoeba-grown bacteria are highly resistant to chemical disinfectants, treatment with biocides and harsh environmental conditions, such as fluctuation in

temperature, osmolarity, pH, and exposure to oxidizing agents (Barker *et al.*, 1992; Abu Kwaik *et al.*, 1997). Amoeba-grown *L. pneumophila* are also more infectious to mammalian cells (Rowbotham, 1986; Cirillo *et al.*, 1994; Cirillo *et al.*, 1999) and more infectious to and lethal in mice. Interestingly, infection with mice with a co-culture of *L. pneumophila* and amoebae resulted in severe lung pathology and higher bacterial counts in the mouse lungs (Brieland *et al.*, 1996; Brieland *et al.*, 1997; Brieland *et al.*, 1997).

The above findings suggest that the legionellae-protozoa interactions not only serve as a shelter for *L. pneumophila* against environmental stress, but also induce the virulence traits that make *L. pneumophila* ready to infect new hosts (Greub & Raoult, 2004).

1.4. Developmental cycle and differentiation of *L. pneumophila*

In the microbial world, resources are almost universally limited and are competed for by billions of organisms. To cope with the environmental fluctuations such as changes in temperature, osmolarity and nutrient availability, bacteria often modify their physiology, and sometimes undergo morphological adaptations through differentiation. Examples of microbial differentiation include fruiting body formation by *Myxococcus xanthus* (Zusman *et al.*, 2007), spore formation by species of *Bacillus* and *Clostridium* (Paredes *et al.*, 2005), and alternation between replication and transmission by the intracellular pathogens *Coxiella burnetti* (Voth & Heinzen, 2007), *Chlamydia trachomatis* (Abdelrahman & Belland, 2005), and *Legionella pneumophila* (Swanson & Hammer, 2000; Faulkner & Garduno, 2002; Molofsky & Swanson, 2004). Much of our current understanding of the life cycle of *L. pneumophila* has been built upon the pioneering work conducted by Rowbotham, who studied the interaction of *L. pneumophila* with freshwater amoebae (Rowbotham, 1980; Rowbotham, 1983; Rowbotham, 1986), and M. Horwitz, who studied the interaction of *L. pneumophila* with macrophages (Horwitz & Maxfield, 1984).

In its natural life cycle, *L. pneumophila* alternates between two main morphological forms; the replicative form (RF) and the mature infectious form (MIF). RFs are replicating, non-flagellated and sodium-resistant forms. MIFs, which may also be referred to as transmissive forms or cyst-like forms (CLFs), are the progenies that emerge

from *L. pneumophila* infections of different host cells (**Figure 1.1.**). MIFs were previously named mature intracellular forms because they were formed only as a result of intracellular growth or intracellular residence. However, since MIFs are primarily found in extracellular compartments and are naturally responsible for initiating new host cell infection, the change of their name to mature infectious forms was implemented. MIFs are non-replicating, flagellated, sodium-sensitive, and stress-resistant forms that are capable of evading phagosome-lysosome fusion and infecting host cells (Garduno *et al.*, 2002; Faulkner & Garduno, 2002) . Similarly, two distinct forms are seen during growth *in vitro*, with the exponential phase of growth, analogous to the replicative phase, and the post-exponential phase of growth analogous to the transmissive phase (Byrne & Swanson, 1998). Stationary phase forms (SPFs) are salt sensitive, motile, resistant to osmotic stress, cytotoxic, infectious to mouse macrophages, and able to escape degradation by the host lysosomes. On the other hand, exponential phase forms (EPFs) do not display these features (Byrne & Swanson, 1998).

1.4.1. The central role of MIFs in the life cycle of *L. pneumophila*

MIFs are unique forms and play a central role in the life cycle of *L. pneumophila*. For instance, MIFs have a unique ultrastructure. Rowbotham provided the first microscopic evidence to demonstrate that the progeny of *L. pneumophila* that comes from infected amoebae displays a unique morphology (Rowbotham, 1986). Morphological differentiation of *L. pneumophila* in protozoa was also reported in early studies (Katz, 1978; Katz *et al.*, 1979; Rodgers, 1979; Hammerschlag, 2002). Direct correlation of the morphological changes to the developmental cycle has been investigated through the ultrastructural analysis of *L. pneumophila* progeny from HeLa cells by electron microscopy (Faulkner & Garduno, 2002). MIFs have an electron-dense cytoplasm largely occupied by poly-β-hydroxybutyrate (PHB) inclusions, thickened cell-wall architecture, unapparent periplasm, and a multi-laminated envelope of intracytoplasmic membranes formed via invagination of the cytoplasmic membrane. These distinct features are unique to MIFs and are thought to enhance their resistance to various stresses (Faulkner & Garduno, 2002).

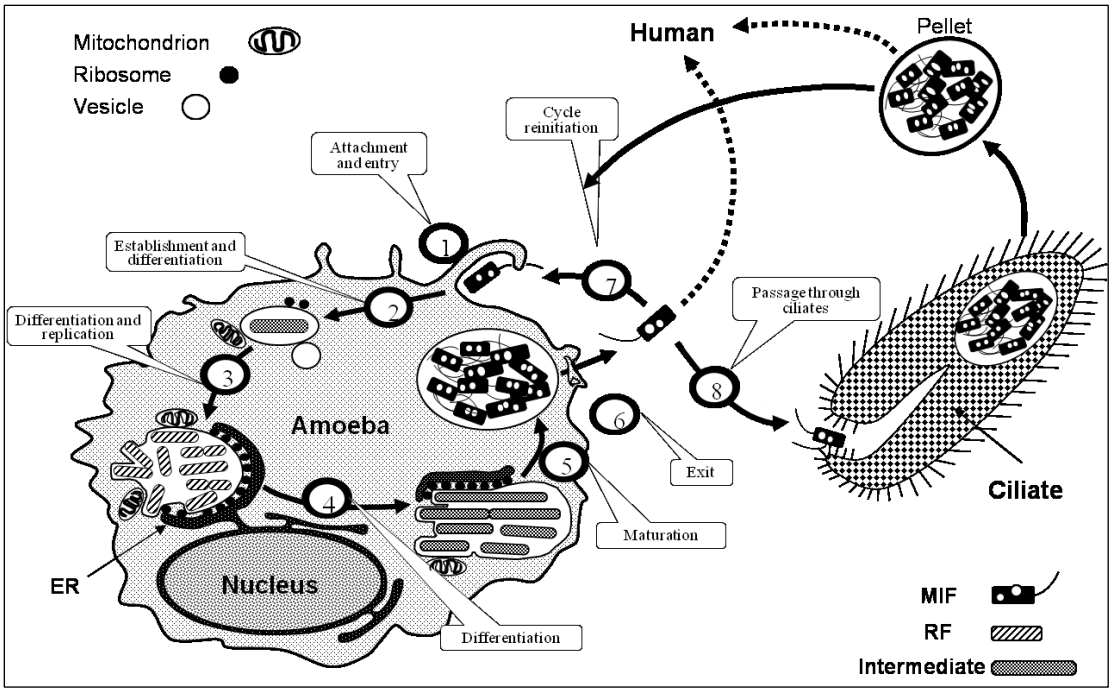

Figure 1.1. The developmental cycle of *L. pneumophila* is integrated into its life cycle.

L. pneumophila attaches to and invades *A. castellanii* where it undergoes replication in ribosome-coated vacuoles that associate with the endoplasmic reticulum. Following replication of the replicative forms (RFs), *L. pneumophila* differentiates into mature infectious forms (MIFs). RFs and MIFs differentiate into each other via various intermediate forms. MIFs are released into the environment where they can once again infect fresh amoebae and start over the whole process. MIFs can also be packaged into pellets by *Tetrahymena* ciliates. MIFs produced in amoebae or packaged by ciliates can infect human alveolar macrophages and transmit Legionnaires' disease (LD). Human infections are a dead end of *L. pneumophila* transmission (Garduno, 2007).

In addition to the unique morphology, MIFs produced in HeLa cells and SPFs (the analogous *in vitro* forms) show distinct physiological and biochemical characteristics (Garduno *et al.*, 2002). MIFs are more infectious to L929 cells, metabolically dormant, more resistant to rifampin and gentamicin challenges, and to detergent lysis than SPFs (Garduno *et al.*, 2002). These observations suggest that MIFs represent distinct differentiated forms of *L. pneumophila* that can survive in the environment for long periods of time, maintain the life cycle in the natural environment, and infect susceptible humans (Skaliy & McEachern, 1979; Schofield, 1985; Lee & West, 1991; James *et al.*, 1999). Once inside the host cells, MIFs differentiate back into RFs in the nutrient-rich intracellular environment. Whether MIFs are the ultimately differentiated forms of *L. pneumophila* still remains to be investigated.

Comparative protein analysis (2-dimentional protein gels) of the two forms has demonstrated that MIFs produced in HeLa cells display a different protein profile. The 20-kDa protein MagA has been shown to be enriched in MIFs, compared to SPFs, and has been suggested as a protein marker for the development of MIFs (Faulkner & Garduno, 2002; Hiltz *et al.*, 2004; Faulkner *et al.*, 2008). Since flagellation and full motility of *L. pneumophila* occur in the transmissive phase (Heuner *et al.*, 1999), the flagellin FlaA protein has been suggested as a marker for the expression of the virulent phenotype of *L. pneumophila* (Byrne & Swanson, 1998; Heuner *et al.*, 2002). However, these markers are unable to distinguish between MIFs and SPFs; therefore, there is still need for better markers that are more specific to MIF formation.

It has not been studied to date whether *L. pneumophila* progeny produced in different hosts share the same characteristics. In contrast to the progeny produced in HeLa cells, the progeny from human macrophages (the primary target cells during human infections) was morphologically undifferentiated and did not have high levels of MIFs (Garduno *et al.*, 2002), suggesting that *L. pneumophila* may reach different levels of differentiation inside different host cells. This could provide a clue for the lack of transmission of LD from person to person. Differentiation is a key factor in the survival and transmission of *L. pneumophila* (Molofsky & Swanson, 2004). The changes in *L. pneumophila* gene expression associated with the formation of MIFs (Molofsky & Swanson, 2004) suggest that MIFs are a truly differentiated form of *L. pneumophila* and

not just a physiological state that is formed as a result of exposute to different stresses (see section 1.5.).

1.4.2. Role of *Tetrahymena* ciliates in the life cycle of *L. pneumophila*.

Tetrahymena ciliates inhabit freshwater environments where they normally engulf bacteria into their intracellular vacuoles and digest them as a source of food. However, *L. pneumophila* cells resist the digestion inside the ciliates and maintain their viability within the food vacuoles.

Tetrahymena ciliates can support the intracellular growth of *L. pneumophila*, depending on the incubation temperature (Barbaree *et al.*, 1986). *L. pneumophila* can grow in *Tetrahymena pyriformis* at 35°C, which is considered a marker for its virulence (Fields *et al.*, 1986) but it is unable to grow in the same ciliate at 25°C (Fields *et al.*, 1984). The *T. pyriformis* ciliates begin to expel the *Legionella*-containing pellets at 6 hours after infection, with maximum production of pellets following 2 days of incubation (Hojo *et al.*, 2012). *L. pneumophila* is also unable to replicate inside *Tetrahymena vorax* at 20-22°C (Smith-Somerville *et al.*, 1991).

The ciliate *Tetrahymena tropicalis* (that has been used throughout my PhD project) is commonly found in freshwater environments. It does not support replication of *L. pneumophila* but has been shown to effectively package legionellae (following incubation for 1-2 hours) into pellets that may contain up to 100 legionellae surrounded by outer membrane fragments (McNealy *et al.*, 2002; Faulkner *et al.*, 2008; Berk *et al.*, 2008). The legionellae-laden pellets are of a respirable size and could be infectious to protozoa and susceptible humans (Rowbotham, 1980; McNealy *et al.*, 2002; Faulkner *et al.*, 2008; Berk *et al.*, 2008). Pellets of legionellae are more resistant to gentamicin and are able to maintain their viability in nutrient-limited environments for longer periods than *in-vitro* grown *L. pneumophila* (Koubar *et al.*, 2011). These findings suggest that *Tetrahymena* ciliates could play a role in the transmission of LD to susceptible humans. Feeding of *T. tropicalis* with SPFs triggers a rapid (within ~ 1 hour) and direct development of MIFs (directly from SPFs without replication intermediates), suggesting that SPFs and MIFs are developmentally linked (SPFs are immature MIFs) and that *Tetrahymena* ciliates may serve as a differentiation model to identify the signals that

trigger the development of MIFs and study the genes that are actively transcribed during *L. pneumophila* differentiation into MIFs (Faulkner *et al.*, 2008).

1.5. Overview of the regulatory network of *L. pneumophila* differentiation

The regulatory network that governs the differentiation cycle in *L. pneumophila* between RFs and MIFs is not well understood. The current understanding of the differentiation process is based mainly on the transition between replicative and transmissive phases *in vitro*. Regulation of *L. pneumophila* differentiation is a complicated process that involves regulation of gene expression through two-component systems, small non-coding RNA, and alternative sigma factors.

Based on *in vitro* studies that have compared exponential phase forms (EPFs) and SPFs of *L. pneumophila*, it is known that the conversion from replicative to transmissive forms is triggered in response to amino acid deficiency and perturbation in fatty acid biosynthesis (Molofsky & Swanson, 2004; Edwards *et al.*, 2009), which result in accumulation of the intracellular alarmone (p)ppGpp (Byrne & Swanson, 1998; Hammer & Swanson, 1999; Swanson & Hammer, 2000). The observation that complete differentiation of *L. pneumophila* into MIFs occurs in the intracellular environments (inside host cells), but not *in vitro*, may suggest that additional signals are also required.

1.5.1. Signals that trigger *L. pneumophila* differentiation

Depletion of amino acids results in limited protein synthesis and accumulation of uncharged transfer RNA (tRNA) molecules, which are then detected by the ribosome-associated RelA synthase (ppGpp synthetase). RelA converts guanosine triphosphate (GTP) or guanosine diphosphate (GDP) to guanosine-3`,5`- bispyrophosphate (ppGpp) (Hammer & Swanson, 1999). Perturbation in fatty acid biosynthesis affects SpoT, a bifunctional enzyme which can both synthesize and hydrolyse ppGpp in response to the intracellular levels of fatty acids (Dalebroux *et al.*, 2009; Dalebroux *et al.*, 2010) (**Figure 1.2.**).

RelA is not essential for *L. pneumophila* growth in macrophages. An *L. pneumophila relA* mutant can grow and spread efficiently in A/J primary mouse macrophages. However, SpoT is essential for *L. pneumophila* transmission in both A/J

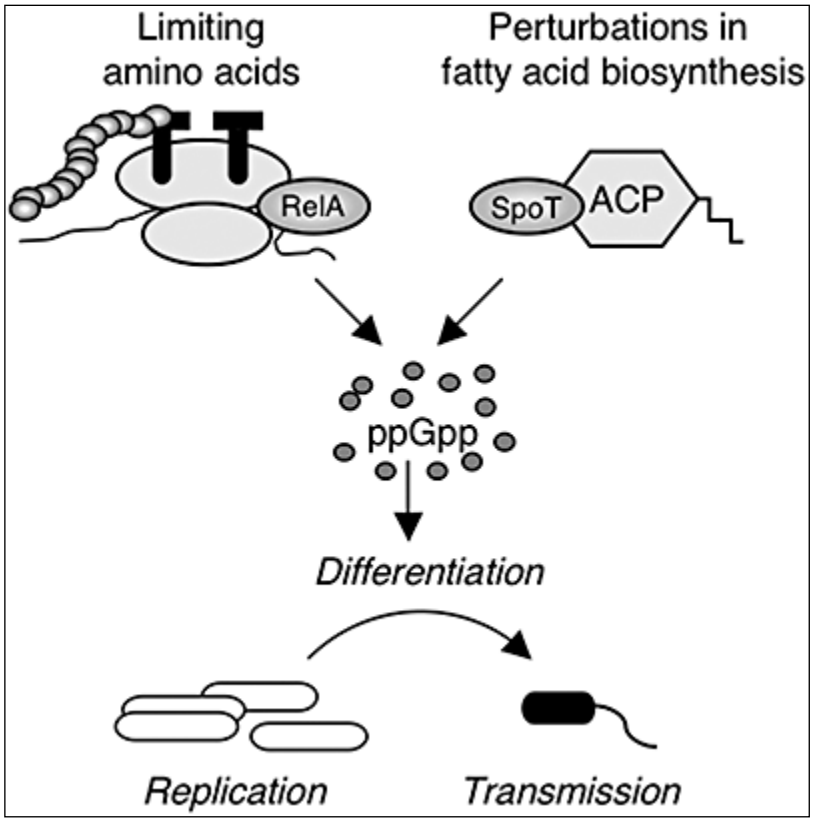

Figure 1.2. Differentiation in *L. pneumophila* is triggered by metabolic changes. Differentiation of *L. pneumophila* into transmissive forms is triggered by low levels of amino acids or fatty acids. In response to such metabolic changes, the proteins RelA and SpoT, respectively, synthesize the alarmone ppGpp. The subsequent interaction of ppGpp with the two-component regulatory system LetA/LetS induces differentiation of RFs to MIFs. When nutrients are abundant, the bifunctional SpoT (which also has a ppGpp hydrolase activity) can degrade ppGpp to induce germination from MIFs to RFs. RFs can then actively multiply until nutrients become limited (Edwards *et al.*, 2009) .

bone marrow- derived mouse macrophages and *in vitro* cultures. *spoT* is not essential for *L. pneumophila* growth when *relA* is deleted. It is possible to obtain a *relA* mutant or a *relA/spoT* double mutant, but not a *spoT* mutant alone. This could be because accumulation of ppGpp, due to the lack of the degrading activity of SpoT, results in cytotoxic effects (Dalebroux *et al.*, 2009) . A *relA/spoT* double mutant is killed during entry to and exit from A/J primary mouse macrophages. Complementation of the *relA/spoT* double mutant with *relA* only does not increase the bacterial counts beyond 24 hours post-infection, while complementation of the double mutant with *spoT* restores growth to parent strain levels. These data indicate that regulation of the ppGpp homeostasis is critical for *L. pneumophila* differentiation (Dalebroux *et al.*, 2009; Dalebroux *et al.*, 2010) .

The accumulation of (p)ppGpp in the bacterial cytosol stimulates the LetAS-RsmYZ-CsrA system to express the transmissive traits. The LetAS-RsmYZ-CsrA system consists of the LetA/LetS two-component system, small non-coding RNAs RsmY and RsmZ and the RNA-binding protein CsrA (Sahr *et al.*, 2009; Rasis and Segal, 2009).

1.5.2. LetA/LetS two-component system

LetA/LetS (*Legionella* transmission activator and sensor, respectively) is the most important and best characterized two-component system (TCS) in *L. pneumophila*. LetA/LetS is a homolog of the GacA/GacS (*Pseudomonas aeruginosa*) and BarA/UvrY (*E. coli*) two-component systems which are global regulators of gene expression. The mechanism by which ppGpp activates the LetA/LetS system and its co-activator LetE is still unknown (Dalebroux *et al.*, 2009; Dalebroux *et al.*, 2010). Once LetS is activated, it phosphorylates LetA, which is the downstream signal effector (**Figure 1.3.**). *L. pneumophila letA* and *letS* mutants are non-motile, sodium resistant, non-cytotoxic and less capable of infecting primary mouse macrophages (Hammer *et al.*, 2002; Gal-Mor & Segal, 2003). The *L. pneumophila letA* mutant displays low expression levels of *flaA* (flagellin-coding gene) from *flaA-gfp* constructs, has no intracellular growth defect in HL-60 human macrophages, but has a severe intracellular growth defect in *A. castellanii* (Gal-Mor & Segal, 2003).

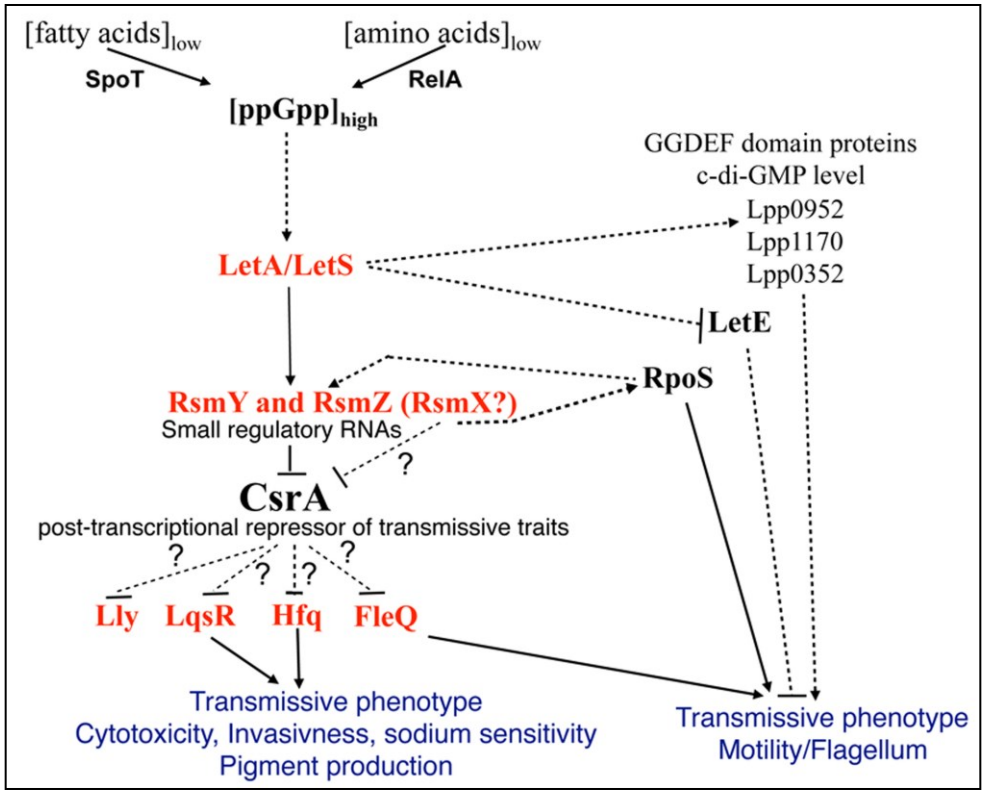

Figure 1.3. A model of the regulatory network governing differentiation of *L. pneumophila* from replicative to transmissive forms.

During the transmissive phase, amino acid starvation and fatty acid starvation triggers the production of the alarmone (p)ppGpp. The changes in (p)ppGpp levels are sensed by the sensor kinase LetS which then phosphorylates LetA. Phosphorylated LetA binds upstream of the small ncRNAs RsmY and RsmZ and activates their transcription. CsrA binds to its mRNA targets and inhibits their translation during bacterial replication. The presence of RsmY and RsmZ titrates CsrA away from its targets, which then enables translation of the mRNAs, thus expressing the transmissive phenotypes. In contrast, flagellum synthesis does not seem to be dependent on the RsmYZ-CsrA pathway but is controlled by the LetA/LetS TCS (Sahr *et al.*, 2009).

The *letA* mutant is more sensitive to oxidative and acidic stresses when grown to the post-exponential (and not to the exponential) phase. The *L. pneumophila letA* mutant has a 2-fold decrease in the expression of *rpoS*, suggesting that *letA* is required for the maximal expression of *rpoS* and the stationary-phase stress response. The reduced infectivity of *letA* mutants in *A. castellanii* may suggest that LetA regulates the expression of virulence genes (Hammer *et al.*, 2002; Molofsky & Swanson, 2004).
The LetA/LetS system belongs to a family of signal-transducing proteins that utilize a four-step phosphorelay system to regulate gene expression and exhibit a rheostat-like behaviour. Histidine 307 of the LetS protein is the primary site of phosphorylation required to activate LetA (Edwards *et al.*, 2010). Additionally, substitution of the threonine residue at position 311 of LetS with methionine generates an *L. pneumophila* mutant (T311M mutant) which displays delayed gene expression of the flagellar regulon and numerous other loci compared to wild-type bacteria, suggesting that histidine 307 and threonine 311 residues are necessary for LetS function (Edwards *et al.*, 2010).
In addition to the LetA/LetS system, several other TCSs are involved in the regulation of the differentiation of *L. pneumophila*. LqsR, the response regulator of the LqsS/LqsR system, controls the genes involved in virulence, motility and cell division, suggesting a role for LqsR in the transition from the replicative to the transmissive phases. The expression of the LqsS/LqsR system is regulated by RpoS and LetA (Tiaden *et al.*, 2007).
The PmrA/PmrS system is a global regulator implicated in the intracellular growth of *L. pneumophila* and in the regulation of its Dot/Icm type IV protein secretion system (Al-Khodor *et al.*, 2009) (**Figure 1.3.**).

1.5.3. Regulation by small non-coding RNA

CsrA (carbon storage regulator A) is an RNA-binding protein which binds to the RNA transcripts encoding the virulence traits of *L. pneumophila* and represses their translation during bacterial replication. Activation of the LetA/LetS system relieves the CsrA repression and induces the expression of *L. pneumophila* virulence traits (Hammer & Swanson, 1999; Hammer *et al.*, 2002; Molofsky & Swanson, 2003) (**Figure 1.3.**).
L. pneumophila encodes two small non-coding RNAs (sRNAs); RsmY and RsmZ (Repressors of stationary phase metabolites) that are involved in the regulation of its

differentiation. The expression of *rsmY* and *rsmZ* increases from exponential phase to post-exponential phase by 3.1 and 6.8 fold respectively (Sahr *et al.*, 2009). Overexpression of *rsmY* or *rsmZ* increases the expression of transmissive genes during exponential growth. RsmY and RsmZ bind to CsrA. A single mutant has no (*ΔrsmY*) or little (*ΔrsmZ*) effect on *L. pneumophila* virulence, but an *rsmY*/Z double mutant has a high resistance to sodium, less pigment production, and displays a severe growth defect in *A. castellanii* or human THP-1 macrophages, suggesting that RsmY and RsmZ have an additive function (Sahr *et al.*, 2009; Rasis & Segal, 2009).

RsmY and RsmZ bind to CsrA. RpoS and LetA regulate the expression of *rsmY* and *rsmZ* in a growth phase-dependent manner. Mutation of *letA* reduces the expression of *rsmY* and *rsmZ* by three- and two-fold respectively. In the stationary phase, LetA becomes phosphorylated and directly binds to its predicted binding box upstream of *rsmY* and *rsmZ* and activates their expression (Quon *et al.*, 1998). RsmY and RsmZ then sequester CsrA and relieve its repressor effect on the expression of *L. pneumophila* virulence traits (Sahr *et al.*, 2009). Therefore, RsmY and RsmZ represent the link between CsrA system and LetA/LetS regulation (**Figure 1.3.**).

1.5.4. Alternative sigma factors

Analysis of the *L. pneumophila* genome has identified six sigma factors: RpoD (σ^D, σ^{70}), RpoE, RpoH (σ^{32}), RpoN (σ^{54}), RpoS (σ^S/σ^{38}), and FliA (σ^{28}) (Chien *et al.*, 2004). Several of the *L. pneumophila* sigma factors have been implicated by genetic analysis to regulate subsets of virulence traits (Bachman & Swanson, 2001; Molofsky *et al.*, 2005). RpoS, RpoN and FliA are associated with bacterial differentiation. RpoS is required for sodium sensitivity, maximal expression of flagellin, and lysosomal evasion, but it is not important for other virulence traits (Bachman & Swanson, 2001). Flagellation and full motility of *L. pneumophila* occur only in the transmissive phase. Therefore, it is expected that flagellum synthesis is regulated by the same mechanisms that allow *L. pneumophila* to switch from the replicative to the transmissive phase (Heuner *et al.*, 1999). Several reports have demonstrated that the expression of the virulent phenotype of *L. pneumophila* is linked to the flagellar regulon and motility (Rowbotham, 1986; Pruckler *et al.*, 1995; Bosshardt *et al.*, 1997; Gao *et al.*, 1997; Byrne & Swanson, 1998;

Heuner *et al.*, 2002). RpoS, LetA, LetE, and probably cyclic-di-GMP (c-di-GMP) levels may have important regulatory influence on motility in *L. pneumophila* (Sahr *et al.*, 2009) (**Figure 1.3.**).

L. pneumophila has a single polar flagellum, which is composed of one major subunit, FlaA (Elliott & Johnson, 1981; Ott *et al.*, 1991; Heuner *et al.*, 1995). The flagellum mediates the invasiveness and cytotoxicity of *L. pneumophila* to macrophages (Dietrich *et al.*, 2001; Hammer *et al.*, 2002). Moreover, the bacterial flagellin is sensed by non-permissive mouse macrophages, resulting in killing of the bacterial cell via activation of the cytosolic Naip5 (Birc1e) receptor (Ren *et al.*, 2006; Molofsky *et al.*, 2006). FliA (σ^{28}) is required to activate the transcription of *flaA* in *L. pneumophila*. The promoter sequence of *flaA* has the typical consensus sequence of σ^{28} (Heuner *et al.*, 1995). An *L. pneumophila fliA* mutant is non-flagellated, and the addition of the *fliA* gene in *trans* restores the expression of *flaA* (Heuner *et al.*, 2002). Expression of *L. pneumophila flaA* gene in *E. coli* requires the presence of the *E. coli* σ^{28} (Heuner *et al.*, 1995; Heuner *et al.*, 2002). FliA of *L. pneumophila* can restore the flagellation and motility in an *E.coli fliA* mutant (Heuner *et al.*, 1999). An *L. pneumophila fliA* mutant displays intracellular growth defects in *Dictyostelium discoideum* and mouse bone marrow-derived macrophages (Heuner *et al.*, 2002; Hammer *et al.*, 2002), suggesting that FliA may play a role in the full fitness of *L. pneumophila*.

L. pneumophila expresses its flagellar genes as a transcriptional hierarchy comprised of at least three steps. The first level of the flagellum regulatory cascade is regulated by the alternative sigma factor RpoN (σ^{54}) together with the transcriptional activator protein FleQ. Putative σ^{54} promoter sites have been found upstream of most of the flagellar operons, suggesting that RpoN and its activator protein FleQ may regulate these operons (Heuner & Steinert, 2003). Both *rpoN* and *fleQ* mutants are non-flagellated and express very small amounts of the flagellin (FlaA) protein (Jacobi *et al.*, 2004; Albert-Weissenberger *et al.*, 2010). RpoN and FleQ activate the expression of *fleN*, *fliM*, *fleSR* and other genes which participate in the synthesis of the flagellum basal body and hook (Jacobi *et al.*, 2004). FliA controls the last step of flagellum synthesis, including *flaA* expression (Heuner & Steinert, 2003; Bruggemann *et al.*, 2006). The activity of FliA is controlled by FlgM protein, an anti-σ^{28} factor. FlgM binds to FliA and prevents the

activation of FliA-dependent gene expression. Consequently, once the flagellum hook-basal body structure is built, FlgM is exported to relieve the repression of FliA so that the flagellum synthesis can be completed (Hughes *et al.*, 1993; Aldridge *et al.*, 2003).

It should be noted that *L. pneumophila rpoS* and *letA* mutants, which are differentiation-deficient, do not grow in amoebae and are completely digested in the ciliate *T. tropicalis*. However, these mutants grow well in HeLa cells and macrophages (Hales & Shuman, 1999; Gal-Mor & Segal, 2003; Lynch *et al.*, 2003; Abu-Zant *et al.*, 2006; Faulkner *et al.*, 2008) suggesting *L. pneumophila* is under strong selective pressure to differentiate inside protozoa, but not in mammalian cells. This may support the hypothesis that *L. pneumophila* does not complete its developmental program in cultured macrophages, since human cells are accidental hosts and not permissive for the completion of the life cycle of *L. pneumophila*.

1.6. *L. pneumophila* intracellular trafficking and replication

The intracellular events that lead to *L. pneumophila* internalization, replication and exit from amoebae are similar to those in human alveolar macrophages, monocytes, and alveolar epithelial cells, suggesting that the infection mechanisms used by *L. pneumophila* are conserved between hosts (Swanson & Hammer, 2000; Garduno, 2007). Following its internalization into host cells, *L. pneumophila* modifies the organelle trafficking of host cells, avoids fusion with the host lysosomes and resides in a unique compartment known as the *Legionella*-containing vacuole (LCV). These processes are chiefly mediated by the secreted effectors of the Dot/Icm system. The LCV does not acquire many of the classical markers of the endocytic pathway, including Rab5 for early endosomes, Rab7 for late endosomes (small GTPases that regulate the endocytic membrane-trafficking interactions) and LAMP-1(lysosome-associated membrane protein 1) for lysosomes (Wieland *et al.*, 2004; Sauer *et al.*, 2005). The LCV does not undergo acidification and maintains a pH value of ~ 6.1 (Horwitz & Maxfield, 1984). Instead, the LCV recruits mitochondria, ribosomes and small vesicles derived from the endoplasmic reticulum (ER) and/or Golgi apparatus (Kagan & Roy, 2002; Robinson & Roy, 2006) and remodels the LCV to an ER-like vacuole. The ability of *L. pneumophila* to escape from lysosomal fusion is a hallmark of its pathogenesis. Bacterial mutants which are deficient

in this capability are essentially avirulent (Horwitz, 1987). *L. pneumophila* replicates actively inside the LCV and eventually ruptures the LCV membrane and lyses the host cells to initiate a new round of infection (Hubber & Roy, 2010). The Dot/Icm system is essential for the virulence of *L. pneumophila*. Phagosomes containing *dot*/*icm* mutants do not exhibit altered organelle trafficking in the host cells and acquire lysosomal markers (Coers *et al.*, 1999; Clemens *et al.*, 2000; Lu & Clarke, 2005).

1.6.1. *L. pneumophila* internalization

Uptake of *L. pneumophila* into amoebae occurs through the characteristic, yet uncommon coiling phagocytosis (Bozue & Johnson, 1996; Venkataraman *et al.*, 1998) and other mechanisms that resemble receptor-mediated endocytosis or macropinocytosis (processes more involved than coiling phagocytosis) (Fields *et al.*, 1993; Abu Kwaik, 1996; Venkataraman *et al.*, 1998), suggesting that different amoebae may use different mechanisms to internalize *L. pneumophila*. Uptake of legionellae by *H. veriformis* is mediated by galactose/N-acetylglucosamine (Gal/GalNAc) lectin, which serves as a receptor for *L. pneumophila* (Venkataraman *et al.*, 1997). Binding to the Gal/GalNAc receptor induces tyrosine dephosphorylation, resulting in the disruption of the host cytoskeleton and entry of *L. pneumophila* by a form of receptor-mediated endocytosis (King *et al.*, 1991; Venkataraman *et al.*, 1997). The bacterial factor that binds to the amoebal Gal/GalNAc lectin has not been identified yet.

Uptake of *L. pneumophila* into macrophages occurs through coiling phagocytosis (Horwitz, 1984), conventional phagocytosis (Horwitz & Silverstein, 1981; Payne & Horwitz, 1987; Steinert *et al.*, 2002) and macropinocytosis (Watarai *et al.*, 2001). Although *L. pneumophila* is taken up by similar mechanisms in both amoebae and human macrophages, some differences in the uptake of *L. pneumophila* by both hosts still exist. Inhibition of actin polymerization by cytochalasin D inhibits the uptake of *L. pneumophila* by human macrophages (but not by *H. vermiformis*), suggesting that actin polymerization is important for the uptake of *L. pneumophila* by human macrophages. In addition, inhibition of host protein synthesis by cycloheximide inhibits uptake of *L. pneumophila* by *H. vermiformis* (but not by human macrophages) suggesting that host

proteins play a more important role in the uptake of *L. pneumophila* into amoebae (Fields *et al.*, 2002).

1.6.2. Inhibition of lysosome fusion with the LCV

L. pneumophila vacuoles do not fuse with the lysosomes, remain non-acidic, and do not acquire endocytic markers such as LAMP-1, Rab5 and Rab7. Instead, they acquire endoplasmic reticulum (ER) markers (Wieland *et al.*, 2004; Sauer *et al.*, 2005). However, another study demonstrated that the LCVs in A/J mouse bone marrow-derived macrophages did acquire LAMP-1 and matured into acidic phagosomes (pH 5.6) after 18 hours of infection. Pharmacological inhibition of LCV acidification inhibits bacterial replication, suggesting that the LCV may act differently in different hosts (Sturgill-Koszycki & Swanson, 2000). The establishment of the unique LCV depends primarily on the Dot /Icm type IV secretion system.

The ability of the LCV to avoid fusion with the host lysosomes is not absolutely dependent on bacterial viability, the Dot/Icm system, or the bacterial active protein synthesis (Horwitz, 1983; Joshi *et al.*, 2001), suggesting that bacterial surface factors also may be involved. HtpB-coated latex beads display delayed fusion with lysosomes (Chong *et al.*, 2009). The Sel-1 repeat-containing LpnE, EnhC and IidL proteins are also involved in manipulating the organelle trafficking of the host cell and avoiding lysosomal fusion (Newton *et al.*, 2007). Latex beads coated with LPS-rich outer membrane vesicles collected from both *L. pneumophila* and *dotA* mutants are also able to inhibit phagosome-lysosome fusion (Fernandez-Moreira *et al.*, 2006).

1.6.3. Recruitment of mitochondria to the LCV

The LCV membrane associates with mitochondria and many small secretory vesicles as early as 15 to 30 minutes post-infection, and becomes surrounded by mitochondria 4 hours post-infection (Horwitz, 1983; Kagan & Roy, 2002). LCVs containing avirulent *dot/icm* mutants do not recruit mitochondria or smooth vesicles (Horwitz, 1987; Marra *et al.*, 1992). The *Legionella* protein HtpB is involved in mitochondria recruitment to the LCV. HtpB-coated beads attract mitochondria to human macrophages and Chinese hamster ovary (CHO) cells (Tilney *et al.*, 2001; Chong *et al.*,

2009). The significance of mitochondrial recruitment and association with the LCV in the pathogenesis of *L. pneumophila* still remains to be determined.

1.6.4. Remodelling of the LCV into an ER-derived replicative organelle

The LCV intercepts early secretory vesicles prior to their transport through the ER-Golgi intermediate compartment (ERGIC) (Horwitz, 1983; Tilney *et al.*, 2001; Kagan & Roy, 2002). The membranes of these vesicles contact with and fuse along the surface of the LCV, which is then followed by exchange of membranes between the two compartments (Tilney *et al.*, 2001). Analysis of the host factors recruited to the LCV reveals that the ER is the source of these secretory vesicles (Swanson & Isberg, 1995; Abu Kwaik, 1996; Tilney *et al.*, 2001; Robinson & Roy, 2006; Ingmundson & Roy, 2008). The LCV becomes studded with ribosomes and surrounded by the ER, and then *L. pneumophila* starts replication inside the LCV (Horwitz, 1983; Swanson & Isberg, 1995; Lu & Clarke, 2005).

1.6.5. Bacterial egress from host cells

L. pneumophila exits infected host cells in two stages: first, by induction of apoptosis during the early stages of infection (Gao *et al.*, 1998; Hagele *et al.*, 1998), followed by induction of necrosis through its pore-forming activity, ultimately resulting in osmotic lysis and egress of the bacteria (Byrne & Swanson, 1998; Alli *et al.*, 2000). It should be noted that *L. pneumophila* induces apoptosis in infected macrophages and alveolar epithelial cells but not in amoebae (Hagele *et al.*, 1998; Gao *et al.*, 1998; Gao & Kwaik, 2000). The pore-forming ability of *L. pneumophila* is essential for its egress from the host cells. *L. pneumophila* mutants termed *rib* (release of intracellular bacteria) are able to evade phagosome-lysosome fusion and replicate inside the host cells, but get trapped inside the host cells due to lack of pore-forming ability (Gao & Kwaik, 2000; Alli *et al.*, 2000; Zink *et al.*, 2002). Eventually, *rib* mutants will induce apoptosis in host macrophages, but not in protozoan hosts. This phenotype of *rib* mutants was found to be associated with a truncated IcmT protein. Complementation of *rib* mutants with a functional *icmT* gene restores the bacterial ability to form pores and exit the host cells (Molmeret *et al.*, 2002; Molmeret *et al.*, 2002; Bitar *et al.*, 2005).

1.7. The Dot/Icm system

The Dot/Icm (defect in organelle trafficking/intracellular multiplication) type IVB protein secretion system is the single most important virulence factor of *L. pneumophila*. It was identified by two independent genetic studies (Marra *et al.*, 1992; Berger & Isberg, 1993), which may explain why some genes are named *dot*, some are named *icm,* and some other genes have both names (e.g. *icmE* = *dotG*).

The Dot/Icm system consists of 26 genes located in two separate regions of the *L. pneumophila* genome. These proteins assemble into a translocation apparatus that allows bacteria to inject effectors into the infected host cells (Sexton & Vogel, 2002). *L. pneumophila* secretes a great number of Dot/Icm effectors. So far, 275 experimentally-confirmed effectors have been identified using bioinformatic analysis (e.g. presence of eukaryotic domains or sequence motifs identified from earlier effectors) and biochemical assays (e.g. translocation assays, protein-protein interactions and yeast genetic screening) (Luo & Isberg, 2004; Burstein *et al.*, 2009; Heidtman *et al.*, 2009; Zhu *et al.*, 2011). This large number of effectors is consistent with the observation that deletion of a single effector rarely results in significant effects on the virulence traits of *L. pneumophila*, suggesting that Dot/Icm effectors have functional redundancy (Ninio & Roy, 2007).

Dot/Icm effectors have diverse structures. However, most proteins are unique to *Legionella* and do not show significant homology to other proteins (Zhu *et al.*, 2011). The individual functions of the majority of the effectors are unknown, although a few have been identified. Some functions include vacuolar remodelling, endosome-lysosome fusion avoidance, and endoplasmic reticulum recruitment (Ensminger & Isberg, 2009). The Dot/Icm system may support the entry of *L. pneumophila* into host cells. An *icmT* mutant (unable to encode one of the inner membrane components of the Dot/Icm apparatus) displays decreased uptake by mouse macrophages and *A. castellanii*, which could be restored by co-infection with wild-type bacteria (Hilbi *et al.*, 2001). Overexpression of *dotA* (which encodes one of the inner membrane components of the Dot/Icm apparatus) enhances *L. pneumophila* invasion of U937 human macrophages and early establishment of LCVs. These findings suggest that upon contact with the host cells, the Dot/Icm system translocates effectors that participate in the entry process either by altering host cellular signals triggered during uptake, or directly by interacting with

the host cell receptors (Segal *et al.*, 1999; Hilbi *et al.*, 2001; Watarai *et al.*, 2001; Molofsky & Swanson, 2004). The Dot/Icm effectors are also important for remodelling of the LCV. The LCV is actively remodelled and acquires markers of the ER, such as calnexin and Bip within minutes of its formation, indicating that LCV interacts with the ER network (Luo, 2012). Host regulators, such as Rab1 and Arf-1 (ADP-ribosylation factor) that are important in the vesicular trafficking from ER and Golgi to the phagosome (ER-Golgi trafficking), are found on LCVs containing wild-type bacteria but not *dot/icm* mutants (Kagan & Roy, 2002; Kagan *et al.*, 2004).

RalF was the first identified *L. pneumophila* Dot/Icm effector. RalF is a guanine-nucleotide exchange factor (GEF), which mediates the recruitment of the host GTPase protein Arf-1(ADP ribosylation factor) to the LCV (Nagai *et al.*, 2002). Although the function of Arf1 is essential for LCV formation and fusion with ER-derived vesicles (Kagan & Roy, 2002; Robinson & Roy, 2006), *ralF* mutants are still capable of evading the endocytic pathway and generating the LCV in protozoa and macrophages (Nagai *et al.*, 2002).

Rab-1 is another GTPase that is targeted by Dot/Icm effectors. SidM (substrate of Icm/Dot transporter M) or DrrA (Defect in Rab1 recruitment A) specifically recruits Rab1 to the LCV membranes (Kagan *et al.*, 2004). SidM/DrrA-mediated recruitment of Rab1 onto the LCV is enhanced by the Dot/Icm effector LidA (Machner & Isberg, 2006; Murata *et al.*, 2006) and can be switched off by two effectors, SidD and LepB (Tan & Luo, 2011; Neunuebel *et al.*, 2011). Although Rab1 is important for LCV biogenesis, *drrA* mutants display no growth defects in A/J primary mouse macrophages (Machner & Isberg, 2006).

The Dot/Icm effector SidK can prevent acidification of the LCV through interaction with the vacuolar H^+-ATPase, which regulates the phagosomal pH. Once translocated into the host cells, SidK can specifically inhibit v-ATPase activity by binding to a VatA subunit and preventing ATP hydrolysis (Xu *et al.*, 2010). Macrophages loaded with SidK are defective in phagosome acidification and less able to digest the internalized non-pathogenic bacteria (Xu *et al.*, 2010).

Dot/Icm effectors can also modulate the host immune defences. Infection by *Legionella* triggers the classical TLR-dependent immune responses (Archer *et al.*, 2009)

and activates caspase1 by the Naip5/Birc1e involved in the detection of flagellin released into the host cytosol by the Dot/Icm transporter (Vance, 2010). Microarray analyses with bacterial flagellin mutants using macrophages derived from mice defective in the TLR pathways have revealed important roles for the Dot/Icm system in the induction of several innate immunity pathways, including the NF-κB pathway (Losick & Isberg, 2006; Shin *et al.*, 2008; Fontana *et al.*, 2011).

Dot/Icm-dependent activation of NF-κB signalling in mammalian cells is a sustained response in both human macrophages and alveolar epithelium (Losick & Isberg, 2006; Abu-Zant *et al.*, 2007; Bartfeld *et al.*, 2009). NF-κB activation is important for bacterial intracellular growth. Activation of certain NF-κB-controlled anti-apoptotic genes decreases the apoptotic death of host macrophages and provides sufficient time for intracellular bacterial replication.

LegK1 and LnaB are Dot/Icm effectors that activate signaling of the host NF-κB. They were identified through NF-κB luciferase reporter screening using HEK 293T cells (Ge *et al.*, 2009; Losick *et al.*, 2010). Interestingly, *legK* mutants*, lnaB* mutants*,* and *legK*/*lnaB* double mutants do not show defects in the NF-κB signaling and viability of A/J mouse primary macrophages or in the intracellular bacterial growth (Ge *et al.*, 2009; Losick *et al.*, 2010).

SidF and SdhA are actively expressed inside human macrophages and may play a role in counteracting the host apoptotic response (Laguna *et al.*, 2006; Banga *et al.*, 2007; Faucher *et al.*, 2011). Mouse macrophages infected with a *sidF* mutant display increased apoptosis and death. The *L. pneumophila sidF* mutant displays a significant decrease in replication inside A/J mouse primary macrophages, but not inside human macrophages or *D. discoideum* (Banga *et al.*, 2007). *L. pneumophila sdhA* mutants display significant growth defects in A/J primary mouse macrophages and less significant defects in *D. discoideum*. Macrophages infected with *sdhA* mutants display increased apoptosis, more drastic than *sidF* mutants (Laguna *et al.*, 2006).

1.8. Transcriptome analysis of *L. pneumophila* inside different hosts

The life cycle of *L. pneumophila* involves two distinct habitats, an extracellular freshwater environment and an intracellular infection vacuole inside host cells. To

survive in both environments, *L. pneumophila* alternates between MIFs and RFs. To reach these distinct forms, *L. pneumophila* undergoes changes in its gene expression during differentiation. Genes induced during the replicative phase (*in vitro* or inside host cells) generally promote bacterial multiplication, and encode components of metabolic pathways and cell division (Bruggemann *et al.*, 2006). However, as nutrients become limited, metabolism slows down. Instead, transmissive traits (*in vitro* or inside host cells) predominate, including genes that encode the flagellar machinery, virulence factors translocated by the Dot/Icm secretion system (Cirillo *et al.*, 1999; Conover *et al.*, 2003; Luo & Isberg, 2004; Shohdy *et al.*, 2005; Campodonico *et al.*, 2005), as well as Dot/Icm-independent virulence factors, e.g. the enhanced entry proteins (Enh). Therefore, the genes upregulated later in the life cycle of *L. pneumophila* are expected to promote transmission and manipulation of new host cells and prepare the bacterium for the next round of infection.

Differentiation is an essential process for *L. pneumophila* and is directly related to its ability to infect both protozoa and mammalian hosts. Therefore, analysing the genetic expression of *L. pneumophila* inside amoebae and human macrophages could improve our understanding of the incomplete differentiation of *L. pneumophila* into MIFs inside macrophages and may help explain why LD is only acquired from the environment and cannot be transmitted from person to person.

1.8.1. The control of differentiation in *L. pneumophila* is not yet fully understood.

There are deficiencies in our current understanding of the differentiation process in *L. pneumophila*. For instance, 23 of the *L. pneumophila* genes upregulated during replication inside amoebae and more than 90 genes upregulated later during differentiation into transmissive forms (MIFs) are hypothetical with no similarity to database entries (Bruggemann *et al.*, 2006). Furthermore, 8 of the 10 most highly induced *L. pneumophila* genes in human macrophages have no assigned functions (Faucher *et al.*, 2011).

The current understanding of the differentiation cycle in *L. pneumophila* is based mainly on *in vitro* growth models. It has been understood that SPFs are the *in vitro* transmissive forms, and therefore were used to study the differentiation mechanisms in *L.*

pneumophila (Byrne & Swanson, 1998). The extent to which the current understanding corresponds to the differentiation process in the intracellular environments is not completely understood.

Gene expression studies have revealed dissimilarity of the genetic expression when *L. pneumophila* grows *in vitro* (BYE broth) or *in vivo* (inside host cells). For instance, about 84% of the replicative phase genes and 77% of the *in vivo* transmissive phase genes characterized in amoebae are also upregulated in the exponential and the post-exponential phases in broth, respectively (Bruggemann *et al.*, 2006). Likewise, comparison of the changes in gene expression in *L. pneumophila* at post-exponential phase (transmissive forms *in vitro*) and inside human macrophages (transmissive forms *in vivo*) to exponential phase forms yields different outcomes, suggesting that the correlation between the *in vivo* MIFs and the *in vitro* SPFs is limited (Faucher *et al.*, 2011). However, similarities in the gene expression profiles *in vivo* and *in vitro* may suggest that there are specific genes that could be essential for the *L. pneumophila* differentiation process in both environments.

1.8.2. Changes in the gene expression of *L. pneumophila* inside *A. castellanii*

To gain insight into the molecular mechanisms controlling the differentiation of *L. pneumophila* inside its natural host, Brüggemann *et al.* (Bruggemann *et al.*, 2006) have analysed the global changes in gene expression profiles of three clinical *L. pneumophila* strains (Philadelphia, Paris and Lens) in *A. castellanii* using microarray analysis. Brüggemann *et al.* (Bruggemann *et al.*, 2006) have analysed the changes in gene expression of *L. pneumophila* at multiple time points (8, 11, and 14 hours postinfection) inside *A. castellanii*. The changes in the gene expression of *L. pneumophila* at 8 hours reflect the replicative traits, the changes at 11 hours reflect the early transmissive traits, and the changes at 14 hours reflect the late transmissive traits. The genes that are upregulated at both 11 and 14 hours reflect the general transmissive traits. Interestingly, the three *L. pneumophila* strains exhibit similar expression profiles, suggesting that the regulatory networks that govern *L. pneumophila* differentiation are conserved (Bruggemann *et al.*, 2006) (**Figure 1.4.**).

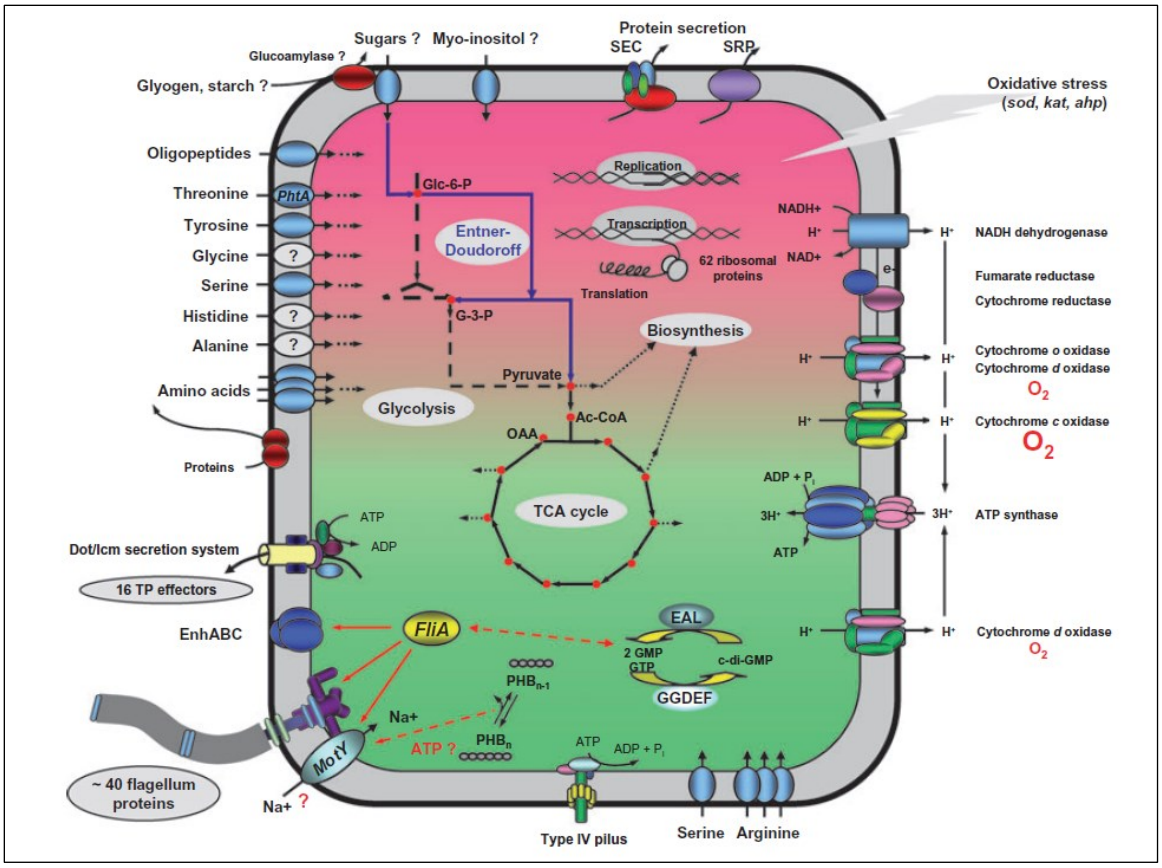

Figure 1.4. Transcriptome changes during the biphasic life cycle of *L. pneumophila* inside *A. castellanii*.

Transcriptome analysis demonstrates the transcriptional changes that occur during the differentiation of RFs (pink background) into MIFs (cyan background) in *A. castellanii*. Main replicative traits are: amino acid and oligopeptide transporters, sugar transporters, glycolysis and the Entner-Doudoroff (ED) pathway, oxidative stress response proteins, and the replication, transcription and translation machinery.

Important transmissive traits are: flagellum biosynthesis, invasion-associated traits (e.g. EnhABC), GGDEF/EAL proteins, type IV pilus biosynthesis, synthesis and degradation of polyhydoxybutyrate (PHB), and the Dot/Icm effectors (Bruggemann *et al.*, 2006).

.

According to microarray analysis, *L. pneumophila* genes that are induced during replication include the ones encoding factors that promote replication such as amino acid transporters, enzymes of the tricarboxylic acid (TCA) cycle, components of the electron transport chain, and some virulence associated factors like CsrA. During replication of *L. pneumophila* in amoebae, genes involved in amino acid degradation pathways are upregulated. Upregulation of several aminopeptidases and proteinases indicates that the pathogen is able to scavenge host proteins (Bruggemann *et al.*, 2006). Eventually, as nutrients and oxygen become scarce, genes involved in bacterial replication are down-regulated and the genes involved in the transmissive phase are up-regulated, including genes encoding Dot/Icm-secreted effector proteins, genes involved in flagellar biosynthesis, genes encoding EnhABC, LetE, integration host factor (IHF), several uncharacterized transcriptional regulators and two-component systems, and many other virulence factors (Bruggemann *et al.*, 2006).

Interestingly, *L. pneumophila* also appears to catabolize carbohydrate-derivatives in the replicative phase. The gene cluster which encodes the Entner-Doudoroff pathway (*lpg0416- lpg0418*, *lpg0420*), the genes which encode a putative glucokinase (*lpg0419*) and a sugar transporter (*lpg0421*) are all upregulated during replication in amoebae (Bruggemann *et al.*, 2006). The expression of the eukaryotic-like glucoamylase (*lpg0422*) *in vivo* could allow *L. pneumophila* to exploit carbohydrates in amoebae. In addition, four out of five genes predicted to encode myo-inositol catabolism proteins are upregulated *in vivo*. Together, the transcriptional profile of *L. pneumophila* inside amoebae suggests that carbohydrates could be used as sources of carbon and energy (Bruggemann *et al.*, 2006).

A family of regulators that possess GGDEF or EAL motifs (GGDEF/EAL proteins) was also up-regulated during the transmissive phase in amoebae (Bruggemann *et al.*, 2006). GGDEF/EAL proteins regulate the intracellular levels of the second messenger cyclic di-guanosine monophosphate (c-di-GMP) through their diguanylate cyclase and phosphodiesterase activities (D'Argenio & Miller, 2004; Romling *et al.*, 2005). GGDEF/EAL proteins regulate the transition between motile and sessile bacteria found in biofilms when nutrients are limited (Romling & Amikam, 2006). In *S. enterica,* mutation in an EAL-domain protein has decreased bacterial resistance to oxidative stress and accelerated its killing by mouse macrophages (Hisert *et al.*, 2005). The roles of

GGDEF/EAL proteins in *L. pneumophila* are yet to be determined.

1.8.3. Changes in the gene expression of *L. pneumophila* inside human macrophages

Faucher *et al*. (Faucher *et al.*, 2011) have analysed the changes in the gene expression of *L. pneumophila* during intracellular infections of THP-1 macrophages at multiple time points (0, 6, and 18 hours postinfection: T_0, T_6, and T_{18}, respectively) by microarray analysis. T_0 is considered an early time point of infection where the bacteria are still adapting to the intracellular environment. At T_6, the bacteria are actively growing inside macrophages (replicative forms) and by T_{18}, the bacteria should stop replicating and start to lyse the host cells (transmissive forms) (Faucher *et al.*, 2011).

Analysis of gene expression of *L. pneumophila* inside human macrophages revealed that genes encoding amino acid biosynthesis and transport systems involved in amino acid transporters and iron uptake are induced during intracellular growth. Genes involved in catabolism of glycerol are induced during intracellular growth, suggesting that glycerol could be used as a carbon source inside macrophages. Iron transport systems are upregulated, including genes involved in legiobactin production (*lbtAB*) and iron acquisition (*iraAB*). Indeed, the *lbtAB* locus is one of the most highly induced *L. pneumophila* genes inside macrophages. Genes involved in glycolysis are not differentially regulated inside human macrophages. Genes encoding the components of ED pathway are not upregulated either, suggesting that carbohydrate metabolism is not important for *L. pneumophila* inside human macrophages.

Several two-component systems, including PmrA/PmrB (Zusman *et al.*, 2007), CpxR/CpxA (Altman & Segal, 2008), and LetA/LetS (Hammer *et al.*, 2002), are involved in the regulation of virulence factors of *L. pneumophila* and are differentially expressed during infection of human macrophages. The *cpxR* and *cpxA* genes are significantly induced at T_6 and T_{18}, and are therefore likely to function late in infection. Although the *pmrA* gene encoding the response regulator is not upregulated inside human macrophages, the *pmrB* gene encoding the cognate sensor kinase is significantly repressed at early time points (T_0 and T_6). In contrast, the gene encoding the LetS sensor is induced inside cells, but the gene encoding its cognate transcription activator, LetA is repressed. The LetA/LetS system controls the expression of two small RNAs (RsmY and

RsmZ), which, in turn, control the activity of CsrA, a global regulator that represses the expression of post-exponential traits during exponential growth (Molofsky & Swanson, 2003; Forsbach-Birk *et al.*, 2004; Rasis & Segal, 2009; Sahr *et al.*, 2009). This may provide clues to the incomplete differentiation of *L. pneumophila* inside human macrophages.

Sigma factors also regulate gene expression in response to stress or other environmental signals. The *rpoD* gene encoding the vegetative sigma factor σ^{70} is repressed during growth inside human macrophages compared to the exponential phase. The *rpoS* gene encoding σ^{S} is strongly induced. The gene *rpoH* is strongly induced at T_6 and T_{18} inside human macrophages.

Phagocytes usually use multiple strategies to kill bacteria. These strategies include acidification of the phagosome, production of reactive oxygen and nitrogen species, and production of antimicrobial peptides (Flannagan *et al.*, 2009). However, infection of macrophages with *L. pneumophila* prevents the formation of ROS (Harada *et al.*, 2007), which may explain why genes involved in oxidative stress adaptation such as *sodB*, *sodC* are not induced during intracellular growth in macrophages (Faucher *et al.*, 2011). *Legionella* also expresses a number of proteases and peptidases during intracellular growth, which could degrade the antimicrobial peptides produced by the host cell (Faucher *et al.*, 2011).

1.8.4. Changes in the gene expression of *L. pneumophila* inside *Tetrahymena* ciliates

Tetrahymena tropicalis ciliates have been proposed as a model to study the differentiation of *L. pneumophila* into mature infectious forms (MIFs). While the development of MIFs inside amoebae usually takes about 3 days and is preceded by bacterial replication, *Tetrahymena* ciliates offer the experimental advantage of rapid (within ~ 1 hour) and direct development of SPFs into MIFs ciliates in the absence of bacterial replication (Faulkner *et al.*, 2008). However, the genetic expression of *L. pneumophila* inside *Tetrahymena* ciliates has not been studied yet. My PhD project is the first study to report the global changes in *L. pneumophila* transcriptome inside *Tetrahymena* ciliates using microarray analysis. Since the development of MIFs inside *Tetrahymena* ciliates has been observed as early as 30 minutes post-ingestion (Faulkner

et al., 2008), I set out to study the changes in gene expression of *L. pneumophila* following 30 minutes of internalization in *Tetrahymena* ciliates compared to SPFs incubated in the infection medium (Tris-buffered Osterhout's Solution; TBOS) for the same period to identify the genes that may be activated early during the differentiation process. The results of my project will also test the validatity of Tetrahymena ciliates as a model to study the differentiation of *L. pneumophila* into MIFs.

1.8.5. Comparison of *L. pneumophila* gene expression in amoebae and macrophages

Analysis of the gene expression profiles of *L. pneumophila* inside amoebae and human macrophages could improve our understanding of the incomplete differentiation into MIFs inside human macrophages, and may help explain why LD is only acquired from the environment and not transmitted among humans. However, direct comparison of the changes in gene expression of *L. pneumophila* inside amoebae and human macrophages has not been done yet. Global gene expression profiles of *L. pneumophila* were studied using microarray analysis, which still requires further confirmation by qRT-PCR analysis (Morey *et al.*, 2006). In addition, the two studies had different designs and targetted different time points during intracellular infections.

1.9. Metabolism of *L. pneumophila*

L. pneumophila grows *in vitro*, in buffered yeast extract (BYE) broth or on buffered charcoal yeast extract (BCYE) agar. The composition of both BCYE agar and BYE broth is described in section (2.1.1.). *L. pneumophila* is a fastidious organism and requires a unique combination of nutrients (which represent the nutrients available inside the host cells) in the laboratory media (Fields *et al.*, 2002). Very little is currently known about the nutritional environment within the LCV. Investigation of the nutrient requirements of *L. pneumophila in vitro* (using laboratory media) might give us a clue for the nutritional requirements inside LCV. Nutrients required for the intracellular multiplication of *L. pneumophila* inside the LCV may also serve as signals that can trigger the germination of MIFs into RFs. *In vitro* studies in broth cultures suggest that *L. pneumophila* mainly depends on amino acids as a primary source of carbon, nitrogen, and energy.

1.9.1. Amino acids

Early reports demonstrated that *L. pneumophila* requires the presence of arginine, isoleucine, leucine, methionine, serine, threonine, valine, cysteine, and glutamic acid to replicate (George *et al.*, 1980; Tesh & Miller, 1981; Tesh *et al.*, 1983), with glutamate serving as the principal energy source (Weiss & Westfall, 1984). This may suggest that *L. pneumophila* has to acquire these amino acids inside LCV from the host cells. In fact, cysteine supplementation is not required for *L. pneumophila* growth inside macrophages, mammalian cells or amoebae, suggesting that *L. pneumophila* obtains cysteine and other essential amino acids from host cells (Wieland *et al.*, 2005). The cysteine requirement of *L. pneumophila* and its inability to utilize the oxidized form cystine may impose an intracellular lifestyle (where cysteine is available) in the natural freshwater environment, and may also guarantee that MIFs do not differentiate into non-infectious RFs outside the host cells (Ewann & Hoffman, 2006). Interestingly, genome sequencing revealed that *L. pneumophila* has genes required for the synthesis of cysteine and methionine, suggesting that *L. pneumophila* may not be auxotrophic for these amino acids under certain conditions (Cazalet *et al.*, 2004; Chien *et al.*, 2004).

The importance of amino acids for *L. pneumophila* replication has been supported by the discovery of a phagosomal transporter (Pht) family. Pht transporters are amino acid transporters which belong to the major facilitator superfamily. They are important for the ability of *L. pneumophila* to differentiate in broth cultures and replicate inside primary mouse macrophages (Sauer *et al.*, 2005; Chen *et al.*, 2008).

PhtA, a threonine transporter, is the first member of the Pht family to be characterized. *L. pneumophila phtA* mutants are unable to replicate in A/J primary mouse macrophages, mainly because of the inability of bacteria to differentiate into the replicative forms inside LCV. This replication defect is restored by in *trans* genetic complementation of *phtA* or by the addition of excess threonine in the infection medium (Sauer *et al.*, 2005). Bioinformatic analysis has demonstrated that *L. pneumophila* possess 11 Pht paralogues, including PhtA. *L. pneumophila* strain Lens also has a strain-specific Pht, PhtL (Chen *et al.*, 2008). Interestingly, several other intracellular human pathogens, including *Chlamydia*, *Coxiella*, and *Francisella* possess *pht* genes, indicating

that this may be a common mechanism for acquisition of nutrients by vacuolar pathogens (Chen *et al.*, 2008).

The putative *L. pneumophila* valine transporter, PhtJ, is required for the differentiation and optimal multiplication of *L. pneumophila* inside U937 human macrophages. *PhtJ* mutants display 100- and 1000-fold growth deficiency inside human macrophages at 24 and 48 hours post-infection, respectively. However, PhtJ is not required for the intracellular growth of *L. pneumophila* inside *A. polyphagia* and *H. vermiformis* (Gao *et al.*, 1998; Harb & Abu Kwaik, 2000).

SLC1A5 is a neutral amino acid transporter located on the surface of LCV. Expression of the *slc1a5* gene is upregulated inside MM6 human monocytes. Pharmacological inhibition of the transporter and RNA silencing of *slc1a5* gene can block the intracellular replication of *L. pneumophila* inside MM6 human monocytes (Wieland *et al.*, 2005). This suggests that in addition to their ability to provide essential nutrients, phagosomal transporters can also assess the nutrient supply in the environment and provide a signal for replication.

1.9.2. Iron

In addition to amino acids, other lines of evidence suggest that growth of *L. pneumophila* inside the host cells is also dependent on iron.

Iron, an essential nutrient for most bacteria, exists in a dynamic equilibrium between the soluble ferrous (Fe^{2+}) and the insoluble ferric (Fe^{3+}) forms. Many studies have highlighted the importance of iron for *L. pneumophila* virulence and replication by exposing *L. pneumophila* bacteria to iron-limiting conditions *in vitro* (Reeves *et al.*, 1981; James *et al.*, 1995). Earlier studies investigating growth requirements of *L. pneumophila* have revealed its need of unusually high amounts of iron for optimal growth (Johnson *et al.*, 1991).

Iron is also important during intracellular replication of *L. pneumophila*. Monocytes and macrophages that have been treated with an iron chelator do not support *L. pneumophila* replication, and this inhibitory effect can be reversed by the addition of iron to the medium (Gebran *et al.*, 1994; Viswanathan *et al.*, 2000). IFN-γ can restrict the intracellular growth of *L. pneumophila* by downregulation of transferrin receptors in the

host cells and thereby maintaining low intracellular levels of iron (Byrd & Horwitz, 1989; Byrd & Horwitz, 2000). Furthermore, the expression level of transferrin receptors in mouse and human macrophages are correlated with the extent to which they are permissive to *L. pneumophila* infections. Low levels of expression of transferrin receptors are associated with higher resistance to *L. pneumophila* intracellular growth (Gebran *et al.*, 1994; Byrd & Horwitz, 2000).

L. pneumophila mutants that display defects in iron acquisition are also defective in infectivity of human macrophages, suggesting that *L. pneumophila* may require an effective iron transport mechanism to utilize iron from the host cells (Pope *et al.*, 1996). Given that a source of iron is essential for *L. pneumophila* replication, it is not surprising that the bacterium has developed regulatory mechanisms to obtain iron from the environment and from host cells (Cianciotto, 2007).

L. pneumophila produces Fur, a protein that can control gene expression in response to changes in iron concentrations. Fur is a transcriptional regulator which is activated under iron-limited conditions. Several Fur-regulated *L. pneumophila* genes that play a role in macrophage infections have been identified (Hickey & Cianciotto, 1994). For instance, a mutation in the Fur-regulated gene, *frgA*, which encodes a homologue of the siderophore-producing aerobactin synthetase in *E. coli*, displays an 80-fold growth defect in U937 human macrophages (Hickey & Cianciotto, 1997).

Our understanding of the acquisition of iron by *L. pneumophila* was greatly improved following the discovery that the bacterium secretes a siderophore (legiobactin) under iron-limiting growth conditions (Liles *et al.*, 2000). Representative strains from all *L. pneumophila* serogroups and other *Legionella* species also display siderophore activity in the presence of low amounts of iron (Starkenburg *et al.*, 2004). The production and export of legiobactin have been linked to the genetic locus *lbtAB*. LbtA is the predicted siderophore synthetase, and LbtB is a member of the major facilitator superfamily of multidrug efflux pumps and is likely responsible for the export of legiobactin (Allard *et al.*, 2006). The genes *lbtA* or *lbtB* are essential for the production of legiobactin. *L. pneumophila lbtAB* mutants display growth defects under low-iron conditions *in vitro* but do not display growth defects in mouse and human macrophages, *H. vermiformis* and alveolar epithelium. However, the *lbtA* mutant is severely attenuated in the intratracheal

infection of A/J mice. In addition, co-infection experiments demonstrate that legiobactin produced by wild-type *L. pneumophila* can rescue the growth defects of *lbtA* mutants in *trans*, suggesting that legiobactin is required for optimal intrapulmonary infections (Allard *et al.*, 2009).

Once the iron-siderophore complex is internalized across the outer membrane, it is likely acted upon by pyomelanin, which has ferric reductase activity, to produce ferrous iron (Chatfield & Cianciotto, 2007), which is then transported across the inner membrane by the ferrous iron transporter, FeoB (Cianciotto, 2007). The gene *feoB* is important for growth of *L. pneumophila in vitro* and for intracellular infections of *H. vermiformis* and human macrophages under low-iron conditions. An *L. pneumophila feoB* mutant shows modest growth defects following pulmonary infection of A/J mice (Robey & Cianciotto, 2002).

In addition to these mechanisms, other factors may also be important for the ability of *L. pneumophila* to acquire iron. The *iraAB* locus (for iron acquisition / assimilation) encodes a putative iron transporter. Deletion of *iraA* significantly impairs growth of *L. pneumophila* inside human macrophages and guinea pigs. *iraB* also contributes to growth of *L. pneumophila* under iron-limiting conditions *in vitro* (Viswanathan *et al.*, 2000). The cytochrome *c* maturation (*ccm*) locus, which is essential for intracellular multiplication, is also important for growth under low-iron conditions *in vitro* and inside amoebae and human macrophages (Viswanathan *et al.*, 2002; Naylor & Cianciotto, 2004).

L. pneumophila also produces McoL, a multicopper oxidase, which is essential for aerobic extracellular growth under low-iron conditions or when ferrous iron is the only available iron source (Huston *et al.*, 2008). McoL is not important for the intracellular growth of *L. pneumophila* in *H. vermiformis* and U937 human macrophages. Therefore, it is suggested that McoL may protect *L. pneumophila* against the toxic effects of utilizing ferrous iron during aerobic growth, rather than aiding iron acquisition (Huston *et al.*, 2008).

Overall, these findings indicate that amino acids and iron availability are required for of *L. pneumophila* growth *in vitro* and *in vivo*.

1.9.3. Carbohydrate metabolism

It has been generally understood that carbohydrate metabolism is unimportant to *L. pneumophila*. According to early growth studies of *L. pneumophila* in broth cultures, amino acids were considered the major source of carbon and energy with no effect of glucose on the growth of the bacterium (Pine *et al.*, 1979; Tesh *et al.*, 1983). In fact, *in vitro* growth studies also suggest that the differentiation of *L. pneumophila* into transmissive forms is mainly triggered by deficiency of amino acids in the growth medium (Molofsky & Swanson, 2004). However, the nature of the energy and carbon sources utilized by intracellular *L. pneumophila* is not well understood.

Recently, several reports have suggested that *L. pneumophila* is able to metabolize carbohydrates, which could serve as a source of carbon and energy when amino acids become deficient. Early reports have demonstrated that *L. pneumophila* has a weak starch-hydrolysing activity (Hebert *et al.*, 1980; Morris *et al.*, 1980; Thorpe & Miller, 1981). The four available genome sequences of *L. pneumophila* (*Lp*) [*Lp* Philadelphia (Cazalet *et al.*, 2004; Chien *et al.*, 2004), *Lp* Paris, *Lp* Lens (Cazalet *et al.*, 2004; Chien *et al.*, 2004), and *Lp* Corby (Glockner *et al.*, 2008)] show that the *L. pneumophila* genome contains genes that code for all proteins of the Embden-Meyerhof-Parnas (EMP) pathway, the complete ED, and the pentose phosphate (PP) pathway. Microarray analysis has demonstrated that genes involved in carbohydrate metabolism are upregulated during infections of *A. castellanii* (Bruggemann *et al.*, 2006). The expression of a genetic locus which codes for components of the ED pathway (*lpg0416-lpg0418*, *lpg0420*), a sugar transporter YwtG (*lpg0421*) and a glucoamylase GamA (*lpg0419*) is upregulated during replication inside amoebae suggesting that *L. pneumophila* can catabolize starch or glycogen stored by amoebic hosts (Bruggemann *et al.*, 2006). Protein analysis has also revealed that the majority of proteins upregulated in SPFs *in vitro* were related to carbohydrate and lipid metabolism (Hayashi *et al.*, 2010). Together, these findings suggest that *L. pneumophila* may utilize carbohydrates as energy sources when amino acids become limited.

Studies have reported that glucose could be metabolized by *L. pneumophila*, mainly through the Entner-Doudoroff (ED) and/or pentose phosphate pathways, rather than glycolysis (Tesh *et al.*, 1983; Weiss & Westfall, 1984; Eylert *et al.*, 2010; Harada *et*

al., 2010). The ED pathway is a NADPH-producing mechanism which is commonly used for sugar assimilation (Peekhaus & Conway, 1998). NADPH is usually generated from endogenous glucose or glucose-6-phosphate. *L. pneumophila* possesses six genes, organized together in a single locus (the *zwf* operon), that are responsible for metabolism of glucose by the Entner-Doudoroff (ED) pathway (Harada *et al.*, 2010). All these genes were upregulated during the replication of *L. pneumophila* inside amoebae (Bruggemann *et al.*, 2006), but not in human macrophages (Faucher *et al.*, 2011). Interestingly, analysis of the metabolism of ^{13}C-labelled glucose by *L. pneumophila* has revealed that the ^{13}C-label is found in various amino acids and in the energy and carbon storage compound poly-3-hydroxybutyrate (PHB) (Eylert *et al.*, 2010).

Carbohydrate analysis of *A. castellanii* trophozoites indicates that carbohydrates make up over 30% of their dry weight, and therefore can provide a significant source of nutrition. *A. castellanii* contains various sugar moieties such as high levels of galactose and glucose and small amounts of mannose and xylose (Dudley *et al.*, 2009). It is very likely that *L. pneumophila* is able to utilize host carbohydrates for replication or differentiation when amino acids become scarce since *L. pneumophila* has established an obligate intracellular relationship with amoebae through evolution (Molmeret *et al.*, 2005).

Although a body of evidence suggests that *L. pneumophila* can utilize carbohydrates, *L. pneumophila* mutants that are defective in carbohydrate metabolism do not seem to have intracellular growth defects. For instance, *L. pneumophila gamA* mutants, which are deficient in glucoamylase, do not display growth defects *in vitro* and inside amoebae or human macrophages (Herrmann *et al.*, 2011). An *L. pneumophila Zwf* mutant, deficient in glucose-6-phosphate dehydrogenase, is slowly outcompeted by the parent strain in successive rounds of infection in *A. castellanii* (Eylert *et al.*, 2010). However, the *L. pneumophila* mutant that lacks the entire genetic locus that codes for the ED pathway enzymes displays growth defects in A549 alveolar epithelium, A/J mouse peritoneal macrophages and the amoeba *Acanthamoeba culbertsoni*, but grows normally *in vitro* (Harada *et al.*, 2010). Taken together, these data suggest that despite being not necessary for *in vitro* growth, carbohydrates could be utilized during the intracellular growth of *L. pneumophila*. It is already known that virulence and differentiation of *L.*

pneumophila are under the control of amino acid and fatty acid metabolism (Hammer & Swanson, 1999; Edwards *et al.*, 2009). It is therefore likely that carbohydrate metabolism can influence the virulence and differentiation of *L. pneumophila* as well.

1.10. Study hypotheses and objectives

Previous studies have suggested that MIFs are poorly produced during *L. pneumophila* infections of human macrophages (Garduno *et al.*, 2002; Faulkner & Garduno, 2002). Since MIFs are thought to be the infectious forms of *L. pneumophila* that can transmit LD to susceptible humans, this observation may have potential impact on our understanding of the transmission of LD. Therefore, I set out to test the hypothesis that *L. pneumophila* progeny from human macrophages is less differentiated and has fitness and infectivity disadvantages compared to *L. pneumophila* progeny produced in protozoa in the natural freshwater environment.

Although the global changes in gene expression of *L. pneumophila* at multiple time points during infection of amoebae (Bruggemann *et al.*, 2006) and human macrophages (Faucher *et al.*, 2011) have been reported using microarray analysis, a direct analysis of gene expression between the two hosts has not been reported. I set out to test the hypothesis that *L. pneumophila* upregulates certain sets of genes in protozoa but not in human macrophages. These genes could be associated with the complete differentiation of *L. pneumophila*. A list of genes that are upregulated during infection of amoebae, but not human macrophages can improve our understanding of *L. pneumophila* differentiation in the natural environment and may help explain why LD is only acquired from the environment and can not be transmitted from person to person. Proteomic analysis of the *L. pneumophila* progeny from amoebae and human macrophages would support the transcriptome analysis.

Tetrahymena tropicalis is a freshwater ciliate that can package *L. pneumophila* MIFs into infectious pellets (Berk *et al.*, 2008). Feeding of *Tetrahymena* ciliates with SPFs of *L. pneumophila* triggers a rapid (within ~ 1 hour) and direct (directly from SPFs without replication intermediates) into MIFs (Faulkner *et al.*, 2008). Therefore, I set out to test the hypothesis that *Tetrahymena* ciliates may serve as a differentiation model to identify the signals that trigger the development of MIFs and study the changes in gene expression

during *L. pneumophila* differentiation from SPFs to MIFs. Therefore, comparison of *L. pneumophila* gene expression inside *Tetrahymena* ciliates and amoebae would test this hypothesis.

According to the aforementioned findings and rationale, the specific objectives of my research project are:

1. To compare the *L. pneumophila* progeny produced in amoebae and the *L. pneumophila* progeny produced in human macrophages according to their morphological differentiation, environmental fitness, and ability to infect host cells.
2. To study the changes in *L. pneumophila* gene expression inside amoebae, human macrophages and *Tetrahymena* ciliates.
3. To assess the role of one of the identified genes (from objective 2) in *L. pneumophila* differentiation.

CHAPTER 2: MATERIALS AND METHODS

2.1. Bacterial strains and growth conditions

All bacterial strains used in my thesis project are described in **Table 2.1**.

2.1.1. *L. pneumophila*

L. pneumophila strains were routinely prepared from crude lysates of infected *A. castellanii* monolayers and kept frozen at -80°C. Frozen stock aliquots were grown on buffered charcoal yeast extract (BCYE) agar (Pasculle *et al.*, 1980) for 3 to 5 days at 37°C in a humid incubator. BCYE was made up of the following ingredients per litre; 10 g yeast extract, 1 g (2-[2-amino-2-oxoethyl]-amino) ethanesulfonic acid (ACES) buffer, 1 g α-ketoglutaric acid, 16 g agar, 1.5 g activated charcoal. The pH of the medium was adjusted to 6.85-6.95 using 6 N KOH. Following autoclaving, 0.4 g L-cysteine (filter sterilized, pH was adjusted to 6-7 with 1 N KOH) and 0.025 % ferric pyrophosphate (filter sterilized) were added to the medium. Plain BCYE was used to grow strain 2064, whereas strains Lp1-SVir and JR32 were grown on BCYE supplemented with 100 µg/ml streptomycin. When required, the following antibiotics were added to the culture medium for selection: kanamycin (Kan) 25 µg/ml, and chloramphenicol (Cm) 5 µg/ml.

L. pneumophila strains were also grown in buffered yeast extract (BYE) broth at 37°C, with agitation (200 rpm) in a New Brunswick C25KC shaker incubator. BYE was based on the same formulation of BCYE, but charcoal and agar were omitted.

2.1.2. *Escherichia coli*

Escherichia coli strains were grown on Luria-Bertani (LB) agar or in LB broth at 37°C with agitation (200 rpm) in a New Brunswick C25KC shaker incubator. LB agar was made up of the following ingredients per litre: 5 g yeast extract, 10 g tryptone, 10 g sodium chloride, and 16 g agar. LB broth was based on the same formulation, with the exception of agar. When required, the following antibiotics were added to the culture medium: ampicillin (Amp) 100 µg/ml, Kan 50 µg/ml, and Cm 20 µg/ml.

Table 2.1. Bacterial strains used in this study

	Selection marker(s)	Characteristics	Reference
L. pneumophila			
Lp1-Svir	Sm^R	A spontaneous streptomycin-resistant Philadelphia-1 virulent strain	(Hoffman *et al.*, 1989)
2064		serogroup 1 (OLDA) clinical isolate from the sputum of LD patient in Halifax, Nova Scotia	(Fernandez *et al.*, 1989)
JR32	Sm^R	Salt sensitive isolate of AM511 (AM511: Philadelphia 1, serogroup 1, restriction deficient, modification positive)	(Sadosky *et al.*, 1993)
JR32-GFP	Sm^R,Cm^R, Kan^R	JR32 constitutively expressing GFP from plasmid pMMB207-Km14-GFP	A gift from G. Nasrallah
JR32-RED	Sm^R,Cm^R	JR32 constitutively expressing DsRed from plasmid pSW001	A gift from G. Nasrallah
JR32 Δ*amyA*	Sm^R, Kan^R	JR32 isogenic mutant that has *amyA* gene replaced with Km^R cassette	This study
JR32 Δ*amyA* (pMMB:*amyA*)	Sm^R,Cm^R, Kan^R	Δ*amyA* carrying pMMB:*amyA*	This study
JR32 Δ*amyA* (pMMB:*amyA*-His_6)	Sm^R,Cm^R, Kan^R	Δ*amyA* carrying pMMB:*amyA*-His_6	This study
E. coli			
DH5α		F–Φ80 ΔlacZΔM15 Δ(lacZYA-argF)U169 supE44 hsdR17 recA1 endA1 gyrA96 thi-1 relA1	Clontech

2.2. Hosts Infected with *L. pneumophila*

2.2.1. Culture and infection of *Acanthamoeba castellanii*

Acanthamoeba castellanii trophozoites (a gift from David Spencer, Dalhousie University) were maintained at room temperature (by subculture) in Neff's medium. Neff's medium was made up of the following ingredients per litre: 15 g glucose, 7.5 g yeast extract, 7.5 g proteose peptone #3, 2 mM KH_2PO_4, 1 mM $MgSO_4$, 0.05 mM $CaCl_2$, 0.1 mM ferric pyrophosphate, and 1% filter-sterilized multivitamin mix (containing, per liter: 1 mg of thiamine hydrochloride, 0.2 mg of *d*-biotin, and 1µg of vitamin B_{12}) (Cursons *et al.*, 1980). *A. castellanii* cultures were routinely collected and stored in sterile tap water at room temperature to form dormant cysts. Cysts were then used to start new cultures in fresh complete Neff's medium. Modified Neff's medium was used to prepare *A. castellanii* for *L. pneumophila* infections. Modified Neff's medium was based on the same formulation of Neff's medium, but yeast extract, proteose peptone, and the multivitamin mix were omitted.

Before infection with *L. pneumophila*, *A. castellanii* trophozoites in suspension were counted by direct microscopy in a Neubauer hemocytometer and were added to 25-cm^2 cell culture flasks (Falcon-BD Biosciences Canada, Mississauga, ON), using about 10^6 trophozoites per flask, and incubated overnight at 37°C until a confluent monolayer (about 10^6 trophozoites) is formed. The growth medium was then removed by pipetting and trophozoites were kept in modified Neff's medium until infected with legionellae. Plate-grown *L. pneumophila* cells were scraped from BCYE agar plates, washed and resuspended in modified Neff's medium to an optical density of 1 unit, which corresponds to $1.9 \pm 0.98 \times 10^9$ legionellae/ml. Optical density was measured at a wavelength of 620 nm (OD_{620}) using UNICO UV-2100 spectrophotometer (Dayton, NJ). The correct amount of this bacterial suspension was added to *A. castellanii* trophozoites to reach a final bacteria:amoeba ratio of 10:1. Infection was allowed to proceed for ~ 3 days at 37°C, and the resulting progeny was then purified.

2.2.2. Culture of *Tetrahymena tropicalis* ciliates and feeding experiments

The ciliate *T. tropicalis* was originally isolated from a cooling tower biofilm and donated by Sharon Berk (Berk *et al.*, 2008). It was first identified as a species of the genus *Tetrahymena* within the *T. mobilis*-*T. tropicalis* group, based on the DNA sequence of its gene encoding the small subunit rRNA. The species was determined according to the DNA sequence of a fragment of the gene encoding the mitochondrial cytochrome *c* oxidase (CO1) (Berk *et al.*, 2008).

T. tropicalis was maintained in axenic culture as lines A, B, and C according to the procedures previously outlined (Berk *et al.*, 2008). Line C *T. tropicalis* ciliates were grown in Plate Count Broth (PCB) at room temperature (RT) in the dark. PCB was made up of the following ingredients per litre; 5 g yeast extract, 10 g tryptone, 2 g glucose (adjusted to pH 7 with 1 M KOH). To prepare *T. tropicalis* for feeding experiments with *L. pneumophila*, the ciliates were gradually transferred into Tris-Buffered Osterhout's Solution (TBOS). TBOS was prepared from 100× stock solutions. 100× TBOS was made up of the following ingredients per litre: 10.5 g NaCl, 0.23 g KCl, 0.1 g $CaCl_2$, 0.4 g $MgSO_4$, 0.85 g $MgCl_2$. After diluting from the 100× stock, the pH of the medium was adjusted to 7 by the addition of 0.121 g of Tris base. TBOS was then sterilized either by autoclaving or filter sterilization.

In preparation for feeding experiments with legionellae, *T. tropicalis* ciliates were grown in PCB and then were gradually transferred into increasing concentrations of modified Tris-Buffered Osterhout's solution, pH 7 (TBOS). Ciliates were pelleted by centrifugation at 500 × *g* for 10 min at room temperature using a Universal 32R centrifuge (Hettich, Concord, Ontario), and then resuspended into PCB-to-TBOS transitions of 75% PCB/25% TBOS, 50% PCB/50% TBOS, and 25% PCB/75% TBOS, with the bacteria-ciliate mixture kept in the dark for 10 minutes in between centrifugations. Ciliates were eventually transferred into 100% TBOS, fixed with Lugol's iodine for 5 min, counted by direct microscopy using a Fuchs-Rosenthal hemocytometer (Bright Line), which is twice as deep as the Neubauer hemocytometer. Ciliates were added to 6-well plates (Falcon-BD Biosciences Canada, Mississauga, ON) at 5×10^4 ciliates/ml and kept overnight in 100% TBOS before infection with legionellae. Plate-grown *L. pneumophila* cells were scraped from BCYE agar plates, washed and

resuspended in TBOS to an OD_{620} of 1 unit ($1.9 \pm 0.98 \times 10^9$ legionellae/ml), and added to the enumerated ciliates to reach a final bacteria:ciliate ratio of 1000:1. The ciliate-bacteria mixture was incubated for 24-48 hours at room temperature and the resulting pellets of MIFs were then purified.

2.2.3. Culture and infection of mammalian cell lines

2.2.3.1. Human U937 and THP-1 cells

Human U937 cells (a gift from Dr. Andrew Issekutz, Dalhousie University) and THP-1 derived macrophages (a gift from Dr. Robert Anderson, Dalhousie University) were routinely cultured in 25-cm^2 flasks (Falcon-BD Biosciences Canada, Mississauga, ON), as a suspension of undifferentiated cells, in complete RPMI-1640 medium (Gibco-Invitrogen Grand Island, NY) supplemented with 10% fetal bovine serum (FBS) (Gibco), 2 mM L-glutamine (Gibco), 100 U/ml penicillin, and 100 μg/ml streptomycin, and incubated at 37°C in a humid incubator in the presence of 5% CO_2.

U937 or THP-1 cells in suspension were washed with RPMI-1640 medium, resuspended in complete RPMI-1640, and enumerated in a Neubauer hemocytometer (Bright Line) by direct microscopy. To prepare U937 and THP-1 cells for infection with legionellae, they were induced to differentiate into adherent, macrophage-like cells using phorbol 12-myristate 13-acetate (PMA, sigma) by activation of mitogen-activated protein kinase (MAPK) (Chi Dug Kang et al., 1996).

Macrophages in suspension were counted by direct microscopy in a Neubauer hemocytometer, pelleted and resuspended in complete RPMI-1640 medium containing 60 ng/ml phorbol-12-myristate 13-acetate (PMA, Sigma), and transferred to 25-cm^2 flasks, (Falcon-BD Biosciences Canada, Mississauga, ON) at $9 \times 10^5 – 1.5 \times 10^6$ cells per flask. Plate-grown *L. pneumophila* cells were washed, resuspended in PBS to an OD_{620} of 1 unit ($1.9 \pm 0.98 \times 10^9$ legionellae/ml), and then added to the enumerated U937 or THP-1 monolayers to a final bacteria:cell ratio of 50:1. Flasks were then centrifuged at $500 \times g$ for 10 min at room temperature, using a Universal 32R centrifuge (Hettich, Concord, Ontario), to maximize the contact of bacteria with the monolayers, and then incubated for 3 hours at 37° C in 5% CO_2, to allow the infection to proceed. Monolayers were then

washed and incubated in RPMI-1640 medium supplemented with 10% FBS and 2 mM glutamine, but without antibiotics. Infection was allowed to proceed for 3 days at 37 ^{o} C, and the resulting MIFs were then purified.

2.2.3.2. Mouse L929 cells

Mouse L929 cells were routinely grown at 37^{o}C with 5% CO_2 in 25-cm^2 flasks (Falcon-BD Biosciences Canada, Mississauga, ON) containing minimal essential medium (MEM) (Gibco) supplemented with 10 % fetal bovine serum (FBS), 100 U/ml penicillin, 100 μg/ml streptomycin. In preparation for infection assays, L929 cells were detached by trypsinization using trypsin-EDTA (0.25% trypsin, 0.1% EDTA), suspended in complete MEM and enumerated by direct microscopy. Then, L929 cells were transferred to 24-well plates at about 5×10^5 cells/well, and allowed to attach and form a monolayer overnight at 37^{o}C.

2.2.3.3. Human HeLa cells

HeLa cells were routinely cultured at 37^{o}C with 5% CO_2 in 25-cm^2 flasks (Falcon-BD Biosciences Canada, Mississauga, ON) containing minimal essential medium (MEM) (Gibco) supplemented with 10 % newborn calf serum (NCS), 100 U/ml penicillin, 100 μg/ml streptomycin (Garduno et al., 1998). Monolayers of HeLa cells were grown until confluent and then removed from the flasks by trypsinization using trypsin-EDTA (0.25% trypsin, 0.1% EDTA). Cells were counted using a Neubauer hemocytometer (Bright Line) and seeded into 75-cm^2 flasks at about 10^6 cells/flask, and allowed to attach and form a monolayer overnight at 37^{o}C. HeLa cells were then infected with *L. pneumophila* using an inoculum of 10^8 plate-grown legionellae in about 1 ml of MEM, following the basic steps described above for macrophages. All infections were monitored using THY-100 inverted microscope (Olympus Canada) until host cell lysis and (or) free legionellae-containing vacuoles were clearly observed.

2.3. Purification of *L. pneumophila* progenies from infected host cells

2.3.1. Purification of *L. pneumophila* progenies from infected cells

The bacterial progenies of *L. pneumophila* produced in *A. castellanii*, HeLa, U937 or THP-1 cells were purified from the lysates of infected cells by high-speed centrifugation in a density gradient of Percoll as previously described (Garduno *et al.*, 1998). Supernatants of wasted cultures of infected cells, containing released MIFs together with host cell debris, were centrifuged at 4020 × *g* for 10 min using a Universal 32R centrifuge (Hettich, Concord, Ontario), and the resulting pellet was resuspended in 1 ml of 0.05% Triton-X 100 in sterile ddH_2O, and vortexed for 1 min at maximum speed (16060 × *g*), using a Heraeus Biofuge Pico centrifuge, to release any remaining intracellular bacteria. The resulting suspension was mixed with 5 ml of MEM and 3 ml of isotonic Percoll, placed in a 9-ml high-speed polycarbonate centrifuge tube, and centrifuged at 20,000 × *g* for 10 min, no brakes at 4°C using an Avanti J-E centrifuge (Beckman Coulter, California, USA). The self-forming density gradient typically yielded two bands. The top band (1.051 to 1.061 *g*/ml) contained mainly cell debris, and the bottom band (~1.074 *g*/ml) contained free MIFs. MIFs recovered from the bottom band were washed twice, by centrifugation, in ddH_2O to remove any residual Percoll and then examined by light microscopy.

2.3.2. Isolation and mechanical disruption of legionellae-laden pellets

The ciliate-bacteria mixture was centrifuged at 500 × *g* for 10 min in 15-ml conical centrifuge tubes (Falcon). Live ciliates were then allowed to swim back into suspension before removing the supernatant. This operation was repeated three times. Alternatively, the ciliate-bacteria mixture was allowed to stand overnight in 15 ml Falcon tubes at room temperature until two layers were visible. Most of the pellets sank down to the bottom layer while *T. tropicalis* ciliates were present in the top layer. The upper layer was discarded and the bottom layer was pelleted at 500 × *g* for 10 min at room temperature to collect the pellets, resuspended in Osterhout's solution, and then examined by light microscopy. To release the legionellae contained inside the pellets, pellets were mechanically sheared by repeatedly passing a very dense suspension of pellets between two 1 ml insulin syringes, with a gauge 22 needle connected to a gauge 27 needle, at least 30 times (Berk & Garduno, 2013).

2.4. Characterization of *L. pneumophila* progenies from infected cells

2.4.1. Transmission electron microscopy (TEM)

Samples of Percoll-purified *L. pneumophila* progeny from the various infected cells or ciliate-produced pellets were fixed in 2.5% glutaraldehyde in 0.1 M cacodylate buffer, postfixed in 1% osmium tetroxide in ddH_2O, in-bloc stained with aqueous uranyl acetate, dehydrated in increasing concentrations of acetone, infiltrated in epoxy resin, hardened, and ultrathin sectioned as previously described (Faulkner & Garduno, 2002). Thin sections post-stained with uranyl acetate and lead citrate were observed in a JEOL JEM-1230 transmission electron microscope using an accelerating voltage of 80 kV. Images were captured digitally (as TIFF files) with an Hamamatsu ORCA-HR high resolution (2K by 2K) camera (Hamamatsu Photonics, Hamamatsu, Japan). To quantify the proportion of bacterial cells showing the typical ultrastructural features of MIFs (Faulkner & Garduno, 2002), multiple sections from each sample were observed and random areas from each section were photographed. At least 100 sectioned bacterial cells per sample were examined for the presence of 3 typical ultrastructural features of MIFs (Faulkner & Garduno, 2002): inconspicuous periplasm, straight and thickened outer membrane and presence of large inclusions. The statistical significance of differences in the proportion of MIFs among samples was calculated using the two-proportion test.

2.4.2. Stress-resistance assays

Survival following exposure to antimicrobial agents was determined through CFU/ml counts (by dilution-plating) performed before and after exposure to each agent. For antibiotic challenges, legionellae were suspended in MEM (Gibco) containing different concentrations of gentamicin (5, 20 or 100 µg/ml) or ciprofloxacin (25 µg/ml) for 3 hours. For chlorine challenges, legionellae were suspended in sterile ddH_2O containing 1 or 5 ppm of chlorine for 30 minutes. All challenges were done using a bacterial cell suspension adjusted to an optical density (OD_{620}) of 0.1 units and incubated at 37°C. CFUs were counted after incubation of agar plates for 3 to 5 days at 37°C, and results were reported as percent survival in relation to the initial number of CFU/ml (time zero counts = 100% before challenges).

Susceptibility to lysis in sodium dodecyl sulphate (SDS) (10 mg/ml in 10 mM Tris, pH 7.5) was tested by making legionellae suspensions with an OD_{620} of 1 unit ($1.9 \pm 0.98 \times 10^9$ legionellae/ml) and measuring the optical density at regular intervals. A graph of OD_{620} versus time (lysis curve) was made and the minutes required for each suspension to reach one-half of the initial OD_{620} was reported as the detergent lysis index.

2.4.3. Intracellular growth experiments

U937-derived macrophages, *A. castellanii*, and L929 cells were seeded in 24-well plates (Falcon-BD Biosciences Canada, Mississauga, ON) at about 5×10^5 cells/well. Purified *L. pneumophila* progeny produced in either *A. castellanii* trophozoites or U937-derived macrophages were added to fresh monolayers of U937-derived human macrophages, *A. castellanii* trophozoites, and L929 cells to reach a bacteria:cell ratio of 50:1, 10:1, and 10:1, respectively. The inoculated plates were centrifuged at 500 × *g* for 10 minutes at room temperature, using a Universal 32R centrifuge (Hettich, Concord, Ontario), to promote initial bacterial contact with the monolayers. Following a 3-hour incubation at 37°C in a humid incubator at 5% CO_2, monolayers were washed vigorously three times with PBS to remove free bacteria. Monolayers were then examined by light microscopy to make sure that the integrity of the monolayer was not compromised. This was considered the zero time for intracellular growth. Since early results demonstrated that the progeny produced in amoeba could have a potential advantage in a gentamicin challenge, the gentamicin treatment used to kill extracellular bacteria was omitted from the infection protocol. At 24 and 48 hours post-infection, 3 wells per sample of infected cells were processed for CFU enumeration by lysing the host cells and dilution-plating of the lysates. Monolayers of U937 macrophages and L929 cells were lysed in 1 ml of ddH_2O, and amoebae monolayers were lysed in 1 ml of ddH_2O containing 0.05% Triton X-100. Results were reported as means ± standard deviations of three independent experiments, each run in triplicate, and the analysis of statistical significance was done using the 2-way ANOVA test.

2.4.4. Attachment experiments

For the attachment-only experiment, the same infection protocol described in section (2.4.3.) was followed, but the experiment was stopped at the time zero point (after 3-hour incubation with the bacterial inoculum and the 3 washes to remove free bacteria). Three wells were processed per sample by lysing the host cell monolayers and dilution-plating the lysates as described above. Results were reported and data were analysed as described before in section (2.4.3.).

2.4.5. Competition assays

The progeny of *L. pneumophila* strain JR32 produced in both amoebae (carrying pMMB207-Km14-GFPc plasmid that constitutively expresses GFP) and U937-derived macrophages (carrying pSW001 plasmid that constitutively expresses dsRed-Express) were tested (Mampel *et al.*, 2006). MIFs produced in both hosts were assayed in direct competition for their ability to infect monolayers of *A. castellanii* trophozoites and U937-derived human macrophages. For the competition assay, trophozoites and PMA-activated macrophages were first added to 12-well plates (Falcon-BD Biosciences Canada, Mississauga, ON) at ~ 10^6 cells/well and allowed to form monolayers overnight. To prepare the bacterial inocula, MIFs were purified from either *A. castellanii* trophozoites or U937 macrophages in Percoll gradients as previously described in section (2.3.4), standardized by adjusting their OD_{620} to 1 unit, mixed in equal proportion (1 part of green-fluorescent MIFs from amoeba and 1 part of red-fluorescent MIFs from macrophages), and added to reach a final bacteria:cell ratio of 10:1 for trophozoites, and 50:1 for macrophages. Infections were performed as above (section 2.4.3). Prior to lysing the infected cells at the indicated time points, fluorescence images were captured from random fields of each well in a THY-100 inverted microscope (Olympus Canada) using an Evolution QEI digital video camera (Media Cybernetics Inc.). Fluorescence was measured using 485 nm excitation and a 510 nm emission spectrum for GFP and 554 nm excitation and 586 nm emission spectrum for DsRed-Express. The number of cells infected by MIFs produced in amoebae (showing green fluorescence) or by MIFs produced in U937 macrophage-like cells (showing red fluorescence), as well as cells with a mixed infection (combined red and green fluorescence) or non-infected cells (not

fluorescent) were scored using the Image Pro Plus image analysis software (Media Cybernetics Inc). The percentages of each type of cells were calculated, and results were shown as mean ± standard deviation from three independent experiments, each run in triplicate. After cells were lysed at the indicated time points, CFU counts were performed by dilution-plating on BCYE agar supplemented with 5 μg/ml chloramphenicol (for total counts of JR32 carrying pMMB207-Km14-GFPc or pSW001), or 25 μg/ml kanamycin (for selection of JR32 carrying pMMB207-Km14-GFPc). Results were shown as mean ± standard deviations of CFU/well from three independent experiments, each run in triplicate. The analysis of statistical significance was done using the 2-way ANOVA test.

2.4.6. Plaque assays

A plaque assay was performed as originally described (Fernandez *et al.*, 1989), except the gentamicin treatment step was omitted. Mouse L929 cells were grown and maintained in MEM as previously described (section 2.2.3.2.). Approximately 5×10^5 cells were added to each well of a 24-well tissue-culture plate (Falcon-BD Biosciences Canada, Mississauga, ON). Plates were then incubated overnight until confluent monolayers were formed. Monolayers were washed six times with PBS to remove the antibiotics in the infection medium. Plate-grown *L. pneumophila* cells were harvested, standardized to an OD_{620} of 0.5 in PBS, and then serially diluted 10-fold in 900 μl of MEM supplemented with 10% FBS, without antibiotics. Immediately after removing the culture medium from L929 monolayers, 400 μl of each dilution (six per strain) were added to duplicate wells. Plates were then subjected to centrifugation (500 × *g*, 10 minutes, room temperature) and incubated for 90 min at 37°C in a CO_2 incubator adjusted to 5% CO_2. Monolayers were washed six times with PBS before the addition of 1 ml of 0.6% agarose in MEM supplemented with 10% FBS, 2 mM glutamine, and 0.225% sodium bicarbonate. Cells were then incubated for 4-5 days at 37°C in a humid incubator in presence of 5% CO_2.

To determine the viable count of each inoculum (cfu/ml), 50 μl of each serial dilution were spread on BCYE plates (cfu/ml). After four days, each monolayer was fixed using 1 ml 4% formaldehyde in PBS and then incubated for 24 hours at room

temperature. PBS/formaldehyde solution was removed, agarose plugs were carefully removed with a spatula, and the monolayers were stained for 20 min with 1% crystal violet in 20% ethanol. Excess stain was removed by washing the wells gently with ddH_2O, and the plates were left for 10 min to air dry. Plaques in the monolayer were counted and plaquing efficiency was calculated according to the formula: plaquing efficiency = (number of plaques formed / viable count of the corresponding inoculum) × 100.

2.4.7. Sodium dodecyl sulphate-polyacrylamide gel electrophoresis (SDS-PAGE)

L. pneumophila Lp1-Svir progeny produced in *A. castellanii* trophozoites or U937-derived human macrophages were centrifuged at 16060 × *g* for 2 min and the pelleted cells were mechanically lysed (via bead beating) with 100-µm diameter zirconia/silica beads (BioSpec Products) at 4800 rpm for 45 seconds using a mini-bead beater (BioSpec Products, Bartlesville, OK USA). The whole cell lysate supernatant (100 µl) was then mixed with 100 µl of 2× sample buffer containing 5-10 % β-mercaptoethanol and placed in boiling water for 5 min. The solubilized proteins were then separated in a 12% acrylamide gel using a Protean-II vertical slab gel apparatus (Bio-rad). Electrophoresis was performed at 10 mA/stacking gel and 20 mA/separating gel in 1× running buffer. Running buffer was prepared from 10X stocks, which contained the following ingredients per litre: 30.27 g Tris, 144.15 g glycine, 10 g SDS.

Coomassie staining was performed to visualize the separated protein bands as follows: gels were submerged in Coomassie stain (0.25 % w/v Coomassie Brilliant Blue R-250 in 50 % [v/v] methanol and 10 % [v/v] acetic acid) for 1 hour, destained in destaining solution I (50% [v/v] methanol, 10 % [v/v] acetic acid) for 1 hour, then destained in destain solution II (5 % [v/v] methanol, 7 % [v/v] acetic acid) for 1 hour, and finally washed in ddH_2O for 20 min. All incubations were done with gentle agitation using a VWR rocking platform-model 200 (Marshall Scientific, NH, USA).

Silver staining of protein gels was done as previously described by Blum et al. (Blum et al., 1987), conducting all incubations with gentle agitation using a VWR rocking platform-model 200 (Marshall Scientific, NH, USA). Briefly, gels were fixed overnight at 4°C in a 50 % (v/v) methanol, 10 % (v/v) acetic acid solution. Following

overnight incubation, gels were immersed in 50% methanol solution for 15 min, and washed 5×5 min each in ddH_2O. Gels were sensitized with 0.2 g/L sodium thiosulfate for 1 min, followed by 2×1 min washes in ddH_2O, and then immersed in a freshly-prepared and chilled 2 g/L silver nitrate solution for 25 min. Gels were developed with a freshly-prepared developing solution of 3% sodium carbonate, 0.025% formalin until the desired staining intensity was achieved. Stain development was stopped by the addition of 14 g/L EDTA sodium salt for 10 min, and then washed 2×1 min with ddH_2O.

Stained protein gels were scanned wet in an EPSON ES-1200C scanner equipped with a transparency unit EU-13 (Seiko Epson Co., Nagano, Japan) to produce digital TIFF images. Bands that were consistently unique to the lanes of MIFs produced in amoebae (from at least 3 independent protein extractions) were cut out from the gels with a sharp scalpel blade (a new blade was used for each band) and sent to the Mass Spectrometry and Proteomics core facility at Dalhousie University for standard protein identification (which involved digestion with trypsin, separation of tryptic peptides by HPLC, and an MS-MS tandem analysis of the separated peptides).

2.5. Molecular techniques

2.5.1. Isolation of *L. pneumophila* genomic DNA

Genomic DNA was isolated from *L. pneumophila* grown overnight in BYE broth at 37°C with agitation (200 rpm) in a New Brunswick C25KC shaker incubator. Bacterial cells were pelleted by centrifugation at 4,020 × *g* at room temperature for 6 min, using a Universal 32R centrifuge (Hettich, Concord, Ontario), and resuspended in 600 µl of Tris-EDTA (TE) buffer (10 mM Tris-HCl pH 7.6 and 1 mM EDTA pH 8). Six µl of 10% SDS and 1.3 µl of 30 mg/ml ribonuclease (RNase) (Sigma) were added, and samples were then mixed and incubated at 37°C for 30 min. Proteinase K (Fermentas) (8 µl) (10 mg/mL in 50 mM Tris-HCl pH 8.0 and 1 mM $CaCl_2$) was added followed by incubation of the samples at 50-55°C for 45 min. The mixture was extracted 2-3 times with phenol/chloroform 1:1 (v/v) and then extracted with chloroform. Between each extraction step, samples were subjected to centrifugation (15,000 × *g*, 10 min, 4°C) and the top aqueous layers were transferred to clean microcentrifuge tubes. The extracted genomic

DNA was precipitated with 0.1 volumes of 5 M sodium chloride and 2 volumes of 95% ethanol and then kept overnight at -20°C. Precipitated DNA was washed with ice-cold 70% ethanol, and air dried (for ~ 10 min) and then resuspended in 100 µl molecular-grade H_2O, and quantified by measuring the absorbance at 260 nm (A_{260}) using UNICO UV-2100 spectrophotometer (Dayton, NJ). DNA samples were then kept at -20°C until used. All centrifugation steps were carried out using a Heraeus Biofuge Pico centrifuge set at the highest speed (16060 × *g*). The quality of the isolated DNA was assessed by measuring the A_{260}:A_{280} ratio (DNA samples with a ratio of 1.8-2 were used in further experiments) and by using the isolated DNA as a template to amplify DNA fragments through PCR reactions.

2.5.2. Isolation of *L. pneumophila* RNA

RNA isolation was performed as previously described (Sahr *et al.*, 2009). All reagents were prepared using molecular grade (DNase-free, RNase-free) water or using DEPC (diethyl pyrocarbonate)-treated water. Fresh gloves were also worn to avoid contamination of the reaction mixtures with RNase enzyme. RNA was isolated from *L. pneumophila* grown in BYE broth to exponential (OD_{620} 1.1) and post-exponential (OD_{620} 2.5-3) phases, *L. pneumophila* obtained 8 hours (mainly replicative forms) and 3 days (the final progeny from infected amoebae) following infection of *A. castellanii* monolayers, *L. pneumophila* obtained 3 days after infection of human U937-derived macrophage monolayers (the final progeny from infected macrophages), *L. pneumophila* obtained 30 minutes after feeding of *Tetrahymena* ciliates, and *L. pneumophila* stationary phase forms (SPFs) grown in BYE broth and then transferred to TBOS for 30 min. Briefly, all samples were pelleted by centrifugation at 16060 × *g* for 2 min. Pellets of *L. pneumophila* cells were then resuspended in a resuspension solution (1 part 20% glucose + 1 part 25 mM Tris), EDTA (0.5 M) and mechanically lysed by beating twice with 100-µm diameter zirconia/silica beads (BioSpec Products) at 4800 rpm for 50 seconds at 4°C using a mini-bead beater (BioSpec Products, Bartlesville, OK USA). Samples were placed on ice between beatings. Following beating, RNA was extracted in trizol (Gibco), and then a series of chloroform/isoamyl alcohol (24:1) purification steps were conducted as previously described (Sahr *et al.*, 2009). Isopropanol was added to the supernatants

containing nucleic acids and samples were kept overnight at -20°C. RNA-containing pellets were then washed with 70% ethanol and allowed to dry for about 10 min at room temperature and were resuspended in 50 µl of molecular-grade water.

To increase the concentration of the isolated RNA, an optional part of the protocol was carried out. Anhydrous ethanol (150 µl) and sodium acetate (3 M, pH 5.2) (5 µl) were added to each sample and samples were kept overnight at -20°C. Samples were washed in ice-cold 70% ethanol. RNA pellets were allowed to dry and were resuspended in 50 µl of molecular grade water. All centrifugation steps were carried out at 4°C using a Heraeus Biofuge Pico microcentrifuge at the highest speed (16060 × *g*). The quality of the isolated RNA was assessed by measuring the A_{260}:A_{280} ratio (RNA samples with a ratio of 1.8-2 were used in further experiments) and by running an aliquot on a 2% agarose gel.

2.5.3. Polymerase chain reaction (PCR)

PCR amplifications were performed in a T-personal thermal cycler (Biometra, Germany) using *Taq* DNA polymerase (New England Biolabs) or Platinum *Pfx* DNA polymerase (Invitrogen) according to the manufacturer's instructions. For PCR reactions using *Taq* DNA polymerase, the following standard conditions were used unless otherwise indicated: 94°C (5 min), followed by 30 cycles of 94°C (30 sec), 55°C (30 sec), and 72°C (for 1 min per kb of the PCR amplification product), and a final extension step at 72°C for 10 min. For PCR reactions using *Pfx* DNA polymerase, the following standard conditions were used unless otherwise indicated: 94°C (5min), followed by 30 cycles of 94°C (15 sec), 55°C (30 sec), and 68°C (for 1 min per kb of the PCR amplification product) and a final extension step at 68°C for 10 min. Primers used for PCR experiments (Table 3) were designed using NCBI Primer-BLAST program (http://www.ncbi.nlm.nih.gov/tools/primer-blast/index.cgi?ORGANISM=9606&INPUT_SEQUENCE=NM_001618.3&log$=seqvies_box_primer) or PrimerQuest program (http://www.idtdna.com/Scitools/Applications/Primerquest/).

All primers were synthesized commercially by Integrated DNA Technologies, Inc. (Coralville, IA). PCR primers were reconstituted in 10 mM concentration using molecular-grade water, and then used for PCR experiments.

2.5.4. Agarose gel electrophoresis

Electrophoresis of DNA was performed using 1% and 2% agarose gels in 1× Tris acetate EDTA (TAE) buffer. TAE buffer was diluted from a 50× stock solution, which were made up of the following ingredients per litre: (242 g Tris base, 57 ml glacial acetic acid, and 100 ml 0.5 M EDTA pH 8). Loading buffer (MBI Fermentas) was added to DNA samples prior to loading into the wells of agarose gels containing 1 µg/ml ethidium bromide. Electrophoresis of the DNA samples was conducted at a constant voltage of 100 V. DNA bands were visualized using the VersaDoc™ Imaging system (Bio-Rad). One kilobase (kb) (MBI Fermentas) or 100 base pair (bp) (New England Biolabs) DNA ladders were used as band-size references. Whenever necessary, DNA bands of interest were excised from the gels using one clean scalpel blade for each band and purified using a gel extraction protocol (see section 2.5.6.).

2.5.5. Restriction endonuclease digestion

Digestion was performed in 25 µl reactions according to instructions provided by the manufacturer of the restriction enzymes used (New England Biolabs). Unless otherwise indicated, restriction digests were generally incubated at 37°C for 2 hours in a reaction consisting of approximately 1 µg of substrate DNA, the appropriate digestion NEB buffer, bovine serum albumin (BSA), and the recommended units (U) of restriction enzyme(s).

2.5.6. Plasmid and DNA purification

Bacterial plasmids used in my thesis project are described in Table 2.2.

Plasmid purification from *E. coli* DH5α or *L. pneumophila* JR32 was performed using the QIAprep Spin Miniprep kit (QIAGEN, Mississauga, Ontario, Canada). Isolation of the digested plasmids or DNA fragments from agarose gels was carried out with a QIAquick Gel Extraction kit (QIAGEN). Digested DNA fragments of low concentrations were purified using the QIAquick PCR Purification kit (QIAGEN). All kits were used according to the manufacturer's detailed instructions (QIAGEN). Constructed plasmids were sent to Genome Québec (McGill University, Québec, Canada) to be verified by DNA sequencing.

Table 2.2. Plasmids used in this study

Plasmid	Selection marker(s)	Characteristics	Reference
pMMB207-Km14-GFPc	Amp^R, Cm^R, Kan^R	pMMB207C derivative, constitutively expressing GFP	(Mampel *et al.*, 2006)
pSW001	Amp^R, Cm^R	pMMB207C derivative, constitutively expressing Ds-Red	(Mampel *et al.*, 2006)
pBluescript II KS	Amp^R	High-copy plasmid used as a general cloning vector in *E. coli*	Stratagene
pBSΔ*amyA*	Amp^R	pBluescript II KS derivative containing the upstream anddownstream fragments of *lpg1669* (*amyA*)	This study
pBSΔ*amyA*::km	Amp^R, Kan^R,	pBluescript II KS derivative containing the upstream anddownstream fragments of *lpg1669* (*amyA*) and a kanamycin resistance cassette	This study
pBRDX	Cm^R	Counterselectable delivery vector with *B. subtilis sacB* (conferring sensitivity to sucrose) and *H. pylori rdxA* (conferring resistance to metronidazole), chloramphenicol acetyltransferase (conferring resistance to chloramphenicol)	(Brassinga *et al.*, 2006)
pBRDXΔ*amyA*:km	Cm^R,kan^R	Counterselectable delivery vector for allelic replacement of *amyA* gene	This study
pMMB207C	Amp^R,Cm^R	RSF1010 (IncQ, lacIq, Ptac, oriT) derivative with ΔmobA and the Ptac IPTG-inducible promoter.	(Chen *et al.*, 2004)
pMMB::*amyA*	Amp^R,Cm^R	pMMB207C derivative carrying *amyA* under the control of its natural promoter P_{amyA}	This study
pMMB::*amyA*-His_6	Amp^R,Cm^R	pMMB207C derivative carrying *amyA-His*$_6$ under the control of its natural promoter P_{amyA}	This study

2.5.7. DNA ligation

DNA ligation reactions containing an insert:vector ratio of 3:1 were performed using T_4 DNA ligase enzyme (New England Biolabs / Fermentas) at 16°C overnight. Ligation mixtures consisted of the appropriate amounts of insert and vector DNA, 1 µl of T_4 DNA ligase, 1 µl of 10× T_4 DNA ligase buffer (New England Biolabs / Fermentas) in a final volume of 10 µl.

2.5.8. Preparation of electrocompetent *E. coli* DH5α cells

E. coli strain DH5α was grown in 10 ml of LB broth overnight at 37°C with agitation (200 rpm). Bacterial cultures were diluted 1:20 into pre-warmed LB broth and grown to an OD_{600} of 0.4-0.6. Bacterial cells were then harvested by centrifugation (3,000 × *g*, 15 min, 4°C) using a Universal 32R centrifuge (Hettich, Concord, Ontario). The cells were washed twice with 50 ml of ice-cold sterile ddH_2O, resuspended twice with 50 ml of ice-cold 10% glycerol, and finally resuspended in 2 ml of cold 10 % glycerol. Electrocompetent *E. coli* DH5α cells were dispensed in 40 µl aliquots into pre-chilled eppendorf tubes and then kept at -80°C until used.

2.5.9. Preparation of electrocompetent *L. pneumophila* cells

L. pneumophila cells grown on BCYE agar were suspended in 100 µl of sterile ddH_2O and spread on BCYE plates and incubated overnight to let them form a thin lawn. The overnight lawns were harvested into 15 ml of ice-cold sterile ddH_2O and centrifuged at 3000 × *g* for 10 min at 4°C. The pelleted cells were then resuspended in 20 ml of ice-cold 10% glycerol, washed twice in 10 ml of ice-cold 10 % glycerol, and finally resuspended in 2 ml of ice-cold 10% glycerol. Electrocompetent *L. pneumophila* cells were dispensed in 40 µl aliquots into pre-chilled eppendorf tubes and kept at -80°C until further use.

2.5.10. Bacterial transformation by electroporation

Electrocompetent *E. coli* DH5α cells (maintained at -80°C) were allowed to thaw on ice. About 1 µL of plasmid DNA in molecular-grade water (~ 1 µg/µl) was added to the thawed cells and incubated on ice for ~ 5 min. The DNA-cell mixture (4 µl) was

transferred to a pre-chilled 2 mm gap electroporation cuvette (Fisher), and electroporated at 2.5 kilovolts (kV) for 0.005 sec using a MicroPulser® (BIO-RAD laboratories Inc.). The entire content of the electroporation cuvette was then transferred to 1 ml of pre-warmed LB broth and incubated at 37°C for ~ 1 hour with gentle agitation (150 rpm), before plating (see below) on selective medium for selection of transformants.

Electrocompetent *L. pneumophila* JR32 cells (maintained at -80°C) were transformed by electroporation as previously described (Viswanathan and Cianciotto, 2001). Briefly, about 1 µg of plasmid DNA (~ 1 µg/µl) was added to thawed electrocompetent *L. pneumophila* cells and incubated on ice for ~ 5 min. The DNA-cell mixture (40 µl) was transferred to a pre-chilled 2 mm gap electroporation cuvette (Fischer), and electroporated at 2.1 kV for 0.005 sec using a MicroPulser® (BIO-RAD laboratories Inc.). The entire content of the electroporation cuvette was then transferred to 1 ml of pre-warmed BYE broth and incubated at 37°C for up to 3 hours with gentle agitation (100 rpm) before plating (see below) on selective medium for selection of transformants.

Different volumes (50 µl, 100 µl, and the remaining volume) of the electroporated cells were then plated onto LB agar (for *E. coli* DH5α) or BCYE agar (for *L. pneumophila*) plates supplemented with the appropriate antibiotic selection. The plates were incubated at 37°C for up to 2 days (for E. coli DH5α) or up to 5 days (for *L. pneumophila*). For every electroporation experiment, positive growth controls (electroporated cells grown on plain medium without antibiotic selection), and negative growth controls (electrocompetent cells grown on medium supplemented with antibiotic selection) were included.

2.6. Transcriptome analysis of *L. pneumophila* inside different hosts

2.6.1. Analysis of the genetic expression of *L. pneumophila* in different hosts

The global changes in gene expression of *L. pneumophila* at different time points inside amoebae (Bruggemann *et al.*, 2006) and human macrophages (Faucher *et al.*, 2011) have been previously published. The changes in gene expression of *L. pneumophila* between 8 hours (replicative traits) and 14 hours (late transmissive traits)

inside amoebae were compared to the changes in gene expression of *L. pneumophila* at 18 hours (transmissive traits) and time zero inside human macrophages to examine whether *L. pneumophila* induces specific sets of genes in different hosts. The microarray analysis of the global changes in gene expression of *L. pneumophila* following 30 minutes of ingestion by *T. tropicalis* ciliates compared to the *in vitro* SPFs was obtained through personal communication with David Allan, Dr. Celia Lima and Dr. Rafael Garduño. Briefly, the microarray slides contained gene-specific 70-mer oligonucleotides based on all predicted genes of the genome of *L. pneumophila* strain Paris (CR628336) and its plasmid (CR628338) as previously described (Bruggemann *et al.*, 2006). Hybridizations were performed following the manufacturer's recommendations (Corning) using 250 pmol of Cy3- and Cy5-labeled cDNA. Slides were scanned on a GenePix 4000A scanner (Axon Instruments), and the laser power and photomultiplier tube (PMT) were adjusted to balance the two channels. The resulting files were analyzed using Genepix Pro version 5.0 software. The statistics and curation of the data following 30 minutes of ingestion by *Tetrahymena tropicalis* ciliates compared to the *in vitro*-grown SPFs were performed by David Allan (Dalhousie University) Dr. Tobias Sahr (Institut Pasteur, Paris, France) as reported in previous transcriptome analyses of *L. pneumophila* in the Buchreiser lab (Institut Pasteur, Paris, France) (Bruggemann *et al.*, 2006; Albert-Weissenberger *et al.*, 2010; Edwards *et al.*, 2010; Edwards *et al.*, 2013). The initial list of the upregulated and downregulated genes was assembled by David Allan in the Garduno lab (Dalhousie University).

2.6.2. Confirmation of microarray data by qRT-PCR

2.6.2.1. RNA isolation and concentration calculation

RNA was isolated as described above (section 2.5.2.). Purity of the isolated RNA was determined by recording the absorbance values at 260 nm and 280 nm (A_{260}, A_{280}) using a UNICO UV-2100 spectrophotometer (Dayton, NJ). RNA samples with an A_{260}/A_{280} ratio of at least 1.8 were used for cDNA production. The total RNA concentration was determined using nucleic acid concentration calculator software (http://www.kenkyuu.net/js/nacalc.html). A small aliquot (~ 1 µg) of RNA from each

sample was also run on a 2% agarose gel. RNA bands were stained with 1 µg/ml ethidium bromide and visualized using a VersaDoc™ Imaging system (Bio-Rad).

2.6.2.2. Deoxyribonuclease (DNase) I treatment of RNA

To make sure that RNA samples used for cDNA synthesis were free from genomic DNA, each sample was treated with RNase-free Deoxyribonuclease (DNase) I enzyme according to the manufacturer's instructions (Ambion). Briefly, 1 µl of DNase enzyme (2 U/µl) (Ambion) was used to digest 10 µg of RNA in a total reaction volume of 50 µl. The reaction mixture was incubated at 37°C for 30 min to ensure complete digestion of any contaminating genomic DNA. DNase I was then inactivated by DNase I inactivation reagent (Ambion). Five µl of vortexed DNase I inactivation reagent were added to the reaction, followed by incubation at room temperature for 5 min. The reaction mixture was then centrifuged at 10,000 × *g* for 2 min, and the supernatant, containing DNA-free RNA, was removed carefully. DNase-treated RNA samples were then tested by *Taq* PCR reactions using 1µl of RNA as a template to make sure that no amplification products were formed (meaning that the genomic DNA is completely digested). DNase-treated RNA samples were then kept at -80°C until used.

2.6.2.3. Reverse transcription and cDNA synthesis

cDNA synthesis reactions were performed using M-MLV reverse transcriptase enzyme, according to detailed manufacturer's instructions (Invitrogen). About 1 µg of DNase-I treated RNA was mixed with 1 µl of 1 µg/µl random hexamer primers (Pharmacia) and 1 µl of 10 mM dNTPs in a total volume of 12 µl. The mixture was incubated at 65°C for 5 min. Then, 4 µl of 5× first-strand buffer (Invitrogen) and 2 µl of 0.1 M dithiothreitol (DTT, Invitrogen) were added and the mixture was incubated at 37°C for 2 min. Following incubation, 1 µl of the M-MLV reverse transcriptase enzyme (Invitrogen) (200 U/µl) was added and the mixture was incubated at 25°C for 10 min, 37°C for 70 min, and 70°C for 15 min. All incubations were done in a T-personal thermal cycler (Biometra, Germany). Negative cDNA synthesis controls (1 µl of molecular-grade water was used instead of the reverse transcriptase enzyme) were produced at the same time. To test for the synthesis of cDNA from each RNA sample, *Taq* PCR reactions were

conducted using 1 µl of cDNA as a template and primers that target the promoter region of *lpg2884* (lpg2884F and lpg2884R) and 5s ribosomal DNA (5srDNAF, 5srDNAR) (Table 3). Lp1-SVir genomic DNA was used for positive PCR reaction controls. Negative PCR reaction controls did not include a DNA template, and had 1 µl of molecular grade water instead. Once cDNA synthesis was confirmed, concentrations of the synthesized cDNA samples were determined according to the measured absorbance values at 260 and 280 nm (A_{260}, A_{280} respectively) with a UNICO UV-2100 spectrophotometer (Dayton, NJ) using nucleic acid concentration calculator software (http://www.kenkyuu.net/js/nacalc.html). cDNA samples were kept at -20°C until used.

2.6.2.4. Primer design

Primers used in qRT-PCR experiments (Table 4) were designed using the PrimerQuest program (http://www.idtdna.com/Scitools/Applications/Primerquest/) after selecting the pre-set parameters for real-time PCR primers, such that the amplified products were in the size range of 70–200 bp. All primers were commercially synthesized by Integrated DNA Technologies, Inc. (Coralville, IA). The synthesized primers were reconstituted into a final concentration of 2 mM with molecular-grade water.

2.6.2.5. qRT-PCR reaction conditions

The qRT-PCR reactions were performed using a real-time DNA amplification system, Rotor-Gene 3000 (Corbett Research) according to the GoTaq® qPCR Master Mix protocol (Promega). Quantitative real time-PCR was performed in 20 µl reaction volume, containing 1 µg of cDNA, 10 µl SYBR green master mix (Promega) and 300 nM of gene-specific primers. The qRT-PCR reactions consisted of an initial heating at 95°C for 5 min of 40 cycles of denaturation at 95°C for 45 sec, annealing at 54°C for 30 sec and extension at 72°C for 30 sec. Final dissociation condition was set according to the manufacturer's instructions (Promega). The fluorescence of SYBR green, a dsDNA-binding dye, was detected and measured at set time points throughout the qRT-PCR cycles. The gene *gyrA*, which encodes subunit A of DNA gyrase enzyme, was used as an internal reference transcript in qRT-PCR experiments to quantify the gene expression of *L. pneumophila* grown in BYE broth, *A. castellanii* and U937-derived human

macrophages. The gene *ftsZ*, which encodes the cell division protein FtsZ, was used as an internal control in qRT-PCR experiments to study the gene expression of *L. pneumophila* inside *T. tropicalis* ciliates, since the expression levels of these genes appear to remain constant throughout the developmental cycle of *L. pneumophila*. qRT-PCR experiments involving the internal controls and the tested genes were conducted at the same time. Each gene was tested in triplicate using the cDNA synthesized from RNA isolated from *L. pneumophila* MIFs, RFs, stationary and exponential phase forms.

2.6.2.6. qRT-PCR data analysis

The qRT-PCR data were analyzed using the comparative $\Delta\Delta C_t$ method according to the Rotor-Gene 3000 manufacturer's protocol (Corbett Research). This method enables the relative quantification of the expression levels of the genes of interest relative to the internal references. The gene *gyrA*, which encodes subunit A of DNA gyrase enzyme, was used as the internal control for qRT-PCR experiments involving *L. pneumophila* grown in BYE broth, *A. castellanii* and U937-derived human macrophages. The gene *ftsZ*, which encodes the cell division protein FtsZ, was used as an internal control for qRT-PCR experiments involving feeding of *T. tropicalis* with legionellae. The cycle threshold (C_t) values of the genes of interest and the internal controls were determined using the linear part of the graph for each replicate. The average C_t-value of the 3 replicates of each gene was calculated, and the differences in C_t-values between the genes of interest and the internal controls were calculated, resulting in the ΔC_t-value [ΔC_t= C_t (target gene) - C_t (internal control)]. The differences in ΔC_t between two sample sets (For example, MIFs vs. RFs) were determined to give the $\Delta\Delta C_t$-value. The comparative expression level (fold-change) was calculated as $2^{\Delta\Delta Ct}$.

2.7. Investigation of the role of *lpg1669* in the differentiation of *L. pneumophila*

2.7.1. Construction of an *L. pneumophila* JR32 Δ*lpg1669* (*amyA*) mutant

amyA (*lpg1669*) chromosomal deletion was made by utilizing an in-house gene counterselectable vector (pBRDX) strategy (Morash *et al.*, 2009) in which I created an allelic replacement construct consisting of a kanamycin-resistance cassette flanked by the

upstream and downstream regions of the target gene. Counterselection of pBRDX constructs is achieved through *sacB* (which confers sensitivity to sucrose) and *rdxA* (which confers sensitivity to metronidazole). Therefore, transformants in which allelic double cross-over replacement has occurred can be selected on solid media containing sucrose and metronidazole.

2.7.2. Complementation of the Δ*amyA* mutant

The promoter and the coding sequence of the *amyA* gene were amplified by PCR using the primer pair amyCo-ApaF and amyCo-XbaR. The amplified fragment was then subcloned into the NotI and XhoI sites of the expression vector pMMB207C, creating the pMMB:*amyA* plasmid, where the *amyA* gene was expressed under its natural promoter (P_{amyA}). The constructed complementing plasmid was then electroporated into an *L. pneumophila* JR32 Δ*amyA* mutant.

2.7.3. Construction of a complemented strain that expresses a His_6-tagged AmyA protein

The promoter and the coding sequence of the *amyA* gene were amplified by PCR using the primer pair amyHisFApaI and amyHisRXbaI. Only the *amyA* coding sequence was amplified by PCR using the primer pair amyHisFSacI and amyHisRXbaI. The amplified fragments were then subcloned into the ApaI and XbaI sites or into the SacI and XbaI sites of pMMB207C, creating pMMB::*amyA-His*$_6$ or pMMB-P_{tac}*: amyA-His*$_6$, where the His_6-tagged *amyA* gene was expressed under its natural promoter (P_{amyA}) or under P_{tac} , respectively. The constructed plasmids were then electroporated into an *L. pneumophila* JR32 Δ*amyA* mutant.

2.7.4. Genetic organization of the *lpg1669* locus

amyA (*lpg1669*) gene is surrounded by two genes; *lpg1668*, a gene predicted to run in the same direction, and *lpg1670*, predicted to run in the opposite direction. To investigate whether *lpg1668* and *lpg1669* form an operon, RNA of *L. pneumophila* JR32 was isolated and converted into cDNA as previously described. The synthesized cDNA was then tested by RT-PCR using the primer pair 1668-1669 FWD and 1668-1669 REV,

which target the intergenic region between *lpg1668* and *lpg1669*. Primer pairs 1668QPCRF / 1668QPCRR (which target the internal region of *lpg1668*) and 1669QPCRF / 1669QPCRR (which target the internal region of *lpg1669*) were used in control RT-PCR reactions to ensure the integrity of the synthesized cDNA.

To investigate whether *lpg1670* and *lpg1671* genes are part of the same operon, the synthesized cDNA was tested by RT-PCR analysis using the primer pair 1670-1671 FWD and 1670-1671 REV (which target the intergenic region between *lpg1670* and *lpg1671*) . Primer pairs1670QPCRF / 1670QPCRR (which target the internal region of *lpg1670*) and 1671QPCRF / 1671QPCRR (which target the internal region of *lpg1671*) were used in control RT-PCR reactions to ensure the integrity of the synthesized cDNA.

2.7.5. Protein quantification

Protein quantification was performed according to the manufacturer's microtitre plate protocol (BIO-RAD). A standard curve using protein concentrations ranging from 0.1 to 0.5 mg/ml with 0.1 mg/ml increments was generated by diluting a stock concentration of 10 mg/ml BSA in 10 mM Tris buffer. Protein samples were diluted 1:5, 1:10, and 1:20 in 10 mM Tris buffer. About 200 µl 1:4 protein assay dye reagent was then added to 10 µL of all protein samples in 96-well plate (Falcon-BD Biosciences Canada, Mississauga, ON). The reactions, for both standard and test samples, were allowed to develop for at least 5 minutes at room temperature and then the intensity of the developed colour was measured at 595 nm using a Benchmark-Plus microplate reader (BIO-RAD).

2.7.6. Western blotting

Western blotting was performed following a protocol modified from that originally described by Towbin et al., (Towbin *et al.*, 1979). Protein bands resolved by SDS-PAGE (see section 2.4.7.) were transferred onto nitrocellulose membranes at a constant voltage of 90 V for 90 minutes using a BIO-RAD electrotransfer apparatus (Model Mini-Protean®II) run in a walk-in cold room maintained at 4^{o}C. Transfer buffer was made up of the following ingredients per litre: 0.192 M glycine, 0.025 M Tris, and 20% methanol. The pH of the buffer was adjusted to 8.2-8.3.

Blotted proteins were stained for 5 min with Ponceau S (2 % w/v Ponceau S in 30 % trichloroacetic acid and 30 % sulfosalicylic acid) and were then destained in PBS. Nitrocellulose membranes were then incubated in a blocking solution (1 % [w/v] skim milk, 1 % [w/v] BSA in TTBS [20mM Tris-HCl {pH 7.6}, 500 mM NaCl, 0.05 % {v/v} Tween 20]) for at least 1 hour, and then washed with TTBS for 10 min. The nitrocellulose membranes were incubated with the primary antibody (1:1,000 monoclonal mouse anti-His_6 in TTBS, a gift from Dr. Nikhil Thomas, Dalhousie University) for 1 hour, washed 3×10 min with TTBS, and then incubated with the secondary antibody (1:5,000 alkaline phosphatase-conjugated goat anti-mouse in TTBS) (Cedarlane) for 1 hour. Membranes were then developed in a solution of 10 ml developing buffer (8 ml dH_2O, 1 ml 1 M Tris pH 9.5, 0.5 ml 1.5 M NaCl, 0.5 ml 1 M $MgCl_2$) containing 1.6 mg of 5-bromo-4-chloro-3-indolylphosphate (BCIP, Sigma) and 44 µL of nitroblue tetrazolium (NBT) solution (75 mg/ml NBT in 70 % dimethylformamide) until the desired color intensity was achieved. The developing reaction was stopped by washing in ddH_2O, and the developed blots were then scanned in an EPSON ES-1200C scanner.

2.7.7. Dot-blotting

Dot-blotting was essentially performed as described above for western blots (section 2.7.6.), except that the electrotransfer of protein bands to nitrocellulose membranes is not necessary. Instead, known volumes of protein samples were directly applied to a nitrocellulose membrane and allowed to dry before immunostaining. The pellet and supernatant fractions of BYE cultures of *L. pneumophila* JR32 Δ*amyA* mutants harbouring pMMB::*amyA-His*$_6$ plasmid were used in this experiment as follows.

Bacterial culture (10 ml) of an OD_{620} value of ~ 2.0 was pelleted down and resuspended in 100 µl 2× sample buffer containing β-mercaptoethanol. Samples were boiled for 5 min as described in section (2.4.7.).

Supernatant proteins were precipitated by the addition of trichloroacetic acid (TCA, Gibco) (100 µl TCA for every 900 µl of supernatant). The mixture was incubated on ice for at least 30 min. Precipitated proteins were then pelleted by centrifugation at 16060 × *g* for 10 min at 4°C using Universal 32R centrifuge (Hettich, Concord, Ontario). Ice-cold (at -80°C) acetone was added to the precipitated proteins, and the mixture was

kept overnight at -80°C. Precipitated proteins were air dried (~ 10 min) and then resuspended in 10 mM Tris.

The protein concentrations were determined, as described in section (2.7.5.). The protein samples were set equal in concentration by diluting in 10 mM Tris. About 15µL of each fraction were spotted onto a nitrocellulose membrane and allowed to air dry. The nitrocellulose membrane was then incubated with the primary antibody (1:1,000 monoclonal mouse anti-His_6) and followed by the secondary antibody (1:5,000 alkaline phosphatase-conjugated goat anti-mouse) (Cedarlane) and then developed as previously described for western blots (section 2.7.6.).

2.8. Bioinformatic analysis

DNA sequences of the genes tested in qRT-PCR experiments were obtained from GenBank®, at the National Center for Biotechnology Information (NCBI) website (http://www.ncbi.nlm.nih.gov). The protein sequences of Lpg1669 (AmyA) and the other α-amylases in *Aspergillus oryzae* and *Bacillus subtilis* were obtained using the National Center for Biotechnology Information (NCBI) website. The Genius Pro™ 5.3 (Biomatters Ltd, New Zealand) and BioEdit (http://www.mbio.ncsu.edu/bioedit/bioedit.html) bioinformatics programs were used for AmyA amino acid sequence alignment.

2.9. Statistical analysis

Statistical analysis (ANOVA, two-proportion test, *t* test as indicated in the relevant figure legends) was performed using Minitab software version 16 (Minitab Inc., State College, PA). *P* values less than 0.05 were considered to represent significant differences.

Table 2.3. Primers used in PCR experiments

Primer	Primer sequence (5`- 3`)	Amplicon size (bp)
amyUSF-NotI	GGCGCGGCCGCGATATGGGCATATTATTATGGC	611
amyUSR-BamHI	GGCGGATCCCATGTACTTATAAATATAAGG	
amyDSF-BamHI	GGCGGATCCTACAGTGATGTCGTGTATCG	818
amyDSR-XhoI	GGCCTCGAGCGAGCAAGTGTAAAATTTC	
amyCo-ApaF	GGCGGGCCCCCTCCACAAAATTTTTAAGTTC	2546
amyCo-XbaR	GCCTCTAGACCACTTTTATTACAGTACTTCT	
amy-intF	CATGCCAAAGGCGGATGTATTGCT	377
amy-intR	TCCAGAGCGTGAACCCTTCTGAAT	
amy-flankF	CGCTCAAAAACATTCAAAGATGAG	N/A[a]
amy-flankR	GAAAGGAACCAATTCCGTGAACC	
amyHisFApaI	CCCCCCGGGCCCTAAATCCTCCACAAAATTTTTAA GTTCAAGACATGTTAGAGAAT	2244
amyHisRXbaI	CCCCCCTCTAGATTAGTGGTGATGGTGATGATGTT TTTTGTTTTCTACAGTTATAG	
amyHisFSacI	CCCCCCGAGCTCATGGCAGAATCAAAATTAGAGA TAGTCAATAAAACAGAACGTG	2262
1668QPCRF	CAACCGTGCCAAAGGTTAGCAGTT	148
1668QPCRR	GCTCTGGCAAAGCAACCATCATCA	
1669QPCRF	TAAATCACGTTGCCGCCGATTCAC	198
1669QPCRR	CAATGCGAACACCCTCAAAGCCAT	
1668-1669 FWD	TCACGCAATTGGTTCCTTTCT	422
1668-1669 REV	TGTGAGGCAGTTGCGTTT	
kmF	GACGGATCCACGTTGTGTCTCAAAATCTCTGA	880
kmR	GACGGATCCCGGCTACCGAGCTCTTAGAA	
1670QCRF	GCGCTCTTGATTGCCCGAAAGTT	94
1670QCRR	TATTGCCATGAATCAGGCCCTTGC	
1671QCRF	TGATGGTGTTCGAGTCGATGCTGT	188
1671QCRR	TTGGGCCTATGCCGGGTAATTTCA	

Table 2.3. continued

1670-1671 FWD	TGCCAGAAGAAGAAAAATTGGAA	162
1670-1671 REV	TCCCATAGAATCGATCACCGTAG	
MDHUSF-NotI	GGCGCGGCCGCCCTAATAGTCCAATTTTAATC	681
MDHUSR-BamHI	GGCGGATCCCAGTGACAACAATTACTTTGG	
MDHDSF-BamHI	GGCGGATCCTACAGGGTATAAAAGAGGGTC	698
MDHDSR-XhoI	GGCCTCGAGGTCAAGGGATGATCCGGGCAT	
MDH-intF	TTATTAGGTGCAGGATCAGCGGGT	378
MDH-intR	TTCTGCGCGAGACGTAGGATTTGA	
MdhCO-ApaF	GGCGGGCCCCCTAATAGTCCAATTTTAATC	1936
MdhCO-XbaR	GCCTCTAGACCAGCAATTTCTACATCGGTT	
Mdh-flankF	CTCGGTTACAAATATTCACAAGGAG	N/A[a]
Mdh-flankR	CAGGATTGGTAGCATCTACAATGG	
lpg2884F	GGCGGGCCCAATTCGAGCACAAATCAAAT	347
lpg2884R	GGCGAATTCAAATAAAATACGCCAGTTGC	
htpBF	AAGACAGCAAAGCTATTG	800
htpBR	GCACGTGTTGAAGATGCT	
5srDNAF	CCCGAATTCTGGCTTAATAAAGCAATCAAAGC	205
5srDNAR	CCCAAGCTTCCTATTTTAATTTAGTCGGCTTTACA	

[a]N/A indicates that the primer pairs were not used together in PCR reactions but were rather used with other primers.

Table 2.4. Primers used in qRT-PCR experiments

Gene ID	Protein Description	Primer sequence	Amplicon size (bp)
lpg1417	DNA gyrase -subunit A (GyrA)	**Forward:** TCGAGCCCATTTATTGGAGGGCTT **Reverse:** AATCATCAGGCCTTGACGCGTTTG	185
lpg2609	FtsZ, cell division protein	**Forward:** TGCTGAGGAAGGTATTCGACGCTT **Reverese:** CCTTTCACAGCACCAAGCAACACA	150
lpg0910	Enhanced entry protein A (EnhA)	**Forward:** GGGGGAAAAGATTTTTGTGAGGACG **Reverse:** GGGAACTTCATAGGCAGCATGTATT	192
lpg0670	Hypothetical protein	**Forward:** AGCTACTAATGTTCGCACAGGTAA **Reverse:** GCTGGATTCCCCATATAACCACCAT	156
lpg1639	Hypothetical protein	**Forward:** ACCTTTGTGCGTAACTACGGGAGA **Reverse:** AAATCAGGTGAATCCTCGCAAGCC	173
lpg0279	Hypothetical protein	**Forward:** CCGTAACCCATCCGCACCAGA **Reverse:** TTCTCCGGCTTCATTGGCGCTG	169
lpg0818	ATP-binding protease component (ClpA)	**Forward:** ACTCTGCGTAACCTGGAACGTGAT **Reverse:** CCAGTTGGTCCGGCAAACAAGAAA	152
lpg0891	Sensory box protein, c-di-GMP synthase	**Forward:** TGGTGTGAAATCAGCGTTGCTCCTG **Reverse:** TGCTTGTAGAATGGCCTGCTCCACT	195
lpg1356	Enhanced entry protein C (EnhC)	**Forward:** AGGTGGGATTGGTGCGGATGATAA **Reverse:** AATTGTGCCTGTGCTTCAGGTTGC	195
lpg1491	Dot/Icm effector	**Forward:** ATGCAGTAGGCCTCAAGGATGAGT **Reverse:** GCTAATTCCGTGGCTGAATCAGGT	157
lpg1540	Universal stress protein A (UspA)	**Forward:** ACCCATCAAAAGAGGATGCCCA **Reverse:** TCCTGTAGCAGAGTGTGAGCCT	170

Table 2.4. continued

lpg1669	Putative α-Amylase	**Forward:** TAAATCACGTTGCCGCCGATTCAC **Reverse:** CAATGCGAACACCCTCAAAGCCAT	198
lpg1950	Dot/Icm effector	**Forward:** CGATTTGGCAGCAAAAGCAGCAG **Reverse:** ACGCCCTCCTTAAGTGCCAGGT	153
lpg2228	3-oxoacyl-[acyl-carrier-protein] synthase	**Forward:** ACCTGAAGTTGAATGCGCCCG **Reverse:** GGCAGCTCCATCAGCCAAACCT	191
lpg2316	3-hydroxybutyrate dehydrogenase (BdhA)	**Forward:** CCTCAGGCAATGGCGGCAGTATT **Reverse:** CGGACAAACCCCGGGCAAATGA	178
lpg2348	Superoxide dismutase (SodC)	**Forward:** CGGGCATTTGGGAGATTTACCTGT **Reverse:** AATGACGCCGCACGCTATACGG	190
lpg2493	Heat shock protein C2 (HspC2)	**Forward:** TGCCTGGTATGGGTGAAGAAGA **Reverse:** CAGTCGCTTTATCCACATCCGC	183
lpg2955	Integration host factor β-subunit (HipB)	**Forward:** TCGCTGCTCGAATGACGCATCTTA **Reverse:** TTTCGCGGTGGTCGGTAATGAAGA	151
lpg1368	Hypothetical protein	**Forward:** TGCAGAAGCAAACCGCCAGATGA **Reverse:** CAGCGACACAGATCGGAGGCA	168
lpg2971	Malate dehydrogenase (MaeA)	**Forward:** TGGCGAACGGATCTTGGGGTT **Reverse:** TCCGAGCGTGTCTCCACCCAA	191
lpg0417	6-phosphoglucono-lactonase (Pgl)	**Forward:** TGCAATCAAACGAAGAGGGCAAGC **Reverse:** AGCAGCTCGTTACGATGTGGATCA	168
lpg0419	Glucokinase (Glk)	**Forward:** AGGAGGGATTATGCCGCGTTTACT **Reverse:** GGTTGAGCGGCTGCAATGACATAA	129

Table 2.4. continued

lpg1887	Hypothetical protein	**Forward:** CAGCAACAACTGGATGCTTTAAATACC **Reverse:** TCCGAGCGTGTCTCCACCCAA	143
lpg0421	D-xylose (galactose, arabinose)-proton symporter (YwtG)	**Forward:** AAGCCCTTGTTGCCTGTGTTGATG **Reverse:** CGTGCTGCCCAAGCCTAAATTCTT	123
lpg1748	Inositol-1-monophosphatase (SuhB)	**Forward:** CCGTGTGTCCAAGCAAACTCAACT **Reverse:** ACCGCTTGCAACATAAGCCAAGTC	175
lpg0136	Pyruvate kinase (PykA)	**Forward:** CTGCTGAAGTTCCCGCCATTCAAA **Reverse:** GCCGAAAGCATCACAGCATCAGTT	181
lpg0948	2-oxoglutarate ferredoxin oxidoreductase β-subunit (KorB)	**Forward:** TTCTCCAACGTCTCAGAAAGGGCA **Reverse:** AAGCACAGAAGCCAAATGGACAGG	154
lpg2495	Hss, homospermidine synthase	**Forward:** TGGACCACAATGCGCGATCTATCT **Reverse:** ATAGGCGTAGTGAACTGTTGGCCT	187

CHAPTER 3: *LEGIONELLA PNEUMOPHILA* PROGENIES PRODUCED IN PROTOZOA AND HUMAN MACROPHAGES DISPLAY DIFFERENT CHARACTERISTICS

3.1. The *L. pneumophila* progenies from human macrophages are less morphologically differentiated than the progenies from protozoa.

Previous electron microscopy studies have shown that MIFs are poorly produced inside human macrophages (Faulkner & Garduno, 2002). To determine whether ultrastructural differences exist between *L. pneumophila* progenies produced in freshwater protozoa (either in a replication-dependent [amoebae] or -independent [ciliates] manner), or in human cells (either epithelial cells or macrophages), a quantitative electron microscopy study was conducted where three typical ultrastructural features (as outlined in Materials and Methods) had to be met for a legionellae cell to be considered a MIF (**Figure 3.1.**). The *L. pneumophila* progeny obtained from HeLa cells was used as a control. I observed a significant difference ($p < 0.001$) between the high proportion of MIFs present in the *L. pneumophila* progeny obtained from HeLa cells, ciliates, and amoebae and the low proportion of MIFs present in the *L. pneumophila* progeny obtained from U937- and THP-1-derived human macrophages. The same results were observed using 2 different strains of *L. pneumophila*; Lp1-SVir (**Table 3.1.)** and 2064 **(Table 3.2.**).

To confirm that the features observed were not fixed traits in the legionellae progeny, but reversible developmental ones, the legionellae progeny produced in U937-derived human macrophages (with a low proportion of MIFs) was allowed to infect *A. castellanii* trophozoites, and the morphology of the amoebal progeny was then re-examined by electron microscopy. As expected for a reversible trait, the proportion of MIFs in this amoebal progeny was high. Collectively, these findings suggest that the intracellular environment of human macrophages does not optimally induce *L. pneumophila* to differentiate.

Of interest was the observation that the legionellae progeny produced in cultured human macrophages had a high proportion of filamentous forms (**Figure 3.2.**). Filamentous *L. pneumophila* forms (F*Lp*) have been shown to interact with lung

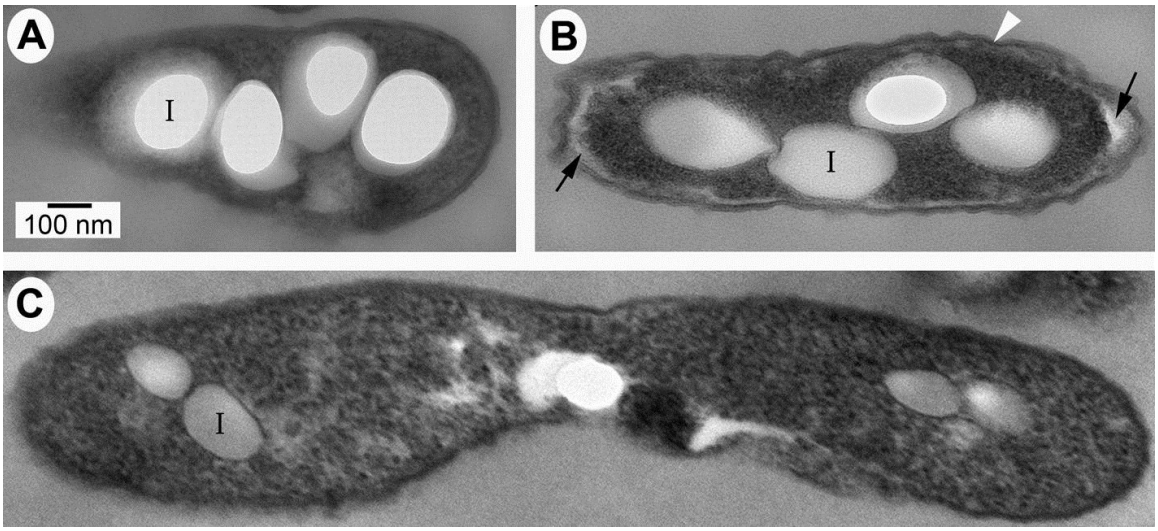

Figure 3.1. Electron micrographs showing the morphological traits of Lp1-SVir progeny from amoebae and from human macrophages.

(A) MIF from amoeba displaying the three traits used to qualify MIFs: a straight outer membrane, an inconspicuous periplasm and the presence of large inclusions. (B) *Legionella pneumophila* cell produced in U937-derived macrophages displaying large inclusions, but lacking a straight outer membrane and an inconspicuous periplasm. The periplasm is quite apparent (black arrows) and the outer membrane is wavy (e.g. white arrowhead). (C) Detail of an *L. pneumophila* cell produced in THP-1-derived macrophages displaying a straight outer membrane and an inconspicuous periplasm, but lacking large inclusions. Bacterial cells shown in (B and C) are not regarded as MIFs. I = inclusion. All micrographs are presented at the same magnification.

Table 3.1. Quantitative analysis of the distribution of MIFs in the Lp1-SVir progeny obtained from different hosts.

Statistical significance was calculated against the percentage of MIFs produced in U937 and THP-1 cells using the two-proportion test. All samples were significant at the 0.001 level.

Host	**Percentage of particles that show the ultrastructural features of MIFs**	
	***L. pneumophila* Lp1-SVir**	
Amoebae (*A. castellanii*)	85 / 107	**79.4 %**
HeLa cells	125 / 149	**83.9 %**
***Tetrahymena tropicalis* ciliates**	109 / 129	**84.5 %**
U937 human macrophages	262 / 536	**48.1 %**
THP-1 human macrophages	62 / 129	**48.9 %**
U937 progeny passed in amoebae	201 / 250	**80.4 %**

Table 3.2. Quantitative analysis of the distribution of MIFs in the progeny of *L. pneumophila* 2064 obtained from different hosts.

Statistical significance was calculated against the percentage of MIFs produced in U937 and THP-1 cells using the two-proportion test. All samples were significant at the 0.001 level. This table was generated by Eman Atwi and Hany Abdelhady.

Host	**Percentage of particles that show the ultrastructural features of MIFs**	
	***L. pneumophila* 2064**	
Amoebae (*A. castellanii*)	130 / 165	**79.0 %**
HeLa cells	76 / 109	**69.7 %**
***Tetrahymena tropicalis* ciliates**	111 / 169	**65.7 %**
U937 human macrophages	196 / 547	**40.0 %**
THP-1 human macrophages	58 / 147	**35.8 %**
U937 progeny passed in amoebae	335 / 402	**83.3 %**

epithelial cells through a mechanism not shared with the bacillary forms (Prashar *et al.*, 2012). This is in sharp contrast with the legionellae progeny obtained from amoebae, which is exclusively formed by short rods. Formation of filamentous forms in macrophages was not a strain-specific trait, since *L. pneumophila* strains Lp1-Svir, and 2064 produced similar proportions of filaments in U937-derived human macrophages (**Figure 3.2.**).

3.2. *L. pneumophila* progeny from amoeba is more resistant to antibiotics, but less resistant to low concentrations of chlorine, than the progeny from macrophages.

Resistance of *L. pneumophila* MIFs to antibiotics was previously reported as a distinct trait of MIFs in relation to SPFs cultured *in vitro* (Garduno *et al.*, 2002). I set out to determine whether differences between the progenies produced in human macrophages, amoebae and the free MIFs released from the ciliate-produced pellets exist in relation to their resistance to gentamicin (used in previous studies with MIFs from HeLa cells) (Garduno *et al.*, 2002), or ciprofloxacin (used clinically for the treatment of LD). The progenies produced in amoebae showed a modestly higher survival in different concentrations of gentamicin (5, 20, and 100 μg/ml) and ciprofloxacin (25μg/ml) than MIFs produced in macrophages (**Table 3.3.**). Resistance to antibiotics represented a reversible developmental trait, rather than a selection of mutants, because macrophage-produced progenies could revert to the higher resistance phenotype after they were passed through amoebae.

In relation to antimicrobial challenges potentially found in man-made water systems (detergents and chlorine) legionellae obtained from amoebae or macrophages were similarly resistant to SDS-mediated lysis, and all showed an infinite lysis index (**Table 3.4.**). However, legionellae obtained from human macrophages demonstrated higher survival in the presence of 1 mg/L chlorine (**Table 3.5.**). Neither progenies produced in amoebae, nor those from U937-derived macrophages showed growth in 5 mg/L chlorine (**Table 3.5.**).

***L. pneumophila* Lp1-SVir**

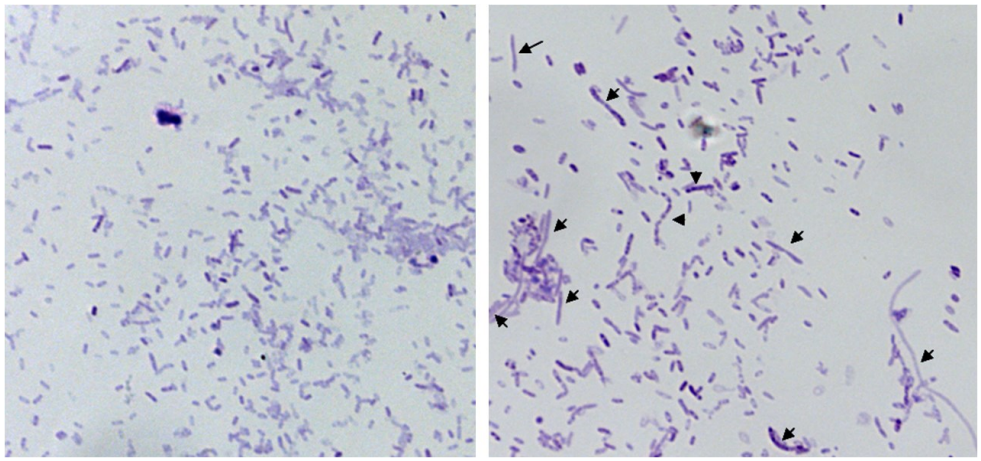

***L. pneumophila* 2064**

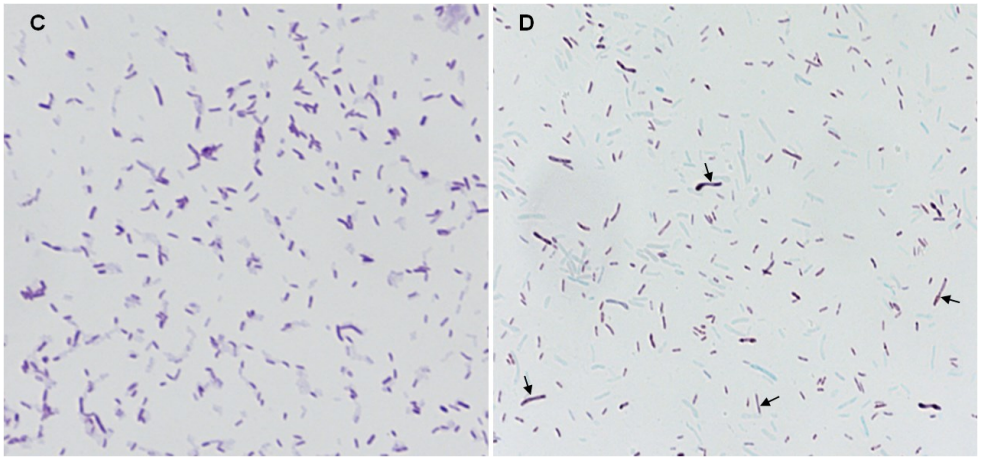

Figure 3.2. The progeny of *L. pneumophila* obtained from U937 cells shows filamentous forms.

Light micrographs of the progeny of *L. pneumophila* strains Lp1-SVir and 2064 obtained from *A. castellanii* (A, C) and U937 human macrophages (B, D). Specimens heat-fixed on glass slides were stained with crystal violet and shown in bright field. Examples of filamentous and elongated legionellae are indicated by the small black arrows. All micrographs were taken with the 100× oil-immersion objective lens.

Table 3.3. The progeny of *L. pneumophila* from amoebae is more resistant to antibiotic challenges than the progeny from human macrophages.

Percent survival (after 3h) of each sample was calculated using this formula [(CFU after challenge / CFU before challenge) × 100]. Results represent the mean ± standard deviations of at least 3 independent experiments. phase forms (SPFs), grown *in vitro*, were used as reference.

***L. pneumophila* Lp1-SVir**

	Gentamicin 5 µg/ml	**Gentamicin 20 µg/ml**	**Gentamicin 100 µg/ml**	**Ciprofloxacin 25 µg/ml**
MIFs produced in amoebae	100%	72.34 ± 4.73 %	5.8 ± 2.6 %	22.58 ± 3.2 %
MIFs produced in U937 macrophages	100%	28.06 ± 3.09 %	1.45 ± 1.19 %	15.12 ± 1.02 %
MIFs produced in U937 macrophages and then passed in amoebae	100%	47.5 ± 6.5 %	7 ± 1.1 %	24.66 ± 1.63 %
Mechanically-disrupted pellets	25.59 ± 4.7%	4.16 ± 1.45%	1 ± 0.6%	18.87 ± 0.33%
Stationary phase froms	0.06 ± 0.004 %	0.005 ± 0.002 %	0.003 ± 0.002 %	6.3 ± 2.3 %

***L. pneumophila* 2064**

MIFs produced in amoebae	43.86 ± 2.1%	20.46 ± 7.8%	0.7 ± 0.45%	21.65 ± 2.9 %
MIFs produced in U937 macrophages	6.93 ± 4.3%	2.44 ± 1.46%	0.045 ± 1.46%	9.95 ± 0.64 %
MIFs produced in U937 macrophages and then passed in amoebae	37.7 ± 8.8%	21.9 ± 6.97%	0.87 ± 0.23%	19.4 ± 0.6 %
Mechanically-disrupted pellets	27.56 ± 13.05%	3.12 ± 1.2 %	0.024 ± 0.02%	16.05 ± 9.8%
Stationary phase forms	0.06 ± 0.04 %	0.002 ± 0.001%	0.001 ± 0.0006 %	9 ± 2.55 %

Table 3.4. SDS challenge experiments of the progeny of two *L. pneumophila* strains (Lp1-SVir and 2064) obtained from different hosts.

Stationary phase forms (SPFs), grown *in vitro*, were used as reference. Results represent the mean ± standard deviations of 3 independent experiments. This table was generated by Eman Atwi and Hany Abdelhady.

	***L.pneumophila* Lp1-Svir**	***L.pneumophila* 2064**
Acanthamoeba castellanii	∞[b]	∞
U937 human macrophages	∞	∞
HeLa cells	∞	∞
Mechanically-disrupted pellets	650 ± 87	600 ± 108
Stationary phase forms	1.3 ± 0.4	1.6 ± 0.2

[a] index lysis is the time (in minutes) required for each sample to reach half of its original optical density (OD_{620}) before treatment with a detergent

[b] ∞, apparently infinite index since the lysis curve becomes asymptotic at a value above 50% of original OD_{620}.

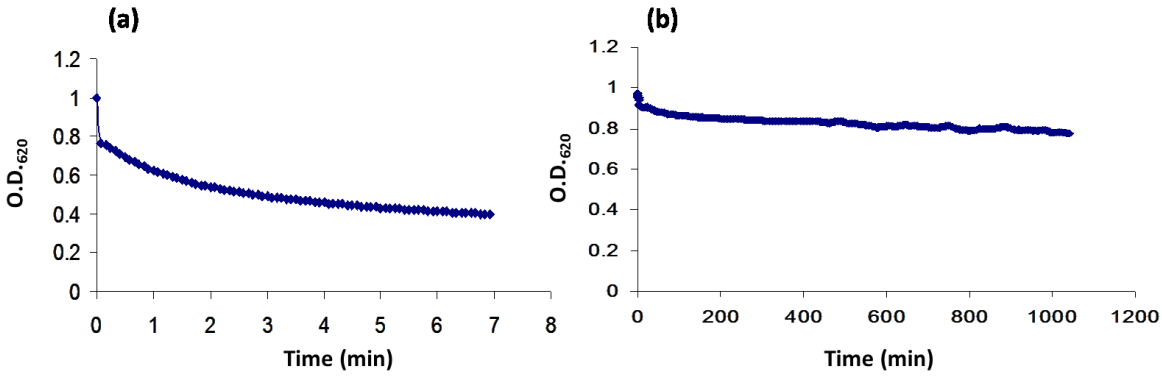

Figure 3.3. *L. pneumophila* progeny from host cells is more resistant to SDS challenge than *L. pneumophila* SPFs.

Typical lysis curves of *L. pneumophila* grown in vitro to SPFs (a) and the progeny of *L. pneumophila* obtained from host cells (b). *In vitro*-grown *L. pneumophila* 2064 is shown as a representative of SPFs (a) and *L. pneumophila* 2064 progeny from amoebae is shown as a representative of MIFs (b). The lysis curve shows changes in OD_{620} nm (an indicator of cell lysis) as a function of time. Lysis index is the time taken for each sample to reach half of its original optical density. The estimated lysis index of *L. pneumophila* SPFs is less than 2 min (a), and for *L. pneumophila* MIFs is infinite (b). Each graph is a representative of 3 different experiments.

Table 3.5. The progeny of *L. pneumophila* from human macrophages is more resistant to chlorine challenge than the progeny from amoebae.

Percent survival (after 30 min) of each sample was calculated using this formula [(CFU after challenge / CFU before challenge) × 100]. Results represent the mean ± standard deviations of at least 3 independent experiments. Stationary phase forms (SPFs), grown *in vitro*, were used as reference.

	Chlorine 1 mg/L (1 ppm)	**Chlorine 5 mg/L (5 ppm)**
***L. pneumophila* Lp1-SVir**		
MIFs produced in amoebae	3.7 ± 1.88 %	No growth
MIFs produced in U937 macrophages	10.9 ± 2.84 %	No growth
Mechanically-disrupted pellets	46.6 ± 5.1 %	2.13 ± 1 %
Stationary phase forms	No growth	No growth
***L. pneumophila* 2064**		
MIFs produced in amoebae	49.15 ± 12.9 %	No growth
MIFs produced in U937 macrophages	92.4 ± 9.1 %	No growth
Mechanically-disrupted pellets	47.12 ± 6.7	No growth
Stationary phase forms	No growth	No growth

3.3. *L. pneumophila* progenies obtained from amoebae are more adherent to host cells than the progenies obtained from macrophages.

L. pneumophila Lp1-Svir progenies produced in amoebae and U937-derived macrophages were tested for their intracellular growth in three types of host cells (*A. castellanii* trophozoites, U937-derived human macrophages and mouse L929 cells) to determine whether infectivity differences exist. Since the aforementioned results demonstrated that legionellae produced in amoebae could have a potential advantage in a gentamicin challenge, the gentamicin treatment step, which is used to kill extracellular bacteria, was omitted from our standard infection protocols. Instead, the monolayers were washed with PBS to more effectively remove unattached bacteria.

My data demonstrated that there were consistently higher numbers of the host cell-associated amoeba progenies than the host cell-associated macrophage progenies at time zero. This difference was maintained along the intracellular growth phase, suggesting that legionellae obtained from macrophages had an early disadvantage in relation to legionellae obtained from amoebae, but no subsequent defect in intracellular growth. In fact, legionellae obtained from macrophages appeared to grow at a higher rate in trophozoites and L929 cells than legionellae obtained from amoebae (**Figure 3.4.**). Subsequent attachment-only assays conducted with *L. pneumophila* strains Lp1-SVir and 2064 confirmed that a consistently higher number of legionellae produced in amoebae were associated with host cells, in relation to legionellae from macrophages (**Figure 3.5.**), and that this trait was developmentally reversible. That is, macrophage-produced legionellae enhanced their adherence after passage in amoebae (**Figure 3.5.**). These results indicate that in relation to *L. pneumophila* progeny produced in amoebae, the progeny produced in macrophages is less adherent and, consequently, initiates fewer host cell infections but does not display intracellular growth defects.

3.4. *L. pneumophila* progeny from macrophages does not show an intracellular growth defect when tested in direct competition with progeny from amoebae.

Although legionellae produced in macrophages showed no apparent intracellular growth defect when tested alone, growth defects sometimes become obvious in competition assays. Therefore, green fluorescent JR32 legionellae (expressing GFP)

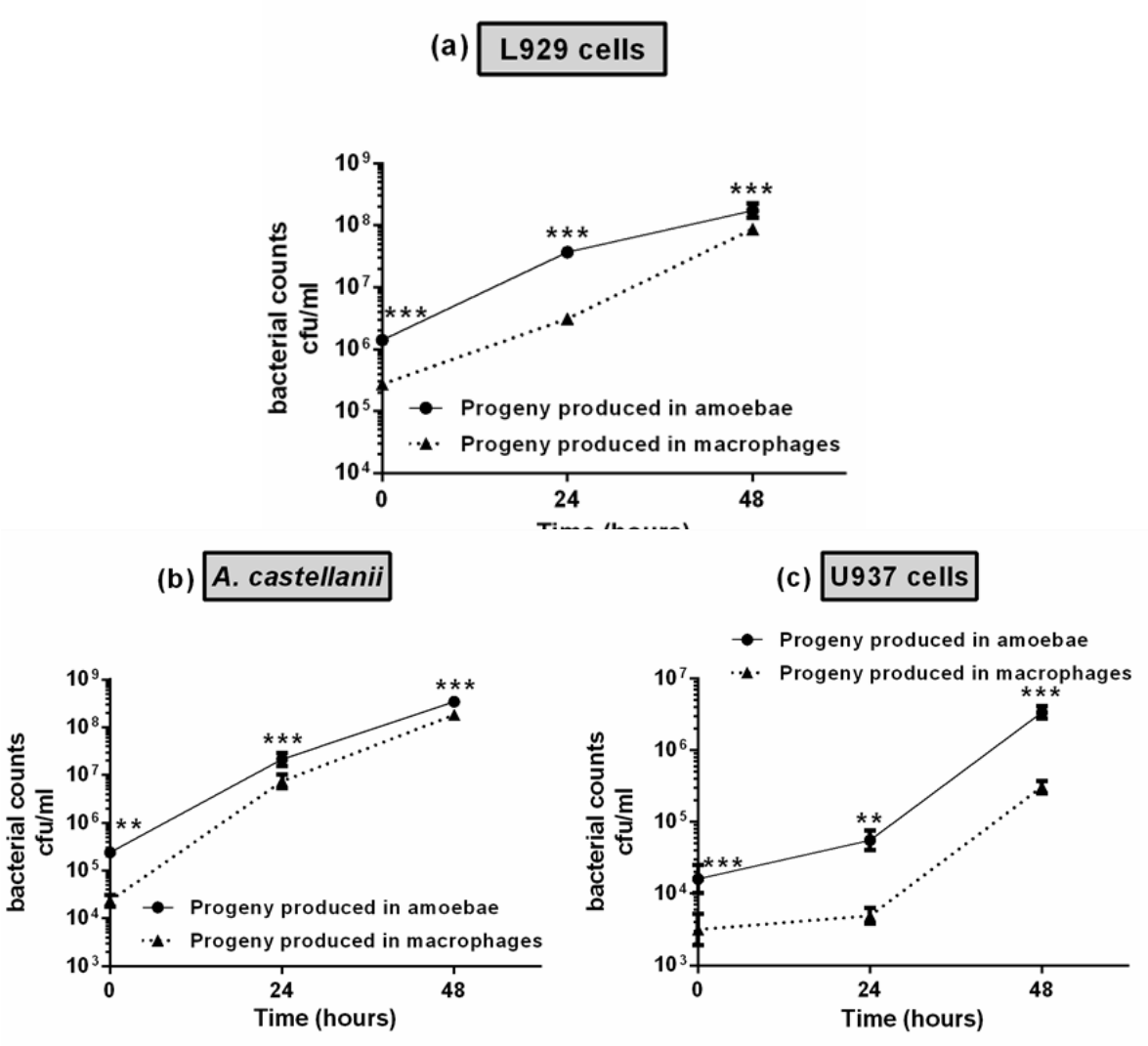

Figure 3.4. *L. pneumophila* Lp1-Svir amoeba progeny is more adherent to L929, U937, and *A. castellanii* monolayers than the macrophage progeny.

Graphs of CFU versus time showing the intracellular growth of legionellae in L929 (a), *A. castellanii* (b), and U937 monolayers (c) infected with the progeny from amoebae or human macrophages at the same bacteria-to-cell ratio. Graph points represent means and error bars represent standard deviations of 3 independent experiments, each run in triplicate. Statistical significance was calculated using 2-way ANOVA. ** $p < 0.01$, *** $p < 0.001$.

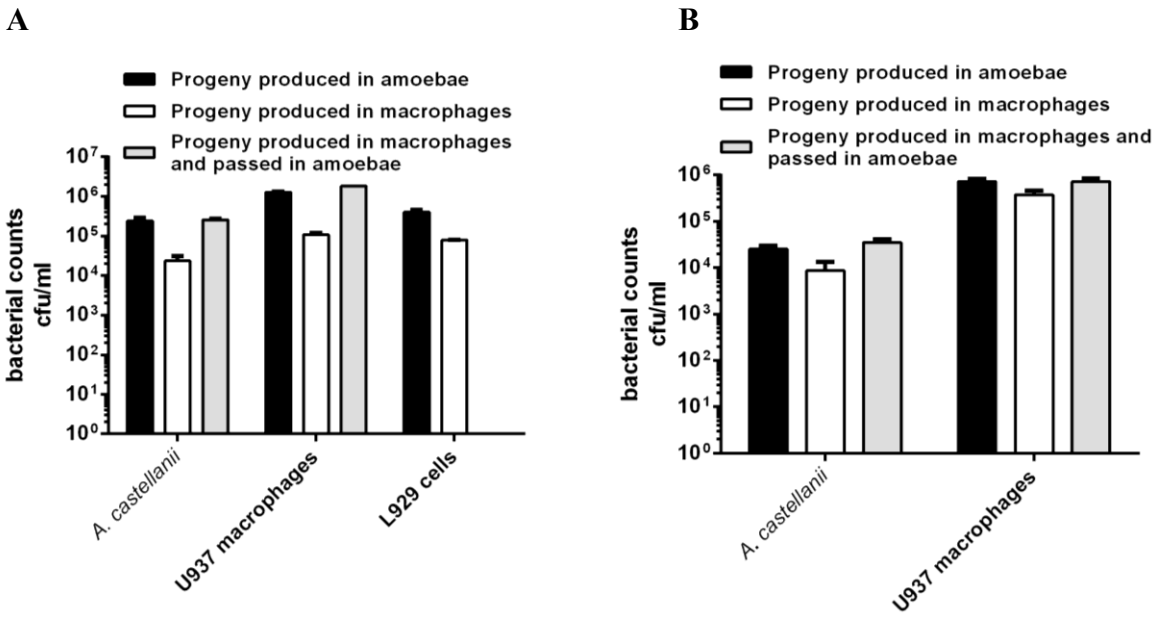

Figure 3.5. *L. pneumophila* progeny produced in amoebae is more adherent to host cells than the progeny produced in human macrophages.

Graphs of CFU versus time showing the adherence of Lp1-SVir (A) and 2064 (B) legionellae to L929, *A. castellanii*, and U937 monolayers infected with the progeny from amoebae, human macrophages, or human macrophages which is then passed in amoebae used at the same bacteria-to-cell ratio. Graph bars represent means and error bars represent standard deviations of 3 independent experiments, each run in triplicate. Statistical significance was calculated using 2-way ANOVA. ** $p < 0.01$, *** $p < 0.001$.

produced in amoebae, and red fluorescent JR32 legionellae (expressing DsRed) produced in macrophages were allowed to compete on monolayers of *A. castellanii* and human U937-derived macrophages. Legionellae produced in amoebae infected a significantly higher number of *A. castellanii* trophozoites (**Figure 3.6. a, b**), but did not produce a more numerous progeny (**Figure 3.6. c**) in relation to legionellae obtained from macrophages, at 24 and 48 h post-infection. These results confirmed that even in direct competition with legionellae obtained from amoebae, legionellae obtained from macrophages did not show a defect in intracellular growth. In fact, the progeny yield per infected cell was higher in cells infected with legionellae from macrophages.

When allowed to compete for infection of a monolayer of human macrophages, legionellae produced in U937 cells did not show intracellular growth defects and were also able to reach higher intracellular counts and produce more progeny than legionellae produced in amoebae (**Figure 3.7. b**) although there was not a significant difference in the percentage of infected human macrophages for both samples following 3 and 4 days of infection (**Figure 3.7. a, c**). Together, these experiments support the initial observation that the *L. pneumophila* progeny from human macrophages does not display intracellular growth defects when compared to the *L. pneumophila* progeny from amoebae.

3.5. *L. pneumophila* MIFs obtained from amoebae is similarly infective to host cells as the free MIFs from the legionellae-laden pellets produced in *Tetrahymena* ciliates.

The role of *Tetrahymena* ciliates in the transmission of LD as packagers of MIFs into respirable pellets has been previously suggested. However, the role of the single MIFs inside these pellets has not been studied. *L. pneumophila* progeny from amoebae (mainly composed of MIFs) and the free MIFs released from legionellae-laden pellets produced in *Tetrahymena* ciliates by mechanical disruption were tested for their ability to infect a monolayer of *A. castellanii* (**Figure 3.8.)** and U937-derived human macrophages (**Figure 3.9.**). Fluorescent legionellae that express GFP were used for this experiement. The results of this experiment demonstrate that *L. pneumophila* MIFs from amoebae infect a similar percentage of *A. castellanii* trophozoites (**Figure 3.8.**) and human macrophages (**Figure 3.9.**) as the free MIFs released by mechanical disruption of the legionellae-laden pellets. These results highlight the potential role *Tetrahymena* ciliates

A

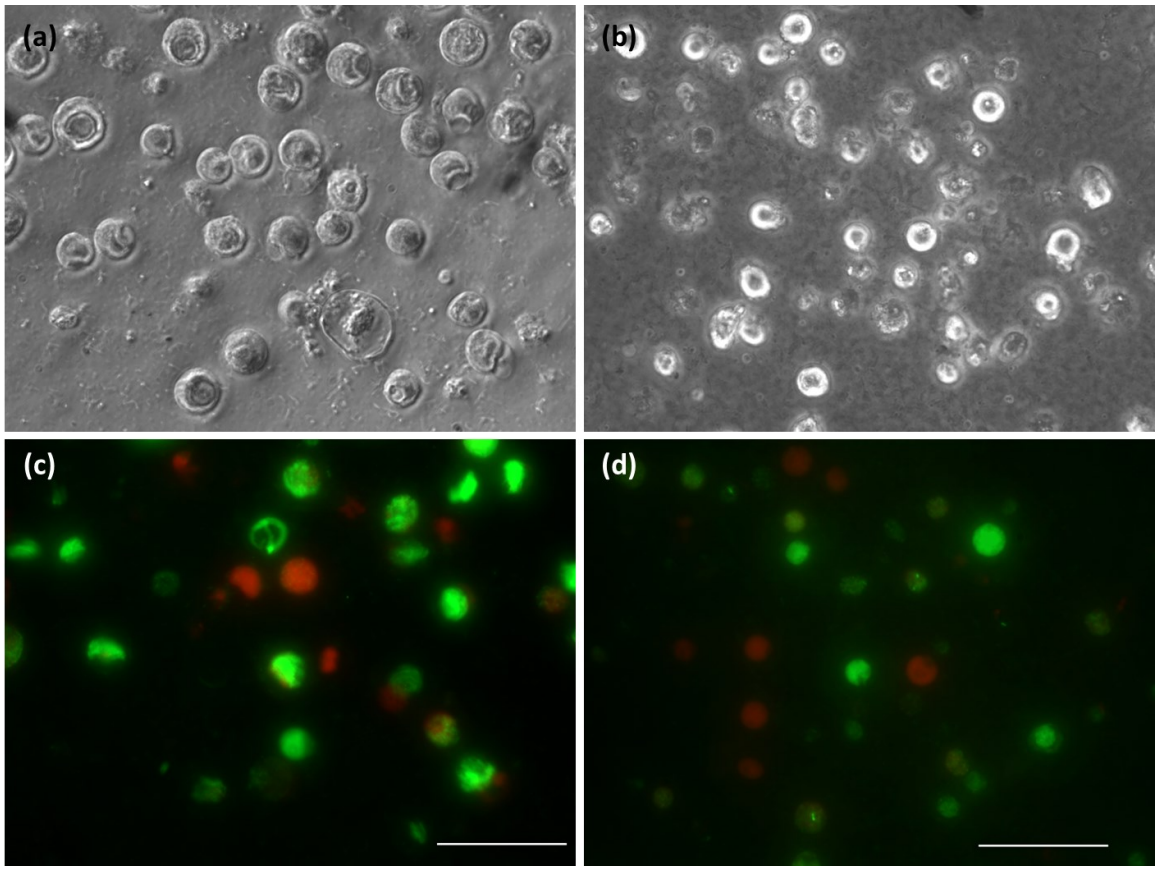

24 hours 48 hours

B

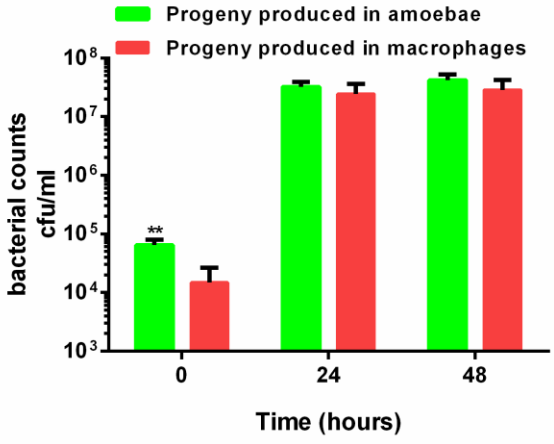

C

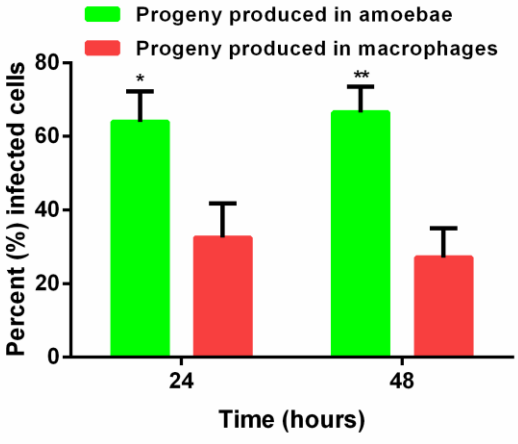

Figure 3.6. *L. pneumophila* progeny from amoebae infects a higher percentage of *A. castellanii* trophozoites in direct competition with the progeny from human macrophages.

(A) Light micrographs captured 24 (a, c) and 48 h (b, d) after infection of *A. castellanii* monolayers with a 1:1 mixture of the *L. pneumophila* progenies obtained from amoebae (green fluorescence) and human macrophages (red fluorescence). Size bars represent 100 μm. (B) A graph of CFU versus time showing the intracellular growth of legionellae in *A. castellanii* monolayers infected with 1:1 mixture of the *L. pneumophila* progeny from amoebae and human macrophages. Green and red bars represent mean CFU counts of the progeny obtained from amoebae and human macrophages, respectively. Error bars represent standard deviations of 3 independent experiments, each run in triplicate. Statistical significance was calculated using 2-way ANOVA. ** $p < 0.01$. (C) A graph of % infected amoeba cells versus time. Green and red bars represent mean % infected cells with the progeny produced in amoebae (green bars) or in human macrophages (red bars), respectively. Error bars represent standard deviations of 3 independent experiments, each run in triplicate. Statistical significance was calculated using two-proportion test. * $p < 0.05$, ** $p < 0.01$.

A

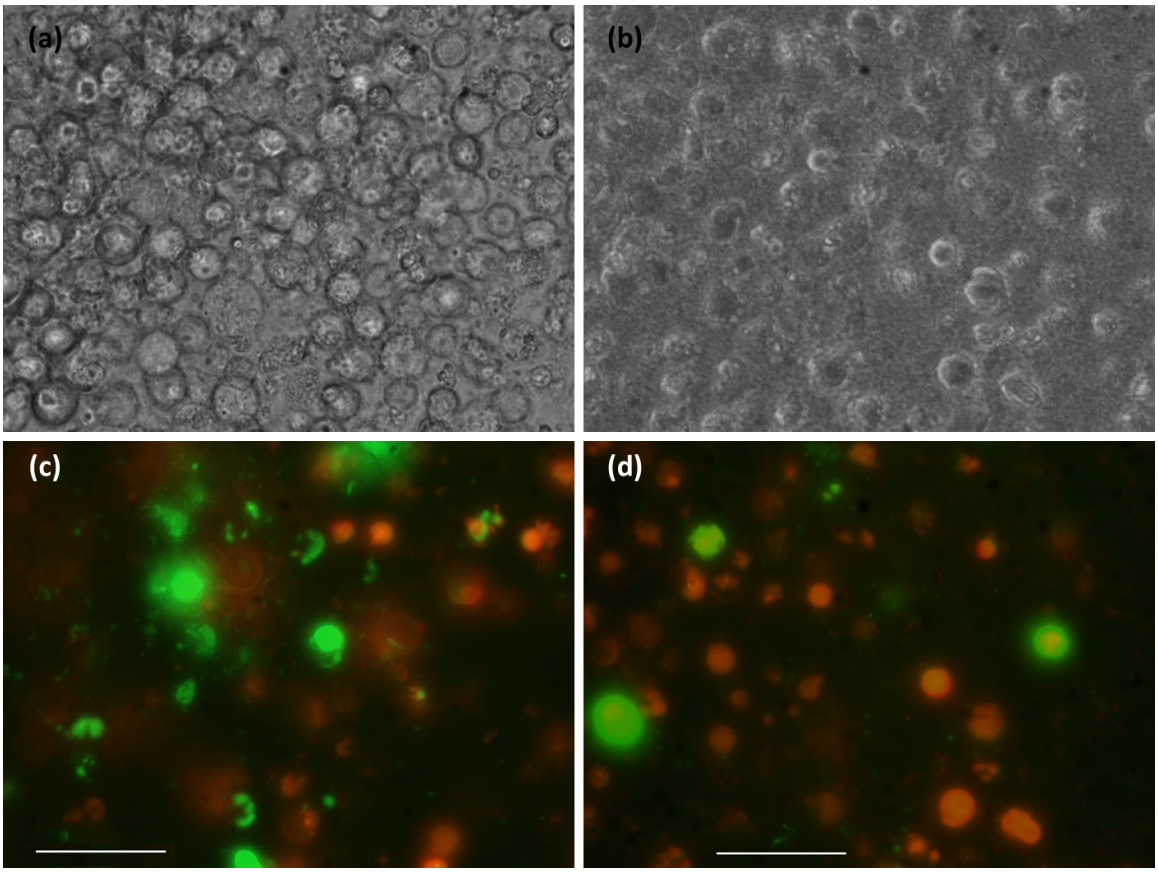

72 hours **96 hours**

B **C**

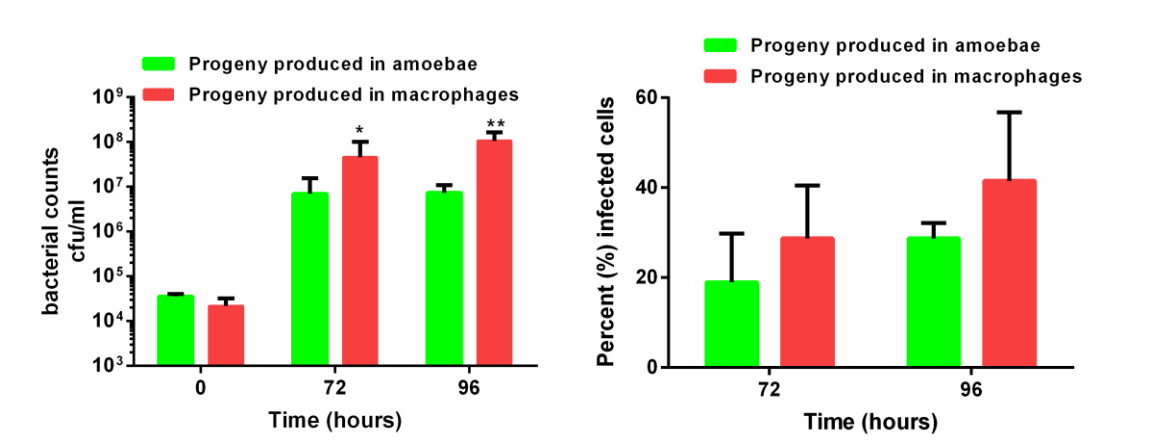

Figure 3.7. *L. pneumophila* progeny from macrophages does not display growth defects inside U937 macrophages in a direct competition with the progeny from amoebae.

(A) Light micrographs captured 72 (a, c) and 96 h (b, d) after infection of U937 macrophages with a 1:1 mixture of the *L. pneumophila* progenies obtained from amoebae (green fluorescence) and human macrophages (red fluorescence). Size bars represent 100 μm. (B) A graph of CFU versus time showing the intracellular growth of legionellae in monolayers of U937 macrophages infected with 1:1 mixture of the progenies obtained from amoebae and human macrophages. Green and red bars represent mean CFU counts of the progenies obtained from amoebae and human macrophages, respectively. Error bars represent standard deviations of 3 independent experiments, each run in triplicate. Statistical significance was calculated using 2-way ANOVA. * $p < 0.05$, ** $p < 0.01$. (C) A graph of % infected amoeba cells versus time. Green and red bars represent mean % infected cells with the progeny produced in amoebae (green bars) or in human macrophages (red bars), respectively. Error bars represent standard deviations of 3 independent experiments, each run in triplicate. No statistical significance was observed using two-proportion test.

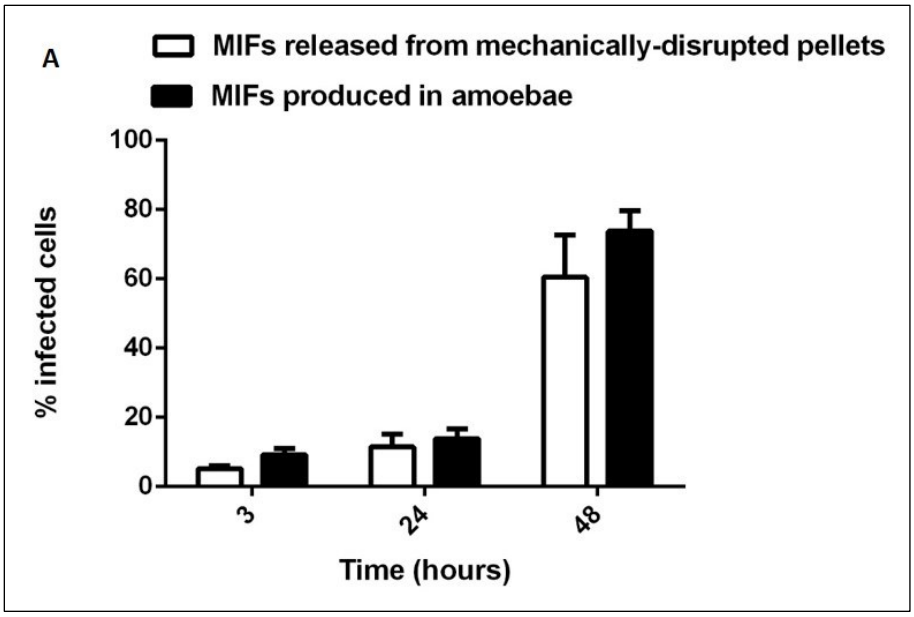
A
MIFs released from mechanically-disrupted pellets
MIFs produced in amoebae
% infected cells
100
80
60
40
20
0
3
24
48
Time (hours)

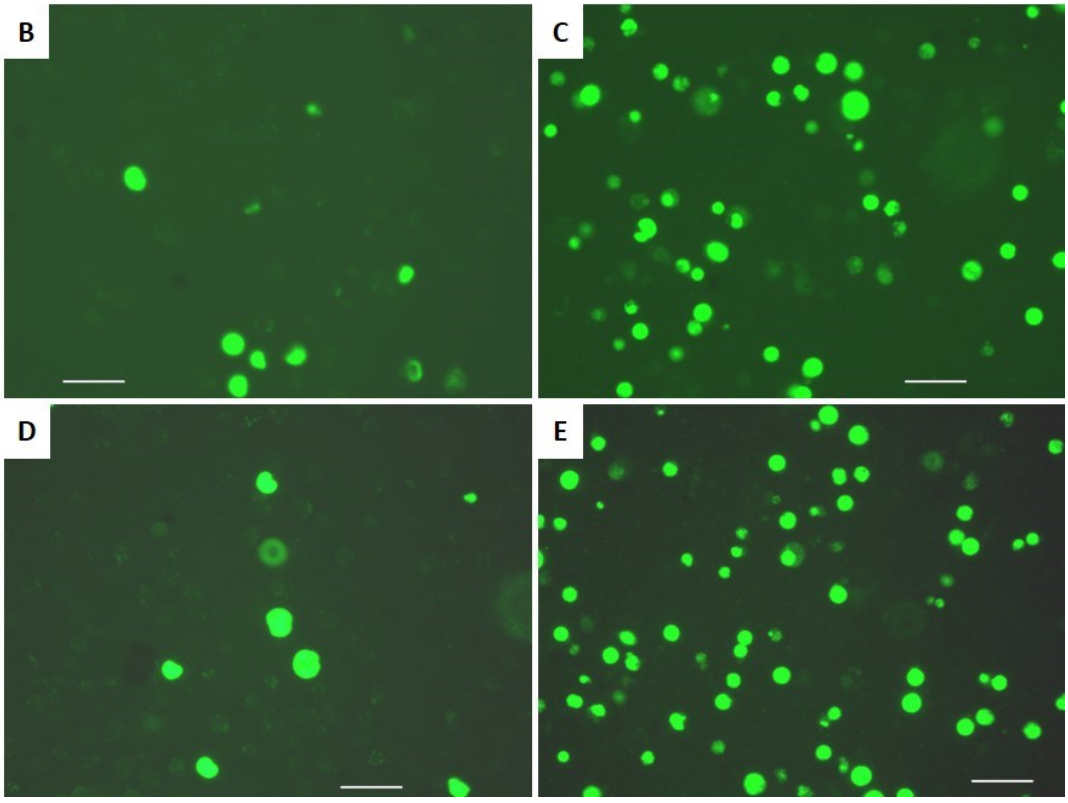
B
C
D
E

Figure 3.8. *L. pneumophila* MIFs from amoebae are similarly infective to *A. castellanii* trophozoites as the free MIFs from the legionellae-laden pellets.
(A) A graph of the percent infected *A. castellanii* trophozoites versus time. Black and white bars represent mean % infected *A. castellanii* trophozoites with *L. pneumophila* MIFs produced in amoebae (black bars) or released from the legionellae-laden pellets produced in *Tetrahymena* ciliates (white bars), respectively. Error bars represent standard deviations of 3 independent experiments, each run in triplicate. (B and C) Light micrographs captured 24 and 48 hours after infection of *A. castellanii* monolayers with free MIFs released from legionellae-laden pellets. (D and E) Light micrographs captured 24 and 48 hours after infection of *A. castellanii* monolayers with MIFs produced in amoebae. Size bars represent 100 μm. Statistical significance was tested using two-proportion test. No statistical significance was observed at any timepoint. This figure was generated by Sachiko Ito and Hany Abdelhady.

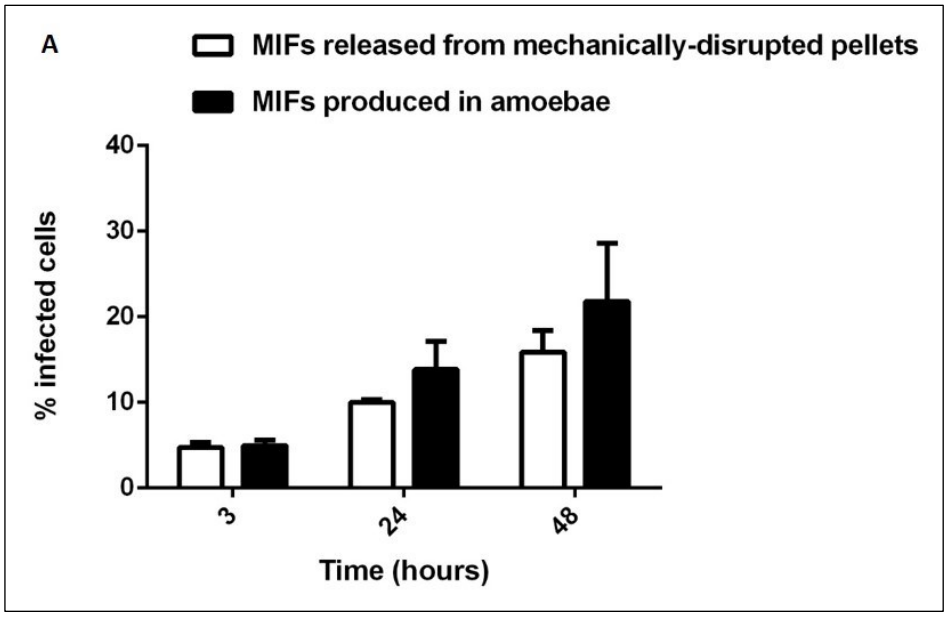
A
MIFs released from mechanically-disrupted pellets
MIFs produced in amoebae
% infected cells
40
30
20
10
0
3
24
48
Time (hours)

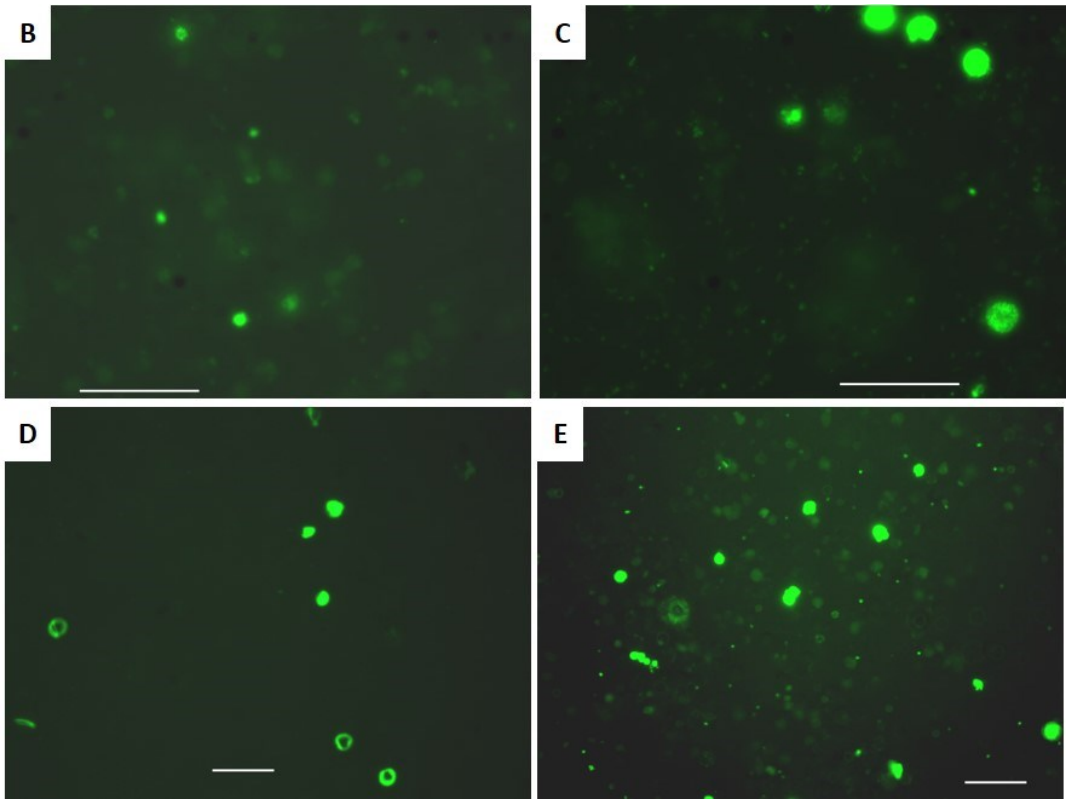
B
C
D
E

Figure 3.9. *L. pneumophila* MIFs from amoebae are similarly infective to U937 human macrophages as the free MIFs from the legionellae-laden pellets.
(A) A graph of the percent infected U937 human macrophages versus time. Black and white bars represent mean % infected mcrophages with *L. pneumophila* MIFs produced in amoebae (black bars) or released from the legionellae-laden pellets produced in *Tetrahymena* ciliates (white bars), respectively. Error bars represent standard deviations of 3 independent experiments, each run in triplicate. (B,C) Light micrographs captured 24 and 48 hours after infection of U937 human macrophage monolayers with free MIFs released from legionellae-laden pellets. (D,E) Light micrographs captured 24 and 48 hours after infection of U937 human macrophage monolayers with MIFs produced in amoebae. Size bars represent 100 μm. Statistical significance was tested using two-proportion test. No statistical significance was observed at any timepoint. This figure was generated by Sachiko Ito and Hany Abdelhady.

can play in maintaining the life cycle of *L. pneumophila* in the natural freshwater environments by infecting amoeba and in the transmission of LD by infecting the macrophages of susceptible humans.

3.6. *L. pneumophila* progeny from amoebae express some unique proteins not found in the progeny from macrophages.

The phenotypic differences between *L. pneumophila* progenies obtained from amoebae and human macrophages were expected to reflect differences in their protein profiles. When the one-dimensional protein profile of whole cell lysates of legionellae produced in amoebae was compared with legionellae obtained from human macrophages, two protein bands were consistently present in the amoeba-produced legionellae lanes (**Figure 3.10.**). The list of proteins represented by the tryptic peptides identified by mass spectrometry in these bands (which were absent from the corresponding gel region of the macrophage MIFs lanes) is shown (**Table 3.6**). To provide more support to the identified list of proteins, the expression profiles of the encoding genes during growth inside amoebae and human macrophages were compared based on previously-published studies (Bruggemann *et al.*, 2006; Faucher *et al.*, 2011). The results are shown in (**Table 3.7**).

3.7. Acknowledgement

I would like also to thank Mary-Ann Trevors for the technical assistance in processing the electron microscopy samples and Dr. Alejandro Cohen for his expertise in mass spectrometry analysis of the excised protein bands. I would like also to acknowledge the contribution of Eman Atwi (an honours student, Department of Biology, Dalhousie University) and Sachiko Ito (a visiting student from Bonn Rhein-Sieg University of Applied Sciences, Germany) to the work presented in this chapter. They both worked under my direct guidance and gave me the opportunity to develop supervisory skills. Eman Atwi analysed the ultrastructural differentiation of the *L. pneumophila* 2064 progeny obtained from amoebae, U937 human macrophages, HeLa cells and *Tetrahymena* ciliates. Eman also performed SDS and gentamicin (100 μg/ml) challenge experiments using the *L. pneumophila* 2064 progeny obtained from amoebae and U937 human macrophages and SPFs. Sachiko Ito performed infection

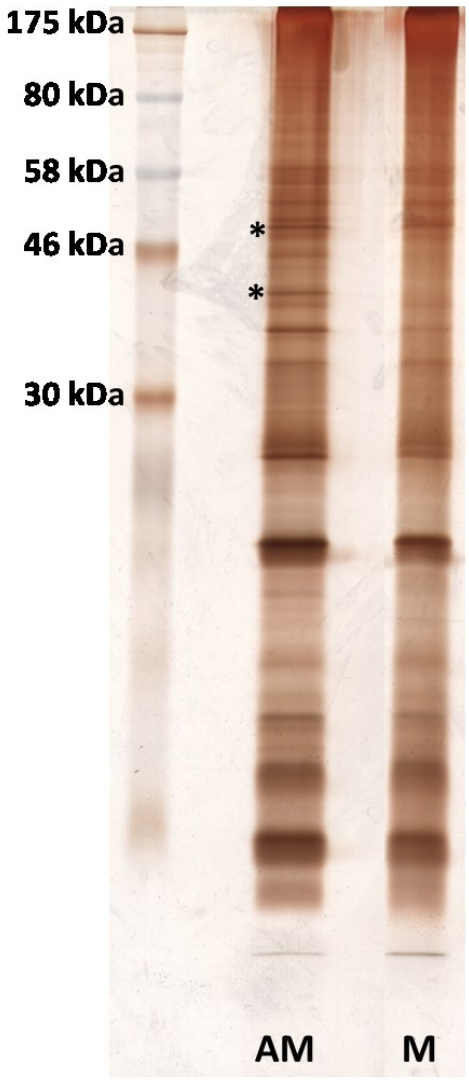

Figure 3.10. *L. pneumophila* progenies produced in amoebae express some unique proteins not found in the progenies from macrophages.

A silver-stained protein gel of the whole cell lysates of the *L. pneumophila* progenies produced in amoebae (AM) and in human macrophages (M) was analyzed by SDS-PAGE and the resolved protein bands were silver-stained (A). The protein bands unique to the progenies from amoebae, marked by the asterisks (*), were selected for analysis by mass spectrometry. This gel is a representative of 3 independent experiments.

Table 3.6. List of proteins for which tryptic peptides were identified by mass spectrometry in two major bands present in the whole cell lysates of Lp1-Svir progeny from amoebae separated by SDS-PAGE.

Tryptic peptides matching these proteins were not found in the corresponding areas of protein SDS-PAGE gels of legionellae from macrophages.

Protein	Predicted Size (kD)	Function
From the higher (~ 50-kDa) band		
Enhanced entry protein C, EnhC	41.4	Toxin production / cell entry
Uroporphyrinogen III methylase	42.5	Metabolism of Cofactors and Vitamins
Hypothetical protein Lpg1368	59.9	Unknown
Nodulation competitiveness protein Lpg2958	54.3	Chemotaxis / motility / Transmembrane protein
Lem9 (Dot/Icm effector)	47.5	Dot/Icm Effectors
Malonate decarboxylase subunit beta	44.5	Energy Metabolism
Hypothetical protein Lpg1639	51.3	ORFs of unknown function (unique)
Hypothetical protein Lpg0670	40.9	Unknown
RalF	44.8	Dot/Icm Effectors
From the lower (~ 40-kDa) band		
Small heat shock protein HspC2	18.9	adaptation to stress
Universal stress protein A (UspA)	15.8	Detoxification / adaptation
Hypothetical protein Lpg0279	42.6	Unknown / hypothetical proteins
Enhanced entry protein EnhA	20.5	Toxin production / cell entry
Malate dehydrogenase	36.33	Carbohydrate Metabolism
3-oxoacyl (acyl carrier protein) synthase III	39.4	Lipid Metabolism
3-hydroxy butyrate dehydrogenase BdhA	27.75	Lipid Metabolism
LirA (Dot/Icm effector)	30.05	Dot/Icm Effectors
RavE (Dot/Icm effector)	37.9	Dot/Icm Effectors

Table 3.7. Transcriptional profiles of the genes encoding the previously identified proteins during infections of *Acanthamoeba castellanii* and human macrophages.

Protein	Gene ID	Human macrophages[a]	*A. castellanii*[b]
		T_{18}/T_0	T_{14}/T_8
Enhanced entry protein EnhC	*lpg1356*	0.77	11.63
Uroporphyrinogen III methylase	*lpg2736*	0.71	1.74
	lpg 2737	2.08	1.29
RavE (Dot/Icm effector)	*lpg0195*	1.19	12.82
3-hydroxy butyrate dehydrogenase (BdhA)	*lpg2316*	0.74	8.82
Small heat shock protein HspC2	*lpg2493*	3.13	18.25
Universal stress protein A (UspA)	*lpg0935*	0.87	2.14
	lpg1540	1.94	4.66
Hypothetical protein Lpg0670	*lpg0670*	0.66	8.94
RalF (Dot/Icm effector)	*lpg1950*	2.50	9.13
Hypothetical protein Lpg1639	*lpg1639*	1.56	13.74
Lpg2958; transmembrane protein (nodulation competitiveness protein)	*lpg2958*	1.11	5.50
Lem9 (Dot/Icm effector)	*lpg1491*	1.78	15.78
Malonate decarboxylase subunit beta	*lpg2427*	1.55	5.67
Hypothetical protein Lpg0279	*lpg0279*	0.67	9.45
Enhanced entry protein EnhA	*lpg0910*	0.99	20.25
	lpg1336	1.62	17.88
	lpg2641	1.29	8.34
Malate dehydrogenase	*lpg2352*	0.55	2.38
	lpg2971	0.60	12.13
3-oxoacyl (acyl carrier protein) synthase III	*lpg2228*	1.55	7.62
Hypothetical protein Lpg1368	*lpg1368*	2.27	3.48
LirA (Dot/Icm effector)	*lpg1960*	3.03	12.21

[a] Data were obtained from Faucher, S. et al. (2011). *Legionella pneumophila* transcriptome during intracellular multiplication in human macrophages. Front Microbiol 2: 1-18. T_{18}: 18 hours after infection, T_0: infection at zero time.

[b] Data were obtained from Brüggemann, H., et al. (2006). Virulence strategies for infecting phagocytes deduced from the *in vivo* transcriptional program of *Legionella pneumophila*. Cell Microbiol 8: 1228-1240. T_{14}: 14 hours after infection, T_8: 8 hours after infection.

experiments of *A. castellanii* and U937 monolayers using the green-fluorescent *L. pneumophila* MIFs obtained from amoebae and released from legionellae-laden pellets. Hany Abdelhady isolated *L. pneumophila* progenies from amoebae, U937 human macrophages, *Tetrahymena tropicalis* ciliates, HeLa cells and passed the progeny from U937 and THP-1 macropahges in amoebae. Hany also performed all the related experimental work; electron microscopy, challenge expeiments with antibiotics (gentamicin [different concentrations], ciprofloxacin), SDS, and chlorine (except for the experiments Eman did as outlined earlier). Hany also performed the intracellular growth and attachment experiments in L929 cells, *A. castellanii*, and U937 monolayers. Hany also performed the competition assay experiments in *A. castellanii*, and U937 monolayers and the proteome analysis the *L. pneumophila* progenies from amoebae and human macrophages and provided technical training and guidance to undergraduate students.

CHAPTER 4: *LEGIONELLA PNEUMOPHILA* UPREGULATES DIFFERENT SETS OF GENES DURING ITS DEVELOPMENTAL DIFFERENTIATION IN AMOEBAE, CILIATES AND HUMAN MACROPHAGES

4.1. Analysis of the gene expression profiles of *L. pneumophila* inside amoebae and macrophages indicates significant differences

We have demonstrated that the *L. pneumophila* progenies obtained from human macrophages are less differentiated and have fitness and infectivity disadvantages when compared to the progenies obtained from freshwater protozoa (Chapter 3). These observations can have potential implications on our understanding of the lack of LD transmission among humans. In order to understand the molecular mechanisms behind such observations, we set out to study the changes in gene expression of *L. pneumophila* during its differentiation into MIFs inside amoebae and human macrophages.

Gene expression analysis of *L. pneumophila* inside amoebae and human macrophages was based on the previously published studies that analyzed the global changes in the gene expression of *L. pneumophila* inside amoebae (Bruggemann *et al.*, 2006) and human macrophages (Faucher *et al.*, 2011) at different time points. The changes in gene expression of *L. pneumophila* between 8h (replicative traits) and 14h (late transmissive traits) post-infection of amoebae (Bruggemann *et al.*, 2006) were compared to the changes in gene expression of *L. pneumophila* at 18 hours (transmissive traits) and time zero inside human macrophages (Faucher *et al.*, 2011). I generated a list of genes that are selectively upregulated (showing at least 2-fold increase in gene expression) inside amoebae (**Appendix I**) or inside human macrophages (**Appendix II**). Genes that were differentially upregulated inside amoebae (in relation to human macrophages) include; hypothetical genes, suggesting that our current knowledge of the differentiation process in *L. pneumophila* is still limited, genes related to motility, genes involved in the synthesis of cyclic-di-GMP, suggesting that it could be important for *L. pneumophila* differentiation, *letE* and *csrA* (*csrA* was downregulated at later time points), suggesting that the differentiation of *L. pneumophila* inside human macrophages is incomplete, and *cpxR* and *uspA*, suggesting that *L. pneumophila* is under selective pressure to differentiate inside amoebae not in human macrophages.

I generated a short list of 20 genes (**Table 4.1.**) that have shown at least 4-fold upregulation during *L. pneumophila* infections of amoebae but are down-regulated (< 1-fold change) or unchanged (< 2-fold increase) in the progeny from human macrophages. I hypothesized that these genes could be important for the full differentiation of *L. pneumophila* inside its natural host and, therefore, could be important for the transmission of LD to susceptible humans. The list includes genes encoding effectors of the Dot/Icm protein secretion system, genes involved in carbohydrate and lipid metabolism, stress response, genes encoding virulence factors, genes required for bacterial adaptation, and hypothetical genes with no assigned functions. These genes were selected for confirmation by qRT-PCR analysis.

4.2. Gene expression profiling of the differentiated forms of *L. pneumophila* inside *Tetrahymena tropicalis* ciliates

Tetrahymena ciliates have been previously proposed as a differentiation model to identify the signals that trigger the development of SPFs into MIFs and study the genes that are actively transcribed during *L. pneumophila* differentiation (Faulkner *et al.*, 2008) because the differentiation process inside the ciliates is direct and rapid. Since the morphological features characteristic of MIFs could be observed as early as 30 minutes following feeding of the ciliates with legionellae in stationary phase (Faulkner *et al.*, 2008), analysis of the changes in gene expression of *L. pneumophila* around that time may identify the genes that are activated early during the differentiation process. The microarray analysis of the global changes in gene expression of the differentiating *L. pneumophila* MIFs recovered from *Tetrahymena tropicalis* 30 minutes after feeding compared to stationary phase forms (SPFs) were obtained through personal communications with David Allan, Dr. Celia Lima and Dr. Rafael Garduño. *L. pneumophila* genes that show at least 2-fold upregulation in expression inside *Tetrahymena* ciliates are listed in **Table 4.2**. *L. pneumophila* genes that are downregulated inside *Tetrahymena* ciliates are listed in **Table 4.3**.

We found that the expression levels of 115 genes were upregulated (at least 2-fold increase) inside *Tetrahymena* ciliates (**Table 4.2.**). These genes are expected to be correlated with the differentiation of *L. pneumophila*. Interestingly, about one third of the

Table 4.1. A short list of *L. pneumophila* genes that are selectively upregulated (≥ 2-fold increase) in amoebae MIFs (in relation to replicative forms in amoebae) but down-regulated (< 1-fold change) or unchanged (< 2-fold increase) in the progeny from human macrophages (in relation to stationary phase forms grown *in vitro*)

Gene ID	Description	*A. castellanii*[a] T_{14}/T_8	Human macrophages[b] T_{18}/T_0
lpg0910	Enhanced entry protein A	20.25	0.99
lpg0818	ATP-dependent Clp A protease	4.66	0.81
lpg0891	Sensory box protein/GGDEF/EAL domains	10.93	0.83
lpg1356	Enhanced entry protein C	11.63	0.77
lpg1491	Lem9 (Dot/Icm effector)	15.78	1.78
lpg0670	Hypothetical protein	8.94	0.66
lpg1669	Putative α-amylase	17.88	0.87
lpg1950	RalF (Dot/Icm effector)	9.13	2.50
lpg2228	3-oxoacyl ACP synthase III	7.62	1.55
lpg2316	3-hydroxybutyrate dehydrogenase	8.82	0.74
lpg1540	Universal stress protein A	4.66	1.94
lpg2348	Superoxide dismutase SodC	6.96	0.84
lpg2493	Heat shock protein HspC2	18.25	3.13
lpg2955	Integration host factor HipB	8.94	0.79
lpg2971	Malate dehydrogenase	12.13	0.60
lpg1639	Hypothetical protein	13.74	1.56
lpg0279	Hypothetical protein	9.45	0.67
lpg2495	Homospermidine synthase	7.26	1.06
lpg1368	Hypothetical protein	3.48	2.27
lpg1887	Hypothetical protein	11.00	0.91

[a] Data were obtained from Bruggemann, H., et al. (2006). Virulence strategies for infecting phagocytes deduced from the *in vivo* transcriptional program of *Legionella pneumophila*. Cell Microbiol 8: 1228-1240. T_{14}: 14 hours after infection, T_8: 8 hours after infection.

[b] Data were obtained from Faucher, S. et al. (2011). *Legionella pneumophila* transcriptome during intracellular multiplication in human macrophages. Front Microbiol 2: 1-18. T_{18}: 18 hours after infection, T_0: infection at zero time.

Table 4.2. List of *L. pneumophila* genes that are upregulated (> 2-fold increase) in differentiating MIFs recovered from *Tetrahymena tropicalis* 30 minutes after feeding, in relation to stationary phase forms grown *in vitro* (which were used to feed the ciliates).

Gene ID	Paris ID	Gene name	Description	Fold Change
lpg2156	***lpp2095***	*sdeB*	Dot/Icm system substrate SdeB	4.33
lpg1368	***lpp1322***	-	Hypothetical protein	4.12
lpg1887	***lpp1854***	-	Q-rich protein	3.89
lpg0818	***lpp0880***	*clpA*	ATP-dependent ClpA protease	3.79
lpg2810	***lpp2856***	-	Similar to conserved hypothetical protein	3.72
lpg1669	***lpp1641***	-	Putative α-amylase	3.57
lpg0817	***lpp0879***	*clpS*	ATP-dependent ClpS protease	3.40
lpg2510	**-**	-	SdcA	3.37
lpg2395	***lpp2461***	-	Hypothetical protein	3.37
lpg2181	***lpp2133***	-	Similar to response regulator	3.36
lpg0798	***lpp0860***	-	similar to proteins	3.34
-	***lpp2578***	*sdcA*	SdcA - paralog of SidC (Dot/Icm substrate)	3.25
lpg0892	***lpp0953***	*kmo*	Kynurenine 3-monooxygenase	3.25
lpg0476	***lpp0541***	-	Putative sigma-54 modulation protein	3.18
lpg1207	***lpp1209***	-	Similar to conserved hypothetical protein	3.15
lpg2521	**lpp2589**	-	Hypothetical protein	3.14
-	***lpp1260***	-	Hypothetical protein	3.06
lpg0009	***lpp0009***	-	Similar to host factor-1 protein	3.05
lpg1206	***lpp1208***	-	similar to protein	3.05
lpg0499	***lpp0561***	-	similar to carboxy-terminal protease family protein	3.05
-	***lpp0460***	-	Hypothetical protein	3.03
lpg1356	***lpp1310***	-	Hypothetical protein	3.02
lpg1154	***lpp1156***	-	Hypothetical protein	2.99
lpg1161	***lpp1163***		Similar to predicted phosphoribosyltransferase	2.98
lpg0847	***lpp0909***	*murA*	UDP-N-acetylglucosamine 1-carboxyvinyltransferase	2.98
lpg1385	***lpp1340***	-	Hypothetical protein	2.96
lpg0967	***lpp1029***	-	Hypothetical protein	2.96
-	***lpp2975***	-	Hypothetical protein	2.93
lpg1715	***lpp1680***	-	16 kD immunogenic protein	2.92
lpg0586	***lpp0636***	-	Similar to conserved hypothetical protein	2.91
lpg1485	***lpp1441***	-	Hypothetical protein	2.88
lpg2495	***lpp2562***	*hss*	Homospermidine synthase	2.87
lpg0848	***lpp0910***	-	Similar to conserved hypothetical protein	2.86

Table 4.1. continued

lpg0625	***lpp0679***	-	Similar to eukaryotic proteins	2.79
lpg0454	***lpp0520***	*icmD*	IcmD (Dot/Icm system substrate)	2.76
lpg1340	***lpp1294***	*flaA*	flagellin	2.75
lpg0846	***lpp0908***	-	Similar to conserved hypothetical protein	2.72
lpg0743	***lpp0808***	-	Hypothetical protein	2.69
lpg2639	***lpp2692***	*enhC*	enhanced entry protein EnhC	2.67
lpg0446	***lpp0512***	*icmO/dotL*	IcmO/DotL (Dot/Icm system substrate)	2.66
lpg0477	***lpp0542***	*rpoN*	RNA polymerase sigma-54 factor (sigma-L)	2.64
lpg1235	***lpp1080***	-	Hypothetical protein	2.62
lpg0267	***lpp0341***	-	Similar to magnesium and cobalt transport proteins	2.62
lpg1118	***lpp1119***	-	similar to D-alanyl-D-alanine carboxypeptidase	2.62
lpg2311	***lpp2259***	-	Hypothetical protein	2.62
lpg1993	***lpp1974***	-	Similar to putative polysaccharide deacetylase	2.61
lpg0853	***lpp0915***	*fleQ*	transcriptional regulator FleQ	2.56
lpg2222	***lpp2174***	-	Hypothetical protein	2.55
lpg2681	***lpp2735***	-	similar to aldolase	2.53
lpg2147	***lpp2086***	-	Hypothetical protein	2.53
lpg1793	***lpp1757***	-	Hypothetical protein	2.51
lpg0453	***lpp0519***	*icmC*/dotE	IcmC/DotE (Dot/Icm system substrate)	2.51
lpg1495	***lpp1452***	-	Hypothetical protein	2.48
lpg2348	***lpp2297***	*sodC*	Superoxide dismutase [Cu-Zn] precursor	2.48
lpg0380	***lpp0447***	-	Hypothetical protein	2.46
lpg1160	***lpp1162***	-	Hypothetical protein	2.45
lpg2971	***lpp3043***	*maeA*	Malate dehydrogenase	2.44
lpg0195	***lpp0253***	-	hypothetical	2.44
lpg2422	***lpp2487***	-	Some similarity with eukaryotic proteins	2.43
lpg1683	**-**	-	Hypothetical protein	2.43
lpg2364	**-**	-	Hypothetical protein	2.43
-	***lpp3061***	-	Hypothetical protein	2.42
lpg0910	***lpp0972***	*enhA*	Similar to enhanced entry protein EnhA	2.42
lpg1355	***lpp1309***	*sidG*	SidG protein- Dot/Icm system substrate	2.41
-	***lpp2559***	-	Similar to small heat shock protein	2.41
lpg2545	***lpp2612***	-	Hypothetical protein	2.41
lpg2073	**-**	-	Hypothetical protein	2.38
lpg1950	***lpp1932***	*ralF*	RalF (Dot/Icm system substrate)	2.34
lpg1526	***lpp1483***	-	Hypothetical protein	2.34
lpg2818	***lpp2871***	-	Similar to hypothetical protein	2.34
lpg2393	***lpp2460***	-	Similar to bacterioferritin	2.31
lpg1145	***lpp1147***	-	Hypothetical protein	2.31
lpg2074	**-**	-	Hypothetical protein	2.30
lpg0940	***lpp1002***	*lidA*	LidA (Dot/Icm system substrate)	2.30

Table 4.1. continued

lpg1055	***lpp2327***	-	Hypothetical protein	2.30
lpg0741	***lpp0806***	-	Hypothetical protein	2.30
lpg2315	***lpp2263***	-	Hypothetical protein	2.28
-	***lpp1652***	-	Hypothetical protein	2.27
-	***lpp0052***	-	Hypothetical protein	2.25
lpg1011	***lpp2368***	-	Hypothetical protein	2.24
lpg1963	**-**	-	Hypothetical protein	2.23
-	***lpp2567***	-	Hypothetical protein	2.23
lpg0245	***lpp0315***	-	NAD-glutamate dehydrogenase	2.22
lpg2157	***lpp2096***	*sdeA*	SdeA	2.21
lpg1782	***lpp1746***	*fliA*	sigma factor 28	2.21
lpg2578	***lpp2630***	-	Hypothetical protein	2.20
lpg1960	***lpp1942***	-	Hypothetical protein	2.20
lpg1309	***lpp1273***	-	Hypothetical protein	2.17
lpg2316	***lpp2264***	*bdhA*	3-hydroxybutyrate dehydrogenase	2.17
lpg1784	***lpp1748***	*flhF*	Flagellar biosynthesis protein FlhF	2.16
-	***lpp1800***	-	Hypothetical protein	2.16
-	***lpl2384***	-	Hypothetical protein	2.16
lpg2811	***lpp2857***	-	Similar to conserved hypothetical protein	2.13
lpg2641	***lpp2694***	*enhA*	EnhA: enhanced entry protein A	2.13
lpg0737	***lpp0802***	-	Similar to conserved hypothetical protein	2.13
lpg2258	***lpp2212***	-	Putative membrane protein	2.09
lpg2301	***lpp2249***	-	Hypothetical protein	2.08
lpg0279	***lpp0354***	-	Similar to conserved hypothetical protein	2.07
lpg1885	***lpp1849***	-	Hypothetical protein	2.07
lpg2351	***lpp2300***	-	Hypothetical protein	2.06
lpg1783	***lpp1747***	*fleN*	similar to flagellar synthesis regulator	2.05
lpg0156	***lpp0220***	-	regulatory protein (EAL domain)	2.04
lpg2524	**-**	-	Hypothetical protein	2.04
lpg0013	***lpp0013***	-	Similar to other protein	2.03
lpg1491	***lpp1447***	-	Some similarity with eukaryotic proteins	2.03
lpg2310	***lpp2258***	*murI*	similar to glutamate racemase	2.02
lpg1925	***lpp1900***	-	Hypothetical protein	2.02
lpg0445	***lpp0511***	*icmP/dotM*	IcmP/DotM (Dot/Icm system substrate)	2.02
lpg2642	***lpp2695***	-	regulatory protein (GGDEF and EAL domains)	2.02
lpg0426	***lpp0493***	*cspD*	similar to Cold shock-like protein CspD	2.01
lpg2017	***lpp1999***	-	Hypothetical protein	2.01
lpg0441	***lpp0507***	*icmT*	IcmT (Dot/Icm system substrate)	2.00

Table 4.3. List of *L. pneumophila* genes that are downregulated (≤ 0.5-fold change) in differentiating MIFs recovered from *Tetrahymena tropicalis* 30 minutes after feeding, in relation to stationary phase forms grown *in vitro* (which were used to feed the ciliates).

Gene ID	Paris ID	Gene name	Description	Fold Change
lpg2884	***lpp2943***	-	Hypothetical protein	0.05
lpg0320	***lpp0385***	*rplJ*	50S ribosomal subunit protein L1	0.07
lpg2668	***lpp2722***	*ftsX*	Cell division protein FtsX	0.08
-	***lpp0392***	*tufA2*	translation elongation factor Tu	0.11
lpg0321	***lpp0386***	*rplL*	50S ribosomal subunit protein L7/L12	0.12
lpg2987	***lpp3058***	*atpE*	H^+-transporting ATP synthase chain c	0.12
lpg0326	***lpp0391***	*fusA*	translation elongation factor G	0.12
lpg0327	**-**	-	Hypothetical protein	0.12
lpg2850	***lpp2908***	-	Similar to cold shock protein	0.13
lpg2825	***lpp2878***	-	Similar to cold shock protein CspC	0.13
lpg2518	***lpp2586***	-	Hypothetical protein	0.14
lpg2650	***lpp2703***	*rpmA*	50S ribosomal protein L27	0.14
lpg2509	***lpp2577***	*sdeD*	SdeD protein (substrate of the Dot/Icm system)	0.14
lpg2769	***lpp2817***	*rpsO*	30S ribosomal protein S15	0.14
lpg0399	***lpp0466***	*rpsP*	Highly similar to 30S ribosomal protein S16	0.14
lpg0301	***lpp0379***	-	similar to eukaryotic proteins	0.15
lpg2636	***lpp2689***	*rpsT*	30S ribosomal subunit protein S20	0.15
lpg2984	***lpp3055***	*atpA*	H^+-transporting ATP synthase chain alpha	0.16
lpg0395	***lpp0463***	*rplS*	50S ribosomal protein L19	0.17
lpg1592	***lpp1550***	*rpsF*	30S ribosomal protein S6	0.17
lpg0325	***lpp0390***	*rpsG*	30S ribosomal protein S7	0.17
lpg0346	***lpp0411***	*rpsE*	30S ribosomal subunit protein S5	0.18
lpg1588	***lpp1546***	*legC6*	Coiled-coil-containing protein	0.18
lpg2652	***lpp2705***	*rplY*	50S ribosomal subunit protein L25- RplY	0.18
lpg1591	***lpp1549***	*rpsR*	30S ribosomal subunit protein S18	0.19
lpg0781	***lpp0845***	*csrA*	global regulator CsrA	0.19
lpg0791	***lpp0855***	*mip*	macrophage infectivity potentiator	0.19
lpg0507	***lpp0570***	-	similar to putative outer membrane proteins	0.19
lpg0436	***lpp0503***	-	Ankyrin repeat protein	0.20
-	***lpp0398***	*rpsS*	30S ribosomal subunit protein S19	0.20
lpg2706	***lpp2761***	*rpsI*	30S ribosomal subunit protein S9	0.20
lpg1548	***lpp1505***	*ndk*	similar to nucleoside diphosphate kinase	0.20
lpg1393	***lpp1348***	*fabH*	3-oxoacyl-[acyl-carrier-protein] synthase III	0.21

Table 4.2. continued

lpg0687	***lpp0742***	*groES*	1 kDa chaperonin (groES protein)	0.21
lpg2976	***lpp3048***	-	Hypothetical protein	0.21
lpg2651	***lpp2704***	*rplU*	50S ribosomal protein L21	0.22
lpg0352	***lpp0417***	*rpsK*	30S ribosomal protein S11	0.22
lpg2702	***lpp2757***	*sspA*	stringent starvation protein A	0.23
lpg0319	***lpp0384***	*rplA*	50S ribosomal protein L1	0.23
lpg1918	***lpp1893***	-	weakly similar to endoglucanase	0.24
lpg2345	***lpp2294***	*deaD*	ATP-dependent RNA helicase	0.24
lpg0518	***lpp0581***	-	Hypothetical protein	0.24
lpg0138	***lpp0153***	*gap*	glyceraldehyde 3-phosphate dehydrogenase	0.25
lpg2361	***lpp2310***	*rpoD*	RNA polymerase sigma factor RpoD	0.25
lpg0024	***lpp0024***	*hbp*	hemin binding protein	0.26
lpg0479	***lpp0544***	*rpmB*	50S ribosomal protein L28	0.26
lpg1697	***lpp1662***	-	conserved hypothetical protein	0.26
lpg0730	***lpp0796***	-	Similar to predicted permease	0.26
lpg0347	***lpp0412***	*rpmD*	50S ribosomal subunit protein L3	0.26
lpg0324	***lpp0389***	*rpsL*	30S ribosomal protein S12	0.27
-	***lpp2768***	*rpmI*	50S ribosomal protein L35	0.27
lpg0810	***lpp0872***	-	Hypothetical protein	0.27
lpg2321	***lpp2269***	*sdaC*	Similar to serine transporter	0.27
lpg2121	***lpp2041***	-	Similar to cold shock protein	0.27
lpg0342	***lpp0407***	*rpsN*	30S ribosomal protein S14	0.27
lpg0351	***lpp0416***	*rpsM*	30S ribosomal protein S13	0.27
lpg0318	***lpp0383***	*rplK*	50S ribosomal protein L11	0.28
lpg2983	***lpp3054***	*atpG*	H^+-transporting ATP synthase chain gamma	0.28
lpg0335	***lpp0400***	*rpsC*	30S ribosomal protein S3	0.28
lpg1858	***lpp1826***	*hubB*	similar to DNA-binding protein HU-beta	0.28
lpg0353	***lpp0418***	*rpsD*	30S ribosomal subunit protein S4	0.28
lpg0345	***lpp0410***	*rplR*	50S ribosomal subunit protein L18	0.29
lpg0322	***lpp0387***	*rpoB*	RNA polymerase B-subunit	0.29
lpg0328	***lpp0393***	*rpsJ*	30S ribosomal subunit protein S1	0.29
lpg2707	***lpp2762***	*rplM*	50S ribosomal subunit protein L13	0.29
lpg1713	***lpp1678***	*tsf*	Elongation factor Ts (EF-Ts)	0.29
lpg0396	***lpp0464***	*trmD*	tRNA (guanine-N1)-methyltransferase	0.29
lpg2508	***lpp2576***	-	Hypothetical protein	0.29
lpg2934	***lpp3002***	*rho*	transcription termination factor Rho	0.29
lpg2814	***lpp2866***	-	Similar to aminopeptidase	0.30
lpg2982	***lpp3053***	*atpD*	H^+-transporting ATP synthase beta chain	0.30
lpg0344	***lpp0409***	*rplF*	50S ribosomal subunit protein L6	0.30
lpg2586	***lpp2639***	-	weakly similar to cysteine protease	0.30
lpg1395	***lpp1350***	*fabG*	3-oxoacyl-[acyl-carrier protein] reductase	0.30

Table 4.2. continued

lpg2248	***lpp2202***	-	Hypothetical protein	0.30
lpg0722	***lpp0788***	-	Hypothetical protein	0.30
lpg1362	***lpp1316***	*lspG*	type II secretory pathway protein LspG	0.31
-	***lpp1220***	-	Simimlar to thiocyanate hydrolase alpha subunit	0.31
lpg0336	***lpp0401***	*rplP*	50S ribosomal protein L16	0.31
lpg0354	***lpp0419***	*rpoA*	DNA-directed RNA polymerase alpha chain	0.31
lpg0339	***lpp0404***	*rplN*	50S ribosomal protein L14	0.31
lpg2791	***lpp2837***	*secG*	Preprotein translocase SecG subunit	0.32
lpg2713	***lpp2769***	*infC*	Translation initiation factor IF-3	0.32
lpg2213	***lpp2164***	-	Similar to hemin binding protein Hbp	0.32
lpg0331	***lpp0396***	*rplW*	50S ribosomal subunit protein L23	0.32
lpg2701	***lpp2756***	*sspB*	similar to stringent starvation protein B	0.32
lpg0316	***lpp0381***	*secE*	Preprotein translocase SecE subunit	0.32
lpg0330	***lpp0395***	*rplD*	50S ribosomal subunit protein L4	0.32
lpg2358	***lpp2307***	*rpsU*	30S ribosomal protein S21	0.32
lpg0334	***lpp0399***	*rplV*	50S ribosomal subunit protein L22	0.32
lpg1743	***lpp1707***	*fis*	DNA-binding protein Fis	0.32
lpg2768	***lpp2816***	*pnp*	Polynucleotide phosphorylase (PNPase)	0.33
lpg1723	***lpp1688***	*guaB*	similar to IMP dehydrogenase/GMP reductase	0.33
lpg1391	***lpp1346***	*rpmF*	50S ribosomal subunit protein L32	0.33
lpg1722	***lpp1687***	*guaA*	similar to GMP synthetase (glutamine-hydrolyzing)	0.33
lpg2577	***lpp2629***	-	Hypothetical protein	0.34
lpg0959	***lpp1021***	-	Similar to extracellular solute-binding protein	0.34
lpg2714	***lpp2770***	*thrS*	Threonyl t-RNA synthetase	0.34
lpg0329	***lpp0394***	*rplC*	50S ribosomal subunit protein L3	0.34
lpg0341	***lpp0406***	*rplE*	50S ribosomal protein L5	0.34
lpg0338	***lpp0403***	*rpsQ*	30S ribosomal protein S17	0.34
lpg0650	***lpp0704***	*rpmE*	50S ribosomal protein L31	0.35
-	***lpp0964***	-	Similar to hypothetical protein	0.35
lpg0340	***lpp0405***	*rplX*	50S ribosomal protein L24	0.35
lpg1590	***lpp1548***	-	Hypothetical protein	0.35
lpg1421	***lpp1376***	*rpsA*	30S ribosomal protein S1	0.35
lpg1396	***lpp1351***	*acp*	Acyl carrier protein (ACP)	0.36
-	***lpp2926***	-	Hypothetical protein	0.36
lpg0214	***lpp0273***	-	Predicted membrane protein- similar to conserved hypothetical protein LrgA	0.36
lpg1453	***lpp1409***	-	Hypothetical protein	0.36
lpg0343	***lpp0408***	*rpsH*	30S ribosomal protein S8	0.36
lpg2882	***lpp2941***	*metG*	methionyl-tRNAsynthetase	0.37
lpg0478	***lpp0543***	*rpmG*	50S ribosomal subunit protein L33	0.37
lpg0394	***lpp0462***	-	similar to methylated-DNA-protein-cysteine S-methyltransferase	0.37

Table 4.2. continued

lpg0349	***lpp0414***	*secY*	Preprotein translocase- SecY subunit	0.37
lpg1156	***lpp1158***	-	Similar to aminopeptidase	0.38
lpg1685	**-**	-	Hypothetical protein	0.38
lpg2985	***lpp3056***	*atpH*	H^+-transporting ATP synthase chain delta	0.38
lpg0019	***lpp0019***	-	Similar to zinc metalloproteinase precursor	0.38
lpg0693	***lpp0748***	-	LigA protein (Legionella Infectivity Gene A)	0.39
lpg1721	***lpp1686***	-	similar to hypothetical proteins	0.39
lpg2986	***lpp3057***	*atpF*	H^+-transporting ATP synthase chain b	0.39
lpg1364	***lpp1318***	*glnA*	glutamine synthetase	0.39
lpg0126	***lpp0140***	-	Hypothetical protein	0.39
lpg2599	***lpp2652***	*topA*	DNA topoisomerase I	0.39
lpg1124	***lpp1125***	-	Hypothetical protein	0.40
lpg0332	***lpp0397***	*rplB*	50S ribosomal subunit protein L2	0.40
lpg1392	***lpp1347***	*plsX*	Fatty acid/phospholipid synthesis protein	0.40
lpg0740	***lpp0805***	*omp*	similar to surface antigens (17 kDa)	0.41
lpg0137	***lpp0152***	*pgk*	phosphoglycerate kinase	0.41
lpg0688	***lpp0743***	*htpB*	60 kDa chaperonin (groEL protein) (Heat shock protein B).	0.42
-	***lpp3032***	-	major outer membrane protein	0.42
lpg1331	***lpp1285***	*htrA*	periplasmic serine protease Do; heat shock protein HtrA	0.42
lpg1776	***lpp1740***	-	Hypothetical protein	0.42
lpg0925	***lpp0987***	*mrcA*	Similar to peptidoglycan synthetase; penicillin-binding protein 1A	0.42
lpg1177	***lpp1180***	*ribD*	Riboflavin biosynthesis protein RibD	0.42
lpg0337	***lpp0402***	*rpmC*	50S ribosomal subunit protein L29	0.42
lpg1861	***lpp1829***	*clpP*	ATP-dependent Clp protease proteolytic subunit	0.42
lpg0540	***lpp0604***	-	similar to putative transport proteins (phagosomal transporter A)	0.42
lpg2327	***lpp2275***	-	Hypothetical protein	0.43
lpg1994	***lpp1975***	*mltA*	Similar to membrane-bound lytic murein transglycosylase	0.43
lpg1547	***lpp1504***	-	similar to conserved hypothetical protein	0.43
lpg1478	***lpp1434***	*aspS*	Aspartyl-tRNAsynthetase	0.44
lpg2625	***lpp2678***	*carB*	carbamoyl-phosphate synthase large subunit	0.44
lpg0634	***lpp0688***	-	Hypothetical protein	0.44
lpg2822	***lpp2875***	*typA*	Similar to GTP-binding protein TypA/BipA	0.44
lpg0005	***lpp0005***	-	similar to peptidyl arginine deiminase	0.44
lpg2623	***lpp2676***	-	Hypothetical protein	0.44
lpg0638	***lpp0692***	-	Similar to major facilitator family transporter	0.45
lpg3005	***lpp3077***	*rpmH*	50S ribosomal protein L34	0.45
lpg0749	***lpp0815***	*hisF1*	imidazole glycerol phosphate synthase subunit HisF	0.45
lpg0355	***lpp0420***	*rplQ*	50S ribosomal protein L17	0.45

Table 4.2. continued

lpg0639	***lpp0693***	*deoB*	Phosphopentomutase	0.45
lpg0317	***lpp0382***	*nusG*	transcription anti-termination protein NusG	0.45
lpg1862	***lpp1830***	*tig*	peptidyl-prolyl cis-trans isomerase (trigger factor)	0.45
lpg1350	***lpp1304***	-	Similar to dehydrogenase	0.45
lpg0467	***lpp0532***	*proA1*	zinc metalloproteinase precursor	0.45
lpg1476	***lpp1432***	-	Similar to conserved hypothetical protein	0.46
lpg2937	***lpp3005***	*fumC*	Fumarate hydratase- class II	0.46
lpg2981	***lpp3052***	*atpC*	H^+-transporting ATP synthase epsilon chain	0.46
lpg2885	***lpp2944***	-	Putative secreted protein	0.46
lpg0275	***lpp0349***	*sdbA*	SdbA protein- Dot/Icm system substrate	0.46
lpg0702	***lpp0757***	*tdh*	threonine dehydrogenase	0.47
lpg1426	***lpp1381***	-	Hypothetical protein	0.48
lpg2924	***lpp2991***	-	conserved lipoprotein	0.48
lpg0903	***lpp0965***	-	Similar to protease	0.48
lpg1137	***lpp1139***	-	Hypothetical protein	0.48
lpg1809	***lpp1772***	-	Hypothetical protein	0.48
lpg1424	***lpp1379***	-	similar to polysaccharide biosynthesis protein	0.48
lpg2052	***lpp2035***	-	Similar to 3-hydroxy-3-methyl glutaryl-coenzyme A reductase	0.48
lpg0811	***lpp0873***	*mreB*	Rod shape-determining protein MreB	0.48
lpg2772	***lpp2820***	*infB*	Translation initiation factor IF-2	0.48
lpg0397	***lpp0465***	*rimM*	similar to 16S rRNA processing protein RimM	0.49
lpg2989	***lpp3060***	*atpI*	Similar to ATP synthase subunit I	0.49
lpg0348	***lpp0413***	*rplO*	50S ribosomal subunit protein L15	0.49
lpg0704	***lpp0759***	*enhA*	Similar to enhanced entry protein EnhA	0.49
lpg0542	***lpp0606***	*fis*	similar to DNA-binding proteins Fis	0.50

genes (48 genes) were hypothetical with no assigned functions, suggesting that our knowledge of the intracellular differentiation mechanisms of *L. pneumophila* is still limited. Other genes encoded Dot/Icm effectors such as RalF, which is involved in the inhibition of phagosome maturation and trafficking (Nagai & Roy, 2003; Luo & Isberg, 2004), the *enhABC* genes which encode the enhanced entry proteins A, B, and C respectively, which are involved with the initial encounters of *L. pneumophila* with host cells (Cirillo *et al.*, 2000), genes involved in utilization and accumulation of energy sources, flagellum biosynthesis, adaptation, detoxification, and modulation of the intracellular levels of c-di-GMP. This is the first report of the *L. pneumophila* transcriptome profile inside the food vacuoles of *Tetrahymena* ciliates. A short list of 15 genes that showed at least 2-fold upregulation inside *Tetrahymena* ciliates, 4-fold upregulation inside *A. castellanii*, and no change or downregulation inside human macrophages was generated (**Table 4.4.**). These genes were selected for confirmation by qRT-PCR analysis.

4.3. Confirmation of the microarray data using qRT-PCR

The integrity and purity of RNA isolated from different *L. pneumophila* samples (exponential phase forms, stationary phase forms, the progenies obtained from *A. castellanii* and U937 human macrophages, the replicative forms recovered from *A. castellanii* 8 hours after infection, and the differentiating MIFs recovered from *Tetrahymena tropicalis* 30 minutes after feeding) were confirmed using agarose gel electrophoresis. Two distinct bands representing 16S and 23S rRNA and a smear that represents mRNA were clearly visible in each sample (**Figure 4.1.**). The quality of the isolated RNA samples was also tested by measuring the absorbance at wavelengths of 260 and 280 nm followed by determination of the A_{260}/A_{280} ratio. Samples that had a ratio of 1.8-2 were selected for further experiments.

The digestion of genomic DNA in the isolated RNA samples using DNase I enzyme and the subsequent synthesis of cDNA were confirmed using PCR experiments. The absence of PCR amplicons when DNaseI-treated RNA samples were used as templates confirms the complete digestion of genomic DNA (lanes labelled RNA). The

Table 4.4. A short list of genes upregulated inside *Tetrahymena* ciliates that were selected for confirmation by qRT-PCR

Gene ID	Description	Expression level (T_{30}/SPFs)
lpg0910	Enhanced entry protein EnhA	2.41
lpg0279	Hypothetical protein	2.07
lpg0818	ATP-dependent Clp protease ATP-binding subunit	3.79
lpg1356	Enhanced entry protein EnhC	2.99
lpg1368	Hypothetical protein	4.12
lpg1491	Dot/Icm effector Lem9	2.02
lpg1540	Universal stress protein A UspA	1.85
lpg1669	A putative alpha-amylase	3.57
lpg1950	Dot/Icm effector RalF	2.34
lpg2316	3-hydroxybutyrate dehydrogenase BdhA	2.16
lpg2348	Cu-Zn Superoxide dismutase SodC	2.46
lpg2493	Similar to small heat shock protein HspC2	2.41
lpg2971	Malate dehydrogenase	2.44
lpg1887	Hypothetical protein	3.89
lpg2495	Similar to homospermidine synthase	2.86

[a] T_{30}: 30 minutes after ingestion, SPFs: stationary phase forms.

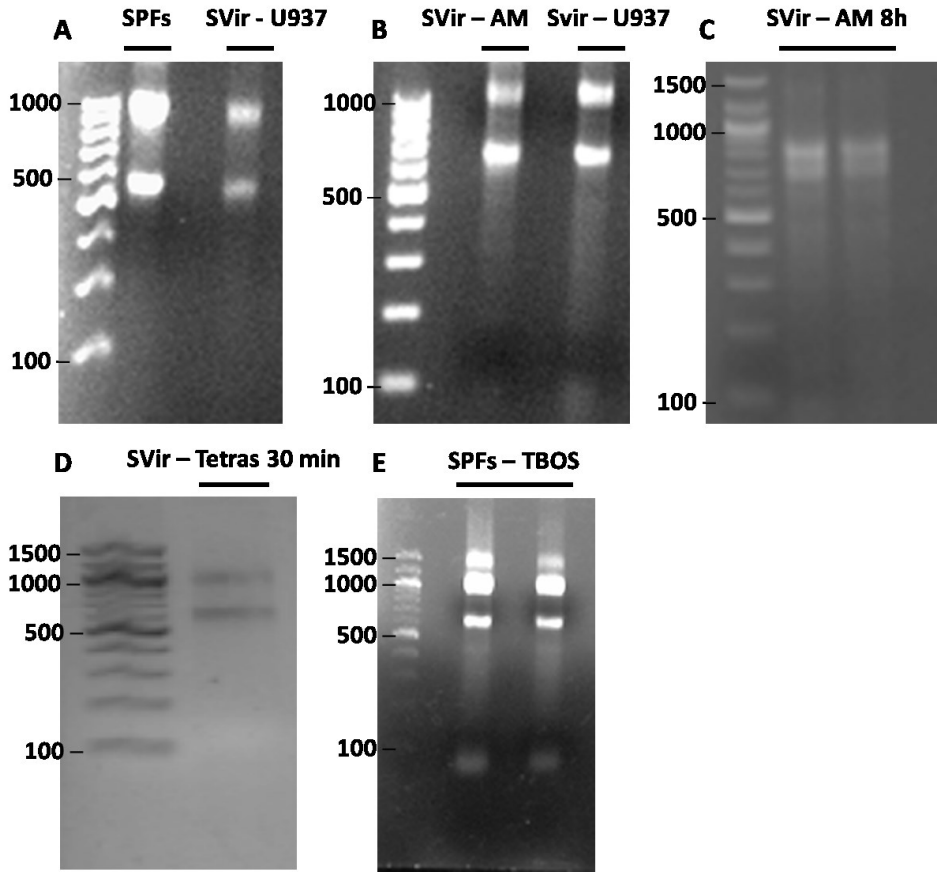

Figure 4.1. Isolation of RNA from *L. pneumophila* Lp1-Svir grown *in vitro* and from the progenies produced in different hosts.

Ethidium bromide-stained agarose gels showing RNA isolated from *L. pneumophila* Lp1-SVir (A) stationary phase forms (SPFs) and the progeny from U937 macrophages (SVir – U937), respectively; (B) the progenies produced in *A. castellanii* (SVir – AM) and U937 cells (SVir – U937), respectively; (C) replicative forms recovered 8 hours after infection of *A. castellanii* (SVir – AM 8h); two independent samples, (D) differentiating MIFs recovered 30 minutes after feeding into *Tetrahymena tropicalis* (SVir – Tetras 30 min), (E) Stationary phase forms incubated in TBOS for 30 minutes (SPFs – TBOS). Two bands representing 23S and 16S rRNA were visible, and the smear in each sample represents mRNA. NEB 100-bp DNA ladder was used as a size reference in all panels. This figure was generated by Emma-Jean Slobodesky, Jungmin Kim, and Hany Abdelhady.

presence of PCR amplicons when the synthesized cDNA samples were used as templates confirms the successful synthesis of cDNA (lanes labelled cDNA) (**Figure 4.2.)**.

Quantitative real-time PCR (qRT-PCR) analysis supported the microarray data for the selected set of genes of *L. pneumophila* (**Table 4.5.**) that are upregulated in *A. castellanii* when comparing expression profiles of *L. pneumophila* progeny obtained after 3 days and RFs collected after 8 hours and downregulated inside human macrophages (**Table 4.6.**). The qRT-PCR analysis serves as a validation tool of the approximate gene expression levels obtained by microarray experiments. The qRT-PCR analysis demonstrated that the expression levels of the tested genes were upregulated in the amoeba-produced progeny and therefore validated the early microarray results. It is important to mention that the expression levels of the majority of the tested genes at 3 days (determined by qRT-PCR analysis) were generally higher than the expression levels at 14 hours [determined by microarray analysis (Bruggemann *et al.*, 2006)], supporting the notion that the tested genes are correlated with *L. pneumophila* differentiation.The gene *lpg1669* which encodes a putative α-amylase had the most dramatic upregulation (166-fold) in the final progenies obtained from amoebae. Interestingly, the protein products of 14 genes in this list were also upregulated in the *L. pneumophila* progenies obtained from amoebae (Chapter 3), which further supports the importance of these genes in the differentiation of *L. pneumophila* in its natural environment and provides a strong correlation between our gene expression and proteome analysis experiments.

The qRT-PCR analysis of the selected 15 upregulated genes inside *Tetrahymena* ciliates was performed to validate the microarray global expression data. The analysis of gene expression in the differentiating *L. pneumophila* MIFs recovered 30 minutes after feeding of *T. tropicalis* ciliates was compared to SPFs incubated in TBOS for a similar period of time. The gene *ftsZ*, which is involved in cell division, was selected as an internal control for the qRT-PCR experiments because its expression levels were constant throughout the feeding experiments, according to the microarray analysis (**Table 4.7.**). The expression levels of the majority of the tested genes had a good correlation between the microarray results and qRT-PCR analysis. Therefore, our qRT-PCR analysis validates the previously published microarray data (Bruggemann *et al.*, 2006). It is of interest to mention that the expression of 12 out of the tested 15 genes was also upregulated at later

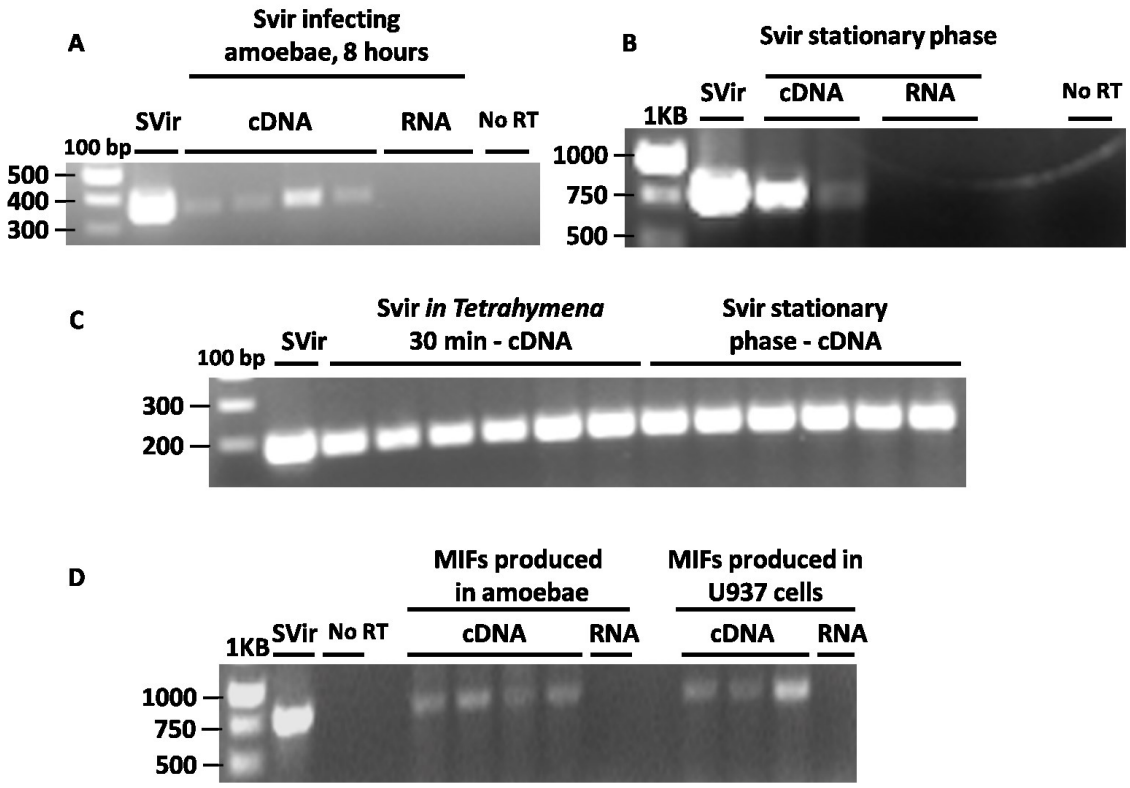

Figure 4.2. Ethidium bromide-stained agarose gels to confirm cDNA synthesis from different samples of RNA isolated from *L. pneumophila* Lp1-SVir.

Synthesis of cDNA was performed on RNA samples isolated from; (A) replicative forms recovered 8 hours after infection of *A. castellanii*, (B) stationary phase forms, (C) differentiating MIFs recovered 30 minutes after feeding of *Tetrahymena tropicalis* ciliates, (D) progenies obtained from amoebae and macrophages. The following primer pairs were used; lpg2884F- lpg2884R (A), htpBF-htpBR (B), 5srDNAF-5srDNAR (C), and htpBF- htpBR (D). Lanes labelled SVir, where the genomic DNA was used as a template, served as (+) controls for the primer performance and PCR amplification. Lanes labelled RNA represent DNase I-treated RNA samples that were used to confirm that RNA samples do not carry contaminating DNA. The absence of visible bands in these lanes confirms the complete digestion of genomic DNA. Lanes labelled no RT represent DNase I-treated RNA samples to which random hexamers, DTT, enzyme buffer, but no reverse transcriptase enzyme were added and serve as (-) controls for the PCR amplification. NEB 100bp and Fermentas 1 kb DNA ladders were used as size

references. This figure was generated by Emma-Jean Slobodesky, Jungmin Kim, and Hany Abdelhady.

Table 4.5. Expression profiles of selected *L. pneumophila* genes during infection of *A. castellanii*

This table was generated by Emma-Jean Slobodesky and Hany Abdelhady.

Gene ID	Description	Level of expression (MIFs)[a]	Level of expression (8 hours)[a]	$\Delta\Delta C_t$	$2^{\Delta\Delta C_t}$
lpg0910	Enhanced entry protein A	1.54 ± 0.42	0.24 ± 1.17	1.3	2.46
lpg0818	ATP-dependent Clp A protease	3.88 ± 0.1	0.48 ± 0.085	3.4	10.56
lpg0891	Sensory box protein/GGDEF/EAL domains	1.41 ± 0.14	-1.54 ± 1.35	2.94	7.69
lpg1356	Enhanced entry protein C	3.49 ± 0.27	-0.323 ± 0.12	3.82	14.09
lpg1491	Lem9 (Dot/Icm effector)	5.32 ± 0.13	1.28 ± 0.01	4.04	16.44
lpg0670	Hypothetical protein	2.47 ± 0.49	-1.32 ± 0.7	3.79	13.8
lpg1669	Putative α-amylase	5.42 ± 0.51	-1.95 ± 0.31	7.38	166
lpg1950	RalF (Dot/Icm effector)	3.58 ± 0.19	-0.16 ± 0.54	3.74	13.4
lpg2228	3-oxoacyl ACP synthase III	1.097 ± 0.83	-0.803 ± 0.37	1.9	3.73
lpg2316	3-hydroxybutyrate dehydrogenase	4.46 ± 1.29	2.84 ± 0.42	1.62	3.1
lpg1540	Universal stress protein A	0.34 ± 0.3	-2.2 ± 0.31	2.54	5.8
lpg2348	Superoxide dismutase SodC	2.97 ± 0.16	0.45 ± 0.86	2.52	5.7
lpg2493	Heat shock protein HspC2	8.36 ± 0.46	4.31 ± 0.48	4.05	16.6
lpg2955	Integration host factor HipB	3.32 ± 0.16	0.29 ± 0.72	3.03	8.15
lpg2971	Malate dehydrogenase	2.11 ± 1.44	0.67 ± 1.7995	1.44	2.71
lpg1639	Hypothetical protein	0.76 ± 0.156	-3.66 ± 0.15	4.42	21.4
lpg0279	Hypothetical protein	2.395 ± 0.09	-2.26 ± 0.38	4.65	25.1
lpg2495	Homospermidine synthase	0.86 ± 0.14	-2.77 ± 0.15	3.63	12.38
lpg1368	Hypothetical protein	5.26 ± 1.13	2.79 ± 0.87	2.47	5.54
lpg1887	Hypothetical protein	3.367 ± 0.15	1.43 ± 0.57	1.93	3.82

[a]Levels of expression were measured relative to the expression of the gene *gyrA*, as an internal control.

Table 4.6. Expression profiles of selected *L. pneumophila* genes during infection of U937 human macrophages.

Gene ID	Description	Level of expression (MIFs)[a]	Level of expression (T_0)[a]	$\Delta\Delta C_t$	$2^{\Delta\Delta C_t}$
lpg0910	Enhanced entry protein A	5.94 ± 0.56	6.93 ± 1.74	-0.99	0.5
lpg0818	ATP-dependent ClpA protease	7.96 ± 0.17	7.24 ± 0.7	0.72	1.64
lpg0891	Sensory box protein/GGDEF/EAL domains	3.62 ± 0.4	4.3 ± 0.264	-0.68	0.62
lpg1356	Enhanced entry protein C	5.18 ± 0.77	4.16 ± 1.09	1.02	2.2
lpg1491	Lem9 (Dot/Icm effector)	5.87 ± 0.44	5.04 ± 1.04	0.83	1.77
lpg0670	Hypothetical protein	4.61 ± 0.55	5.82 ± 0.35	-1.21	0.43
lpg1169	Putative α-amylase	7.09 ± 1.66	7.55 ± 1.95	-0.46	0.72
lpg1950	RalF (Dot/Icm effector)	6.12 ± 0.22	5.06 ± 0.42	1.06	2.08
lpg2228	3-oxoacyl ACP synthase III	3.93 ± 1.59	3.39 ± 1.96	0.54	1.45
lpg2316	3-hydroxybutyrate dehydrogenase	7.69 ± 0.17	10.47 ± 2.08	-2.79	0.15
lpg1540	Universal stress protein A	0.69 ± 0.18	1.06 ± 0.22	-0.37	0.77
lpg2348	Superoxide dismutase SodC	4.16 ± 1.19	4.09 ± 0.39	0.07	1.04
lpg2493	Heat shock protein HspC2	10.08 ± 0.77	10.9 ± 2.83	-0.81	0.56
lpg2955	Integration host factor HipB	3.4 ± 0.67	3.13 ± 0.78	0.27	1.2
lpg2971	Malate dehydrogenase	5.52 ± 0.88	8.07 ± 1.8	-2.55	0.17
lpg1639	Hypothetical protein	3.69 ± 0.44	5.4 ± 0.72	-1.72	0.304
lpg0279	Hypothetical protein	4.29 ± 0.49	3.12 ± 0.2	1.17	2.26
lpg2495	Homospermidine synthase (*hss*)	1.17 ± 0.3	3.09 ± 0.68	-1.92	0.26
lpg1368	Hypothetical protein	5.99 ± 0.35	6.25 ± 0.87	-0.26	0.83
lpg1887	Hypothetical protein	5.42 ± 0.2	5.04 ± 0.5	0.38	1.3

[a]Levels of expression were measured relative to the expression of the gene *gyrA*, as an internal control. T_0: infection at zero time.

Table 4.7. Expression profiles of selected *L. pneumophila* genes inside *Tetrahymena tropicalis* ciliates.

This table was generated by Jungmin Kim and Hany Abdelhady.

Gene ID	Description	Level of expression (T30)[a]	Level of expression (SPF)[a]	$\Delta\Delta C_t$	$2^{\Delta\Delta C_t}$
lpg0910	Enhanced entry protein A, EnhA	4.7 ± 1.3	4.17 ± 0.88	0.54	1.45
lpg0818	ATP-dependent ClpA protease	3.88 ± 0.33	3.48 ± 0.55	0.41	1.33
lpg1356	Enhanced entry protein C, EnhC	2.98 ± 0.34	0.46 ± 0.06	2.53	5.76
lpg1491	Lem9 (Dot/Icm effector)	0.76 ± 0.38	-2.03 ± 0.329	2.8	6.9
lpg1540	Universal stress protein A	0.34 ± 0.4	0.037 ± 0.29	0.3	1.3
lpg1669	Putative α-amylase	3.48 ± 0.68	2.43 ± 0.96	1.05	2.1
lpg1950	RalF (Dot/Icm effector)	1.19 ± 0.9	-0.38 ± 0.83	1.57	2.97
lpg1368	Hypothetical protein	1.86 ± 0.26	0.67 ± 0.015	1.19	2.27
lpg2316	3-hydroxybutyrate dehydrogenase	6.56 ± 0.16	5.4 ± 0.77	1.16	2.23
lpg2348	Superoxide dismutase SodC	3.17 ± 0.28	2.29 ± 0.22	0.88	1.8
lpg2493	Heat shock protein HspC2	6.46 ± 0.15	5.34 ± 0.265	1.123	2.2
lpg1887	Hypothetical protein	4.16 ± 0.59	2.94 ± 0.97	1.22	2.32
lpg2971	Malate dehydrogenase	3.65 ± 0.73	2.44 ± 0.51	1.21	2.3
lpg2495	Homospermidine synthase	1.27 ± 0.42	0.94 ± 0.46	0.34	1.26
lpg0279	Hypothetical protein	2.16 ± 0.435	0.22 ± 0.28	1.94	3.5

[a]Levels of expression were measured relative to the expression of the gene *ftsZ*, as an internal control. T_{30}: 30 minutes after ingestion, SPF: stationary phase forms.

time points in *A. castellanii*, supporting our earlier findings and suggesting that *Tetrahymena* ciliates are a good model to study the changes in gene expression of *L. pneumophila* during differentiation into MIFs.

4.4. Expression profiles of *L. pneumophila* genes involved in carbohydrate metabolism

The expression of *lpg1669*, which encodes a putative α-amylase, is dramatically upregulated (166-fold) in the progeny obtained from *A. castellanii*. The expression of *lpg2971* and the encoded malate dehydrogenase are also upregulated in the amoeba progeny. Together, this suggests that carbohydrate metabolism could play a role in the differentiation of *L. pneumophila* RFs into MIFs in amoebae. This is particularly interesting because it has been understood for years that *L. pneumophila* neither ferments nor oxidizes carbohydrates.

The expression of *L. pneumophila* genes involved in carbohydrate metabolism was found to be upregulated in amoebae (Bruggemann *et al.*, 2006). The endocyst of *A. castellanii* is mainly composed of cellulose and approximately 10% of the dry weight of trophozoites is composed of glycogen (Dudley *et al.*, 2009). Together, this may suggest that *L. pneumophila* can exploit polysaccharides during intracellular infections of amoebae.

To further test the possibility that carbohydrate metabolism could be important for intracellular growth and differentiation of *L. pneumophila* inside amoebae, we set out to test the expression levels of six genes that are related to carbohydrate metabolism at different time points during the transition between replicative and transmissive forms in the natural host (*A. castellanii*) and *in vitro* (in BYE broth) using qRT-PCR. The genes *lpg0417*, *lpg0419,* and *lpg0421* were all upregulated during replication in amoebae as determined by microarray analysis (Bruggemann *et al.*, 2006). The genes *lpg0417* and *lpg0419* encode 6-phosphogluconolactonase and glucokinase, which are components of the ED pathway. The gene *lpg0421* encodes an associated sugar transporter. The gene *lpg1748* encodes inositol-1-monophosphatase. *L. pneumophila* genes predicted to encode myo-inositol catabolism proteins were upregulated inside amoebae (Bruggemann *et al.*,

2006). The gene *lpg0136* encodes a pyruvate kinase, which is a component of the glycolysis pathway. The gene *lpg0948* encodes 2-oxoglutarate ferredoxin oxidoreductase.

Analysis of gene expression was perfomed in the final progeny (after 3 days) and in RFs collected at 8 hours following infection of *A. castellanii* and at stationary and exponential growth phases in BYE broth (**Table 4.8.**).

The expression of *lpg0417, lpg0419*, and *lpg1748* was upregulated at 8 hours in amoebae, suggesting that these genes are important during *L. pneumophila* replication inside amoebae. The expression of *lpg0417, lpg0419* was also uppregulated during exponential growth in BYE broth. However, the expression of *lpg1748* increased markedly in SPFs *in vitro*.

The expression of *lpg0136* and *lpg0948* was upregulated after 3 days in amoebae, suggesting that these genes are important during *L. pneumophila* differentiation into MIFs inside amoebae. While the expression of *lpg0948* was similarly upregulated in SPFs *in vitro*, the expression of *lpg0136* was upregulated during replication in BYE broth.

The gene *lpg0421* which encodes a putative sugar transporter does not show changes in its expression levels at the tested time points inside amoebae. However, it is upregulated during growth in BYE broth (**Table 4.8.**).

Taken together, the changes in the expression of genes that are involved in carbohydrate metabolism during *L. pneumophila* replication or differentiation inside amoebae suggest that *L. pneumophila* can utilize carbohydrates as a source of energy. The changes in gene expression *in vitro* (BYE broth) do not necessarily represent the changes in gene expression *in vivo* (inside amoebae).

In addition, the expression of the genes *lpg1669*, which encodes a putative α-amylase, and *lpg2971*, which encodes a malate dehydrogenase, previously shown to be upregulated during differentiation in amoebae, are also upregulated in SPFs *in vitro*. The gene *lpg1669* shows a dramatic 1000-fold increase in expression and the gene *lpg2971* shows an 80-fold increase in expression in SPFs compared to EPFs. The observation that these two genes are consistently upregulated in both environments suggests that they could play a role in the differentiation of *L. pneumophila* when amino acids become scarce.

Table 4.8. Expression profiles of genes involved in carbohydrate metabolism during infection of *A. castellanii* and during *in vitro* growth in BYE broth.

This table was generated by Emma-Jean Slobodesky and Hany Abdelhady.

During *in vitro* growth

Gene ID	Description	Level of expression (E)[a]	Level of expression (SPFs)[a]	$\Delta\Delta C_t$	$2^{\Delta\Delta C_t}$
lpg0417	6-phosphogluconolactonase	0.68 ± 0.23	-0.93 ± 0.33	1.61	3.06
lpg0419	Glucokinase	0.78 ± 0.47	-0.93 ± 0.33	1.71	3.27
lpg0948	2-oxoglutarate ferredoxin oxidoreductase β subunit	-0.88 ± 0.38	0.82 ± 0.27	-1.7	0.31
lpg0421	D-xylose (galactose, arabinose)-proton symporter, similar to sugar transport protein	0.097 ± 0.22	-1.34 ± 0.43	1.44	2.71
lpg1748	Inositol monophosphatase	-1.18 ± 0.52	1.54 ± 0.56	-2.73	0.15
lpg0136	Pyruvate kinase	1.38 ±0.38	0.14 ± 0.39	1.24	2.36

During replication inside *Acanthamoeba castellanii*

	Description	Level of expression (AM – 8 hours)[a]	Level of expression (SPFs)[a]	$\Delta\Delta C_t$	$2^{\Delta\Delta C_t}$
lpg0417	6-phosphogluconolactonase	0.87 ± 0.09	-0.61 ± 0.26	1.48	2.79
lpg0419	Glucokinase	0.57 ± 0.34	-0.93 ± 0.33	1.5	2.83
lpg0948	2-oxoglutarate ferredoxin oxidoreductase β subunit	-0.88 ± 0.51	0.83 ± 0.27	-1.7	0.31
lpg0421	D-xylose (galactose, arabinose)-proton symporter, similar to sugar transport protein	-3.65 ± 0.56	-1.34 ± 0.43	-2.3	0.2
lpg1748	Inositol monophosphatase	0.92 ± 0.39	1.54 ± 0.56	-0.62	0.65
lpg0136	Pyruvate kinase	-0.6 ± 0.08	0.14 ± 0.39	-0.74	0.599

During later growth stages in *Acanthamoeba castellanii*

Gene ID	Description	Level of expression (MIFs)[a]	Level of expression (8 hours)[a]	$\Delta\Delta C_t$	$2^{\Delta\Delta C_t}$
lpg0417	6-phosphogluconolactonase	-0.72 ± 0.25	0.87 ± 0.09	-1.59	0.33
lpg0419	Glucokinase	-1.66 ± 0.37	0.57 ± 0.34	-2.22	0.21

Table 4.8. continued

lpg0419	Glucokinase	-1.66 ± 0.37	0.57 ± 0.34	-2.22	0.21
lpg0948	2-oxoglutarate ferredoxin oxidoreductase β subunit	-0.087 ± 0.53	-0.88 ± 0.51	0.79	1.73
lpg0421	Tra: -D-xylose (galactose, arabinose)-proton symporter, similar to sugar transport protein	-3.54 ± 0.32	-3.65 ± 0.55	0.11	1.08
lpg1748	Inositol monophosphatase	-1.25 ± 0.52	0.92±0.38	-2.17	0.22
lpg0136	Pyruvate kinase	0.54 ± 0.2	-0.6 ± 0.08	1.14	2.21

[a]Levels of expression were measured relative to the expression of the gene *gyrA*, as an internal control. E: exponential phase, PE: post-exponential phase.

4.5. Acknowledgement

I would like to acknowledge the contribution of Emma-Jean Slobodesky and Jungmin Kim (honours students, Department of Microbiology and Immunology, Dalhousie University) to the work presented in this chapter. They both worked under my direct guidance and gave me the opportunity to develop supervisory skills. Emma-Jean Slobodesky isolated RNA and synthesized cDNA from the replicative forms (RFs) of *L. pneumophila* obtained following 8 hours of infection of *A. castellanii* trophozoites. Emma-Jean also performed qRT-PCR analysis of the expression of the short list of *L. pneumophila* genes in *A. castellanii* and the *L. pneumophila* genes involved in carbohydrate metabolism. Jungmin Kim isolated RNA and synthesized cDNA from the differentiating MIFs recovered from *Tetrahymena* ciliates 30 minutes after feeding and from SPFs incubated in TBOS for 30 minutes. Jungmin also performed qRT-PCR analysis of the expression of the short list of *L. pneumophila* genes inside *Tetrahymena* ciliates. Hany Abdelhady analyzed the microarray data in *Tetrahymena tropicalis* ciliates, generated a short list of target genes for qRT-PCR analysis, isolated RNA, and synthesized cDNA from *L. pneumophila* RFs and SPFs grown in BYE broth and from the *L. pneumophila* progenies obtained from amoebae and U937 macrophages following 3 days of infection. Hany also performed qRT-PCR analysis of the expression of the short list of *L. pneumophila* genes inside U937 human macrophages and provided technical training and guidance to honours students.

CHAPTER 5: THE GENE *LPG1669*, WHICH ENCODES A PUTATIVE ALPHA-AMYLASE, IS NOT ESSENTIAL FOR THE INTRACELLULAR DIFFERENTIATION OF *LEGIONELLA PNEUMOPHILA*

The gene *lpg1669* which encodes a putative α-amylase demonstrated the highest level of upregulation inside amoebae (out of the tested list of genes presented in chapter 4). This gene is also upregulated inside *Tetrahymena* ciliates, massively upregulated in SPFs *in vitro*, but downregulated inside human macrophages (**Table 5.1.**). Together, the qRT-PCR analysis of the expression of *lpg1669* suggests that it could be associated with the full differentiation of *L. pneumophila* into MIFs in freshwater protozoa. Therefore, I set out to assess the role of *lpg1669* in the intracellular growth and differentiation of *L. pneumophila*.

5.1. Lpg1669 displays the D-E-D catalytic triad characteristic of α-amylases

The α-amylase family possesses no universally conserved features in primary sequence with the exception of the catalytic D-E-D motif (Janecek & Blesak, 2011). Despite this, several regions of well conserved residues exist, allowing for examination of Lpg1669 with respect to these regions. Seven regions have been identified as relatively well conserved in the α-amylase family, including the region containing an invariant arginine and the first catalytic aspartic acid (domain II), the region containing the catalytic glutamic acid (domain III), and the region containing a well conserved histidine followed by the second catalytic aspartic acid (domain IV).

Protein BLAST was used to compare the small regions of conserved sequences identified in the α-amylase from *Aspergillus oryzae* (Taka A; accession number: P0C1B4) against Lpg1669, as well as to perform a whole-protein sequence alignment between the two enzymes. Comparison of the small conserved regions of Taka A to Lpg1669 revealed that the putative α-amylase of *L. pneumophila* possesses regions similar to domains I and VI of Taka A (**Figure 5.1.**). Additionally, whole-protein alignment revealed some homology between Lpg1669 and Taka A at domain II, the domain of Taka A containing the first catalytic aspartic acid of the D-E-D motif. Alignment of both the whole proteins and the small, conserved α-amylase features using

Table 5.1. Expression levels of *amyA* (*lpg1669*) under different conditions

This table was generated by Emma-Jean Slobodesky, Jungmin Kim, and Hany Abdelhady

Intracellular infections of *Acanthamoeba castellanii*	**Expression level (MIFs)[a]**	**Expression level (8 hours)[a]**	**$\Delta\Delta C_t$**	**$2^{\Delta\Delta C_t}$**
	5.42 ± 0.51	-1.95 ± 0.31	7.38	166
Intracellular infections of U937 human macrophages	**Expression level (3 days)[a]**	**Expression level (SPFs)[a]**	**$\Delta\Delta C_t$**	**$2^{\Delta\Delta C_t}$**
	7.09 ± 1.66	7.55 ± 1.95	-0.46	0.72
Inside the food vacuoles of *Tetrahymena tropicalis* ciliates	**Expression level (T_{30})[b]**	**Expression level (SPF)[b]**	**$\Delta\Delta C_t$**	**$2^{\Delta\Delta C_t}$**
	3.48 ± 0.68	2.43 ± 0.96	1.05	2.1
During *in vitro* growth (BYE broth)	**Expression level (SPF)[a]**	**Expression level (E)[a]**	**$\Delta\Delta C_t$**	**$2^{\Delta\Delta C_t}$**
	5.68 ± 0.48	-4.42 ± 0.16	10.1	1102.6

Levels of expression were measured relative to the expression of the gene *gyrA*[a], or ftsZ[b]as an internal control. T_{30}: 30 minutes after ingestion, E: exponential phase, SPF: stationary phase form, MIF: mature infectious form.

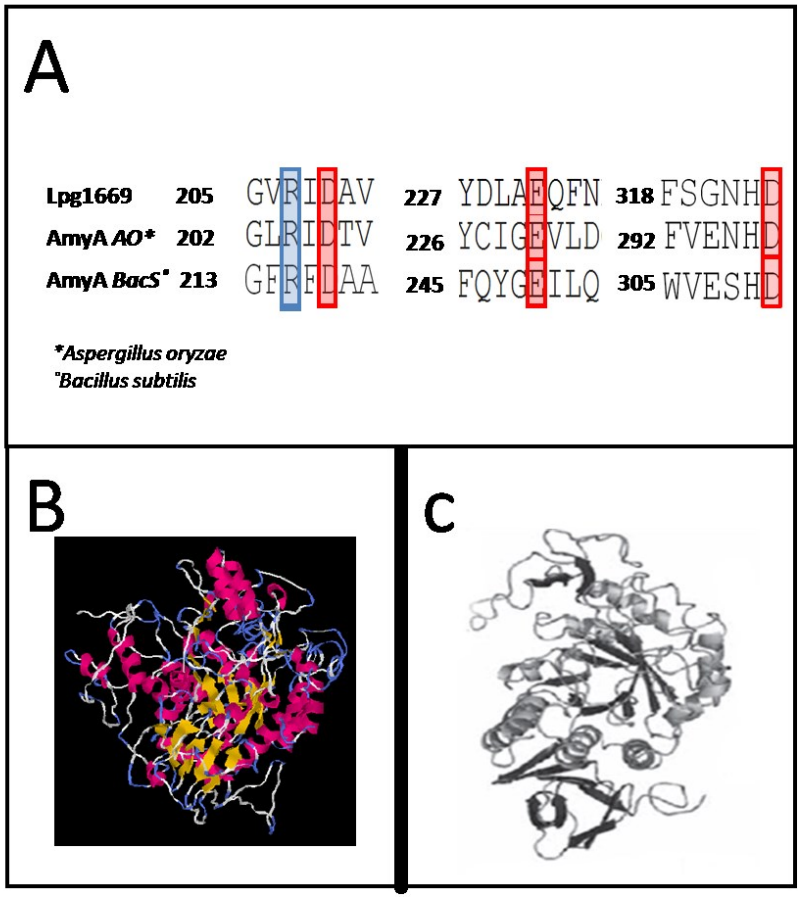

Figure 5.1. Lpg1669 displays the D-E-D catalytic triad characteristic of α-amylases. (A) Lpg1669 possesses a conserved catalytic D-E-D motif present in other α-amylases from *Aspergillus oryzae* and *Bacillus subtilus* (red boxes).This motif is responsible for the nucleophilic attack on α-1,4-glucosidic bonds in polysaccharide substrates. (B) A predicted 3D structure of Lpg1669 was generated using the I-TASSER v2.1 program. Pink areas correspond to an α-helix and yellow areas to a β-sheet. (C) The 3D structure of a characterized amylase from *A. oryzae* is shown for comparison (adapted from Matsuura *et al.*, 1984). This figure was generated by Peter Robertson and Hany Abdelhady.

protein BLAST did not yield any further homology. Because the primary sequence of α-amylases is known to be highly variable, and would therefore resist conventional algorithm-based sequencing to some degree, the primary sequence of Lpg1669 was aligned to Taka A using the BioEdit program and visually screened for residues exhibiting homology to the catalytic triad. The visual screen demonstrated the probable location of the second catalytic aspartic acid, based primarily on the presence of a preceding histidine (a known feature of α-amylases). The location of the catalytic glutamic acid was already predicted by NCBI.

The regions surrounding catalytic triad in both Taka A and Lpg1669 were then aligned to those in a well characterized and commercially available amylase from *Bacillus subtilis*, in order to further examine homology of Lpg1669 to known α-amylases. While homology between Lpg1669 and *B. subtilis* α-amylase at their respective catalytic sites was minimal, significant homology between the two confirmed α-amylases (*B. subtilis* and Taka A) was also not observed, illustrating the difficulties in predicting the catalytic triad based on primary sequence.

A well characterized and commercially available α-amylase from *Bacillus subtilis* (accession number: P00691) was also aligned to the three potentially catalytic regions of Lpg1669 and Taka A, demonstrating that homology is partial at best, even between confirmed amylases. To help further characterize Lpg1669, I generated a three-dimensional model of the protein's predicted structure using the I-TASSERv2.1 program (Zhang, 2008) (**Figure 5.1.**).

5.2. Genetic organization of the *lpg1669* locus

The gene *lpg1670* is located 300 bp downstream of *lpg1669*, but is encoded on the opposite strand from *lpg1669*. The closest gene to *lpg1669* that runs in the same direction is *lpg1668*, roughly 900 bp upstream. To study the genetic organization of the *lpg1669* locus, the Neural Network Promoter Prediction program (http://www.fruitfly.org/seq_tools/promoter.html) was used to predict the presence of promoter sequences in the intergenic regions between *lpg1668*-*lpg1669* and *lpg1670*-*lpg1671*. The program predicted the presence of a promoter between *lpg1668* and *lpg1669*, suggesting that they do not form an operon together. The genes *lpg1670* and

lpg1671 are separated by a 100 bp intergenic region. The gene *lpg1671* encodes another putative α-amylase and could possibly be regulated through the same regulatory machinery with *lpg1669*. The Neural Network Promoter Prediction program was unable to predict a promoter sequence between *lpg1670* and *lpg1671*.

To assess these predictions and evaluate the putative operon structures, RT-PCR experiments were performed using the primer pairs 1668-1669 FWD and 1668-1669 REV (which target the intergenic region between *lpg1668* and *lpg1669*) and 1670-1671 FWD and 1670-1671 REV (which target the intergenic region between *lpg1670* and *lpg1671*) (**Figure 5.2.**). Generation of amplicons that span these intergenic regions would indicate that the corresponding gene sets are transcribed as polycistronic messages. Proper controls were also included to make sure that the absence of amplicons was a result of the absence of operon structures, rather than poor cDNA sample quality. The results of the RT-PCR experiments indicate that *lpg1669* does not form an operon with *lpg1668* and that *lpg1670* and *lpg1671* are found in a single operon. This indicates that the deletion of *lpg1669* is not expected to have no polar effects on downstream genes.

5.3. Construction of *L. pneumophila* JR32 Δ*lpg1669* (*amyA*) mutant

To assess the role of *lpg1669* in the intracellular differentiation of *L. pneumophila*, a chromosomal deletion mutant was constructed utilizing an gene counterselectable vector (pBRDX) strategy (Morash *et al.*, 2009) in which an allelic replacement construct consisting of a kanamycin-resistance cassette flanked by the upstream and downstream regions of the target gene was used to replace *lpg1669* (**Figure 5.3.**).

The upstream (611 bp) and downstream (818 bp) flanking DNA sequences to *lpg1669* were amplified by PCR, using the primer pairs amyUSF-NotI / amyUSR-BamHI to amplify the upstream fragment and amyDSF-BamHI / amyDSR-XhoI to amplify the downstream fragment. The amplified fragments were ligated into pBluescript (pBS), creating pBSΔ*amyA* plasmid. Then, the kanamycin resistance determinant of plasmid p34S-*km3* (Dennis & Zylstra, 1998) was inserted into the BamHI site between the upstream and downstream fragments, creating pBSΔ*amyA*::km. The construct was subcloned into the NotI and XhoI sites of pBRDX (Brassinga *et al.*, 2006), a suicide

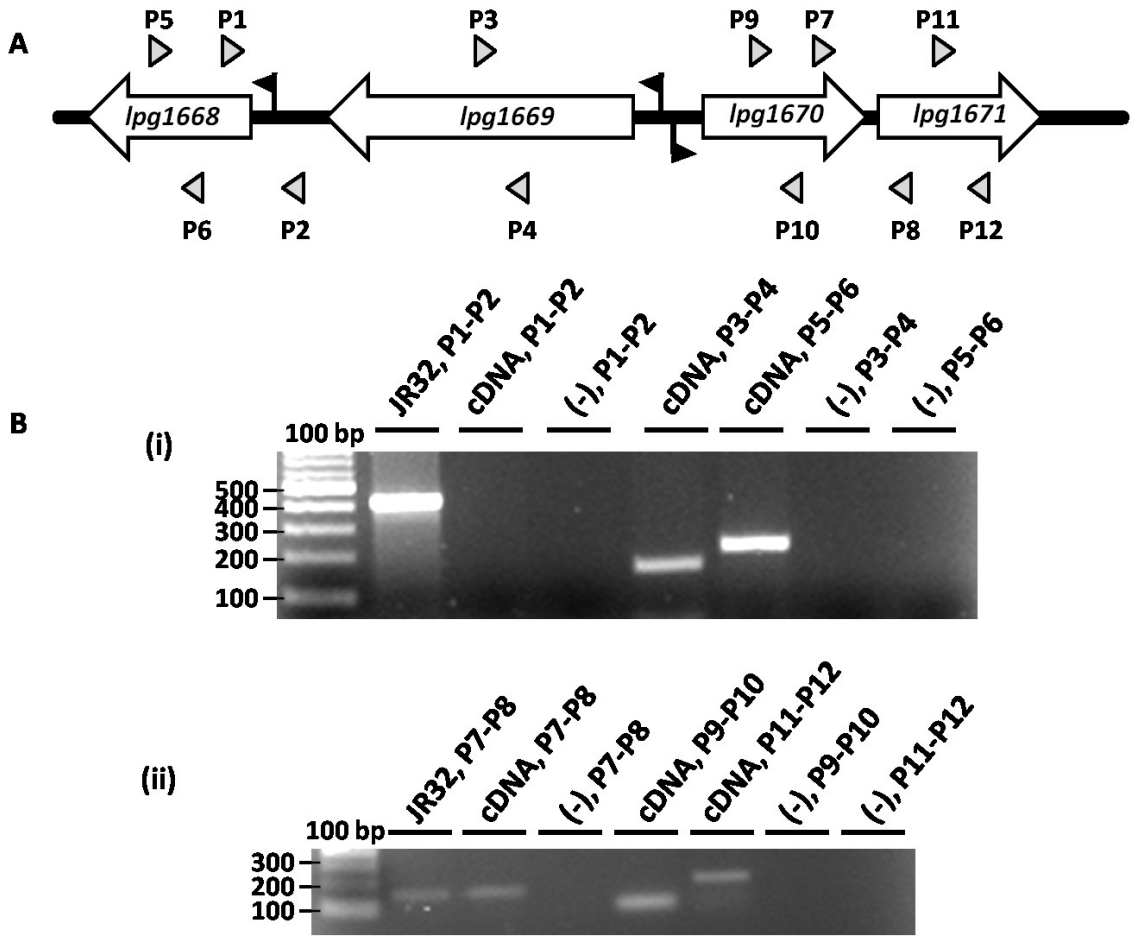

Figure 5.2. Genetic organization of the *lpg1669* locus.

(A) Schematic representation (not to scale) of the *lpg1669* gene locus. Arrowheads represent the binding sites of the primers (P1-P12) used in the RT-PCR reactions. Black arrows indicate the putative promoter regions identified using the Neural Network Promoter Prediction program (http://www.fruitfly.org/seq_tools/promoter.html). (B) Ethidium-bromide stained agarose gels showing the RT-PCR confirmation of the predicted organization of the intergenic regions between *lpg1668* and *lpg1669* (i), and between *lpg1670* and *lpg1671* (ii). Lanes labelled (-) indicate a negative control reaction (no template) was performed. NEB 100-bp DNA ladder was used as a size reference. P1: 1668-1669 FWD, P2: 1668-1669 REV, P3: 1669QPCRF, P4: 1669QPCRR, P5: 1668QPCRF, P6: 1668QPCRR, P7: 1670-1671 FWD, P8: 1670-1671 REV, P9: 1670QPCRF, P10: 1670QPCRR, P11: 1671QPCRF, P12: 1671QPCRR. This figure was generated by Peter Robertson and Hany Abdelhady.

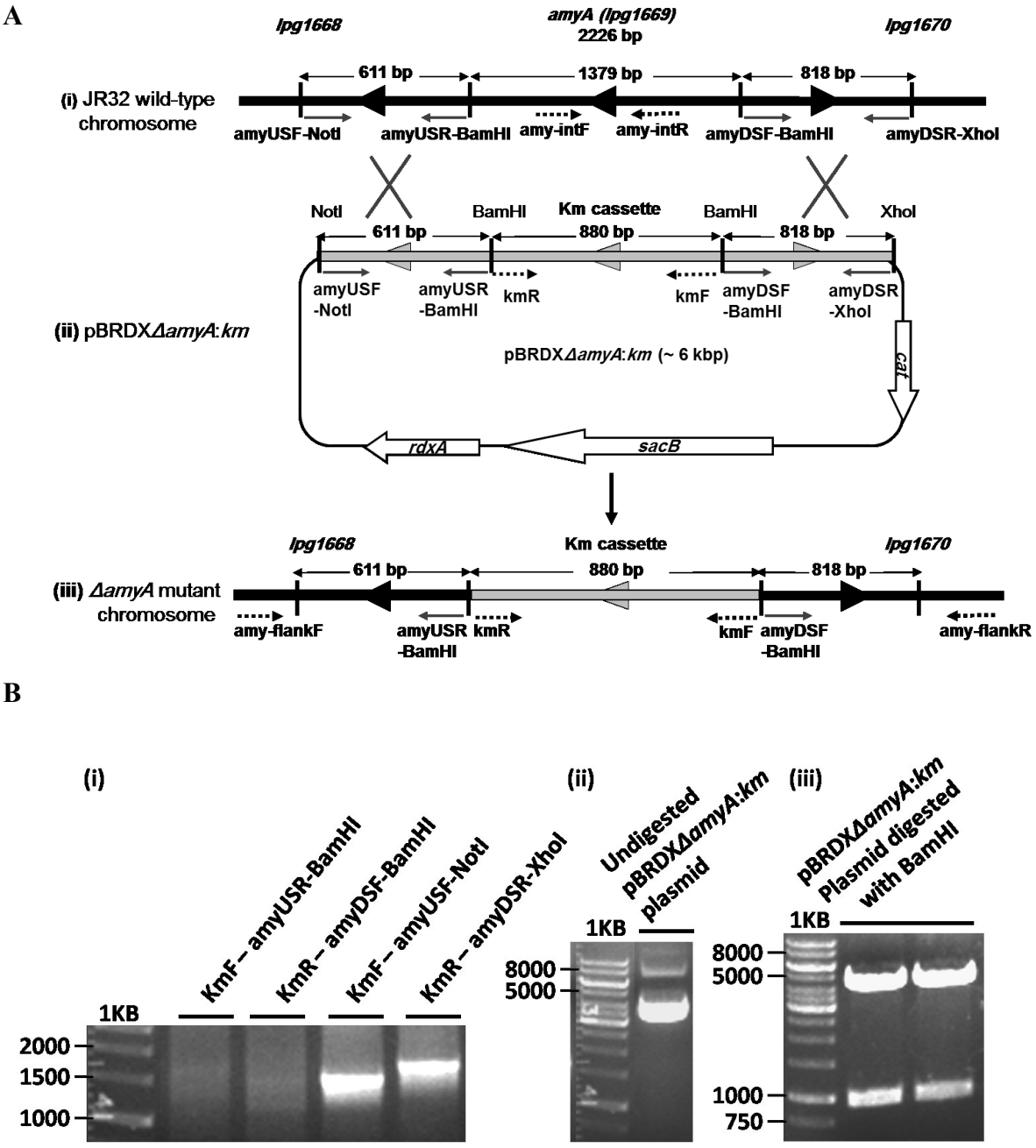

Figure 5.3. Construction of the *L. pneumophila* JR32Δ*amyA* mutant.

(A) Schematic representation (not to scale) of the allelic replacement approach used to replace *lpg1669* from the genome of *L. pneumophila* JR32 with a Km^R cassette present in the counter selectable plasmid pBRDXΔ*amyA:km*. (i) Area of the JR32 chromosome (not to scale) showing the *amyA* (*lpg1669*) locus and its flanking genes (*lpg1668* and *lpg1670*). Direction of the transcription of each gene is indicated by black arrowheads.

Figure 5.3. continued

The size of *lpg1669* gene is 2226 bp. However, the portion of the gene to be replaced by the kanamycin resistance cassette is 1379bp (ii) Map of plasmid pBRDXΔ*amyA:km*. Primer pairs amyUSR-NotI/amyUSRBamHI - and amyDSF-BamHI/amyDS-XhoI were used to generate the upstream and downstream flanking regions to *amyA* (*lpg1669*), respectively by PCR. The large Xs indicate the areas of recombination between the JR32 chromosome and pBRDXΔ*amyA:km*. (iii) The expected outcomes following an allelic replacement. Primers used to confirm the loss of *amyA* and the insertion of Km^R cassette are indicated by small broken arrows.

(B) Genetic confirmation of the construction of pBRDXΔ*amyA:km* plasmid. Ethidium bromide-stained agarose gels showing; (i) the PCR amplicons generated using primers (KmF-amyUSF-NotI) and (KmR-amyDSR-XhoI), (ii) pBRDXΔ*amyA:km* plasmid, and (iii) the pBRDXΔ*amyA:km* plasmid after digestion with BamHI enzyme. Kanamycin cassette was released from the plasmid and detected around 900 bp. Fermentas 1 kb DNA ladder was used as a size reference. This figure was generated by Peter Robertson and Hany Abdelhady.

vector containing *sacB* and *rdxA* genes as counter-selection markers, creating pBRDXΔ*amyA*:km (**Figure 5.3. A**).

Following electroporation into *E. coli* DH5α cells and confirmation by PCR analysis, the plasmid pBRDXΔ*amyA*::km was electroporated into *L. pneumophila* JR32. Allelic recombinants of *L. pneumophila* were selected for the loss of plasmid from a population of kanamycin resistant (Kan^R) colonies, grown on BCYE supplemented with 25 μg/ml kan, by replica-plating onto BCYE medium supplemented with 5% (w/v) sucrose or 5 μg/ml chloramphenicol.

Colonies that were kanamycin-resistant (Kan^R), streptomycin-resistant (Sm^R), sucrose-resistant (Suc^R) and chloramphenicol-sensitive (Cm^S) strains were screened by PCR using primers that bind internal to the deleted DNA region (amy-intF and amy-intR), primers that bind outside of the cloned upstream and downstream regions (amy-flankF and amy-flankR) and primers that bind to the kanamycin resistance cassette (kmF and kmR) (**Figure 5.4.**). Reverse transcription PCR (RT-PCR) was also used to confirm the absence of *amyA* mRNA in the Δ*amyA* mutant (**Figure 5.6.**).

5.4. Complementation of the *L. pneumophila lpg1669* (*amyA*) mutant.

The promoter and the coding sequence of the *amyA* gene were amplified by PCR using the primer pair amyCo-ApaF and amyCo-XbaR. The amplified fragment was then subcloned into the NotI and XhoI sites of the expression vector pMMB207C, creating the pMMB:*amyA* plasmid, where the *amyA* gene was expressed under its natural promoter (P_{amyA}) (**Figure 5.5.**). The constructed complementing plasmid was then electroporated into an *L. pneumophila* JR32 Δ*amyA* mutant. Reverse transcription PCR (RT-PCR) was also used to confirm that the complemented strain is able to express *lpg1669* (*amyA*) (**Figure 5.6.**).

5.5. Construction of a 6xHis_6-tagged copy of *lpg1669*

In order to study the putative α-amylase Lpg1669 (AmyA), I set out to construct a His_6-tagged copy of *lpg1669*. The gene *lpg1669* (*amyA*) together with its upstream promoter region were amplified with the primer pair amyHisFApaI and amyHisRXbaI, a primer pair that adds a 6xHis residues and ApaI and XbaI restriction sites to *lpg1669*. The

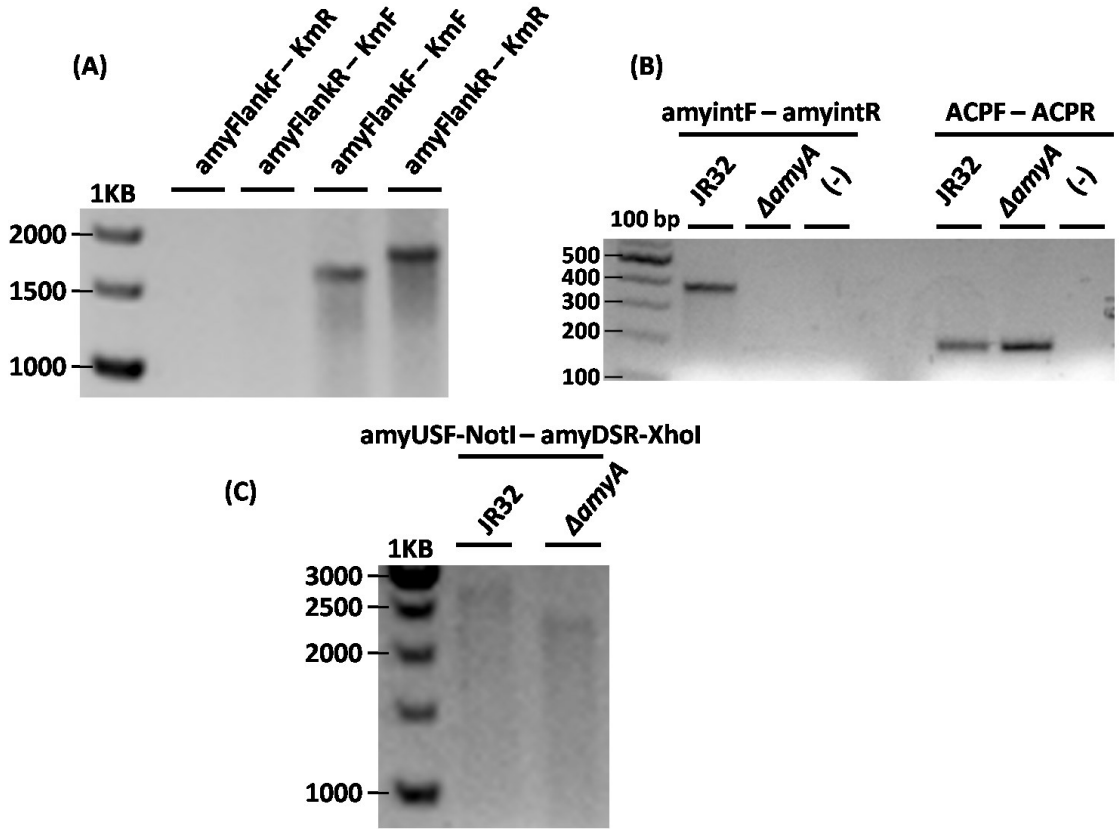

Figure 5.4. Genetic confirmation of the construction of the JR32 Δ*amyA* mutant. Ethidium bromide-stained agarose gels showing; (i) the PCR amplicons generated using primers (kmF – amy-flankF) and (kmR – amy-flankR), (ii) the absence of the PCR amplicon of the internal region of *amyA* (*lpg1669*) gene (using amy-intF and amy-intR primers) in theJR32 Δ*amyA* mutant. The primers ACPF and ACPR were used as a control, and (iii) the PCR amplicons generated using primers amyUSF-NotI and amyUSR-BamHI using JR32 and JR32 Δ*amyA* genomic DNA as templates. The size difference of ~ 500 bp of the amplicons confirms the construction of JR32 Δ*amyA* mutant. Lanes labelled (-) indicate a negative control reaction (no template) was performed. NEB 100bp and Fermentas 1 kb DNA ladders were used as size references. This figure was generated by Peter Robertson and Hany Abdelhady.

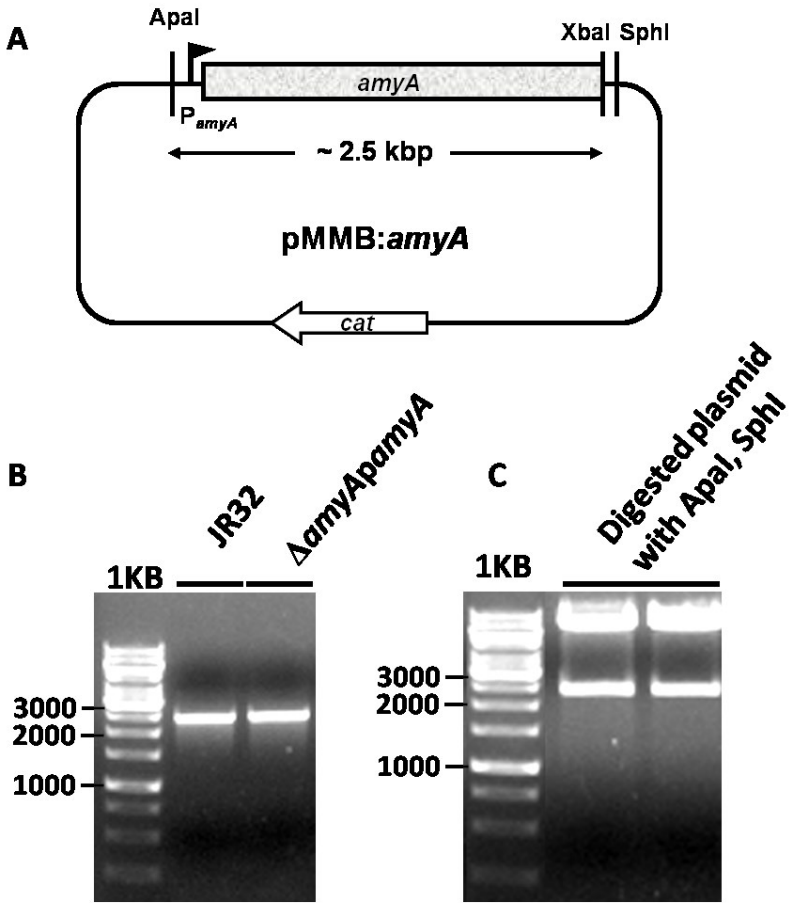

Figure 5.5. Construction of complement strain Δ*amyA*-pMMB:*amyA*.
(A) Schematic representation (not to scale) of the plasmid pMMB:*amyA*. Ethidium bromide-stained agarose gels showing the PCR amplicons generated using primers (amyCo-ApaF – amyCo-XbaR) and the genomic DNA of JR32 and JR32Δ*amyA*-pMMB:*amyA* as templates (B) and the digestion products of pMMB:*amyA* plasmid after digestion with ApaI and SphI enzymes (C). SphI enzyme was used instead of XbaI because XbaI is sensitive to DNA methylation. Fermentas 1 kb DNA ladder was used as a size reference. This figure was generated by Peter Robertson and Hany Abdelhady.

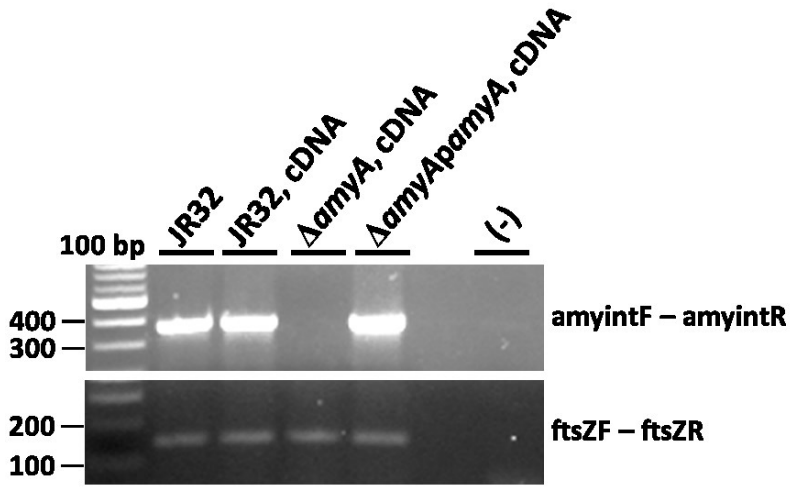

Figure 5.6. The gene *amyA* (*lpg1669*) is transcribed in JR32, JR32 Δ*amyA*-pMMB:*amyA* but not transcribed in the Δ*amyA* mutant.

Ethidium bromide-stained agarose gels showing the RT-PCR analysis of the transcription of *amyA* (*lpg1669*) gene in JR32, Δ*amyA* mutant and Δ*amyA*-pMMB:*amyA* using the amy-intF and amy-intR primers. FtsZF and FtsZR primers were used as a control. Lanes labelled (-) indicate a negative control reaction (no template) was performed. NEB 100-bp DNA ladder was used as a size reference.

amplified DNA as well as the plasmid pMMB207C were digested with XbaI and ApaI, and then ligated to form the plasmid pMMB:*amyA*-His_6 (**Figure 5.7. A**). The construction of the pMMB:*amyA*-His_6 plasmid was confirmed by PCR experiments using the primer pair amyHisFApaI and amyHisRXbaI and the internal primers amy-intF and amy-intR (**Figure 5.7. B**). The ligated plasmid was then electroporated into JR32 Δ*lpg1669* mutants to create a strain of *L. pneumophila* that can express 6xHis tagged *lpg1669*.

5.6. The construct pMMB:*amyA*-His_6 expresses Lpg1669 (AmyA) protein.

To make sure that the constructed pMMB::*amyA*-His_6 plasmid was able to express the protein Lpg1669, we performed an immunoblotting experiment using the whole cell lysate of the JR32 Δ*lpg1669* mutant harbouring the pMMB::*amyA*-His_6 plasmid. The whole cell lysates of the strains Δ*lpg1669*, Δ*lpg1669* harbouring the untagged pMMB::*lpg1669* were used as negative controls. The nitrocellulose membrane containing the separated protein bands was incubated with a monoclonal anti-His_6 antibody. The protein lysates from the Δ*lpg1669* mutant harbouring pMMB::*amyA*-His_6 developed a band, confirming that *lpg1669* was successfully translated into a protein of the predicted size (84.7 kDa). The protein lysates from the Δ*lpg1669* mutant or Δ*lpg1669* harbouring pMMB::*lpg1669* did not show any bands, confirming that neither of the background proteins of *L. pneumophila* nor the untagged Lpg1669 cross-reacted on the immunoblot. The purified truncated ComB-His_6 protein (which lacks the signal sequence and transmembrane domains) from *Streptococcus gordonii* (a gift from Lauren Davey, Dalhousie University), used as a positive control, developed a band at its known molecular weight of 29 kDa (**Figure 5.8.**).

5.7. Lpg1669 (AmyA) is an intracellular, not secreted protein

Signal P4 software (http://www.cbs.dtu.dk/services/SignalP/) was unable to detect a secretion signal in the primary sequence of Lpg1669 (AmyA) protein, suggesting that Lpg1669 (AmyA) is an intracellular protein that is not secreted by bacterial cells. To assess this prediction, we performed a dot blot experiment using equivalent concentrations of the whole cell lysate and the culture supernatant proteins of JR32

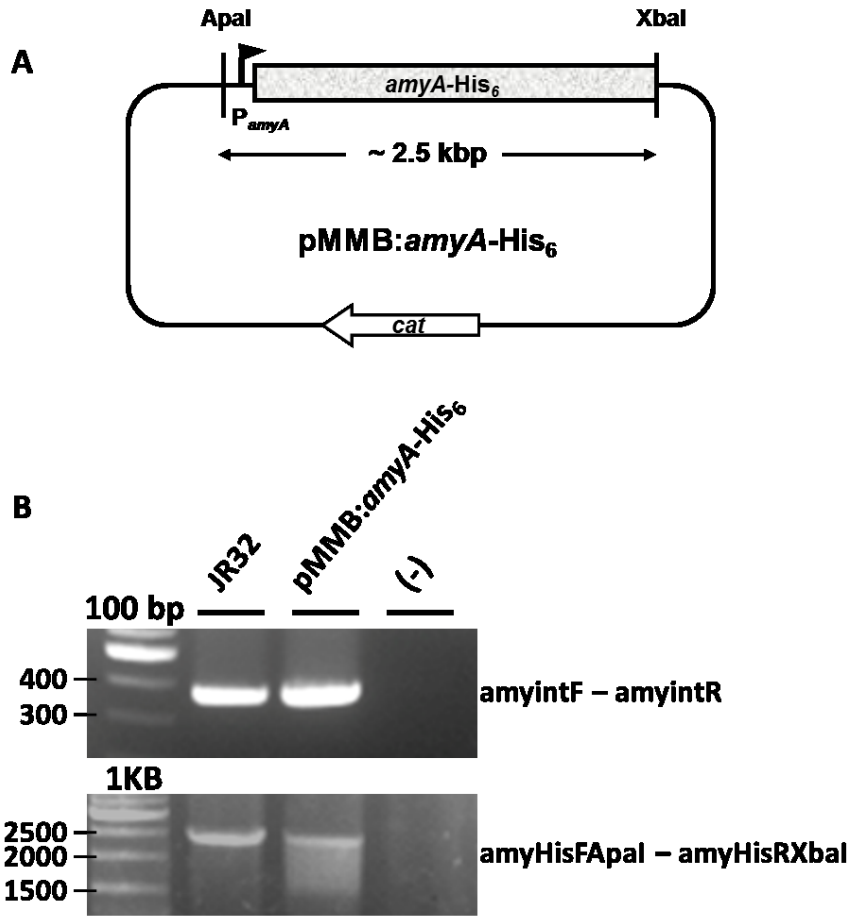

Figure 5.7. Construction of the pMMB:*amyA*-His$_6$ plasmid.

(A) Schematic representation (not to scale) of the plasmid pMMB:*amyA*-His$_6$. (B) Ethidium bromide-stained agarose gels showing the PCR amplicons generated using primers (amy-intF– amy-intR) and (amyHisFApaI – amyHisRXbaI) and the genomic DNA of JR32 and the pMMB:*amyA*-His$_6$ plasmid as templates. Lanes labelled (-) indicate a negative control reaction (no template) was performed. NEB 100-bp and Fermentas 1 kb DNA ladders were used as a size reference. This figure was generated by Peter Robertson and Hany Abdelhady.

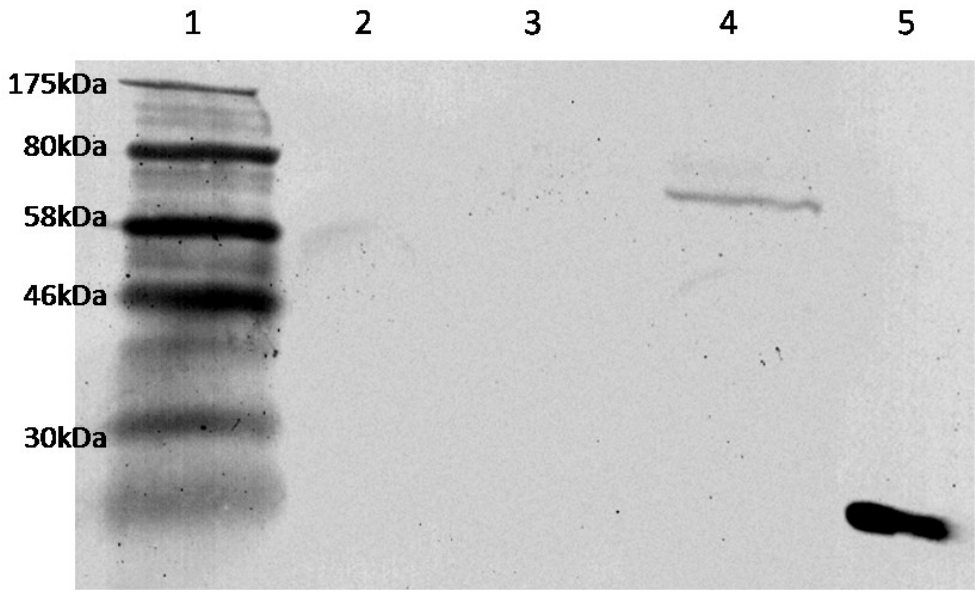

Figure 5.8. AmyA is expressed in the JR32 Δ*amyA* mutant harbouring the plasmid pMMB:*amyA*(His)$_6$.

An immunoblot performed on the whole cell lysate of JR32 Δ*amyA* (lane 2), JR32Δ*amyA* harbouring pMMB:*amyA* (lane 3), JR32 Δ*amyA* harbouring pMMB:*amyA*-His$_6$(lane 4) using a monoclonal anti-His$_6$ antibody. AmyA showed a band at the predicted molecular weight (84.7 kDa), confirming that the gene *lpg1669* is expressed into a protein. A purified ComB-His$_6$ protein from *S. gordonii* was used as a positive control and showed a band at the expected size of 29kDa (lane 5). NEB protein ladder was used as a size reference (Lane 1). This figure was generated by Peter Robertson and Hany Abdelhady.

Δ*lpg1669* mutant harbouring pMMB:*amyA*-His_6. The whole cell lysate of JR32 Δ*lpg1669* and the purified truncated ComB-His_6 protein (which lacks the signal sequence and transmembrane domains) from *Streptococcus gordonii* (a gift from Lauren Davey, Dalhousie University) were included as negative and positive controls, respectively. Following incubation of the blot with a monoclonal anti-His_6 antibody, the dot corresponding to the whole cell lysate developed a positive colour while the dot corresponding to the supernatant fraction developed no colour. Positive and negative controls showed the expected results, confirming the early prediction that Lpg1669 is not secreted (**Figure 5.9.**). It should be noted that the objective of this experiment was to assess whether Lpg1669 (AmyA) is secreted or not. The exact subcellular localization of Lpg1669 (AmyA) still remains to be determined.

5.8. The JR32 Δ*lpg1669* mutant displays no growth defects (*in vitro* or *in vivo*) or defects in morphological differentiation.

To assess the role of Lpg1669 (AmyA) in the intracellular growth and differentiation of *L. pneumophila in vitro* and *in vivo*, *L. pneumophila* strains JR32, the Δ*lpg1669* mutant, and the complemented Δ*lpg1669* (pMMB:*lpg1669*) were allowed to grow in BYE broth, and monolayers of *A. castellanii* trophozoites and U937 macrophages (**Figure 5.10.**).

Analysis of the growth curve in BYE broth demonstrated that the Δ*lpg1669* mutant did not display any growth defects and was able to grow at comparable rates to both JR32 and the *Δlpg1669* (pMMB:*lpg1669*) strains. Moreover, Δ*lpg1669* did not show any intracellular growth defects in monolayers of *A. castellanii* or U937 macrophages. These data suggest that despite the massive upregulation of *lpg1669* in SPFs and the amoeba-produced progeny, Lpg1669 is not important for *L. pneumophila* growth *in vivo* or *in vitro* (**Figure 5.10.**).

Analysis of the ultrastructural features of the progeny of *L. pneumophila* strains JR32, Δ*lpg1669* mutant, and the complemented Δ*lpg1669* (pMMB:*lpg1669*) strain obtained from amoebae, macrophages, and *Tetrahymena* ciliates did not demonstrate significant differences in the ultrastructural differentiation of the Δ*lpg1669* mutant (using the criteria described in materials and methods and previously demonstrated in **Figure**

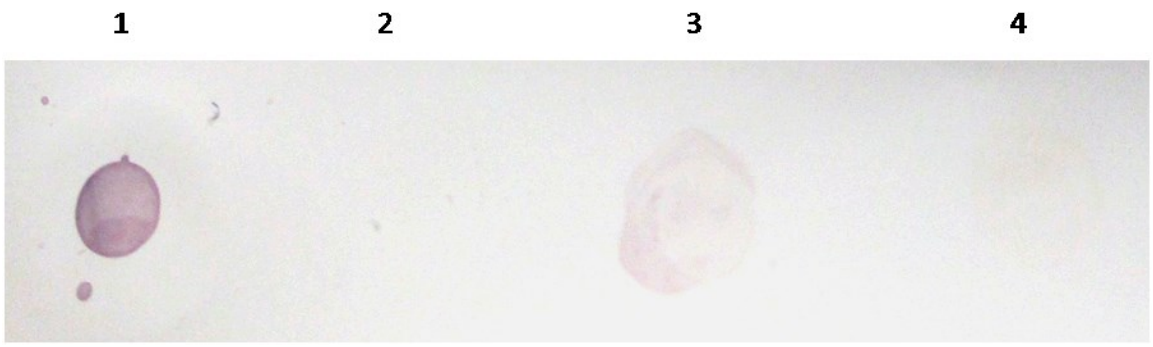

Figure 5.9. Lpg1669 (AmyA) is a soluble protein and not secreted into the growth medium.

Dot-blot analysis of the culture supernatant (lane 2) and the whole cell lysate proteins (lane 3) of JR32 Δ*amyA* harbouring the plasmid pMMB:*amyA*-His_6 using a monoclonal anti-His_6 antibody. The purified ComB-His_6 protein of *S. gordonii* was used as a positive control (lane 1) and the whole cell lysate of JR32 Δ*amyA* was used as a negative control (lane 4). This figure was generated by Peter Robertson and Hany Abdelhady.

Table 5.2. *L. pneumophila* JR32 Δ*amyA* does not display defects in ultrastructural features following infection of different hosts.

Quantitative electron microscopic analysis of the distribution of the ultrastructural traits of MIFs in the progeny of *L. pneumophila* JR32, the Δ*amyA* mutant and JR32 Δ*amyA*-pMMB:*amyA* strain obtained from *A. castellanii*, U937 human macrophages and the ciliate *Tetrahymena tropicalis.*

	Percentage of particles that show the ultrastructural features of MIFs					
	***L.pneumophila* JR32**		**JR32Δ*amyA***		**JR32Δ*amyA*-pMMB:*amyA***	
Amoebae (*A. castellanii*)	279/412	**67.7%**	277/398	**69.6%**	312/490	**63.7%**
***Tetrahymena tropicalis* ciliates**	208/305	**68.2%**	187/278	**67.3%**	189/251	**75.3%**
U937 human macrophages	42/81	**51.6%**	56 / 109	**51.4%**	202/401	**50.4%**

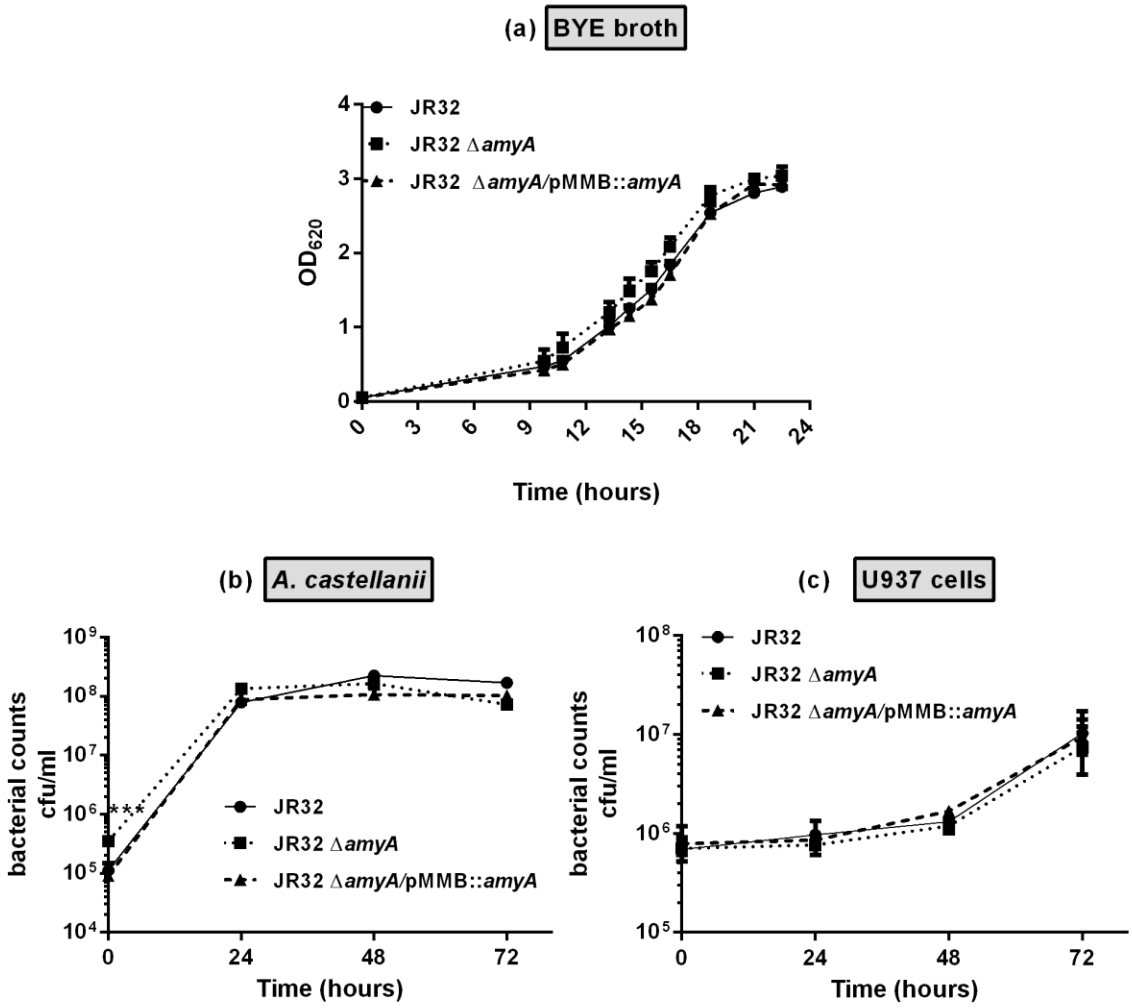

Figure 5.10. *L. pneumophila* JR32 Δ*amyA* does not show *in vitro* or *in vivo* growth defects.

Graphs of optical density or CFU versus time showing the growth of legionellae in BYE broth (a), *A. castellanii* (b), and U937 monolayers (c) infected with JR32, Δ*amyA*, and Δ*amyA*-pMMB:*amyA* at the same bacteria-to-cell ratio. Graph points represent means and error bars represent standard deviations of 3 independent experiments, each run in triplicate. Statistical significance was calculated using 2-way ANOVA test. *** $p < 0.001$. This figure was generated by Peter Robertson and Hany Abdelhady.

3.1.) compared to the other strains, suggesting that Lpg1669 does not play an important role in the differentiation of *L. pneumophila* into MIFs (**Table 5.2.**).

5.9. Acknowledgement

I would like to thank Mary-Ann Trevors for the technical assistance in processing the electron microscopy samples. I would like also to acknowledge the contribution of Peter Robertson (a summer student and an honours student, Department of Microbiology and Immunology, Dalhousie University) to the work presented in this chapter. Peter worked under my direct guidance and gave me the opportunity to develop supervisory skills. Peter provided technical assistance in the construction of the JR32 Δ*lpg1669* mutant and complemented strains, analysis of the sequence homology of Lpg1669 protein to other well-characterized α-amylases and RT-PCR experiment to analyze the organization of the *lpg1669* genetic locus. Peter also performed western blot and dot blot experiments, growth analysis experiment in BYE broth. Hany Abdelhady made the major contribution to the construction of the JR32 Δ*lpg1669* mutant, complemented strains and the pMMB:*amyA*-His_6 plasmid, sequence homology, and RT-PCR experiments. Hany also performed electron microscopy analysis, intracellular growth experiments in *A. castellanii* and U937 human macrophages monolayers, RNA isolation and cDNA synthesis of all samples used in this chapter, and prepared protein samples for western and dot blot experiments.

CHAPTER 6: DISCUSSION

6.1. *L. pneumophila* reaches different stages of development inside different host cells

While the differences between SPFs and MIFs have been previously reported (Garduno *et al.*, 2002; Garduno, 2007), it is not similarly documented whether the progeny of *L. pneumophila* produced in different host cells share the same characteristics. This study is the first report to indicate that *L. pneumophila* reaches different developmental stages in different hosts, and that the progeny produced in freshwater amoebae (the natural host) and cultured human macrophages display different characteristics that could improve our understanding for the lack of transmission of LD among humans.

6.1.1. *L. pneumophila* progeny produced in amoebae and human macrophages

Data in chapter 3 have demonstrated that the *L. pneumophila* progeny produced in amoebae is more morphologically differentiated, more resistant to antibiotics (but less resistant to chlorine), and more able to adhere to and initiate infections in host cells when compared to the progeny obtained from macrophages. These findings may provide a clue to explain the lack of transmission of LD from person to person. When allowed to infect amoebae trophozoites, the progeny produced in human macrophages displayed similar levels of morphological differentiation, antibiotic resistance, and adherence to the host cells as the progeny produced in amoebae, suggesting that the observed phenotypes were reversible developmental traits. The fact that these traits were observed in the progeny produced in macrophages by different strains of *L. pneumophila* provides more strength to the data and rules out strain-specific phenotypes. Collectively, these findings suggest that the intracellular environment of human macrophages does not optimally induce *L. pneumophila* differentiation.

Although the progeny of *L. pneumophila* from cultured human macrophages was less able to adhere to different host cells, it did not show any intracellular growth defects inside amoebae trophozoites or human macrophages, compared to the *L. pneumophila* progeny from amoebae. In fact, they were able to multiply at a similar, or even better,

growth rate. This was also evident in the competition assay experiments where the macrophage progeny was able to produce a higher yield per infected cell. It should be noted that the red fluorescence of RFP usually takes a long time to develop because RFP has to polymerize first into tetramers. This could hamper the use of RFP in live cell imaging (Rizzo *et al.*, 2009). However, the DsRed-Express system used in my research has been engineered to express RFP constitutively and has been previously used in live cell imaging experiments (Mampel *et al.*, 2006). Previous experiments in our laboratory that swapped the plasmids pMMB207-Km14-GFPc and pSW001 (that account for the green and red fluorescence, respectively) in the competing *L. pneumophila* populations did not display significant effects on the experiment outcomes (unpublished data). Together, these findings rule out the possibility that the lower infectivity of the *L. pneumophila* progeny from macrophages is due to the inefficient production of red fluorescence. However, better fluorescence alternatives may be considered for future experiments.

The presence of filamentous forms in the progeny of *L. pneumophila* produced in human macrophages has been frequently observed during my PhD project. Filamentous *L. pneumophila* (F*Lp*) forms have been found in the lung tissue from autopsies and bronchoalveolar lavage from infected patients and are able to invade the lung epithelium by a unique mechanism, not shared by non-filamentous *L. pneumophila* (Prashar *et al.*, 2012). F*Lp* forms are gradually internalized into the lung epithelium through a zipper mechanism of phagocytosis, which involves the engagement of host cell β1 integrin and E-cadherin receptors (Prashar *et al.*, 2012) . F*Lp* can also outcompete rod-shaped legionellae in the attachment to the lung epithelium, which can play an important role in the pathogenesis of *L. pneumophila* (Prashar *et al.*, 2012).

It has been previously proposed (Garduno *et al.*, 2002; Garduno, 2007) that the early apoptotic demise of *Legionella*-infected macrophages and (or) the lack of proper signals, may lead to an incomplete (or defective) differentiation of the *L. pneumophila* progeny inside these host cells. Furthermore, after analyzing the intracellular survival and morphological differentiation patterns of *L. pneumophila* mutants unable to produce transmissive forms *in vitro*, it was suggested that *L. pneumophila* is under a strong selective pressure to differentiate in nature, but not in the human host (Faulkner *et al.*,

2008). That is, *rpoS* and *letA* mutants, which are unable to survive or grow in amoebae and are effectively digested in *T. tropicalis* (Faulkner *et al.*, 2008), can still grow in HeLa cells (Faulkner *et al.*, 2008), and mouse or human macrophages (Hales & Shuman, 1999; Gal-Mor & Segal, 2003; Lynch *et al.*, 2003; Abu-Zant *et al.*, 2006; Faulkner *et al.*, 2008). These previous observations, together with the results presented in chapter 3, provide sufficient experimental evidence to support the notion that *L. pneumophila* can not fully complete its developmental program in cultured macrophages. Therefore, it could also be argued that the progeny of *L. pneumophila* produced in macrophages during the accidental infections of susceptible humans are not fully differentiated.

6.1.2. Free MIFs released from *Tetrahymena*-produced pellets and MIFs produced in amoebae

The importance of amoebae in the life cycle of *L. pneumophila* and their central role in supporting bacterial replication and development has been investigated in previous studies. However, the investigation of legionellae-laden pellets produced by the ciliate *T. tropicalis* is a relatively new field. *T. tropicalis* survives in both freshwater environments and man-made water systems, chiefly cooling towers. This is particularly important, since many outbreaks of LD, including the recent ones, have been traced to *L. pneumophila*-contaminated cooling towers (McCormick *et al.*, 2012). It has been previously suggested that pellets can act as complex infectious particles to both protozoa and susceptible humans and, therefore, may help in the transmission of LD to susceptible individuals. Pellets are more resistant to gentamicin and are able to maintain their viability in nutrient-limited environments for longer periods than the *in vitro* SPFs (Koubar *et al.*, 2011). Although the different phases of pellet production inside the food vacuoles of the ciliates have been thoroughly studied (Berk *et al.*, 2008), little is known about the behavior of the free legionellae MIFs released from the pellets. It should also be noted that the interaction between *L. pneumophila* and *Tetrahymena* ciliates and the production of legionellae-laden pellets are two events that are exclusive to the natural environment. This may also help explain (in addition to the findings in chapter 3) why *L. pneumophila* MIFs produced in the natural environment are able to transmit LD to susceptible humans.

When compared to free MIFs from amoebae, free MIFs from mechanically-disrupted pellets were less resistant to gentamicin, similarly resistant to ciprofloxacin, more resistant to chlorine (*L. pneumophila* 2064 progenies from amoebae and disrupted pellets were similarly resistant), and less resistant to SDS challenge. These findings were reported using 2 different strains of *L. pneumophila*, to rule out strain-specific phenotypes and support the idea that *L. pneumophila* progenies from different hosts may display different characteristics. MIFs released from *Tetrahymena*-produced pellets were similarly infectious to monolayers of amoebae and U937 macrophages as to the free MIFs from amoebae. Together, these findings highlight the potential role *Tetrahymena* ciliates can play in maintaining the life cycle of *L. pneumophila* in natural freshwater environments and in the transmission of LD to susceptible humans. It should be noted that in future comparisons between the mechanically-disrupted pellets and free progenies produced in other hosts, mechanical shearing of both samples should be performed to make the comparison more accurate.

6.2. Transcriptomic and proteomic analyses provide clues for the incomplete differentiation inside macrophages.

The mechanisms behind the incomplete differentiation of *L. pneumophila* in cultured macrophages are not completely understood. The early detachment and lysis of macrophages after infection with *L. pneumophila* may determine whether or not replicative forms can continue the developmental cycle and fully differentiate into MIFs (Garduno *et al.*, 2002). However, the rapid differentiation of *L. pneumophila* into MIFs inside *Tetrahymena* ciliates suggests that the intracellular environment of human macrophages does not support the full differentiation of *L. pneumophila*. Human macrophages may be deficient in one or more signals that trigger the differentiation of *L. pneumophila*. Analysis of the differences in gene expression and protein profiles of *L. pneumophila* progenies produced in amoebae and cultured human macrophages constitute an initial contribution to the understanding of some of the molecular mechanisms behind the observed phenotypes.

6.2.1. The current understanding of the differentiation process of *L. pneumophila* is not complete.

The regulatory networks that govern the differentiation process in *L. pneumophila* are not completely understood, mainly because the current understanding is largely based on studying the differentiation process *in vitro*. The extent to which this reflects the differentiation process inside the host cells is not known. For instance, the results of qRT-PCR analysis in chapter 4 have demonstrated that the changes in *L. pneumophila* gene expression in BYE broth do not necessarily agree with the corresponding changes inside amoebae. Faucher et al. have also found significant differences in *L. pneumophila* grown inside human macrophages to later stages (18 hours post-infection) and the *in vitro* SPFs. This could argue that the differentiation mechanisms that occur in PE phase are not essentially representative of what happens inside host cells (Faucher *et al.*, 2011).

Moreover, it was also interesting that almost a third of the upregulated *L. pneumophila* genes inside *T. tropicalis* were hypothetical with no assigned functions. The list of *L. pneumophila* genes selectively upregulated inside amoebae, compared to human macrophages also included hypothetical genes. Together, these findings strongly suggest that our understanding of the differentiation process in *L. pneumophila* is still limited.

6.2.2. Gene expression analysis demonstrates that *L. pneumophila* upregulates specific sets of genes in the natural environment

The genes that are upregulated late in the life cycle of *L. pneumophila* are expected to promote transmission and manipulation of new host cells (Bruggemann *et al.*, 2006). Genes that are upregulated during the transition of RFs into MIFs could be directly involved in or upregulated as a result of the intracellular differentiation process. Therefore, analysis of the gene expression during RFs-to-MIFs transition inside *A. castellanii* can help us understand the differentiation process in the natural host.
The changes in the transcriptome of *L. pneumophila* during infections of amoebae (Bruggemann *et al.*, 2006) and human macrophages (Faucher *et al.*, 2011) have been reported using microarray analysis; however, no direct comparison of the *L. pneumophila* transcription profiles has been reported to date. Quantitative real-time PCR (qRT-PCR), a more sensitive tool to determine gene expression levels, was used in this study to confirm

prior microarray data (Morey *et al.*, 2006). The findings of the qRT-PCR experiments demonstrated that *L. pneumophila* upregulates specific sets of genes inside amoebae, relative to human macrophages. These genes are expected to be correlated with the full differentiation of *L. pneumophila* into MIFs in the natural environment, and therefore, with the transmission of LD to susceptible humans.

Perturbations in fatty acid biosynthesis can affect the intracellular levels of ppGpp (through their effect on SpoT) and trigger the differentiation of *L. pneumophila* into MIFs (Dalebroux *et al.*, 2009; Dalebroux *et al.*, 2010). The SpoT response to perturbations in fatty acid biosynthesis requires an interaction with acyl carrier protein (ACP) (Dalebroux *et al.*, 2009; Dalebroux *et al.*, 2010). The findings that *lpg2228*, which encodes for 3-oxoacyl ACP synthase III (Chapter 4) is selectively upregulated inside amoebae (downregulated in human macrophages) supports the notion that the differentiation of *L. pneumophila* inside human macrophages in incomplete. Moreover, microarray and qRT-PCR transcriptional analyses have shown that *bdhA*, which encodes a β-hydroxybutyrate dehydrogenase (BdhA) enzyme, is selectively upregulated inside amoebae and *Tetrahymena* ciliates, suggesting that *bdhA* is correlated with the differentiation of *L. pneumophila.* BdhA enzyme is responsible for the synthesis of poly β-hydroxy butyrate (PHB) inclusions, which serve as an energy source to help the survival of *L. pneumophila* in the nutrient-limited extracellular environments (James *et al.*, 1999). *bdhA* is co-transcribed with *patD*, which encodes a phospholipase A enzyme. *L. pneumophila bdhA-patD* mutants dispaly severe intracellular growth defects inside amoebae and human macrophages, suggesting that the *bdhA-patD* operon is important for *L. pneumophila* virulence (Aurass *et al.*, 2009). Unpublished data from our lab suggest that BdhA is important in the extended survival of *L. pneumophila* in water in a viable-but-non-culturable (VBNC) state. *L. pneumophila bdhA* mutants lose their viability following extended incubation in water much sooner compared to wild-type bacteria (Badii Al-Banna and Rafael Garduño, personal communication).

Polyamines are small flexible organic polycationic compounds that are important for normal growth of both prokaryotic and eukaryotic cells (Cohen, 1998) and for the bacterial ability to survive in acidic environments with limited nutrients (Jung *et al.*, 2003). The gene *hss* (*lpg2495*), which encodes the enzyme homospermidine synthase,

(important for the synthesis of the polyamine homospermidine) was upregulated in both amoebae and *Tetrahymena* ciliates, but not inside human macrophages. Polyamines are required for the optimal growth of *L. pneumophila* inside host cells (Nasrallah *et al.*, 2011). They are important for the ability of *L. pneumophila* to form biofilms (Mampel *et al.*, 2006) and persist in low pH environments (Sheehan *et al.*, 2005). The induction of polyamine synthesis is therefore likely to enhance the pathogenesis of *L. pneumophila*. The importance of the enhanced entry proteins EnhA and EnhC in the early interactions of *L. pneumophila* with host cells has been previously established (Cirillo *et al.*, 1994; Cirillo *et al.*, 2000). The finding that the expression of *enhA* and *enhC* are selectively upregulated inside amoebae compared to human macrophages certainly contributes towards explaining their low adherence and efficiency of the progeny produced in human macrophages to initiate infections of host cells.

The *clpA* gene encodes the ATP-binding subunit of the ATP-dependent Clp proteolytic complex. Since proteolysis of the misfolded proteins is critical, *L. pneumophila* requires the Clp protease system for intracellular growth. In addition, the Clp proteolytic complex also influences the expression of virulence traits such as cytotoxicity against amoebae (Li *et al.*, 2010), suggesting that the Clp protease system plays a role in the virulence of *L. pneumophila*.

The selective upregulation of *uspA* and *hspC2*, which encode two stress proteins (UspA and HspC2, respectively) inside amoebae, but not inside human macrophages, supports the concept that *L. pneumophila* is not under strong selective pressure to differentiate inside macrophages. Perhaps macrophages in culture do not create intracellular conditions that are stressful enough to force *L. pneumophila* to differentiate into environmentally fit MIFs. This could imply that some forms of intracellular stress may act as a signal for the full differentiation of *L. pneumophila* into MIFs.

The gene *sodC* encodes the periplasmic protein zinc-copper superoxide dismutase (ZnCuSOD), which decomposes superoxide radicals (Steinman & Ely, 1990; Stabel *et al.*, 1994). ZnCuSOD displays a higher activity during the transition of *L. pneumophila* into SPFs, suggesting that ZnCuSOD is important for survival of *L. pneumophila* at stationary phase (St John & Steinman, 1996). Although ZnCuSOD could possibly decompose the superoxide radicals generated during phagocytosis, *sodC* mutants are not

defective in the intracellular growth inside human macrophages (St John & Steinman, 1996). Harada et al. have shown that the infection of macrophages with *L. pneumophila* prevents the formation of reactive oxygen species (ROS) (Harada *et al.*, 2007), which may explain why genes involved in oxidative stress e.g. *sodC* are not induced during intracellular growth. The qRT-PCR analysis has also confirmed that ZnCuSOD is not upregulated inside human macrophages. The importance of ZnCuSOD in growth inside amoebae remains to be studied.

The expression of *lpg1669*, which encodes a putative α-amylase, is quite significant. The expression of *lpg1669* had the most dramatic upregulation (out of the tested genes) inside amoebae. In addition, it was also upregulated inside *Tetrahymena* ciliates, and BYE broth, but downregulated inside human macrophages. The expression of *lpg2352*, which encodes a malate dehydrogenase enzyme, was also upregulated inside amoebae, in SPFs, and in ciliates and downregulated inside human macrophages. Together, these findings may suggest that carbohydrate metabolism plays a role in the differentiation of *L. pneumophila* into MIFs in the natural environment, when amino acid levels become limited.

Analysis of the expression of genes involved in carbohydrate metabolism by qRT-PCR has confirmed the early observations of the microarray analysis that genes coding for the components of the ED pathway (for instance, 6-phosphogluconolactonase, glucokinase, and the sugar transporter) and inositol-1-monophosphatase are upregulated during *L. pneumophila* replication inside amoebae (Bruggemann *et al.*, 2006).

The freshwater amoeba *A. castellanii* contains various sugar moieties such as high levels of galactose and glucose and small amounts of mannose and xylose (Dudley *et al.*, 2009). Starvation of *Tetrahymena* ciliates (for example, by incubation in TBOS) results in the loss of cellular proteins and utilization of glycogen as an energy source (Levy & Elliott, 1968). The availability of carbohydrates inside these host cells further supports the notion that carbohydrates can be a potential source of energy when amino acid levels become limited and that carbohydrate metabolism could play a role in the replication and differentiation of *L. pneumophila* inside amoebae.

6.2.3. *Tetrahymena* ciliates are a good model to study the differentiation process in *L. pneumophila*

Tetrahymena ciliates have been previously proposed as a differentiation model to identify the signals that trigger the development of MIFs and study the genes that are actively transcribed during *L. pneumophila* differentiation (Faulkner *et al.*, 2008) because the differentiation process into MIFs inside the ciliates is direct and rapid. Since the morphological features of MIFs could be observed as early as 30 minutes following feeding of the ciliates with SPFs legionellae (Faulkner *et al.*, 2008), global changes in the gene expression of *L. pneumophila* were studied at the same time (by microarray analysis) to identify the genes that may be activated early during the differentiation process. Analysis of the changes in gene expression of *L. pneumophila* from SPFs to MIFs in *Tetrahymena* ciliates could identify potential markers that are specific for MIF formation.

The qRT-PCR analysis of the selected 15 genes during feeding of *Tetrahymena* ciliates showed a very good correlation with the results of microarray analysis. In addition, 12 of the 15 genes were also upregulated inside the natural amoebic host (but not inside human macrophages), suggesting that the differentiation process of *L. pneumophila* in both amoebae and ciliates involves expression of a similar set of genes. These findings support that *Tetrahymena* ciliates are a valid model to study the differentiation of *L. pneumophila* into MIFs and may also provide insights into the incomplete differentiation of *L. pneumophila* inside human macrophages.

However, it could still be argued that the changes in the gene expression of *L. pneumophila* inside *Tetrahymena* ciliates (where *L. pneumophila* changes from SPFs to MIFs) are only a subset of the changes *L. pneumophila* undergoes inside amoebae (where *L. pneumophila* changes from RFs to MIFs). Therefore the gene expression analysis inside *Tetrahymena* may not be a true representative of the changes in gene expression of *L. pneumophila* inside amoebae. In addition, the release of legionellae-laden pellets into the infection medium or freshwater environments may trigger further changes in *L. pneumophila* gene expression.

6.2.4. Protein analysis supports the results of transcriptome analysis

Analysis of the protein profiles of the *L. pneumophila* progeny obtained from amoebae and human macrophages using one-dimensional protein gel has identified 18 proteins that were not present in the proteome of *L. pneumophila* progeny produced in cultured human macrophages, suggesting that the identified proteins are potential targets for future studies of legionellae differentiation and fitness (chapter 3).

The results of the protein analysis have also supported the findings of the transcriptome analysis (chapter 4). The genes that encode 14 of the identified 18 proteins had also high expression levels during *L. pneumophila* infections of amoebae.
For instance, 3-oxoacyl ACP synthase and BdhA proteins that are involved in lipid metabolism are upregulated in the *L. pneumophila* progeny in amoebae. 2-D protein gel analysis has previously shown that BdhA is also upregulated in SPFs *in vitro* (Hayashi *et al.*, 2010). Together, these findings could explain the low proportion of progenies from macrophages that display large inclusions, or a thickened membranous envelope.

The enhanced entry proteins EnhA and EnhC were also upregulated in the *L. pneumophila* progeny from amoebae, supporting the earlier transcriptome findings and providing a reasonable explanation for the low adherence and efficiency of the *L. pneumophila* progeny from macrophages to initiate cell infections.

The two stress proteins UspA and HspC2 were also upregulated in the *L. pneumophila* progeny from amoebae, supporting the earlier transcriptome data and supporting the concept that *L. pneumophila* is not under strong selective pressure to differentiate inside macrophages.

In addition, hypothetical proteins were also identified supporting the concept that our understanding of the differentiation of *L. pneumophila* is limited.

Protein analysis of *L. pneumophila* has revealed that proteins associated with glycolysis (pyruvate kinase, malate dehydrogenase) and the TCA cycle (2-oxoglutarate ferredoxin oxidoreductase) are upregulated at the stationary phase *in vitro* (Hayashi *et al.*, 2010). Earlier protein analysis (Chapter 3) has also demonstrated that malate dehydrogenase is upregulated in the *L. pneumophila* progeny produced in amoebae. Together, these findings suggest that *L. pneumophila* may be able to utilize carbohydrates as an energy source, when amino acid levels become limited.

A more refined proteomic analysis (perhaps involving 2-D protein gels, or comparative shotgun mass spectrometry) could be required to substantiate the initial observations of my PhD project. In addition, it should be noted that my protein analysis did not include secreted *L. pneumophila* proteins, because the progenies used to generate the whole cell lysate samples had been extensively washed off the culture supernatants during the purification process.

6.3. Carbon metabolism of intracellular bacteria

Our knowledge about the metabolism of bacteria in their natural habitats is very limited, mainly because our understanding of the microbial physiology is largely based on *in vitro* studies which may not represent the actual events that happen to the bacterium in its intracellular niche. For instance, very little is known about the metabolism of *E. coli* in its natural habitat, the human intestine. Interestingly, *E. coli* displays different patterns of carbohydrate metabolism in different environments. When *E. coli* is grown *in vitro*, glucose is primarily metabolized through the glycolytic and the pentose phosphate pathways with no role for the ED pathway (Fuhrer *et al.*, 2005). In contrast, *E. coli* grown on mucus upregulates the enzymes involved in the ED pathway (Chang *et al.*, 2004), which are essential for colonization of the mouse intestine (Sweeney *et al.*, 1996; Chang *et al.*, 2004).

Induction of amino acid transport genes was also observed during intracellular growth of *Yersinia pestis*, *Salmonella typhimurium*, *Salmonella typhi*, *Shigella flexneri*, and *Bacillus anthracis* (Eriksson *et al.*, 2003; Lucchini *et al.*, 2005; Faucher *et al.*, 2006; Bergman *et al.*, 2007; Fukuto *et al.*, 2010). Moreover, many amino acid transporters were identified as essential for intracellular growth of *L. monocytogenes* (Schauer *et al.*, 2010).

The ED pathway is the major pathway for carbohydrate metabolism in *L. pneumophila* (Harada *et al.*, 2010). The ED pathway is also important for the survival of *Salmonella enterica* inside macrophages. Microarray analysis of *S. typhimurium* inside cultured macrophages has shown that the ED pathway is the dominant mode of sugar metabolism and that the majority of genes encoding components of the TCA cycle are downregulated (Eriksson *et al.*, 2003; Lucchini *et al.*, 2005; Faucher *et al.*, 2006; Bergman *et al.*, 2007; Fukuto *et al.*, 2010). Although glucose is the main carbon source

inside the *Salmonella*-containing vacuole (SCV) (Bowden *et al.*, 2009), *Salmonella* mutants defective in glucose uptake can still replicate in Caco-2 cells at a slower rate, suggesting that *Salmonella* can switch to other carbon sources in the absence of glucose (Garcia-del Portillo *et al.*, 2008). Other studies have suggested that catabolism of fatty acids seems to play a role in *Salmonella* metabolism *in vivo*. *Salmonella* mutants unable to metabolize fatty acids display attenuated virulence in mice (Krivan *et al.*, 1992; Utley *et al.*, 1998).

Genes involved in the catabolism of glycerol are induced during growth of *L. pneumophila* inside human macrophages, suggesting that glycerol could be used as a carbon source (Faucher *et al.*, 2011). Glycerol could be the major carbon source for *Listeria monocytogenes* (Eylert *et al.*, 2008) and *Shigella flexneri* (Lucchini *et al.*, 2005) inside murine cultured macrophages. *L. monocytogenes* genes involved in the facilitated uptake (*glpF*) and catabolism (glycerol kinase (*glpK*), glycerol-3-phosphate (glycerol-3P) dehydrogenase (*glpD*) and dihydroxyacetone kinase subunit K (*dhaK*)) of glycerol are significantly upregulated during growth of this pathogen in the cytoplasm of epithelial or macrophage cell lines (Chatterjee *et al.*, 2006; Joseph *et al.*, 2006). Moreover, *L. monocytogenes* mutants lacking *glpD*, *glpF*, *glpK*, and *dhaK* display defects in their intracellular growth rates (Joseph *et al.*, 2006; Joseph *et al.*, 2008).

Although the hexose-phosphate transporter Hpt is required for normal replication and virulence in cultured mammalian cells and in mice (Goetz *et al.*, 2001; Chico-Calero *et al.*, 2002), *L. monocytogenes* mutants impaired in glucose uptake replicate as efficiently as the wild-type strains in the cytosol of J774 macrophages and Caco-2 epithelial cells (Stoll & Goebel, 2010), suggesting that glucose does not serve as a major substrate for carbon metabolism of intracellular *L. monocytogenes*.

Although differential gene expression studies of *S. flexneri* and ^{13}C-isotopologue profiling studies of an EIEC strain confirm a carbon metabolism using C_3 substrates (Gotz *et al.*, 2010), ^{13}C-isotopologue profiling studies of another EIEC strain suggests that glucose is the primary carbon source during intracellular growth (Gotz *et al.*, 2010), suggesting that EIEC (and possibly *S. flexneri*) exhibit strain-dependent preferences. The genes required for glycerol-3-P uptake and metabolism (*ugp* and *glpD*) are also upregulated during growth of *M. tuberculosis* inside primary mouse macrophages

(Schnappinger *et al.*, 2003). In addition, differential gene expression data of *M. tuberculosis* growing in primary mouse macrophages have shown that all of the genes characteristic for a C_2-based metabolism are significantly upregulated with genes required for gluconeogenesis showing a modest upregulation (Schnappinger *et al.*, 2003). Together, these data suggest that fatty acids and possibly glycerol or glycerol-3-P are the preferred carbon sources for *M. tuberculosis* in bone marrow-derived macrophages. Indeed, the dependency on fatty acids in acute and persistent *M. tuberculosis* infections in mice is a hallmark of its *in vivo* carbon metabolism (McKinney *et al.*, 2000; Munoz-Elias & McKinney, 2005; Munoz-Elias *et al.*, 2006).

In conclusion, metabolic studies of intracellular bacteria have shown that intracellular pathogens are capable of adapting to the host cell environments in a pathogen-specific way. This adaptation process seems to be controlled mainly by the pathogen's metabolic capacities. It could also be possible that intracellular bacteria influence the metabolism of host cells to fulfill their metabolic requirements. Studies have also shown that metabolism of intracellular bacteria seems to be flexible and that carbon metabolism is not restricted to a single preferred carbon substrate but may switch to alternative sources when the primary source becomes unavailable.

6.4. Lpg1669 (AmyA) protein is not essential for *L. pneumophila* growth and differentiation inside amoebae

Previous studies have shown that *L. pneumophila* genes involved in carbohydrate metabolism are upregulated during intracellular growth and could allow the bacterium to scavenge host carbohydrates (Bruggemann *et al.*, 2006). The gene *lpg1669* could be one such gene. As a putative α-amylase, it could provide a means for *L. pneumophila* to exploit carbohydrate resources from the amoebic hosts during replication. The qRT-PCR experiments have demonstrated that the expression of *lpg1669* is upregulated inside amoebae, *Tetrahymena* ciliates, BYE broth and downregulated in human macrophages, suggesting that *lpg1669* could be associated with *L. pneumophila* differentiation. Previous studies have shown that *lpg1669* is upregulated at the stationary phase, inside amoebae (Bruggemann *et al.*, 2006) and following the treatment of *L. pneumophila* with nicotinic acid to induce its virulence traits (Edwards *et al.*, 2013). The expression of

lpg1669 was upregulated 20-fold over a 6-hour period inside amoebae (Bruggemann *et al.*, 2006) and was dramatically upregulated (166-fold) in the amoeba progeny (composed mainly of MIFs) compared to RFs. The expression of *lpg1669* is repressed in the $LetS^{T311M}$ mutant, suggesting that it could be regulated either directly or indirectly by the LetAS-RsmYZ-CsrA system (Edwards *et al.*, 2010).

Lpg1669 displays the D-E-D catalytic triad characteristic of α-amylases and sequence features of the α-amylase family. While being a powerful tool, sequence homology is at best an approximation (Devos & Valencia, 2000). Although the D-E-D catalytic triad is the only universally conserved sequence in the α-amylase family, seven regions of primary sequence are also predicted to be well conserved among the α-amylase family (Janecek & Blesak, 2011). Comparing the primary sequence of the well-characterized α-amylase from *Aspergillus oryzae* (Taka A) to Lpg1669 reveals significant homology in three of these regions, including the region containing the first catalytic aspartic acid residue. The region containing the catalytic glutamic acid residue in Lpg1669 was not homologous to the corresponding regions in the α-amylases of *A. oryzae* or *B. subtilis*. Tertiary structural features are also important in identifying α-amylases. The presence of a TIM-barrel in conjunction with the D-E-D motif strongly implies an α-amylase activity (Janecek & Blesak, 2011). However, the presence of the TIM-barrel in Lpg1669 was not supported by the TIM-finder program (http://202.112.170.199/TIM-Finder/).

Expression of a His_6-tagged copy of Lpg1669 (AmyA) has demonstrated that AmyA is an intracellular protein and is not secreted outside the bacterial cell. *E. coli* possesses both cytoplasmic (AmyA) (Raha *et al.*, 1992) and periplasmic (MalS) α-amylase proteins. The two proteins act on maltodextrins after they enter the periplasm via the outer membrane porin LamB (Freundlieb *et al.*, 1988). In the periplasm, maltodextrins are either cleaved by the periplasmic amylase, MalS, or are transported to the cytoplasm via a transport complex (Schneider *et al.*, 1992) where they are further processed. The exact subcellular location of Lpg1669 and the role it plays in the carbohydrate metabolism of *L. pneumophila* still remain to be determined.

Electron microscopy analysis has revealed that the progeny of the *lpg1669* (*amyA*) mutant obtained from amoebae, macrophages, and ciliates displays no

ultrastructural differentiation defects, compared to its parent strain. Intracellular growth experiments have also revealed that the *lpg1669* (*amyA*) mutant did not display intracellular growth defects inside amoebae and human macrophages. These findings clearly suggest that the absence of Lpg1669 does not affect the intracellular growth or differentiation of *L. pneumophila*. It could be due to the fact that *L. pneumophila* possesses two other putative α-amylases encoded by *lpg1671* and *lpg2528* and a glucoamylase encoded by *gamA* (Herrmann *et al.*, 2011) which could compensate for the loss of *lpg1669*. Moreover, previous studies have shown that deletion of *L. pneumophila* genes associated with carbohydrate metabolism do not usually result in significant growth defects, and *L. pneumophila* mutants deficient in the entire ED pathway components had growth defects inside amoeba, macrophages, and alveolar epithelium (Harada *et al.*, 2010). While the expression levels of *lpg1671* and *lpg2528* are upregulated at stationary phase and following nicotinic acid treatment, their expression levels were not repressed in the $LetS^{T311M}$ mutant, suggesting that the expression of *lpg1669* is regulated by different machinery than the other putative α-amylases (Edwards *et al.*, 2010).

While *lpg1669*, *lpg 2352*, and other genes associated with carbohydrate metabolism do not affect differentiation, their massive upregulation at later points inside amoebae could allow their use as genetic markers for the *L. pneumophila* differentiation into MIFs.

Previous studies have also reported that ^{13}C derived from labelled glucose is found in various amino acids and in poly-3-hydroxybutyrate (PHB) (Eylert *et al.*, 2010). A recent study in our lab (unpublished data) has demonstrated the importance of *bdhA*, the gene that is responsible for the synthesis of PHB, in the extended survival of *L. pneumophila* in water. Indeed, PHB inclusions are gradually degraded during the prolonged survival of *L. pneumophila* in water. This could suggest that carbohydrate metabolism may be important for survival of *L. pneumophila* in the environment rather than intracellular growth inside the host cells.

6.5. Conclusions and Future Directions

The findings of my PhD project have demonstrated that *L. pneumophila* reaches different development endpoints inside amoebae, ciliates, and cultured human macrophages. The reported differences between the *L. pneumophila* progeny from the natural environment and the progeny from human macrophages could provide initial insights into understanding the lack of LD transmission among humans. I have performed a one-dimensional protein analysis to study the differences in the protein profiles of the *L. pneumophila* progeny from amoebae and human macrophages (**Table 3.6.**). More refined proteome analysis (two-dimensional protein gels or shotgun proteomics) could substantiate my early findings and identify more proteins that could be targets for future studies to understand the molecular mechanisms behind the differentiation of *L. pneumophila* in its natural environment.

This study has also identified, through analysis of the microarray data for gene expression of *L. pneumophila* in amoebae and human macrophages, a list of *L. pneumophila* genes that are upregulated in amoebae and downregulated in human macrophages (**Appendix I**). A short list of 20 genes (**Table 4.3.**) was selected for confirmation by qRT-PCR analysis. The remainder of the genes in Appendix I are also potential targets for future studies.

This study has also identified a list of *L. pneumophila* genes that are upregulated inside human macrophages, but downregulated inside amoebae (**Appendix II**). These genes represent targets for future studies that focus on understanding the specific virulence mechanisms *L. pneumophila* employs to infect susceptible humans.

This study has demonstrated that *Tetrahymena* ciliates are a good model to study the differentiation of *L. pneumophila*. A good correlation has been observed between the upregulated *L. pneumophila* genes in both amoebae and ciliates, suggesting that *L. pneumophila* upregulates certain sets of genes required for its full differentiation in freshwater protozoa. Although a short list of 15 *L. pneumophila* genes was selected for confirmation by qRT-PCR analysis, the expression of other *L. pneumophila* genes (**Table 4.4.**) could also be tested in future studies. Moreover, analysis of the proteome of the *L. pneumophila* progeny from amoebae and from ciliates could also be tested to understand the similarities and differences in their protein profiles.

This study has investigated the role of the gene *lpg1669* (*amyA*) which encodes a putative α-amylase in the intracellular growth and differentiation of *L. pneumophila*. The remainder of the genes, other than *lpg1669*, (**Table 4.5.**) are also potential targets for future studies. These genes have demonstrated a high level of expression inside amoebae and a low level of expression inside human macrophages, suggesting that they could be associated with the full differentiation of *L. pneumophila* in its natural environment.

Despite the high levels of gene expression, AmyA (Lpg1669) does not seem to play an important role in the differentiation of *L. pneumophila*. This is not completely unexpected given that other studies have shown that although *L. pneumophila* genes involved in carbohydrate metabolism are upregulated inside amoebae to allow the bacterium to metabolize the host carbohydrates, carbohydrate metabolism seems not essential for the intracellular growth of *L. pneumophila*. That is, *L. pneumophila* mutants deficient in carbohydrate metabolism do not generally tend to display growth defects *in vitro* or *in vivo*. Therefore, the role of carbohydrate metabolism in the differentiation of *L. pneumophila* is still not understood. Construction of an *L. pneumophila* strain that is defective in the 3 genes that encode putative α-amylase enzymes and *gamA* that encodes a glucoamylase and investigation of the ability of this strain to grow and differentiate inside host cells could be considered in future studies. Transcriptome and proteome studies have indicated that the gene *lpg2971* which encodes a malate dehydrogenase enzyme can be a target for future studies. These future studies could help us gain a better understanding of the differentiation process in *L. pneumophila* and subsequently gain a better understanding of the transmission of LD.

REFERENCES

Abdelrahman YM & Belland RJ (2005) The chlamydial developmental cycle FEMS Microbiol Rev **29:** 949-959.

Abu Kwaik Y (1996) The phagosome containing *Legionella pneumophila* within the protozoan *Hartmannella vermiformis* is surrounded by the rough endoplasmic reticulum Appl Environ Microbiol **62:** 2022-2028.

Abu Kwaik Y, Gao LY, Harb OS & Stone BJ (1997) Transcriptional regulation of the macrophage-induced gene (*gspA*) of *Legionella pneumophila* and phenotypic characterization of a null mutant Mol Microbiol **24:** 629-642.

Abu-Zant A, Asare R, Graham JE & Abu Kwaik Y (2006) Role for RpoS but not RelA of *Legionella pneumophila* in modulation of phagosome biogenesis and adaptation to the phagosomal microenvironment Infect Immun **74:** 3021-3026.

Abu-Zant A, Jones S, Asare R, Suttles J, Price C, Graham J & Kwaik YA (2007) Anti-apoptotic signalling by the Dot/Icm secretion system of *L. pneumophila* Cell Microbiol **9:** 246-264.

Albert-Weissenberger C, Sahr T, Sismeiro O, Hacker J, Heuner K & Buchrieser C (2010) Control of flagellar gene regulation in *Legionella pneumophila* and its relation to growth phase J Bacteriol **192:** 446-455.

Al-Khodor S, Kalachikov S, Morozova I, Price CT & Abu Kwaik Y (2009) The PmrA/PmrB two-component system of *Legionella pneumophila* is a global regulator required for intracellular replication within macrophages and protozoa Infect Immun **77:** 374-386.

Allard KA, Viswanathan VK & Cianciotto NP (2006) *lbtA* and *lbtB* are required for production of the *Legionella pneumophila* siderophore legiobactin J Bacteriol **188:** 1351-1363.

Allard KA, Dao J, Sanjeevaiah P, McCoy-Simandle K, Chatfield CH, Crumrine DS, Castignetti D & Cianciotto NP (2009) Purification of Legiobactin and importance of this siderophore in lung infection by *Legionella pneumophila* Infect Immun **77:** 2887-2895.

Alli OA, Gao LY, Pedersen LL, Zink S, Radulic M, Doric M & Abu Kwaik Y (2000) Temporal pore formation-mediated egress from macrophages and alveolar epithelial cells by *Legionella pneumophila* Infect Immun **68:** 6431-6440.

Altman E & Segal G (2008) The response regulator CpxR directly regulates expression of several *Legionella pneumophila* icm/dot components as well as new translocated substrates J Bacteriol **190:** 1985-1996.

Archer KA, Alexopoulou L, Flavell RA & Roy CR (2009) Multiple MyD88-dependent responses contribute to pulmonary clearance of *Legionella pneumophila* Cell Microbiol **11:** 21-36.

Aurass P, Pless B, Rydzewski K, Holland G, Bannert N & Flieger A (2009) *bdhA-patD* operon as a virulence determinant, revealed by a novel large-scale approach for identification of *Legionella pneumophila* mutants defective for amoeba infection Appl Environ Microbiol **75:** 4506-4515.

Bachman MA & Swanson MS (2001) RpoS co-operates with other factors to induce *Legionella pneumophila* virulence in the stationary phase Mol Microbiol **40:** 1201-1214.

Banga S, Gao P, Shen X, Fiscus V, Zong WX, Chen L & Luo ZQ (2007) *Legionella pneumophila* inhibits macrophage apoptosis by targeting pro-death members of the Bcl2 protein family Proc Natl Acad Sci U S A **104:** 5121-5126.

Barbaree JM, Fields BS, Feeley JC, Gorman GW & Martin WT (1986) Isolation of protozoa from water associated with a legionellosis outbreak and demonstration of intracellular multiplication of *Legionella pneumophila* Appl Environ Microbiol **51:** 422-424.

Barker J, Brown MR, Collier PJ, Farrell I & Gilbert P (1992) Relationship between *Legionella pneumophila* and *Acanthamoeba polyphaga*: physiological status and susceptibility to chemical inactivation Appl Environ Microbiol **58:** 2420-2425.

Bartfeld S, Engels C, Bauer B, Aurass P, Flieger A, Bruggemann H & Meyer TF (2009) Temporal resolution of two-tracked NF-kappaB activation by *Legionella pneumophila* Cell Microbiol **11:** 1638-1651.

Beaute J, Zucs P, de Jong B & European Legionnaires' Disease Surveillance Network (2013) Legionnaires disease in Europe, 2009-2010 Euro Surveill **18:** 20417.

Benin AL, Benson RF, Arnold KE, Fiore AE, Cook PG, Williams LK, Fields B & Besser RE (2002) An outbreak of travel-associated Legionnaires disease and Pontiac fever: the need for enhanced surveillance of travel-associated legionellosis in the United States J Infect Dis **185:** 237-243.

Berger KH & Isberg RR (1993) Two distinct defects in intracellular growth complemented by a single genetic locus in *Legionella pneumophila* Mol Microbiol **7:** 7-19.

Bergman NH, Anderson EC, Swenson EE, Janes BK, Fisher N, Niemeyer MM, Miyoshi AD & Hanna PC (2007) Transcriptional profiling of *Bacillus anthracis* during infection of host macrophages Infect Immun **75:** 3434-3444.

Berk SG & Garduno RA (2013) The *tetrahymena* and *acanthamoeba* model systems Methods Mol Biol **954:** 393-416.

Berk SG, Faulkner G, Garduno E, Joy MC, Ortiz-Jimenez MA & Garduno RA (2008) Packaging of live *Legionella pneumophila* into pellets expelled by *Tetrahymena spp*. does not require bacterial replication and depends on a Dot/Icm-mediated survival mechanism Appl Environ Microbiol **74:** 2187-2199.

Berk SG, Faulkner G, Garduno E, Joy MC, Ortiz-Jimenez MA & Garduno RA (2008) Packaging of live *Legionella pneumophila* into pellets expelled by *Tetrahymena spp*. does not require bacterial replication and depends on a Dot/Icm-mediated survival mechanism Appl Environ Microbiol **74:** 2187-2199.

Bitar DM, Molmeret M & Kwaik YA (2005) Structure-function analysis of the C-terminus of IcmT of *Legionella pneumophila* in pore formation-mediated egress from macrophages FEMS Microbiol Lett **242:** 177-184.

Bosshardt SC, Benson RF & Fields BS (1997) Flagella are a positive predictor for virulence in *Legionella* Microb Pathog **23:** 107-112.

Bowden SD, Rowley G, Hinton JC & Thompson A (2009) Glucose and glycolysis are required for the successful infection of macrophages and mice by *Salmonella enterica* serovar typhimurium Infect Immun **77:** 3117-3126.

Bozue JA & Johnson W (1996) Interaction of *Legionella pneumophila* with *Acanthamoeba castellanii*: uptake by coiling phagocytosis and inhibition of phagosome-lysosome fusion Infect Immun **64:** 668-673.

Brassinga AK, Mathew AC, Hoemaker CJ, Morash MG, Leblanc JJ & Hoffman PS (2006) Novel use of *Helicobacter pylori* nitroreductase (*rdxA*) as a counterselectable marker in allelic vector exchange to create *Legionella pneumophila* Philadelphia-1 mutants. *Legionella*: state of the art 30 years after its recognition (N. P. Cianciotto, Y. Abukwaik, P. H. Edelstein, B. S. Fields, D. F. Geary, T. G. Harrison, C. A. Joseph, R. M. Ratcliff, J. E. Stout, and M. S. Swanson, ed), pp.339-342. ASM Press, Washington, DC.

Brenner DJ, Steigerwalt AG & McDade JE (1979) Classification of the Legionnaires' disease bacterium: *Legionella pneumophila*, genus novum, species nova, of the family Legionellaceae, familia nova Ann Intern Med **90:** 656-658.

Brieland J, McClain M, LeGendre M & Engleberg C (1997) Intrapulmonary *Hartmannella vermiformis*: a potential niche for *Legionella pneumophila* replication in a murine model of legionellosis Infect Immun **65:** 4892-4896.

Brieland J, McClain M, Heath L, Chrisp C, Huffnagle G, LeGendre M, Hurley M, Fantone J & Engleberg C (1996) Coinoculation with *Hartmannella vermiformis* enhances replicative *Legionella pneumophila* lung infection in a murine model of Legionnaires' disease Infect Immun **64:** 2449-2456.

Brieland JK, Fantone JC, Remick DG, LeGendre M, McClain M & Engleberg NC (1997) The role of *Legionella pneumophila*-infected *Hartmannella vermiformis* as an infectious particle in a murine model of Legionnaire's disease Infect Immun **65:** 5330-5333.

Bruggemann H, Cazalet C & Buchrieser C (2006) Adaptation of *Legionella pneumophila* to the host environment: role of protein secretion, effectors and eukaryotic-like proteins Curr Opin Microbiol **9:** 86-94.

Bruggemann H, Hagman A, Jules M *et al.* (2006) Virulence strategies for infecting phagocytes deduced from the in vivo transcriptional program of *Legionella pneumophila* Cell Microbiol **8:** 1228-1240.

Burstein D, Zusman T, Degtyar E, Viner R, Segal G & Pupko T (2009) Genome-scale identification of *Legionella pneumophila* effectors using a machine learning approach PLoS Pathog **5:** e1000508.

Byrd TF & Horwitz MA (2000) Aberrantly low transferrin receptor expression on human monocytes is associated with nonpermissiveness for *Legionella pneumophila* growth J Infect Dis **181:** 1394-1400.

Byrd TF & Horwitz MA (1989) Interferon gamma-activated human monocytes downregulate transferrin receptors and inhibit the intracellular multiplication of *Legionella pneumophila* by limiting the availability of iron J Clin Invest **83:** 1457-1465.

Byrne B & Swanson MS (1998) Expression of *Legionella pneumophila* virulence traits in response to growth conditions Infect Immun **66:** 3029-3034.

Campodonico EM, Chesnel L & Roy CR (2005) A yeast genetic system for the identification and characterization of substrate proteins transferred into host cells by the *Legionella pneumophila* Dot/Icm system Mol Microbiol **56:** 918-933.

Cazalet C, Rusniok C, Bruggemann H *et al.* (2004) Evidence in the *Legionella pneumophila* genome for exploitation of host cell functions and high genome plasticity Nat Genet **36:** 1165-1173.

CDC (Centres for Disease Prevention and Control) (1997). Guidelines for prevention and control of nosocomial pneumonia. *Morbidity and Mortality Weekly Report*, 46:31–34.

Chang DE, Smalley DJ, Tucker DL *et al.* (2004) Carbon nutrition of *Escherichia coli* in the mouse intestine Proc Natl Acad Sci U S A **101:** 7427-7432.

Chatfield CH & Cianciotto NP (2007) The secreted pyomelanin pigment of *Legionella pneumophila* confers ferric reductase activity Infect Immun **75:** 4062-4070.

Chatterjee SS, Hossain H, Otten S, Kuenne C, Kuchmina K, Machata S, Domann E, Chakraborty T & Hain T (2006) Intracellular gene expression profile of Listeria monocytogenes Infect Immun **74:** 1323-1338.

Chen DE, Podell S, Sauer JD, Swanson MS & Saier MH,Jr (2008) The phagosomal nutrient transporter (Pht) family Microbiology **154:** 42-53.

Chen J, de Felipe KS, Clarke M, Lu H, Anderson OR, Segal G & Shuman HA (2004) *Legionella* effectors that promote nonlytic release from protozoa Science **303:** 1358-1361.

Chico-Calero I, Suarez M, Gonzalez-Zorn B, Scortti M, Slaghuis J, Goebel W, Vazquez-Boland JA & European Listeria Genome Consortium (2002) Hpt, a bacterial homolog of the microsomal glucose- 6-phosphate translocase, mediates rapid intracellular proliferation in Listeria Proc Natl Acad Sci U S A **99:** 431-436.

Chien M, Morozova I, Shi S *et al.* (2004) The genomic sequence of the accidental pathogen *Legionella pneumophila* Science **305:** 1966-1968.

Chong A, Lima CA, Allan DS, Nasrallah GK & Garduno RA (2009) The purified and recombinant *Legionella pneumophila* chaperonin alters mitochondrial trafficking and microfilament organization Infect Immun **77:** 4724-4739.

Cianciotto NP (2007) Iron acquisition by *Legionella pneumophila* Biometals **20:** 323-331.

Cirillo JD, Falkow S & Tompkins LS (1994) Growth of *Legionella pneumophila* in *Acanthamoeba castellanii* enhances invasion Infect Immun **62:** 3254-3261.

Cirillo JD, Cirillo SL, Yan L, Bermudez LE, Falkow S & Tompkins LS (1999) Intracellular growth in *Acanthamoeba castellanii* affects monocyte entry mechanisms and enhances virulence of *Legionella pneumophila* Infect Immun **67:** 4427-4434.

Cirillo JD, Cirillo SL, Yan L, Bermudez LE, Falkow S & Tompkins LS (1999) Intracellular growth in *Acanthamoeba castellanii* affects monocyte entry mechanisms and enhances virulence of *Legionella pneumophila* Infect Immun **67:** 4427-4434.

Cirillo SL, Lum J & Cirillo JD (2000) Identification of novel loci involved in entry by *Legionella pneumophila* Microbiology **146 (Pt 6):** 1345-1359.

Clemens DL, Lee BY & Horwitz MA (2000) Deviant expression of Rab5 on phagosomes containing the intracellular pathogens *Mycobacterium tuberculosis* and *Legionella pneumophila* is associated with altered phagosomal fate Infect Immun **68:** 2671-2684.

Coers J, Monahan C & Roy CR (1999) Modulation of phagosome biogenesis by *Legionella pneumophila* creates an organelle permissive for intracellular growth Nat Cell Biol **1:** 451-453.

Conover GM, Derre I, Vogel JP & Isberg RR (2003) The *Legionella pneumophila* LidA protein: a translocated substrate of the Dot/Icm system associated with maintenance of bacterial integrity Mol Microbiol **48:** 305-321.

Cohen S (1998) A Guide to the Polyamines (ed). Oxford University Press, New York.

Cursons RT, Brown TJ & Keys EA (1980) Effect of disinfectants on pathogenic free-living amoebae: in axenic conditions Appl Environ Microbiol **40:** 62-66.

Dalebroux ZD, Edwards RL & Swanson MS (2009) SpoT governs *Legionella pneumophila* differentiation in host macrophages Mol Microbiol **71:** 640-658.

Dalebroux ZD, Svensson SL, Gaynor EC & Swanson MS (2010) ppGpp conjures bacterial virulence Microbiol Mol Biol Rev **74:** 171-199.

D'Argenio DA & Miller SI (2004) Cyclic di-GMP as a bacterial second messenger Microbiology **150:** 2497-2502.

Den Boer JW, Yzerman E, Van Belkum A, Vlaspolder F & Van Breukelen FJ (1998) Legionnaire's disease and saunas Lancet **351:** 114.

Den Boer JW, Yzerman EP, Schellekens J *et al.* (2002) A large outbreak of Legionnaires' disease at a flower show, the Netherlands, 1999 Emerg Infect Dis **8:** 37-43.

Dennis JJ & Zylstra GJ (1998) Improved antibiotic-resistance cassettes through restriction site elimination using Pfu DNA polymerase PCR BioTechniques **25:** 772-4, 776.

Devos D & Valencia A (2000) Practical limits of function prediction Proteins **41:** 98-107.

Dietrich C, Heuner K, Brand BC, Hacker J & Steinert M (2001) Flagellum of *Legionella pneumophila* positively affects the early phase of infection of eukaryotic host cells Infect Immun **69:** 2116-2122.

Dudley R, Jarroll EL & Khan NA (2009) Carbohydrate analysis of *Acanthamoeba castellanii* Exp Parasitol **122:** 338-343.

Edelstein PH & Meyer RD (1984) Legionnaires' disease. A review Chest **85:** 114-120.

Edwards RL, Dalebroux ZD & Swanson MS (2009) *Legionella pneumophila* couples fatty acid flux to microbial differentiation and virulence Mol Microbiol **71:** 1190-1204.

Edwards RL, Jules M, Sahr T, Buchrieser C & Swanson MS (2010) The *Legionella pneumophila* LetA/LetS two-component system exhibits rheostat-like behavior Infect Immun **78:** 2571-2583.

Edwards RL, Bryan A, Jules M, Harada K, Buchrieser C & Swanson MS (2013) Nicotinic acid modulates *Legionella pneumophila* gene expression and induces virulence traits Infect Immun **81:** 945-955.

Elliott JA & Johnson W (1981) Immunological and biochemical relationships among flagella isolated from *Legionella pneumophila* serogroups 1, 2, and 3 Infect Immun **33:** 602-610.

Ensminger AW & Isberg RR (2009) *Legionella pneumophila* Dot/Icm translocated substrates: a sum of parts Curr Opin Microbiol **12:** 67-73.

Eriksson S, Lucchini S, Thompson A, Rhen M & Hinton JC (2003) Unravelling the biology of macrophage infection by gene expression profiling of intracellular *Salmonella enterica* Mol Microbiol **47:** 103-118.

Ewann F & Hoffman PS (2006) Cysteine metabolism in *Legionella pneumophila*: characterization of an L-cystine-utilizing mutant Appl Environ Microbiol **72:** 3993-4000.

Eylert E, Schar J, Mertins S, Stoll R, Bacher A, Goebel W & Eisenreich W (2008) Carbon metabolism of *Listeria monocytogenes* growing inside macrophages Mol Microbiol **69:** 1008-1017.

Eylert E, Herrmann V, Jules M, Gillmaier N, Lautner M, Buchrieser C, Eisenreich W & Heuner K (2010) Isotopologue profiling of *Legionella pneumophila*: role of serine and glucose as carbon substrates J Biol Chem **285:** 22232-22243.

Faucher SP, Mueller CA & Shuman HA (2011) *Legionella pneumophila* Transcriptome during Intracellular Multiplication in Human Macrophages Front Microbiol **2:** 60.

Faucher SP, Porwollik S, Dozois CM, McClelland M & Daigle F (2006) Transcriptome of *Salmonella enterica* serovar Typhi within macrophages revealed through the selective capture of transcribed sequences Proc Natl Acad Sci U S A **103:** 1906-1911.

Faulkner G & Garduno RA (2002) Ultrastructural analysis of differentiation in *Legionella pneumophila* J Bacteriol **184:** 7025-7041.

Faulkner G, Berk SG, Garduno E, Ortiz-Jimenez MA & Garduno RA (2008) Passage through *Tetrahymena tropicalis* triggers a rapid morphological differentiation in *Legionella pneumophila* J Bacteriol **190:** 7728-7738.

Fernandez RC, Lee SH, Haldane D, Sumarah R & Rozee KR (1989) Plaque assay for virulent *Legionella pneumophila* J Clin Microbiol **27:** 1961-1964.

Fernandez-Moreira E, Helbig JH & Swanson MS (2006) Membrane vesicles shed by *Legionella pneumophila* inhibit fusion of phagosomes with lysosomes Infect Immun **74:** 3285-3295.

Fields BS, Benson RF & Besser RE (2002) *Legionella* and Legionnaires' disease: 25 years of investigation Clin Microbiol Rev **15:** 506-526.

Fields BS, Shotts EB,Jr, Feeley JC, Gorman GW & Martin WT (1984) Proliferation of *Legionella pneumophila* as an intracellular parasite of the ciliated protozoan *Tetrahymena pyriformis* Appl Environ Microbiol **47:** 467-471.

Fields BS, Fields SR, Loy JN, White EH, Steffens WL & Shotts EB (1993) Attachment and entry of *Legionella pneumophila* in *Hartmannella vermiformis* J Infect Dis **167:** 1146-1150.

Fields BS, Barbaree JM, Shotts EB,Jr, Feeley JC, Morrill WE, Sanden GN & Dykstra MJ (1986) Comparison of guinea pig and protozoan models for determining virulence of *Legionella* species Infect Immun **53:** 553-559.

Fields BS, Nerad TA, Sawyer TK, King CH, Barbaree JM, Martin WT, Morrill WE & Sanden GN (1990) Characterization of an axenic strain of *Hartmannella vermiformis* obtained from an investigation of nosocomial legionellosis J Protozool **37:** 581-583.

Flannagan RS, Cosio G & Grinstein S (2009) Antimicrobial mechanisms of phagocytes and bacterial evasion strategies Nat Rev Microbiol **7:** 355-366.

Fontana MF, Banga S, Barry KC, Shen X, Tan Y, Luo ZQ & Vance RE (2011) Secreted bacterial effectors that inhibit host protein synthesis are critical for induction of the innate immune response to virulent *Legionella pneumophila* PLoS Pathog **7:** e1001289.

Forsbach-Birk V, McNealy T, Shi C, Lynch D & Marre R (2004) Reduced expression of the global regulator protein CsrA in *Legionella pneumophila* affects virulence-associated regulators and growth in *Acanthamoeba castellanii* Int J Med Microbiol **294:** 15-25.

Fraser DW, Tsai TR, Orenstein W *et al.* (1977) Legionnaires' disease: description of an epidemic of pneumonia N Engl J Med **297:** 1189-1197.

Freundlieb S, Ehmann U & Boos W (1988) Facilitated diffusion of p-nitrophenyl-alpha-D-maltohexaoside through the outer membrane of *Escherichia coli*. Characterization of LamB as a specific and saturable channel for maltooligosaccharides J Biol Chem **263:** 314-320.

Fuhrer T, Fischer E & Sauer U (2005) Experimental identification and quantification of glucose metabolism in seven bacterial species J Bacteriol **187:** 1581-1590.

Fukuto HS, Svetlanov A, Palmer LE, Karzai AW & Bliska JB (2010) Global gene expression profiling of *Yersinia pestis* replicating inside macrophages reveals the roles of a putative stress-induced operon in regulating type III secretion and intracellular cell division Infect Immun **78:** 3700-3715.

Gal-Mor O & Segal G (2003) The *Legionella pneumophila* GacA homolog (LetA) is involved in the regulation of *icm* virulence genes and is required for intracellular multiplication in *Acanthamoeba castellanii* Microb Pathog **34:** 187-194.

Gao LY & Kwaik YA (2000) The mechanism of killing and exiting the protozoan host *Acanthamoeba polyphaga* by *Legionella pneumophila* Environ Microbiol **2:** 79-90.

Gao LY, Harb OS & Kwaik YA (1998) Identification of macrophage-specific infectivity loci (mil) of *Legionella pneumophila* that are not required for infectivity of protozoa Infect Immun **66:** 883-892.

Gao LY, Harb OS & Abu Kwaik Y (1997) Utilization of similar mechanisms by *Legionella pneumophila* to parasitize two evolutionarily distant host cells, mammalian macrophages and protozoa Infect Immun **65:** 4738-4746.

Garcia-Fulgueiras A, Navarro C, Fenoll D *et al.* (2003) Legionnaires' disease outbreak in Murcia, Spain Emerg Infect Dis **9:** 915-921.

Garcia-del Portillo F, Nunez-Hernandez C, Eisman B & Ramos-Vivas J (2008) Growth control in the *Salmonella*-containing vacuole Curr Opin Microbiol **11:** 46-52.

Garduno RA (2007) Life cycle, growth cycles and developmental cycle of *Legionella pneumophila*. *Legionella pneumophila*: Pathogenesis and Immunity (P.S. Hoffman, T. Klein, and H. Friedman, ed), pp. 65-84. Springer, New York.

Garduno RA, Quinn FD & Hoffman PS (1998) HeLa cells as a model to study the invasiveness and biology of *Legionella pneumophila* Can J Microbiol **44:** 430-440.

Garduno RA, Garduno E, Hiltz M & Hoffman PS (2002) Intracellular growth of *Legionella pneumophila* gives rise to a differentiated form dissimilar to stationary-phase forms Infect Immun **70:** 6273-6283.

Ge J, Xu H, Li T, Zhou Y, Zhang Z, Li S, Liu L & Shao F (2009) A Legionella type IV effector activates the NF-kappaB pathway by phosphorylating the IkappaB family of inhibitors Proc Natl Acad Sci U S A **106:** 13725-13730.

Gebran SJ, Newton C, Yamamoto Y, Widen R, Klein TW & Friedman H (1994) Macrophage permissiveness for *Legionella pneumophila* growth modulated by iron Infect Immun **62:** 564-568.

George JR, Pine L, Reeves MW & Harrell WK (1980) Amino acid requirements of *Legionella pneumophila* J Clin Microbiol **11:** 286-291.

Gilmour MW, Bernard K, Tracz DM *et al.* (2007) Molecular typing of a *Legionella pneumophila* outbreak in Ontario, Canada J Med Microbiol **56:** 336-341.

Glick TH, Gregg MB, Berman B, Mallison G, Rhodes WW,Jr & Kassanoff I (1978) Pontiac fever. An epidemic of unknown etiology in a health department: I. Clinical and epidemiologic aspects Am J Epidemiol **107:** 149-160.

Glockner G, Albert-Weissenberger C, Weinmann E, Jacobi S, Schunder E, Steinert M, Hacker J & Heuner K (2008) Identification and characterization of a new conjugation/type IVA secretion system (trb/tra) of *Legionella pneumophila* Corby localized on two mobile genomic islands Int J Med Microbiol **298:** 411-428.

Goetz M, Bubert A, Wang G, Chico-Calero I, Vazquez-Boland JA, Beck M, Slaghuis J, Szalay AA & Goebel W (2001) Microinjection and growth of bacteria in the cytosol of mammalian host cells Proc Natl Acad Sci U S A **98:** 12221-12226.

Guerin JC (1992) Epidemiology of legionnaires' disease. From myth to reality Rev Mal Respir **9 Suppl 1:** R53-6.

Fallon RJ & Rowbotham TJ (1990) Microbiological investigations into an outbreak of Pontiac fever due to *Legionella micdadei* associated with use of a whirlpool J Clin Pathol **43:** 479-483.

Fields BS, Haupt T, Davis JP, Arduino MJ, Miller PH & Butler JC (2001) Pontiac fever due to *Legionella micdadei* from a whirlpool spa: possible role of bacterial endotoxin J Infect Dis **184:** 1289-1292.

Girod JC, Reichman RC, Winn WC,Jr, Klaucke DN, Vogt RL & Dolin R (1982) Pneumonic and nonpneumonic forms of legionellosis. The result of a common-source exposure to Legionella pneumophila Arch Intern Med **142:** 545-547.

Goldberg DJ, Wrench JG, Collier PW, Emslie JA, Fallon RJ, Forbes GI, McKay TM, Macpherson AC, Markwick TA & Reid D (1989) Lochgoilhead fever: outbreak of non-pneumonic legionellosis due to *Legionella micdadei* Lancet **1:** 316-318.

Gotz A, Eylert E, Eisenreich W & Goebel W (2010) Carbon metabolism of enterobacterial human pathogens growing in epithelial colorectal adenocarcinoma (Caco-2) cells PLoS One **5:** e10586.

Greig JE, Carnie JA, Tallis GF, Ryan NJ, Tan AG, Gordon IR, Zwolak B, Leydon JA, Guest CS & Hart WG (2004) An outbreak of Legionnaires' disease at the Melbourne Aquarium, April 2000: investigation and case-control studies Med J Aust **180:** 566-572.

Greub G & Raoult D (2004) Microorganisms resistant to free-living amoebae Clin Microbiol Rev **17:** 413-433.

Hagele S, Hacker J & Brand BC (1998) *Legionella pneumophila* kills human phagocytes but not protozoan host cells by inducing apoptotic cell death FEMS Microbiol Lett **169:** 51-58.

Hales LM & Shuman HA (1999) The *Legionella pneumophila* rpoS gene is required for growth within *Acanthamoeba castellanii* J Bacteriol **181:** 4879-4889.

Hammer BK & Swanson MS (1999) Co-ordination of *legionella pneumophila* virulence with entry into stationary phase by ppGpp Mol Microbiol **33:** 721-731.

Hammer BK, Tateda ES & Swanson MS (2002) A two-component regulator induces the transmission phenotype of stationary-phase *Legionella pneumophila* Mol Microbiol **44:** 107-118.

Hammerschlag MR (2002) The intracellular life of chlamydiae Semin Pediatr Infect Dis **13:** 239-248.

Harada E, Iida K, Shiota S, Nakayama H & Yoshida S (2010) Glucose metabolism in *Legionella pneumophila*: dependence on the Entner-Doudoroff pathway and connection with intracellular bacterial growth J Bacteriol **192:** 2892-2899.

Harada T, Miyake M & Imai Y (2007) Evasion of *Legionella pneumophila* from the bactericidal system by reactive oxygen species (ROS) in macrophages Microbiol Immunol **51:** 1161-1170.

Harb OS & Abu Kwaik Y (2000) Characterization of a macrophage-specific infectivity locus (*milA*) of *Legionella pneumophila* Infect Immun **68:** 368-376.

Hayashi T, Nakamichi M, Naitou H, Ohashi N, Imai Y & Miyake M (2010) Proteomic analysis of growth phase-dependent expression of *Legionella pneumophila* proteins which involves regulation of bacterial virulence traits PLoS One **5:** e11718.

Hebert GA, Thomason BM, Harris PP, Hicklin MD & McKinney RM (1980) "Pittsburgh pneumonia agent": a bacterium phenotypically similar to *Legionella pneumophila* and identical to the TATLOCK bacterium Ann Intern Med **92:** 53-54.

Heidtman M, Chen EJ, Moy MY & Isberg RR (2009) Large-scale identification of *Legionella pneumophila* Dot/Icm substrates that modulate host cell vesicle trafficking pathways Cell Microbiol **11:** 230-248.

Herrmann V, Eidner A, Rydzewski K, Bladel I, Jules M, Buchrieser C, Eisenreich W & Heuner K (2011) GamA is a eukaryotic-like glucoamylase responsible for glycogen- and starch-degrading activity of *Legionella pneumophila* Int J Med Microbiol **301:** 133-139.

Heuner K & Steinert M (2003) The flagellum of *Legionella pneumophila* and its link to the expression of the virulent phenotype Int J Med Microbiol **293:** 133-143.

Heuner K, Brand BC & Hacker J (1999) The expression of the flagellum of *Legionella pneumophila* is modulated by different environmental factors FEMS Microbiol Lett **175:** 69-77.

Heuner K, Dietrich C, Skriwan C, Steinert M & Hacker J (2002) Influence of the alternative sigma-28 factor on virulence and flagellum expression of *Legionella pneumophila* Infect Immun **70:** 1604-1608.

Heuner K, Bender-Beck L, Brand BC, Luck PC, Mann KH, Marre R, Ott M & Hacker J (1995) Cloning and genetic characterization of the flagellum subunit gene (*flaA*) of *Legionella pneumophila* serogroup 1 Infect Immun **63:** 2499-2507.

Hickey EK & Cianciotto NP (1997) An iron- and fur-repressed *Legionella pneumophila* gene that promotes intracellular infection and encodes a protein with similarity to the *Escherichia coli* aerobactin synthetases Infect Immun **65:** 133-143.

Hickey EK & Cianciotto NP (1994) Cloning and sequencing of the *Legionella pneumophila* fur gene Gene **143:** 117-121.

Hilbi H, Segal G & Shuman HA (2001) Icm/dot-dependent upregulation of phagocytosis by *Legionella pneumophila* Mol Microbiol **42:** 603-617.

Hiltz MF, Sisson GR, Brassinga AK, Garduno E, Garduno RA & Hoffman PS (2004) Expression of *magA* in *Legionella pneumophila* Philadelphia-1 is developmentally regulated and a marker of formation of mature intracellular forms J Bacteriol **186:** 3038-3045.

Hisert KB, MacCoss M, Shiloh MU *et al.* (2005) A glutamate-alanine-leucine (EAL) domain protein of *Salmonella* controls bacterial survival in mice, antioxidant defence and killing of macrophages: role of cyclic diGMP Mol Microbiol **56:** 1234-1245.

Hoffman PS, Butler CA & Quinn FD (1989) Cloning and temperature-dependent expression in *Escherichia coli* of a *Legionella pneumophila* gene coding for a genus-common 60-kilodalton antigen Infect Immun **57:** 1731-1739.

Hojo F, Sato D, Matsuo J *et al.* (2012) Ciliates expel environmental *Legionella*-laden pellets to stockpile food Appl Environ Microbiol **78:** 5247-5257.

Horwitz MA (1987) Characterization of avirulent mutant *Legionella pneumophila* that survive but do not multiply within human monocytes J Exp Med **166:** 1310-1328.

Horwitz MA (1984) Phagocytosis of the Legionnaires' disease bacterium (*Legionella pneumophila*) occurs by a novel mechanism: engulfment within a pseudopod coil Cell **36:** 27-33.

Horwitz MA (1983) Symbiotic interactions between *Legionella pneumophila* and human leukocytes Int Rev Cytol Suppl **14:** 307-328.

Horwitz MA (1983) Cell-mediated immunity in Legionnaires' disease J Clin Invest **71:** 1686-1697.

Horwitz MA & Maxfield FR (1984) *Legionella pneumophila* inhibits acidification of its phagosome in human monocytes J Cell Biol **99:** 1936-1943.

Horwitz MA & Silverstein SC (1981) Interaction of the legionnaires' disease bacterium (*Legionella pneumophila*) with human phagocytes. II. Antibody promotes binding of L. pneumophila to monocytes but does not inhibit intracellular multiplication J Exp Med **153:** 398-406.

Hubber A & Roy CR (2010) Modulation of host cell function by *Legionella pneumophila* type IV effectors Annu Rev Cell Dev Biol **26:** 261-283.

Hughes KT, Gillen KL, Semon MJ & Karlinsey JE (1993) Sensing structural intermediates in bacterial flagellar assembly by export of a negative regulator Science **262:** 1277-1280.

Huston WM, Naylor J, Cianciotto NP, Jennings MP & McEwan AG (2008) Functional analysis of the multi-copper oxidase from *Legionella pneumophila* Microbes Infect **10:** 497-503.

Ingmundson A & Roy CR (2008) Analyzing association of the endoplasmic reticulum with the *legionella pneumophila*-containing vacuoles by fluorescence microscopy Methods Mol Biol **445:** 379-387.

Jacobi S, Schade R & Heuner K (2004) Characterization of the alternative sigma factor sigma-54 and the transcriptional regulator FleQ of *Legionella pneumophila*, which are both involved in the regulation cascade of flagellar gene expression J Bacteriol **186:** 2540-2547.

James BW, Mauchline WS, Dennis PJ, Keevil CW & Wait R (1999) Poly-3-hydroxybutyrate in *Legionella pneumophila*, an energy source for survival in low-nutrient environments Appl Environ Microbiol **65:** 822-827.

James BW, Mauchline WS, Fitzgeorge RB, Dennis PJ & Keevil CW (1995) Influence of iron-limited continuous culture on physiology and virulence of *Legionella pneumophila* Infect Immun **63:** 4224-4230.

Janecek S & Blesak K (2011) Sequence-structural features and evolutionary relationships of family GH57 alpha-amylases and their putative alpha-amylase-like homologues Protein J **30:** 429-435.

Johnson W, Varner L & Poch M (1991) Acquisition of iron by *Legionella pneumophila*: role of iron reductase Infect Immun **59:** 2376-2381.

Joseph B, Przybilla K, Stuhler C, Schauer K, Slaghuis J, Fuchs TM & Goebel W (2006) Identification of *Listeria monocytogenes* genes contributing to intracellular replication by expression profiling and mutant screening J Bacteriol **188:** 556-568.

Joseph B, Mertins S, Stoll R, Schar J, Umesha KR, Luo Q, Muller-Altrock S & Goebel W (2008) Glycerol metabolism and PrfA activity in *Listeria monocytogenes* J Bacteriol **190:** 5412-5430.

Joshi AD, Sturgill-Koszycki S & Swanson MS (2001) Evidence that Dot-dependent and -independent factors isolate the *Legionella pneumophila* phagosome from the endocytic network in mouse macrophages Cell Microbiol **3:** 99-114.

Jung IL, Oh TJ & Kim IG (2003) Abnormal growth of polyamine-deficient *Escherichia coli* mutant is partially caused by oxidative stress-induced damage Arch Biochem Biophys **418:** 125-132.

Kagan JC & Roy CR (2002) *Legionella phagosomes* intercept vesicular traffic from endoplasmic reticulum exit sites Nat Cell Biol **4:** 945-954.

Kagan JC, Stein MP, Pypaert M & Roy CR (2004) *Legionella* subvert the functions of Rab1 and Sec22b to create a replicative organelle J Exp Med **199:** 1201-1211.

Katz SM (1978) The morphology of the Legionnaires' disease organism Am J Pathol **90:** 701-722.

Katz SM, Brodsky I & Kahn SB (1979) Legionnaires' disease: ultrastructural appearance of the agent in a lung biopsy specimen Arch Pathol Lab Med **103:** 261-264.

King CH, Fields BS, Shotts EB,Jr & White EH (1991) Effects of cytochalasin D and methylamine on intracellular growth of *Legionella pneumophila* in amoebae and human monocyte-like cells Infect Immun **59:** 758-763.

King CH, Shotts EB,Jr, Wooley RE & Porter KG (1988) Survival of coliforms and bacterial pathogens within protozoa during chlorination Appl Environ Microbiol **54:** 3023-3033.

Koubar M, Rodier MH, Garduno RA & Frere J (2011) Passage through *Tetrahymena tropicalis* enhances the resistance to stress and the infectivity of *Legionella pneumophila* FEMS Microbiol Lett **325:** 10-15.

Krivan HC, Franklin DP, Wang W, Laux DC & Cohen PS (1992) Phosphatidylserine found in intestinal mucus serves as a sole source of carbon and nitrogen for salmonellae and *Escherichia coli* Infect Immun **60:** 3943-3946.

Laguna RK, Creasey EA, Li Z, Valtz N & Isberg RR (2006) A *Legionella pneumophila*-translocated substrate that is required for growth within macrophages and protection from host cell death Proc Natl Acad Sci U S A **103:** 18745-18750.

Lee JV & West AA (1991) Survival and growth of *Legionella* species in the environment Soc Appl Bacteriol Symp Ser **20:** 121S-129S.

Lettinga KD, Verbon A, Weverling GJ *et al.* (2002) Legionnaires' disease at a Dutch flower show: prognostic factors and impact of therapy Emerg Infect Dis **8:** 1448-1454.

Levy MR & Elliott AM (1968) Biochemical and ultrastructural changes in *Tetrahymena pyriformis* during starvation J Protozool **15:** 208-222.

Li XH, Zeng YL, Gao Y, Zheng XC, Zhang QF, Zhou SN & Lu YJ (2010) The ClpP protease homologue is required for the transmission traits and cell division of the pathogen *Legionella pneumophila* BMC Microbiol **10:** 54-2180-10-54.

Liles MR, Scheel TA & Cianciotto NP (2000) Discovery of a nonclassical siderophore, legiobactin, produced by strains of *Legionella pneumophila* J Bacteriol **182:** 749-757.

Losick VP & Isberg RR (2006) NF-kappaB translocation prevents host cell death after low-dose challenge by *Legionella pneumophila* J Exp Med **203:** 2177-2189.

Losick VP, Haenssler E, Moy MY & Isberg RR (2010) LnaB: a *Legionella pneumophila* activator of NF-kappaB Cell Microbiol **12:** 1083-1097.

Lu H & Clarke M (2005) Dynamic properties of *Legionella*-containing phagosomes in *Dictyostelium* amoebae Cell Microbiol **7:** 995-1007.

Lucchini S, Liu H, Jin Q, Hinton JC & Yu J (2005) Transcriptional adaptation of *Shigella flexneri* during infection of macrophages and epithelial cells: insights into the strategies of a cytosolic bacterial pathogen Infect Immun **73:** 88-102.

Luck C (2010) Legionella - a case for culture Indian J Med Res **131:** 736-738.

Luo ZQ (2012) Legionella secreted effectors and innate immune responses Cell Microbiol **14:** 19-27.

Luo ZQ & Isberg RR (2004) Multiple substrates of the *Legionella pneumophila* Dot/Icm system identified by interbacterial protein transfer Proc Natl Acad Sci U S A **101:** 841-846.

Luttichau HR, Vinther C, Uldum SA, Moller J, Faber M & Jensen JS (1998) An outbreak of Pontiac fever among children following use of a whirlpool Clin Infect Dis **26:** 1374-1378.

Lynch D, Fieser N, Gloggler K, Forsbach-Birk V & Marre R (2003) The response regulator LetA regulates the stationary-phase stress response in *Legionella pneumophila* and is required for efficient infection of *Acanthamoeba castellanii* FEMS Microbiol Lett **219:** 241-248.

Machner MP & Isberg RR (2006) Targeting of host Rab GTPase function by the intravacuolar pathogen *Legionella pneumophila* Dev Cell **11:** 47-56.

Mampel J, Spirig T, Weber SS, Haagensen JA, Molin S & Hilbi H (2006) Planktonic replication is essential for biofilm formation by *Legionella pneumophila* in a complex medium under static and dynamic flow conditions Appl Environ Microbiol **72:** 2885-2895.

Marra A, Blander SJ, Horwitz MA & Shuman HA (1992) Identification of a *Legionella pneumophila* locus required for intracellular multiplication in human macrophages Proc Natl Acad Sci U S A **89:** 9607-9611.

Marrie TJ, De Carolis E, Yu VL, Stout J & Canadian Community-Acquired Pneumonia Investigators (2003) Legionnaires' disease - Results of a multicentre Canadian study Can J Infect Dis **14:** 154-158.

Marrie TJ, Raoult D, La Scola B, Birtles RJ, de Carolis E & Canadian Community-Acquired Pneumonia Study Group (2001) *Legionella*-like and other amoebal pathogens as agents of community-acquired pneumonia Emerg Infect Dis **7:** 1026-1029.

Marston BJ, Lipman HB & Breiman RF (1994) Surveillance for Legionnaires' disease. Risk factors for morbidity and mortality Arch Intern Med **154:** 2417-2422.

Marston BJ, Plouffe JF, File TM,Jr, Hackman BA, Salstrom SJ, Lipman HB, Kolczak MS & Breiman RF (1997) Incidence of community-acquired pneumonia requiring hospitalization. Results of a population-based active surveillance Study in Ohio. The Community-Based Pneumonia Incidence Study Group Arch Intern Med **157:** 1709-1718.

Matsuura Y, Kusunoki M, Harada W & Kakudo M (1984) Structure and possible catalytic residues of Taka-amylase A J Biochem **95:** 697-702.

McCormick D, Thorn S, Milne D, Evans C, Stevenson J, Llano M, Donaghy M & Incident Management Team (2012) Public health response to an outbreak of Legionnaires' disease in Edinburgh, United Kingdom, June 2012 Euro Surveill **17:** 20216.

McDade JE, Shepard CC, Fraser DW, Tsai TR, Redus MA & Dowdle WR (1977) Legionnaires' disease: isolation of a bacterium and demonstration of its role in other respiratory disease N Engl J Med **297:** 1197-1203.

McKinney JD, Honer zu Bentrup K, Munoz-Elias EJ, Miczak A, Chen B, Chan WT, Swenson D, Sacchettini JC, Jacobs WR,Jr & Russell DG (2000) Persistence of *Mycobacterium tuberculosis* in macrophages and mice requires the glyoxylate shunt enzyme isocitrate lyase Nature **406:** 735-738.

McNealy T, Newsome AL, Johnson RA & Berk SG (2002) Impact of amoebae, bacteria and *Tetrahymena* on *L. pneumophila* multiplication and distribution in an aquatic environment. *Legionella* (Marre R, AbuKwaik Y, Bartlett C, Cianciotto NP, Fields BS, Frosch M, Hacker J & Lück PC, eds), pp. 170-175. ASM press, Washington.

Molmeret M, Horn M, Wagner M, Santic M & Abu Kwaik Y (2005) Amoebae as training grounds for intracellular bacterial pathogens Appl Environ Microbiol **71:** 20-28.

Molmeret M, Alli OA, Zink S, Flieger A, Cianciotto NP & Kwaik YA (2002) icmT is essential for pore formation-mediated egress of *Legionella pneumophila* from mammalian and protozoan cells Infect Immun **70:** 69-78.

Molmeret M, Alli OA, Radulic M, Susa M, Doric M & Kwaik YA (2002) The C-terminus of IcmT is essential for pore formation and for intracellular trafficking of *Legionella pneumophila* within *Acanthamoeba polyphaga* Mol Microbiol **43:** 1139-1150.

Molofsky AB & Swanson MS (2004) Differentiate to thrive: lessons from the *Legionella pneumophila* life cycle Mol Microbiol **53:** 29-40.

Molofsky AB & Swanson MS (2003) *Legionella pneumophila* CsrA is a pivotal repressor of transmission traits and activator of replication Mol Microbiol **50:** 445-461.

Molofsky AB, Shetron-Rama LM & Swanson MS (2005) Components of the *Legionella pneumophila* flagellar regulon contribute to multiple virulence traits, including lysosome avoidance and macrophage death Infect Immun **73:** 5720-5734.

Molofsky AB, Byrne BG, Whitfield NN, Madigan CA, Fuse ET, Tateda K & Swanson MS (2006) Cytosolic recognition of flagellin by mouse macrophages restricts *Legionella pneumophila* infection J Exp Med **203:** 1093-1104.

Morash MG, Brassinga AK, Warthan M, Gourabathini P, Garduno RA, Goodman SD & Hoffman PS (2009) Reciprocal expression of integration host factor and HU in the developmental cycle and infectivity of *Legionella pneumophila* Appl Environ Microbiol **75:** 1826-1837.

Morey JS, Ryan JC & Van Dolah FM (2006) Microarray validation: factors influencing correlation between oligonucleotide microarrays and real-time PCR Biol Proced Online **8:** 175-193.

Morris GK, Steigerwalt A, Feeley JC, Wong ES, Martin WT, Patton CM & Brenner DJ (1980) *Legionella gormanii* sp. nov J Clin Microbiol **12:** 718-721.

Muder RR & Yu VL (2002) Infection due to *Legionella* species other than *L. pneumophila* Clin Infect Dis **35:** 990-998.

Munoz-Elias EJ & McKinney JD (2005) *Mycobacterium tuberculosis* isocitrate lyases 1 and 2 are jointly required for in vivo growth and virulence Nat Med **11:** 638-644.

Munoz-Elias EJ, Upton AM, Cherian J & McKinney JD (2006) Role of the methylcitrate cycle in *Mycobacterium tuberculosis* metabolism, intracellular growth, and virulence Mol Microbiol **60:** 1109-1122.

Murata T, Delprato A, Ingmundson A, Toomre DK, Lambright DG & Roy CR (2006) The *Legionella pneumophila* effector protein DrrA is a Rab1 guanine nucleotide-exchange factor Nat Cell Biol **8:** 971-977.

Nagai H & Roy CR (2003) Show me the substrates: modulation of host cell function by type IV secretion systems Cell Microbiol **5:** 373-383.

Nagai H, Kagan JC, Zhu X, Kahn RA & Roy CR (2002) A bacterial guanine nucleotide exchange factor activates ARF on *Legionella* phagosomes Science **295:** 679-682.

Nasrallah GK, Riveroll AL, Chong A, Murray LE, Lewis PJ & Garduno RA (2011) *Legionella pneumophila* requires polyamines for optimal intracellular growth J Bacteriol **193:** 4346-4360.

Naylor J & Cianciotto NP (2004) Cytochrome c maturation proteins are critical for in vivo growth of *Legionella pneumophila* FEMS Microbiol Lett **241:** 249-256.

Neunuebel MR, Chen Y, Gaspar AH, Backlund PS,Jr, Yergey A & Machner MP (2011) De-AMPylation of the small GTPase Rab1 by the pathogen *Legionella pneumophila* Science **333:** 453-456.

Newton HJ, Sansom FM, Dao J, McAlister AD, Sloan J, Cianciotto NP & Hartland EL (2007) Sel1 repeat protein LpnE is a *Legionella pneumophila* virulence determinant that influences vacuolar trafficking Infect Immun **75:** 5575-5585.

Nguyen TM, Ilef D, Jarraud S *et al.* (2006) A community-wide outbreak of legionnaires' disease linked to industrial cooling towers--how far can contaminated aerosols spread? J Infect Dis **193:** 102-111.

Ninio S & Roy CR (2007) Effector proteins translocated by *Legionella pneumophila*: strength in numbers Trends Microbiol **15:** 372-380.

Ott M, Messner P, Heesemann J, Marre R & Hacker J (1991) Temperature-dependent expression of flagella in *Legionella* J Gen Microbiol **137:** 1955-1961.

Paredes CJ, Alsaker KV & Papoutsakis ET (2005) A comparative genomic view of clostridial sporulation and physiology Nat Rev Microbiol **3:** 969-978.

Pasculle AW, Feeley JC, Gibson RJ, Cordes LG, Myerowitz RL, Patton CM, Gorman GW, Carmack CL, Ezzell JW & Dowling JN (1980) Pittsburgh pneumonia agent: direct isolation from human lung tissue J Infect Dis **141:** 727-732.

Payne NR & Horwitz MA (1987) Phagocytosis of *Legionella pneumophila* is mediated by human monocyte complement receptors J Exp Med **166:** 1377-1389.

Peekhaus N & Conway T (1998) What's for dinner?: Entner-Doudoroff metabolism in *Escherichia coli* J Bacteriol **180:** 3495-3502.

Pine L, George JR, Reeves MW & Harrell WK (1979) Development of a chemically defined liquid medium for growth of *Legionella pneumophila* J Clin Microbiol **9:** 615-626.

Pope CD, O'Connell W & Cianciotto NP (1996) *Legionella pneumophila* mutants that are defective for iron acquisition and assimilation and intracellular infection Infect Immun **64:** 629-636.

Prashar A, Bhatia S, Tabatabaeiyazdi Z, Duncan C, Garduno RA, Tang P, Low DE, Guyard C & Terebiznik MR (2012) Mechanism of invasion of lung epithelial cells by filamentous *Legionella pneumophila* Cell Microbiol.

Pruckler JM, Benson RF, Moyenuddin M, Martin WT & Fields BS (1995) Association of flagellum expression and intracellular growth of *Legionella pneumophila* Infect Immun **63:** 4928-4932.

Quon KC, Yang B, Domian IJ, Shapiro L & Marczynski GT (1998) Negative control of bacterial DNA replication by a cell cycle regulatory protein that binds at the chromosome origin Proc Natl Acad Sci U S A **95:** 120-125.

Raha M, Kawagishi I, Muller V, Kihara M & Macnab RM (1992) *Escherichia coli* produces a cytoplasmic alpha-amylase, AmyA J Bacteriol **174:** 6644-6652.

Rasis M & Segal G (2009) The LetA-RsmYZ-CsrA regulatory cascade, together with RpoS and PmrA, post-transcriptionally regulates stationary phase activation of *Legionella pneumophila* Icm/Dot effectors Mol Microbiol **72:** 995-1010.

Reeves MW, Pine L, Hutner SH, George JR & Harrell WK (1981) Metal requirements of *Legionella pneumophila* J Clin Microbiol **13:** 688-695.

Reimer AR, Au S, Schindle S & Bernard KA (2010) *Legionella pneumophila* monoclonal antibody subgroups and DNA sequence types isolated in Canada between 1981 and 2009: Laboratory Component of National Surveillance Eur J Clin Microbiol Infect Dis **29:** 191-205.

Ren T, Zamboni DS, Roy CR, Dietrich WF & Vance RE (2006) Flagellin-deficient *Legionella* mutants evade caspase-1- and Naip5-mediated macrophage immunity PLoS Pathog **2:** e18.

Rizzo MA, Davidson MW & Piston DW (2009) Fluorescent protein tracking and detection: fluorescent protein structure and color variants Cold Spring Harb Protoc **2009:** pdb.top63.

Robey M & Cianciotto NP (2002) *Legionella pneumophila* feoAB promotes ferrous iron uptake and intracellular infection Infect Immun **70:** 5659-5669.

Robinson CG & Roy CR (2006) Attachment and fusion of endoplasmic reticulum with vacuoles containing *Legionella pneumophila* Cell Microbiol **8:** 793-805.

Rodgers FG (1979) Ultrastructure of *Legionella pneumophila* J Clin Pathol **32:** 1195-1202.

Roig J & Rello J (2003) Legionnaires' disease: a rational approach to therapy J Antimicrob Chemother **51:** 1119-1129.

Romling U & Amikam D (2006) Cyclic di-GMP as a second messenger Curr Opin Microbiol **9:** 218-228.

Romling U, Gomelsky M & Galperin MY (2005) C-di-GMP: the dawning of a novel bacterial signalling system Mol Microbiol **57:** 629-639.

Rowbotham TJ (1980) Pontiac fever explained? Lancet **2:** 969.

Rowbotham TJ (1986) Current views on the relationships between amoebae, legionellae and man Isr J Med Sci **22:** 678-689.

Rowbotham TJ (1983) Isolation of *Legionella pneumophila* from clinical specimens via amoebae, and the interaction of those and other isolates with amoebae J Clin Pathol **36:** 978-986.

Rowbotham TJ (1980) Preliminary report on the pathogenicity of *Legionella pneumophila* for freshwater and soil amoebae J Clin Pathol **33:** 1179-1183.

Sadosky AB, Wiater LA & Shuman HA (1993) Identification of *Legionella pneumophila* genes required for growth within and killing of human macrophages Infect Immun **61:** 5361-5373.

Sahr T, Bruggemann H, Jules M, Lomma M, Albert-Weissenberger C, Cazalet C & Buchrieser C (2009) Two small ncRNAs jointly govern virulence and transmission in *Legionella pneumophila* Mol Microbiol **72:** 741-762.

Sauer JD, Bachman MA & Swanson MS (2005) The phagosomal transporter A couples threonine acquisition to differentiation and replication of *Legionella pneumophila* in macrophages Proc Natl Acad Sci U S A **102:** 9924-9929.

Sauer JD, Shannon JG, Howe D, Hayes SF, Swanson MS & Heinzen RA (2005) Specificity of *Legionella pneumophila* and *Coxiella burnetii* vacuoles and versatility of *Legionella pneumophila* revealed by coinfection Infect Immun **73:** 4494-4504.

Schauer K, Geginat G, Liang C, Goebel W, Dandekar T & Fuchs TM (2010) Deciphering the intracellular metabolism of *Listeria monocytogenes* by mutant screening and modelling BMC Genomics **11:** 573-2164-11-573.

Schnappinger D, Ehrt S, Voskuil MI *et al.* (2003) Transcriptional Adaptation of *Mycobacterium tuberculosis* within Macrophages: Insights into the Phagosomal Environment J Exp Med **198:** 693-704.

Schneider E, Freundlieb S, Tapio S & Boos W (1992) Molecular characterization of the MalT-dependent periplasmic alpha-amylase of *Escherichia coli* encoded by *malS* J Biol Chem **267:** 5148-5154.

Schofield GM (1985) A note on the survival of *Legionella pneumophila* in stagnant tap water J Appl Bacteriol **59:** 333-335.

Segal G, Russo JJ & Shuman HA (1999) Relationships between a new type IV secretion system and the icm/dot virulence system of *Legionella pneumophila* Mol Microbiol **34:** 799-809.

Sexton JA & Vogel JP (2002) Type IVB secretion by intracellular pathogens Traffic **3:** 178-185.

Sheehan KB, Henson JM & Ferris MJ (2005) *Legionella* species diversity in an acidic biofilm community in Yellowstone National Park Appl Environ Microbiol **71:** 507-511.

Shin S, Case CL, Archer KA, Nogueira CV, Kobayashi KS, Flavell RA, Roy CR & Zamboni DS (2008) Type IV secretion-dependent activation of host MAP kinases induces an increased proinflammatory cytokine response to *Legionella pneumophila* PLoS Pathog **4:** e1000220.

Shohdy N, Efe JA, Emr SD & Shuman HA (2005) Pathogen effector protein screening in yeast identifies *Legionella* factors that interfere with membrane trafficking Proc Natl Acad Sci U S A **102:** 4866-4871.

Skaliy P & McEachern HV (1979) Survival of the Legionnaires' disease bacterium in water Ann Intern Med **90:** 662-663.

Smith-Somerville HE, Huryn VB, Walker C & Winters AL (1991) Survival of *Legionella pneumophila* in the cold-water ciliate *Tetrahymena vorax* Appl Environ Microbiol **57:** 2742-2749.

St John G & Steinman HM (1996) Periplasmic copper-zinc superoxide dismutase of *Legionella pneumophila*: role in stationary-phase survival J Bacteriol **178:** 1578-1584.

Stabel TJ, Sha Z & Mayfield JE (1994) Periplasmic location of *Brucella abortus* Cu/Zn superoxide dismutase Vet Microbiol **38:** 307-314.

Starkenburg SR, Casey JM & Cianciotto NP (2004) Siderophore activity among members of the Legionella genus Curr Microbiol **49:** 203-207.

Steele TW, Moore CV & Sangster N (1990) Distribution of *Legionella longbeachae* serogroup 1 and other legionellae in potting soils in Australia Appl Environ Microbiol **56:** 2984-2988.

Steele TW, Lanser J & Sangster N (1990) Isolation of *Legionella longbeachae* serogroup 1 from potting mixes Appl Environ Microbiol **56:** 49-53.

Steinert M, Hentschel U & Hacker J (2002) *Legionella pneumophila*: an aquatic microbe goes astray FEMS Microbiol Rev **26:** 149-162.

Steinman HM & Ely B (1990) Copper-zinc superoxide dismutase of *Caulobacter crescentus*: cloning, sequencing, and mapping of the gene and periplasmic location of the enzyme J Bacteriol **172:** 2901-2910.

Stoll R & Goebel W (2010) The major PEP-phosphotransferase systems (PTSs) for glucose, mannose and cellobiose of *Listeria monocytogenes*, and their significance for extra- and intracellular growth Microbiology **156:** 1069-1083.

Stout JE & Yu VL (1997) Legionellosis N Engl J Med **337:** 682-687.

Sturgill-Koszycki S & Swanson MS (2000) *Legionella pneumophila* replication vacuoles mature into acidic, endocytic organelles J Exp Med **192:** 1261-1272.

Swanson MS & Hammer BK (2000) *Legionella pneumophila* pathogesesis: a fateful journey from amoebae to macrophages Annu Rev Microbiol **54:** 567-613.

Swanson MS & Isberg RR (1995) Association of *Legionella pneumophila* with the macrophage endoplasmic reticulum Infect Immun **63:** 3609-3620.

Sweeney NJ, Laux DC & Cohen PS (1996) *Escherichia coli* F-18 and *E. coli* K-12 *eda* mutants do not colonize the streptomycin-treated mouse large intestine Infect Immun **64:** 3504-3511.

Tan Y & Luo ZQ (2011) *Legionella pneumophila* SidD is a deAMPylase that modifies Rab1 Nature **475:** 506-509.

Taniguchi M & Honnda Y (2009) Amylases. Encyclopedia of Microbiology (Third Edition) (ed), pp.158-173. Academic Press, Massachussetts

Tesh MJ & Miller RD (1981) Amino acid requirements for *Legionella pneumophila* growth J Clin Microbiol **13:** 865-869.

Tesh MJ, Morse SA & Miller RD (1983) Intermediary metabolism in *Legionella pneumophila*: utilization of amino acids and other compounds as energy sources J Bacteriol **154:** 1104-1109.

Thomas V, Bouchez T, Nicolas V, Robert S, Loret JF & Levi Y (2004) Amoebae in domestic water systems: resistance to disinfection treatments and implication in Legionella persistence J Appl Microbiol **97:** 950-963.

Thomas DL, Mundy LM & Tucker PC (1993) Hot tub legionellosis. Legionnaires' disease and Pontiac fever after a point-source exposure to *Legionella pneumophila* Arch Intern Med **153:** 2597-2599.

Thorpe TC & Miller RD (1981) Extracellular enzymes of *Legionella pneumophila* Infect Immun **33:** 632-635.

Tiaden A, Spirig T, Weber SS, Bruggemann H, Bosshard R, Buchrieser C & Hilbi H (2007) The *Legionella pneumophila* response regulator LqsR promotes host cell interactions as an element of the virulence regulatory network controlled by RpoS and LetA Cell Microbiol **9:** 2903-2920.

Tilney LG, Harb OS, Connelly PS, Robinson CG & Roy CR (2001) How the parasitic bacterium *Legionella pneumophila* modifies its phagosome and transforms it into rough ER: implications for conversion of plasma membrane to the ER membrane J Cell Sci **114:** 4637-4650.

Towbin H, Staehelin T & Gordon J (1979) Electrophoretic transfer of proteins from polyacrylamide gels to nitrocellulose sheets: procedure and some applications Proc Natl Acad Sci U S A **76:** 4350-4354.

Tsai TF, Finn DR, Plikaytis BD, McCauley W, Martin SM & Fraser DW (1979) Legionnaires' disease: clinical features of the epidemic in Philadelphia Ann Intern Med **90:** 509-517.

Utley M, Franklin DP, Krogfelt KA, Laux DC & Cohen PS (1998) A *Salmonella typhimurium* mutant unable to utilize fatty acids and citrate is avirulent and immunogenic in mice FEMS Microbiol Lett **163:** 129-134.

Vance RE (2010) Immunology taught by bacteria J Clin Immunol **30:** 507-511.

Venkataraman C, Gao LY, Bondada S & Kwaik YA (1998) Identification of putative cytoskeletal protein homologues in the protozoan host *Hartmannella vermiformis* as substrates for induced tyrosine phosphatase activity upon attachment to the Legionnaires' disease bacterium, *Legionella pneumophila* J Exp Med **188:** 505-514.

Venkataraman C, Haack BJ, Bondada S & Abu Kwaik Y (1997) Identification of a Gal/GalNAc lectin in the protozoan *Hartmannella vermiformis* as a potential receptor for attachment and invasion by the Legionnaires' disease bacterium J Exp Med **186:** 537-547.

Viswanathan VK, Edelstein PH, Pope CD & Cianciotto NP (2000) The *Legionella pneumophila iraAB* locus is required for iron assimilation, intracellular infection, and virulence Infect Immun **68:** 1069-1079.

Viswanathan VK, Kurtz S, Pedersen LL, Abu-Kwaik Y, Krcmarik K, Mody S & Cianciotto NP (2002) The cytochrome c maturation locus of *Legionella pneumophila* promotes iron assimilation and intracellular infection and contains a strain-specific insertion sequence element Infect Immun **70:** 1842-1852.

Voth DE & Heinzen RA (2007) Lounging in a lysosome: the intracellular lifestyle of *Coxiella burnetii* Cell Microbiol **9:** 829-840.

Watarai M, Derre I, Kirby J, Growney JD, Dietrich WF & Isberg RR (2001) *Legionella pneumophila* is internalized by a macropinocytotic uptake pathway controlled by the Dot/Icm system and the mouse Lgn1 locus J Exp Med **194:** 1081-1096.

Weiss E & Westfall HN (1984) Substrate utilization by *Legionella* cells after cryopreservation in phosphate buffer Appl Environ Microbiol **48:** 380-385.

Wieland H, Goetz F & Neumeister B (2004) Phagosomal acidification is not a prerequisite for intracellular multiplication of *Legionella pneumophila* in human monocytes J Infect Dis **189:** 1610-1614.

Wieland H, Ullrich S, Lang F & Neumeister B (2005) Intracellular multiplication of *Legionella pneumophila* depends on host cell amino acid transporter SLC1A5 Mol Microbiol **55:** 1528-1537.

Xu L, Shen X, Bryan A, Banga S, Swanson MS & Luo ZQ (2010) Inhibition of host vacuolar H^+-ATPase activity by a *Legionella pneumophila* effector PLoS Pathog **6:** e1000822.

Yu VL, Plouffe JF, Pastoris MC *et al.* (2002) Distribution of *Legionella* species and serogroups isolated by culture in patients with sporadic community-acquired legionellosis: an international collaborative survey J Infect Dis **186:** 127-128.

Zhang Y (2008) I-TASSER server for protein 3D structure prediction BMC Bioinformatics **9:** 40-2105-9-40.

Zhu W, Banga S, Tan Y, Zheng C, Stephenson R, Gately J & Luo ZQ (2011) Comprehensive identification of protein substrates of the Dot/Icm type IV transporter of *Legionella pneumophila* PLoS One **6:** e17638.

Zink SD, Pedersen L, Cianciotto NP & Abu-Kwaik Y (2002) The Dot/Icm type IV secretion system of *Legionella pneumophila* is essential for the induction of apoptosis in human macrophages Infect Immun **70:** 1657-1663.

Zusman DR, Scott AE, Yang Z & Kirby JR (2007) Chemosensory pathways, motility and development in *Myxococcus xanthus* Nat Rev Microbiol **5:** 862-872.

APPENDICES

Appendix I. A List of *L. pneumophila* genes that are selectively upregulated (≥ 2-fold increase) in amoebae MIFs (in relation to replicative forms in amoebae) but down-regulated (< 1-fold change) or unchanged (< 2-fold increase) in the progeny from human macrophages (in relation to stationary phase forms grown *in vitro*)

Gene ID	Gene name	Description	*A. castellanii*[a] (T_{14}/T_8)	Human THP-1 macrophages[b] (T_{18}/T_0)
lpg1340	*fliC*	Flagellin	83.29	0.57
lpg1093	*pacL*	Cation efflux transporter (calcium transporting ATPase) (cation transporting ATPase)	47.64	1.84
lpg2957	-	Stomatin-like transmembrane protein	29.86	0.64
lpg1160	-	Hypothetical protein	29.65	0.88
lpg2334	-	Hypothetical protein	29.45	1.60
lpg0499	-	Similar to carboxy-terminal protease	23.26	1.74
lpg0672	-	Similar to acetoacetate decarboxylase (ADC)	22.01	1.82
lpg0671	*ndh*	NADH-dehydrogenase transmembrane protein	21.41	0.94
lpg0910	*enhA*	Enhanced entry protein EnhA	20.25	0.99
lpg2222	*lpnE*	TPR repeat protein, protein-protein interaction	19.84	1.14
lpg2803	-	Hypothetical protein	19.56	1.49
lpg2268	-	Hypothetical protein	18.00	1.61
lpg1336	*enhA*	Enhanced entry protein EnhA	17.88	1.62
lpg1669	-	alpha-amylase, putative	17.88	0.87
lpg1889	-	Similar to Lipase (triacyglycerol lipase)	16.45	1.68
lpg2257	-	Hypothetical protein	16.45	0.90
lpg1491	*lem9*	Lem9 (Dot/Icm system substrate)	15.78	1.78
lpg2157	*SdeA*	SdeA, IMH1; Encodes a protein implicated in protein transport; induced under stress conditions.	14.83	0.84
lpg0245	-	NAD-glutamate dehydrogenase	14.62	1.72
lpg1206	-	Predicted sigma 54 modulation protein YhbH	14.62	0.94
lpg0009	*hfq*	Host factor-I protein for bacteriophage Q beta replication (RNA binding regulator)	14.52	1.54
lpg1639	-	Hypothetical protein	13.74	1.56
lpg2482	-	SdbC (putative Dot/Icm substrate)	13.64	1.45
lpg0244	-	Pyridine nucleotide-disulfide oxidoreductase, FAD-dependent disulfide oxidoreductase	13.55	0.78
lpg0967	-	Hypothetical protein	13.55	1.13
lpg1039	-	Hypothetical protein	13.55	0.97
lpg1636	-	Similar to Acetyltransferase, GNAT family	13.09	1.72
lpg0037	*artJ*	Arginine 3rd transport system periplasmic binding protein	13.00	1.44
lpg0195	*ravE*	Dot/Icm system substrate	12.82	1.19
lpg1915	*pilE*	Tfp pilus assembly protein, major type IV pilin class A	12.73	0.77
lpg2149	-	Hypothetical protein	12.73	0.99

lpg2393	-	Similar to bacterioferritin (cytochrome b1)	12.38	1.46
lpg1338	*fliD*	FliD: Flagellar hook associated protein 2	12.13	1.37
lpg2971	*maeA*	Malate dehydrogenase (NAD-linked)	12.13	0.60
lpg1091	-	Hypothetical protein	11.91	1.96
lpg0901	-	Hypothetical protein	11.63	1.07
lpg1356	*enhC*	Enhanced entry protein EnhC	11.63	0.77
lpg2187	-	Hypothetical protein	11.63	1.05
lpg1135	-	Similar to bacterial regulatory proteins, TetR family	11.55	1.26
lpg1993	-	Similar to polysaccharide deacetylase	11.16	1.76
lpg0632	-	Similar to type IV pre-pilin (type IV fimbrial pilin)	11.08	0.65
lpg1887	-	Hypothetical protein	11.00	0.91
lpg0891	-	Putative sensory box protein/GGDEF/EAL domains	10.93	0.82
lpg2395	-	Hypothetical protein	10.85	1.16
lpg2831	*vipD*	VipD (Dot/Icm system substrate)	10.70	1.35
lpg0415	-	Hypothetical protein	10.56	1.69
lpg2813	-	Hypothetical protein	10.56	0.83
lpg1220	*flgF*	flagellar basal body rod protein FlgF	10.34	1.28
lpg0878	-	Hypothetical protein	10.27	1.85
lpg2258	-	Hypothetical protein	10.27	1.97
lpg1782	*fliA*	Flagellar biosynthesis sigma factor FliA	10.20	0.91
lpg0383	-	ORF, very weak IcmL homolog	9.99	1.61
lpg0669	-	Hypothetical exported protein	9.99	1.18
lpg2028	*hemE*	Uroporphyrinogen decarboxylase	9.99	0.69
lpg2537	-	Similar to 5-carboxy vanillate decarboxylase	9.85	1.44
lpg1454	-	Multidrug efflux protein (MFS transporter)	9.78	1.54
lpg2520	-	Hypothetical protein	9.78	1.85
lpg1490	*cyaA*	Adenylate cyclase PLUS two component hybrid sensor and regulator	9.71	0.65
lpg0279	-	Hypothetical protein	9.45	0.67
lpg0631	*pilV*	Type IV fimbrial biogenesis protein PilV	9.45	1.71
lpg2153	*sdeC*	SdeC protein (substrate of the Dot/Icm system)	9.38	0.94
lpg0670	-	Hypothetical protein	8.94	0.66
lpg2955	*hipB*	Integration host factor beta subunit	8.94	0.79
lpg2761	-	Hypothetical protein	8.88	1.13
lpg2316	*bdhA*	3-hydroxybutyrate dehydrogenase	8.82	0.74
lpg2311	*ceg28*	interaptin	8.75	1.64
lpg2849	-	Hypothetical (TPR repeat)	8.75	0.77
lpg0906	-	Flagellar biosynthesis/type III secretory pathway chaperone	8.63	0.73
lpg1117	*paiA*	Putative uncharacterized protein paiA	8.63	0.94
lpg1145	-	Hypothetical protein	8.51	0.78
lpg0074	-	Glutamate synthase	8.40	0.85
lpg1522	*pilB*	(type IV) pilus assembly protein PilB	8.40	1.41
lpg2641	*enhA*	enhanced entry protein EnhA	8.34	1.29
lpg2907	-	Hypothetical protein	8.00	1.08

lpg0717	-	ORF	7.94	0.92
lpg2721	-	glutamine amidotransferase	7.78	1.72
lpg2511	*sidC*	SidC, interaptin	7.73	1.61
lpg2147	-	Hypothetical protein	7.67	0.80
lpg2228	-	3-oxoacyl (acyl carrier protein) synthase III	7.62	1.55
lpg1925	-	Hypothetical protein	7.57	1.49
lpg0013	-	Pirin-like protein	7.41	0.71
lpg1032	-	Hypothetical protein	7.36	1.51
lpg1885	-	Hypothetical protein	7.36	1.83
lpg2495	*hss*	Homospermidine synthase	7.26	1.06
lpg0156	-	Signal transduction protein (EAL/GGDEF domain protein) - 2 component response regulator (c-di-GMP phosphodiesterase A)	7.21	0.94
lpg0782	-	O-antigen acetylase (lipopolysaccharide modification acyl transferase)	7.11	1.11
lpg1161	-	Phosphoribosyltransferase	7.11	0.43
lpg1783	*minD*	Flagellar biosynthesis MinD	6.96	1.25
lpg2348	*sodC*	Superoxide dismutase (copper-zinc)	6.96	0.84
lpg2457	-	Two component response regulator	6.92	1.24
lpg1207	-	Hypothetical protein	6.82	1.27
lpg2189	*ygjT*	Drug efflux protein	6.63	1.92
lpg1025	*yegE*	Sensory box/GGDEF/EAL family (membrane protein)	6.59	1.41
lpg0665	-	Putative transmembrane protein	6.45	1.33
lpg2509	*sdeD*	SdeD (Dot/Icm substrate)	6.45	0.78
lpg2132	-	Sensory box/GGDEF family protein (regulatory components of sensory transduction system), PleD	6.32	1.62
lpg0817	-	Hypothetical protein	6.28	1.15
lpg1339	-	Hypothetical protein	6.28	0.93
lpg0589	-	Hypothetical protein	6.19	1.95
lpg1055	-	Hypothetical protein	6.19	1.49
lpg0666	-	Hypothetical protein	6.15	1.84
lpg0267	*corA*	magnesium and cobalt transport protein CorA	6.11	1.92
lpg2310	*murI*	Glutamate racemase	6.11	1.35
lpg0847	*murA*	UDP-N-acetylglucosamine 1-carboxyvinyltransferase (3-phosphoshikimate-1-carboxyvinyl transferase)	6.02	0.61
lpg1090	-	Hypothetical protein	5.95	1.80
lpg1226	*flgL*	flagellar hook associated protein type 3 FlgL	5.94	0.46
lpg2526	-	Hypothetical protein	5.90	0.65
lpg2969	-	Hypothetical protein	5.90	0.79
lpg1155	-	Pyruvate decarboxylase	5.82	0.92
lpg0737	-	hypothetical signal peptide protein	5.74	1.07
lpg2427	*mdcB*	acetyl coenzyme A carboxylase, carboxyltransferase subunit β (malonate decarboxylase β subunit)	5.70	1.55
lpg2962	-	Sodium-type flagellar protein	5.70	1.86
lpg1985	*gad*	guanine aminohydrolase (guanine deaminase)	5.66	1.75
lpg0879	-	two component response regulator with GGDEF domain	5.62	1.10
lpg1451	-	Hypothetical phosphatidylethanolamine binding protein	5.62	0.57

lpg2017	-	Hypothetical protein	5.58	1.49
lpg0854	-	Hypothetical protein	5.50	1.02
lpg0893	-	Hypothetical protein	5.50	0.90
lpg2958	-	Transmembrane protein	5.50	1.11
lpg1386	*enhA*	enhanced entry protein EnhA	5.39	1.92
lpg1635	-	Dienelactone hydrolase	5.39	1.71
lpg2180	-	Sensory box histidine kinase/response regulator	5.39	1.85
lpg0537	*letE*	Transmission trait enhancer LetE	5.35	0.93
lpg0744	-	GGDEF domain protein	5.35	0.78
lpg0526	-	Hypothetical protein	5.28	0.96
lpg2201	-	replication factor C subunit (activator I)	5.28	0.72
lpg2318	*motA*	chemotaxis (motility protein A) transmembrane (proton conductor component of motor)	5.28	1.59
lpg2197	-	Ketosteroid isomerase	5.21	0.76
lpg0846	*yrbA*	Hypothetical BolA-like protein	5.13	0.98
lpg1279	-	Hypothetical protein	5.13	1.71
lpg2655	-	Sensory box protein, EAL domain, GGDEF domain, signal transduction protein	5.10	0.99
lpg2196	-	Ornithine cyclodeaminase	5.06	1.43
lpg2818	-	Hypothetical protein	5.03	1.20
lpg0525	-	Hypothetical virulence protein	4.92	1.46
lpg2229	-	saframycin Mx1 synthetase B	4.69	1.62
lpg0818	*cl*	ATP-binding protease component ClpA	4.66	0.81
lpg1526	-	Hypothetical protein	4.66	0.95
lpg1540	*uspA*	universal stress protein A (UspA)	4.66	1.94
lpg2681	-	4-hydroxy-2-oxovalerate aldolase (aldolase/synthase)	4.66	1.42
lpg1415	*gltA*	Citrate synthase	4.50	0.60
lpg2687	*icmV*	IcmV (Dot/Icm substrate)	4.50	6.46
lpg1596	*yfcX*	Enoyl CoA hydratase	4.41	0.58
lpg1898	*moxR*	MoxR: Methanol dehydrogenase regulatory protein	4.41	1.15
lpg1951	-	Hypothetical protein	4.38	1.59
lpg0135	*sdhB*	SdhB	4.35	1.89
lpg0446	*icmO*	IcmO/DotL (Dot/Icm substrate)	4.35	0.72
lpg0586	-	Transcriptional regulator	4.35	1.95
lpg1121	-	Hypothetical protein	4.35	0.78
lpg1058	*phbC*	Polyhydroxyalkanoic synthase	4.26	0.82
lpg2639	*enhC*	Enhanced entry protein EnhC	4.26	1.09
lpg2212	*bcp*	Acetylpolyamine aminohydolase	4.23	1.09
lpg2312	-	Hypothetical protein	4.23	1.03
lpg0035	-	Hypothetical protein	4.20	1.40
lpg1221	*flgG*	Flagellar basal body rod protein FlgG	4.20	1.89
lpg2931	-	Hypothetical protein	4.17	0.90
lpg2210	-	Hypothetical protein	4.14	1.08
lpg1495	-	Hypothetical protein	4.11	1.15
lpg1523	*pilC*	(Type IV) pilus assembly protein PilC (bacterial type II secretion system protein)	4.08	1.16

lpg1792	*fliM*	Flagellar motor switch protein FliM	4.06	0.87
lpg2844	-	Hypothetical histidine-rich protein	4.00	0.46
lpg0842	-	Similar to permease of ABC transporter	3.97	0.76
lpg0969	-	Hypothetical protein	3.97	0.97
lpg2952	-	Hypothetical protein	3.97	1.53
lpg2333	-	Similar to membrane-associated metalloprotease	3.94	1.81
lpg0165	-	Hypothetical protein	3.92	1.10
lpg2810	-	Hypothetical protein	3.92	0.93
lpg0667	-	Hypothetical protein	3.86	0.90
lpg2759	-	Hypothetical protein	3.84	0.70
lpg1527	-	Hypothetical protein	3.78	1.46
lpg0197	-	Hypothetical protein	3.73	0.77
lpg0364	-	Hypothetical protein	3.71	1.91
lpg0894	-	Similar to eukaryotic cytokinin oxidase	3.71	0.91
lpg1836	-	Some similarity with eukaryotic protein	3.71	0.64
lpg0242	*serA*	SerA; D-3-phosphoglycerate dehydrogenase	3.66	1.16
lpg2918	-	Highly similar to putative lytic murein transglycosylase	3.66	0.67
lpg2111	-	peptide methionine sulfoxide reductase	3.66	1.20
lpg0940	*lidA*	LidA (Dot/Icm substrate)	3.63	0.64
lpg1551	-	Hypothetical protein	3.63	0.74
lpg2829	*sidH*	SidH (Dot/Icm substrate)	3.63	1.23
lpg1278	-	Hypothetical protein	3.61	0.87
lpg0644	-	hypothetical protein	3.61	0.97
lpg0445	*icmP*	IcmP/DotM (Dot/ Icm substrate)	3.58	0.95
lpg2442	-	Hypothetical protein	3.58	0.79
lpg0280	-	similar to transcriptional regulator lysR family	3.56	0.97
lpg0848	-	Hypothetical protein	3.56	0.62
lpg0269	-	Hypothetical protein	3.43	1.26
lpg2261	-	similar to phosphotransacetylase	3.39	1.33
lpg2807	-	Similar to conserved hypothetical protein	3.39	0.86
lpg2018	-	Similar to conserved hypothetical protein	3.36	1.18
lpg1216	*flgB*	Flagellar basal-body rod protein FlgB	3.32	1.33
lpg0026	-	similar to amino acid permease	3.29	1.28
lpg0557	*mutM*	Formamidopyrimidine-DNA glycosylase	3.27	1.43
lpg0689	-	Weakly similar to DNA-binding ferritin-like protein (oxidative damage protectant)	3.25	1.23
lpg2709	*ihfA*	Integration host factor- alpha	3.25	0.62
lpg1243	-	hypothetical protein	3.25	1.36
lpg1172	-	TPR repeat protein	3.23	1.41
lpg1796		similar to transcriptional regulator (LysR family)	3.23	1.36
lpg2640	*enhB*	enhanced entry protein EnhB	3.20	0.61
lpg0401	-	hypothetical protein	3.18	0.92
lpg1555	*artJ*	arginine 3rd transport system periplasmic binding protein	3.18	1.32
lpg2131	*legA6*	ankyrin 3	3.18	1.27

lpg2155	-	Hypothetical protein	3.16	0.84
lpg0585	-	Hypothetical protein	3.14	0.77
lpg1030	-	Chemiosmotic efflux system C protein A	3.14	0.68
lpg1173	*pilS*	Sensor protein PilS	3.12	1.21
lpg1293	-	Similar to intracellular septation protein	3.12	1.30
lpg0587	-	Hypothetical protein	3.07	1.57
lpg2626	-	Hypothetical protein	3.03	1.08
lpg1217	*flgC*	Flagellar basal-body rod protein FlgC	2.99	0.83
lpg2248	-	Hypothetical protein	2.99	0.63
lpg1225	*flgK*	Flagellar hook-associated protein 1FlgK	2.97	1.31
lpg1127	-	Similar to long-chain acyl-CoA synthetase	2.95	1.17
lpg2406	-	Hypothetical protein	2.95	0.96
lpg2576	-	Similar to conserved hypothetical protein	2.93	0.92
lpg0845	*rsbV*	weakly similar to anti-anti-sigma factor	2.89	0.69
lpg1439	-	Similar to magnesium and cobalt efflux protein CorC	2.89	0.86
lpg1097	*phbC*	polyhydroxyalkanoic synthase	2.87	0.80
lpg0230	*pleD*	Sensor histidine kinase	2.85	1.35
lpg1597	-	thiolase	2.83	0.63
lpg1044	-	Similar to NADH oxidoreductase	2.81	1.22
lpg1440	-	similar to conserved hypothetical protein	2.81	1.03
lpg2225	-	similar to other proteins	2.81	1.03
lpg2456	*legA15*	ankyrin repeat protein	2.79	0.57
lpg1130	*cyaA4*	adenylate cyclase	2.75	1.05
lpg2976	-	Hypothetical protein	2.75	0.89
lpg2998	-	Similar to sulfate permease	2.75	1.11
lpg1456	*rumA*	Similar to 23S rRNA (Uracil-5-)-methyltransferase	2.73	1.45
lpg2431	-	Similar to malonyl-CoA acyl-carrier-protein transacylase	2.73	1.43
lpg1952	-	Similar to predicted phosphohydrolases	2.71	1.59
lpg2156	*sdeB*	SdeB (substrate of the Dot/Icm system)	2.71	0.94
lpg2970	-	Similar to glycerophosphoryl diester phosphodiesterase (ATA start codon)	2.71	1.18
lpg0294	-	Hypothetical protein	2.69	0.78
lpg0843	-	Hypothetical protein	2.69	0.88
lpg2561	-	hypothetical protein	2.68	1.24
lpg0120	-	Some similarity with - IcmL/DotI	2.66	0.75
lpg2396	-	Hypothetical protein	2.66	1.16
lpg0081	-	Hypothetical protein	2.62	0.96
lpg0386	-	Highly similar to *C. burnetii* heat shock protein HtpX	2.62	1.18
lpg0790	-	Similar to L-serine dehydratase	2.62	0.96
lpg0841	-	Similar to ABC transporter- ATP-binding protein	2.62	0.80
lpg2205	-	Predicted integral membrane protein	2.60	0.82
lpg2458	-	Similar to two-component sensor histidine kinase	2.57	1.25
lpg2508	-	Hypothetical protein	2.57	0.62

lpg1726	-	similar to acyl-CoA dehydrogenase	2.55	0.65
lpg0629	-	Similar to Tfp pilus assembly protein PilX	2.53	0.78
lpg1690	*acn*	Aconitate hydratase	2.51	1.01
lpg1043	-	Hypothetical protein	2.48	1.33
lpg0452	*icmG*	IcmG/DotF	2.46	1.09
lpg0010	*hflX*	Similar to GTP-binding protein HflX	2.45	1.07
lpg0456	*icmB*	IcmB/DotO	2.45	0.82
lpg1750	*clpB*	endopeptidase Clp ATP-binding chain B (ClpB)	2.41	1.34
lpg0012	-	Hypothetical protein	2.39	0.45
lpg2101	*merA1*	mercuric reductase	2.39	0.87
lpg2352	*mdh*	Malate dehydrogenase	2.38	0.55
lpg0673	-	Hypothetical protein	2.35	1.10
lpg2198	-	Similar to transporters	2.35	0.93
lpg0995	-	Hypothetical protein	2.33	0.96
lpg0686	*dsbD*	Similar to thiol:disulfide interchange protein DsbD	2.30	0.55
lpg0443	*icmR*	IcmR	2.28	1.03
lpg2422	-	Some similarity with eukaryotic proteins	2.28	0.67
lpg0630	-	Similar to Tfp pilus assembly protein PilW	2.27	0.66
lpg2685	*sbpA*	small basic protein SbpA	2.27	0.77
lpg2804	-	Hypothetical protein	2.27	1.40
lpg0453	*icmC*	IcmC/DotE	2.25	0.89
lpg1292	-	similar to two component response regulator	2.25	0.89
lpg1588	*legC6*	Coiled-coil-containing protein	2.25	0.70
lpg2500	-	similar to carbonic anhydrase	2.25	0.67
lpg1438	*cpxR*	transcriptional regulatory protein CpxR	2.22	1.08
lpg2186	*pksJ*	polyketide synthase of type I	2.22	0.61
lpg1582	-	similar to unknown proteins	2.20	0.52
lpg1888	-	lpp1855 unknown	2.20	1.13
lpg0408	-	Predicted membrane protein	2.19	0.88
lpg1148	-	Putative coiled-coil protein	2.19	0.83
lpg2664	-	Similar to biotin carboxylase (A subunit of acetyl-CoAcarboxylase)	2.19	0.87
lpg1497	-	Similar to aminopeptidase N	2.17	1.16
lpg1918	-	weakly similar to endoglucanase	2.17	0.72
lpg2191		global stress protein GspA	2.17	1.10
lpg2577	-	Hypothetical protein	2.17	0.64
lpg0935	*ibpA*	Similar to universal stress protein A	2.14	0.87
lpg2372	-	Hypothetical protein	2.14	1.31
lpg1956	-	similar to chloromuconate cycloisomerase	2.13	0.64
lpg1369	*htpG*	Class III heat-shock protein HtpG	2.10	1.07
lpg1236	-	modification methylase (Eco47II, Sau96I)	2.10	1.10
lpg0696	-	Hypothetical protein	2.08	1.07
lpg2683	*dlpA*	DlpA protein	2.08	1.05
lpg1056	-	Hypothetical protein	2.07	0.98
lpg1672	-	Phosphoribosylglycinamide formyltransferase	2.07	0.98

lpg1745	-	similar to iron-sulpher cluster proteins NifU	2.04	0.91
lpg1263	-	Hypothetical protein	2.04	0.80
lpg2742	*cca*	tRNA nucleotidyltransferase	2.03	0.87
lpg2260	*phbC*	Poly(3-hydroxyalkanoate) synthetase	2.00	0.90
lpg2315	-	Hypothetical protein	2.00	0.96

[a] Data were obtained from Bruggemann, H., et al. (2006). Virulence strategies for infecting phagocytes deduced from the *in vivo* transcriptional program of *Legionella pneumophila*. Cell Microbiol 8: 1228-1240. T_{14}: 14 hours after infection, T_8: 8 hours after infection.

[b] Data were obtained from Faucher, S. et al. (2011). *Legionella pneumophila* transcriptome during intracellular multiplication in human macrophages. Front Microbiol 2: 1-18. T_{18}: 18 hours after infection, T_0: infection at zero time.

Appendix II. A List of *L. pneumophila* genes that are selectively upregulated (≥ 2-fold increase) in the progeny from human macrophages (relative to stationary phase forms grown *in vitro*) but down-regulated (< 1-fold change) or unchanged (< 2-fold increase) in MIFs from amoebae (in relation to replicative forms in amoebae).

Gene ID	Gene name	Product	Human THP-1 macrophages[a] (T_{18}/T_0)	*A. castellanii*[b] (T_{14}/T_8)
lpg2383	-	Transcriptional regulator, LysR family	41.45	1.73
lpg0997	-	small ORF (108aa)	38.84	1.73
lpg1739	*gidA*	adenylate/guanylate cyclase transmembrane protein	30.22	-1.34
lpg1610	*proB*	glutamate-5-kinase (gamma-glutamyl kinase)	26.80	1.13
lpg0494	*argG*	argininosuccinate synthase	22.36	-1.23
lpg0065	-	Hypothetical protein	20.64	1.18
lpg0988	-	Hypothetical protein	15.93	1.07
lpg1004	-	Hypothetical protein	15.64	1.83
lpg0150	-	Putative phage protein	14.22	1.15
lpg2432	*phoA*	Alkaline phosphatase	11.97	-2.50
lpg1971	-	Organic hydroperoxide resistance protein, OsmC: predicted redox protein	11.91	-1.41
lpg0174	*pvcA*	Pyoverdine biosynthesis protein PvcA	11.73	-1.47
lpg1002	-	Putative exported protein	11.40	1.21
lpg0994	-	Hypothetical protein	11.23	-1.06
lpg2365	-	Plasmid transfer protein TraK	10.98	1.30
lpg1617	-	probable signal peptide protein	10.98	1.69
lpg0829	-	Two component histidine kinase, GGDEF domain protein/EAL domain protein (sensory box) (c-di-GMP phosphodiesterase A?)	10.94	-1.39
lpg0622	-	Transmembrane protein	10.65	-1.21
lpg1070	*int*	Integrase (phage related)	10.64	-1.24
lpg0715	-	Two component response regulator	9.99	-2.16
lpg0682	-	ABC transporter ATP-binding protein	9.86	1.47
lpg1003	*csrA-2*	carbon storage regulator	9.75	1.93
lpg2534	-	Hypothetical protein	9.47	-1.55
lpg1962	*lirB*	peptidyl-prolyl cis-trans isomerase (rotamase)	9.32	-1.80
lpg1021	-	metallo-beta lactamase family	9.27	1.47
lpg1001	-	Hypothetical protein	8.70	1.31
lpg2373	-	Hypothetical protein	8.66	-1.13
lpg1933	-	Hypothetical protein	8.42	1.86
lpg1074	-	Hypothetical protein	8.36	-1.3
lpg0491	-	Amino acid (glutamine) ABC transporter, periplasmic amino acid binding protein)	8.28	-1.04
lpg1230	-	Hypothetical protein	8.13	1.35
lpg1995	-	Hypothetical protein	8.12	1.13
lpg1958	*legL5*	Leucine-rich repeat-containing protein	8.10	-1.10

lpg0683	-	Transmembrane protein, ABC-type multidrug transport system	8.07	1.05
lpg1794	-	Oxidoreductase (L-gululonolactone oxidase)	8.02	-1.41
lpg1227	-	Hypothetical protein	8.01	1.20
lpg0897	-	Na/Ca antiporter	7.99	1.07
lpg2491	-	Hypothetical protein	7.94	1.97
lpg1262	-	Hypothetical protein	7.87	1.42
lpg1020	*cebA*	Chemiosmotic efflux system B protein A	7.86	-2.19
lpg0919	-	Transmembrane protein	7.78	-1.76
lpg1946	*lpnR2*	Transcriptional regulator LuxR	7.77	-1.44
lpg2423	-	Hypothetical protein	7.76	1.64
lpg1981	-	Hypothetical protein	7.71	1.14
lpg2129	-	Hypothetical protein	7.58	1.71
lpg0787	-	Hypothetical protein	7.40	1.63
lpg1395	*fabG*	3-oxoacyl-(acyl carrier protein) reductase	7.39	-2.89
lpg0024	*hbp*	Hemin binding protein Hbp	7.35	-1.37
lpg0220	-	Hypothetical protein	7.30	1.31
lpg0986	-	Membrane protein	7.23	-1.01
lpg1000	-	Putative exported protein	7.18	1.22
lpg2460	-	Hypothetical protein	6.89	1.16
lpg2140	-	Hypothetical transcriptional regulator, MarR family	6.80	-1.18
lpg1649	*iolE*	myo-inositol catabolism protein IolE	6.79	-3.39
lpg2536	-	Ferredoxin reductase	6.71	-1.42
lpg2324	*Gulo*	L-gulono-gamma-lactone oxidase	6.65	1.65
lpg1229	-	Site specific recombinase	6.62	1.16
lpg1612	-	transcriptional regulator SkgA (mercury resistance)	6.60	-1.08
lpg1732	*qor*	quinone oxidoreductase	6.58	1.33
lpg2247	-	DedA family protein	6.52	-1.24
lpg1902	-	Hypothetical protein	6.50	1.03
lpg0498	-	leucine-, isoleucine-, valine-, threonine-, and alanine-binding protein	6.47	1.02
lpg2165	-	Hypothetical protein	6.36	-1.40
lpg1118	-	serine-type D-Ala-D-Ala carboxypeptidase	6.35	1.16
lpg1110	-	Hypothetical protein	6.17	1.07
lpg2418	-	Putative penicillin-binding protein AmpH	6.13	-1.67
lpg1370	*fis*	Putative DNA-binding protein Fis	6.11	-2.31
lpg0219	-	Hypothetical protein	6.05	1.62
lpg2530	*aroF*	Phospho-2-dehydro-3-deoxy-phosphoheptonate aldolase	6.02	1.00
lpg0058	-	Hypothetical protein	6.02	1.57
lpg0983	*traD*	conjugative coupling factor TraD	5.94	1.48
lpg1124	-	Hypothetical protein	5.91	1.73
lpg0978	-	Hypothetical protein	5.87	1.38
lpg0431	-	Hypothetical protein	5.87	1.11
lpg2531	*pheA*	Chorismate mutase/prephenate dehydratase (P-protein)	5.86	1.37
lpg2523	-	Hypothetical protein	5.81	-1.35

lpg0066	-	Phosphoribosylglycinamide synthetase ATP-grasp (A) domain protein	5.81	1.04
lpg2382	-	Hypothetical protein	5.74	1.81
lpg1738	-	Hypothetical protein	5.72	-1.43
lpg1656	-	Hypothetical protein	5.67	-1.20
lpg2562	-	Phage repressor	5.66	1.13
lpg0991	-	Exported protein?	5.64	1.81
lpg0681	-	Putative lipoprotein	5.62	1.24
lpg1938	-	Coenzyme F390 synthetase (capsular polysaccharide biosynthesis protein)	5.62	1.04
lpg0613	-	Hypothetical protein	5.60	-1.71
lpg0495	*argH*	Argininosuccinate lyase	5.58	1.27
lpg1979	-	Hypothetical protein	5.56	-1.07
lpg1050	-	ATP synthase C subunit (H^+-transporting ATP synthase)	5.56	1.94
lpg0430	*pmrA*	Multidrug resistance efflux pump PmrA	5.55	1.31
lpg1249	*virB8*	LvhB8 (conjugal transfer protein)	5.52	-2.19
lpg1561	*kefA*	potassium efflux system KefA	5.44	1.24
lpg1999	*phhB*	Pterin-4-alpha carbinolamine dehydratase	5.42	-1.74
lpg0770	-	Hypothetical protein	5.40	1.10
lpg1023	-	ribose-phosphate pyrophosphokinase	5.40	1.07
lpg1134	-	nitropropane dioxygenase/(trans-enoyl-CoA reductase)	5.35	1.05
lpg1740	-	Hypothetical protein	5.28	-1.10
lpg1006	-	Cobalt/zinc/cadmium efflux RND transporter, outer membrane protein	5.27	-1.09
lpg1177	*ribD*	Riboflavin biosynthesis protein RibD	5.26	-1.25
lpg2400	*legL7*	Leucine-rich repeat-containing protein	5.17	1.24
lpg2535	-	Limited homology to myoglobin (hemoglobin, cyanoglobin)	5.13	1.02
lpg2411	-	Hypothetical protein	5.10	-1.95
lpg1169	-	Hypothetical protein (dioxygenase)	5.09	1.90
lpg1980	-	Hypothetical protein	5.06	-1.15
lpg0176	-	FAD monooxygenase, PheA/TfdB family	5.04	-1.47
lpg0159	-	Hypothetical protein	5.03	1.31
lpg1668	-	Hypothetical protein	4.99	1.34
lpg0272	-	Cysteine transferase	4.98	-1.85
lpg1321	-	Oxidoreductase	4.96	-1.05
lpg1900	-	Transglutaminase domain protein	4.95	1.37
lpg1890	*legLC8*	Leucine-rich repeat- and coiled coil-containing protein	4.94	1.06
lpg1211	-	Transporter, LysE family	4.92	1.02
lpg0067	-	Similar to unknown protein YdeN of *Bacillus subtilis*	4.91	1.10
lpg2762	-	Hypothetical protein	4.90	1.55
lpg1517	-	HlyD family secretion protein (hemoloysin) (type I secretion system LssD)	4.90	1.52
lpg1234	-	Hypothetical protein	4.89	1.73
lpg0675	-	Hypothetical protein	4.88	-1.17
lpg0955	-	Transmembrane protein	4.87	-1.82
lpg2319	*motB*	chemotaxis (motility protein B) transmembrane (flagellar motor rotation)	4.84	1.95

lpg1191	-	Glycosyl hydrolase family 3	4.83	-1.05
lpg0521	-	Hypothetical protein	4.82	1.11
lpg0998	-	Hypothetical protein	4.80	1.17
lpg0188	-	Acyl CoA transferase/carnitine dehydratase	4.79	1.08
lpg1667	-	Hypothetical protein	4.79	1.44
lpg2430	*mdcB*	2-(5-triphosphoribosyl)-3'-dephosphocoenzyme A synthase CitG (modifier of citrate lyase)	4.78	1.75
lpg1473	*bioF*	8-amino-7-oxononanoate synthase	4.77	-2.51
lpg1246	*virB11*	LvhB11 (VirB11)	4.77	-1.21
lpg0127	*acsB*	acetyl-coenzyme A synthetase	4.76	-1.79
lpg2503	-	Hypothetical protein	4.75	1.93
lpg1566	-	Thiamine biosynthesis oxidoreductase ThiO	4.73	1.36
lpg0989	-	H ypothetical Type IV secretory protein VirB4 components	4.73	1.76
lpg0433	-	Hypothetical protein	4.73	1.82
lpg1749	*sppA*	signal peptide peptidase	4.72	-2.45
lpg0113	*yuxH*	Putative uncharacterized protein yuxH	4.72	-1.11
lpg2235	-	Sterol desaturase	4.70	1.10
lpg1751	-	Hypothetical protein	4.64	1.35
lpg1054	*atpD*	ATP synthase F1, beta chain (F_0F_1-type ATPase beta subunit)	4.62	1.70
lpg1233	-	Hypothetical protein	4.56	1.25
lpg0268	-	Hypothetical (hydrolase?)	4.55	1.70
lpg1255	*lvhB3*	LvhB3 (type IV secretion system protein B3)	4.53	-1.31
lpg0167	-	Peptide chain release factor	4.52	-1.45
lpg2539	-	Hypothetical protein	4.52	1.19
lpg2454	-	acetyltransferase, GNAT family, ElaA-like protein	4.51	1.01
lpg1899	-	Transmembrane protein	4.49	1.43
lpg0742	-	Hypothetical protein	4.49	1.63
lpg0153	-	Hypothetical protein	4.48	1.18
lpg2555	-	Hypothetical protein	4.46	1.27
lpg2474	*hypF*	Hydrogenase maturation protein HypF	4.46	-1.91
lpg1123	*artJ*	Peb1 (Arginine binding periplasmic protein (amino acid ABC transporter)	4.44	-1.39
lpg1073	-	Hypothetical protein	4.43	1.54
lpg0795	-	ISI400 transposase B	4.41	-1.49
lpg1786	*flhB*	flagellar biosynthetic protein FlhB	4.39	1.14
lpg1077	-	Inner membrane protein	4.39	-1.26
lpg2380	-	Hypothetical protein	4.38	1.46
lpg0590	*comM*	Competence-related protein ComM	4.34	1.07
lpg1005	*lvrA*	LvrA	4.32	1.16
lpg2827	-	Hypothetical protein	4.31	-1.42
lpg0517	*ytbE*	Aldo/keto reductases	4.30	1.08
lpg2560	-	Hypothetical protein	4.29	1.03
lpg0515	*legD2*	Phytanoyl-CoA dioxygenase	4.25	-1.08
lpg1325	*frgA*	siderophore biosynthetic enzyme FrgA	4.25	1.17

lpg0519	*ceg17*	Hypothetical protein	4.25	1.56
lpg1430	*ubiA*	4-hydroxybenzoate octaprenyltransferase UbiA	4.21	-1.16
lpg0971	-	Hypothetical protein	4.15	1.44
lpg2199	-	Hypothetical protein	4.14	1.89
lpg0281	-	Amino acid transporter	4.13	1.38
lpg1521	-	Generic methyl-transferase	4.12	-1.30
lpg0152	-	Hypothetical protein	4.10	-1.72
lpg0554	*dinP*	DNA-damage inducible protein P (DNA polymerase IV)	4.08	-1.11
lpg1611	-	transcriptional regulator, MerR family (mercury resistance)	4.07	1.08
lpg0032	*lapB*	Leucine aminopeptidase	4.07	-1.27
lpg0201	-	Hypothetical protein	4.03	-1.05
lpg1982	-	hypothetical protein	4.00	-2.66
lpg0516	-	conserved hypothetical protein	3.94	-1.11
lpg2115	-	hypothetical (phage AbiD protein)	3.94	-1.17
lpg0663	-	soluble lytic murein transglycosylase	3.92	1.22
lpg0714	-	sensor histidine kinase (two component sensor)	3.91	2.01
lpg2667	*rpoH*	RNA polymerase sigma-32 factor (sigma factor RpoH)	3.90	-1.25
lpg1484	-	Hypothetical protein	3.90	1.05
lpg0432	-	Hypothetical protein	3.88	1.15
lpg2254	-	Conserved hypothetical protein	3.87	-3.73
lpg0469	-	Endonuclease/exonuclease/phosphatase family protein	3.84	1.93
lpg1741	-	Conserved hypothetical protein	3.83	-1.00
lpg0202	-	Conserved hypothetical protein	3.81	-1.18
lpg1758	*fliH*	flagellar assembly protein FliH	3.81	1.12
lpg2494	-	Conserved hypothetical protein	3.73	-2.48
lpg1085	-	phage related integrase (site specific recombinase)	3.73	-1.01
lpg1486	-	AsnC family transcription regulator protein (amino acid metabolism)	3.70	-1.28
lpg2179	-	peptide synthetase (non-ribosomal)	3.69	1.32
lpg1882	*gloA*	lactoylglutathione lyase	3.67	1.72
lpg2035	-	transporter, Zip family (solute carrier; Fe(II) transporter)	3.66	-1.81
lpg1248	*virB9*	LvhB9 (probable conjugal transfer protein TrbG)	3.66	1.68
lpg1047	*atpG*	ATP synthase gamma subunit C-terminus homolog	3.63	1.50
lpg1996	-	ORF (PilW?)	3.62	-1.67
lpg0064	-	Hypothetical protein	3.61	1.57
lpg1142	-	Hypothetical protein	3.60	-1.13
lpg2371	-	Hypothetical protein	3.60	-1.28
lpg2379	-	Hypothetical protein	3.59	1.22
lpg1075	-	Hypothetical protein	3.55	1.21
lpg1468	-	Hypothetical protein	3.54	1.74
lpg0973	-	Hypothetical protein	3.53	-2.14
lpg0788	-	Hypothetical protein	3.53	-2.14
lpg2183	-	regulatory protein, SyrP-like (antibiotic production)	3.53	-1.49
lpg2596	-	signal peptide protein (LysM domain protein)	3.49	-1.46

lpg1650	*iolD*	myo-inositol catabolism protein IolD	3.48	-1.57
lpg0551	*plsC*	1-acyl-sn-glycerol-3-phosphate acetyltransferase	3.48	-1.63
lpg0975	-	transmembrane protein (transporter, DME family)	3.48	-1.42
lpg0660	-	ABC transporter permease protein	3.48	-1.84
lpg1300	-	integral membrane protein COG5528	3.48	-1.15
lpg0214	-	murein hydrolase exporter (LrgA family protein)	3.46	1.38
lpg1176	-	Zn-dependent protease (zinc metalloprotease)	3.45	1.63
lpg1069	-	similar to AbiD phage protein	3.44	-1.56
lpg1018	-	chemiosmotic efflux system B protein C (outer membrane efflux protein)	3.43	1.32
lpg1329	-	hypothetical protein	3.42	-2.45
lpg1556	-	MutT/nudix family protein (phosphohydrolase)	3.42	-1.33
lpg0209	-	hypothetical protein	3.42	1.75
lpg1564	-	membrane protein (nodulin 21?)	3.41	1.60
lpg2264	-	hypothetical protein	3.41	1.45
lpg1648	-	signal peptide protein	3.40	1.23
lpg0422	*gamA*	glucoamylase (glucan-1,4 alpha glucosidase)	3.40	-2.38
lpg2544	*mltA*	membrane-bound lytic murein transglycosylase A	3.40	1.60
lpg2084	-	putative conjugative transfer protein TrbC	3.40	1.60
lpg1789	-	flagellar biosynthetic protein FliP	3.40	1.73
lpg2656	-	octaprenyl diphosphate synthase IspB	3.40	-3.61
lpg0777	*lag-1*	O-acetyltransferase (glycosyltransferase)	3.37	-5.06
lpg1762	*fleR*	sigma 54-dependent response regulator	3.36	1.72
lpg1326	-	conserved hypothetical protein	3.36	1.32
lpg2602	-	conserved domain protein	3.35	1.48
lpg2020	*oruR*	transcriptional regulator OruR, AraC family	3.35	1.42
lpg1382	-	dehydrogenase, short chain (dhs-6C) (hydroxysteroid dehydrogenase)	3.34	-1.49
lpg1936	-	methoxymalonyl CoA synthase	3.34	1.60
lpg1266	-	methylase	3.34	1.59
lpg1528	-	conserved hypothetical protein	3.32	1.44
lpg1247	-	LvhB10 (type IV secretion system protein B10)	3.32	1.10
lpg1260	*prpA*	phage repressor (putative repressor protein of prophage)	3.32	-1.15
lpg1998	*hisC2*	histidinol phosphate aminotransferase	3.31	-1.62
lpg1257	*csrA*	LvrC (carbon storage regulator)	3.31	-2.35
lpg0171	*LegU1*	FBOX-containing protein	3.30	1.02
lpg2717	-	Hypothetical protein	3.28	1.20
lpg2497	-	conserved hypothetical protein	3.28	1.16
lpg0265	-	multicopper oxidase	3.26	1.44
lpg0533	*sucB*	dihydrolipoamide succinyltransferase (2-oxoglutarate dehydrogenase E2 component)	3.25	1.12
lpg0981	-	Hypothetical protein	3.25	-4.00
lpg0435	-	SAM-dependent methyltransferase	3.24	1.14
lpg1716	-	Hypothetical protein	3.24	-1.46
lpg1089	-	methyltransferase (N-methyltransferase?)	3.23	1.21
lpg2082	*traF*	sex pilus assembly TraF	3.22	-1.03

lpg0992	-	Hypothetical protein	3.22	-1.05
lpg0063	*aroH*	phospho-2-dehydro-3-deoxyheptonate aldolase	3.22	-1.21
lpg1299	-	transmembrane protein FimV	3.21	-1.04
lpg1594	-	Hypothetical protein	3.20	-1.32
lpg2332	-	competence protein ComF (phosphoribosyltransferase)	3.20	-1.13
lpg2618	*murF*	UDP-N-acetylmuramoylalanyl-D-glutamyl-2, 6-diaminopimelate-D-alanyl-D-alanyl ligase	3.19	1.08
lpg1704	-	SOS (error prone) mutagenesis protein UmuD (RumA)	3.19	-1.04
lpg2244	-	Hypothetical protein	3.18	1.20
lpg1212	-	IAA acetyltransferase/MarR transcriptional regulatory protein	3.18	-1.17
lpg2014	-	pyridoxal-5'-phosphate dependent enzyme family	3.17	1.37
lpg2920	-	Hypothetical (nucleotidyltransferase?)	3.16	1.14
lpg1494	-	Hypothetical protein	3.15	1.34
lpg1009	*cadA-1*	Cadmium translocating P-type ATPase CadA (Pb-efflux ATPase?)	3.15	1.30
lpg1680	*dsbD*	thiol:disulfide interchange protein DsbD	3.15	-1.04
lpg1068	-	Hypothetical protein	3.14	1.08
lpg1467	*coaE*	dephospho-CoA kinase (DNA repair protein?)	3.14	1.31
lpg0493	-	amino acid (glutamine) ABC transporter, ATP binding component	3.14	1.12
lpg0902	-	Hypothetical protein	3.14	-13.64
lpg2003	*tgt*	queuine tRNA-ribosyltransferase	3.12	-1.61
lpg1884	*legC2/ylfb*	Microtubule binding protein, putative	3.11	1.45
lpg1200	*hisG*	ATP phosphoribosyltransferase HisG	3.10	-1.88
lpg0549	-	gamma-glutamyltranspeptidase	3.10	-2.23
lpg0610	-	major facilitator family transporter (multidrug efflux transporter)	3.10	1.19
lpg1259	*lvrA*	LvrA	3.09	-1.38
lpg0611	-	metal ion transporter	3.09	1.48
lpg2267	-	prolidase (aryldialkylphosphatase)	3.08	-7.46
lpg1245	*virD4*	LvhD4 (VirD4)	3.06	-1.05
lpg1989	-	Glutathione S-transferase?	3.06	-1.12
lpg0175	-	Pyoverdine biosynthesis protein PvcB	3.03	1.32
lpg1815	*oxyR*	hydrogen peroxide-inducible genes activator OxyR	3.03	-1.22
lpg1222	*flgH*	flagellar L-ring protein FlgH	3.02	1.53
lpg0434	-	Hypothetical protein	3.02	-2.04
lpg0996	-	Hypothetical protein	3.02	1.05
lpg1755	-	transmembrane protein (protease?)	3.02	1.16
lpg1607	*capP*	phosphoenolpyruvate carboxylase	3.01	-1.06
lpg1228	-	Hypothetical protein	2.99	-1.06
lpg1327	-	Hypothetical protein	2.99	1.47
lpg0712	*yjeA*	similar to endo-1,4-beta-xylanase	2.99	-1.32
lpg1943	-	Hypothetical protein	2.98	-1.30
lpg0208	*pkn5*	serine/threonine-protein kinase	2.98	1.19
lpg1258	*lvrB*	LvrB	2.97	-1.11
lpg0429	*oprM*	outer membrane efflux protein	2.97	1.20

lpg2127	-	Hypothetical protein	2.97	-3.07
lpg1275	-	Transporter, TrkA family	2.97	-1.15
lpg0330	*rplD*	50S ribosomal protein L4	2.95	-6.11
lpg1965	-	Hypothetical protein	2.94	1.51
lpg0615	*def*	polypeptide deformylase	2.94	-1.82
lpg0106	-	xanthine/uracil permease	2.94	-2.55
lpg1841	*com1*	27 kDa outer membrane protein	2.94	-2.14
lpg0289	*ppk*	polyphosphate kinase (polyphosphoric acid kinase)	2.94	-1.06
lpg2151	-	aminoglycoside 6-adenylyltransferase	2.93	1.28
lpg2718	-	Hypothetical protein	2.93	-1.18
lpg0275	*SdbA*	SdbA	2.92	1.36
lpg0054	-	Hypothetical protein	2.91	-1.19
lpg2059	-	hypothetical (phage repressor) (putative regulator)	2.90	-1.34
lpg0999	-	Hypothetical protein	2.89	1.20
lpg0959	*hbpA*	bacterial extracellular solute-binding protein (peptide ABC transporter, periplasmic peptide-binding protein)	2.89	1.10
lpg2880	*nth*	endonuclease III (DNA	2.89	-1.72
lpg1253	*virB5*	LvhB5 (plasmid-related export protein)	2.89	-1.06
lpg0247	-	Hypothetical protein	2.89	-1.17
lpg0931	*pilQ*	type IV pilus biogenesis protein PilQ	2.88	-1.23
lpg0769	-	Hypothetical protein	2.88	-2.45
lpg1022	*deoA*	thymidine phosphorylase	2.88	1.10
lpg0169	-	probable transmembrane protein	2.87	-1.17
lpg1818	-	tetraacyl disaccharide 4'-kinase	2.87	-1.49
lpg2855	-	TPR (repeat) domain protein	2.86	-1.57
lpg1470	-	serine-type D-Ala-D-Ala carboxypeptidase	2.85	1.35
lpg0635	-	melitin resistance protein	2.84	-1.94
lpg1616	*uup*	ABC transporter ATP-binding protein Uup (erythromycin resistance)	2.84	1.19
lpg1937	-	pyoverdine biosynthesis regulatory gene (SyrP-like protein)	2.83	-1.93
lpg1967	-	transcriptional regulator, TetR family	2.82	-1.40
lpg1328	-	conserved repeat domain protein	2.81	-1.91
lpg0042	-	Hypothetical protein	2.81	-2.62
lpg2632	*holC*	DNA polymerase III, chi subunit	2.80	-2.46
lpg0701	*kbl*	2-amino-3-ketobutyrate coenzyme A ligase	2.80	-1.95
lpg0616	-	GTP cyclohydrolase I PLUS perhaps regulatory protein: fused protein?	2.80	1.43
lpg0263	-	MFS transporter family protein (major facilitator superfamily)	2.79	1.05
lpg1671	-	alpha-amylase, putative	2.79	-1.10
lpg0876	*pntAa*	NAD(P) transhydrogenase subunit alpha	2.79	-1.03
lpg0490	*argR*	arginine repressor (transcriptional regulator)	2.79	-1.17
lpg0658	-	HlyD family secretion protein	2.78	1.18
lpg0802	-	sulfate transporter (sulfate permease)	2.77	-1.12
lpg1806	-	outer membrane protein	2.76	1.19
lpg0832	-	oxidoreductase dehydrogenase, short chain	2.75	-1.31

lpg0743	-	glutamate synthetase	2.75	1.65
lpg1250	*virB6*	LvhB6 (conjugal transfer protein)	2.75	1.50
lpg0921	-	Hypothetical protein	2.74	-1.01
lpg1159	-	Hypothetical (transporter?)	2.74	-1.63
lpg2062	-	methylase	2.74	-1.82
lpg0609	*alaS*	alanyl tRNA synthetase	2.74	1.35
lpg2048	-	Hypothetical protein	2.73	1.08
lpg0582	-	Hypothetical protein	2.73	-2.66
lpg1126	-	calcium-transporting ATPase	2.72	1.60
lpg0700	*pcm*	protein-L-isoaspartate-O-methyltransferase	2.72	-1.82
lpg3000	-	Hypothetical protein	2.70	1.42
lpg1731	*ugpA*	sn-glycerol-3-phosphate transmembrane ABC transporter	2.70	1.32
lpg1048	*atpA1*	ATP synthase F1, subunit alpha (F0F1-type ATP synthase alpha subunit)	2.70	1.39
lpg1184	-	Outer membrane protein RomA	2.70	1.02
lpg1487	-	acetyltransferase, GNAT family	2.69	1.22
lpg2015	*proC*	pyrroline-5-carboxylate reductase	2.69	1.13
lpg0794	-	Transposase B	2.67	-1.13
lpg1188	*kup2*	Kup system potassium uptake protein	2.67	-1.63
lpg2162	-	Hypothetical protein	2.67	1.37
lpg1167	-	hypothetical (cytoplasmic protein)	2.67	-2.38
lpg1194	-	imidazoleglycerol-phosphate synthase, cyclase subunit HisF	2.67	-1.22
lpg0692	*dppF*	ABC type dipeptide/oligopeptide/nickel transport, ATPase component	2.66	1.00
lpg1894	-	Chloride channel protein (voltage gated?)	2.66	-1.74
lpg0105	-	Cytochrome oxidase-like	2.66	1.35
lpg1830	*mvaB*	hydroxymethylglutaryl-CoA lyase	2.66	-1.04
lpg0626	-	DNA uptake/competence protein ComA	2.65	-1.45
lpg0520	-	methyltransferase (ubiE/COQ5 family)	2.64	1.11
lpg1662	-	Putative transport protein	2.64	-2.16
lpg2604	-	Hypothetical	2.63	1.21
lpg2058	-	hypothetical	2.62	-1.15
lpg2627	-	hypothetical (periplasmic flavoprotein)	2.59	-1.43
lpg1301	-	oxidoreductase	2.59	1.16
lpg2940	*waaM*	lipid A lauroyl acyltransferase	2.59	-1.74
lpg1190	-	SAM-dependent methyltransferase	2.58	-3.39
lpg0423	*yozG*	transcriptional regulator (cro family)	2.58	-1.51
lpg2538	-	Hypothetical	2.57	-1.02
lpg1544	*hisS*	histidyl tRNA synthetase	2.57	-3.97
lpg0466	-	oxaloacetate decarboxylase alpha subunit	2.57	-1.69
lpg1569	-	sulfurylase (ThiF family protein)	2.56	1.16
lpg1851	-	Hypothetical	2.56	-1.85
lpg1153	-	amine oxidase	2.56	-1.25
lpg0372	*smpA*	COG2913 small protein A (tmRNA-binding), outer membrane lipoprotein	2.54	-2.58

lpg1743	*fis*	Fis transcriptional activator	2.54	1.13
lpg1990	-	Hypothetical protein	2.54	-1.45
lpg2828	-	Hypothetical protein	2.54	1.20
lpg2572	-	Hypothetical protein	2.54	-1.59
lpg1514	-	lipoprotein (inner membrane protein)	2.54	-1.34
lpg2416	*legA1*	ankyrin repeat containing protein?	2.53	-2.20
lpg2169	-	Hypothetical protein	2.53	1.13
lpg2114	-	Transposase	2.53	-2.46
lpg0464	*aroQ*	3-dehydroquinate dehydratase type	2.53	1.06
lpg2415	-	Transmembrane protein	2.52	-1.18
lpg0857	*ccmB*	Heme exporter protein CcmB	2.52	-1.60
lpg1847	-	glutamate-cysteine ligase	2.52	-1.02
lpg2070	-	reverse transcriptase	2.52	-1.13
lpg0680	-	dipeptidyl aminopeptidase/acylaminoacyl peptidase	2.51	1.29
lpg0224	-	toxin secretion ABC transporter HlyB/MsbA family	2.50	-1.67
lpg2357	*gcp*	O-sialoglycoprotein endopeptidase	2.49	-1.62
lpg0161	-	Hypothetical protein	2.49	-1.12
lpg0015	-	multidrug resistance protein (efflux pump protein FarA)	2.49	1.19
lpg0853	*fleQ*	transcriptional regulator FleQ (sigma 54 dependent transcriptional activator)	2.48	1.11
lpg2757	-	hypothetical protein	2.48	-1.31
lpg1166	-	Hypothetical protein	2.48	1.21
lpg2439	-	NADPH-dependent FMN reductase domain protein (chromate reductase)	2.47	-1.40
lpg2387	*pla*	plasminogen activator (coagulase/fibrinolysin) (outer membrane protease E)	2.47	1.02
lpg0883	-	Hypothetical protein	2.47	1.33
lpg0659	-	ABC transporter ElsE	2.47	-2.27
lpg2306	-	Rhodanese domain protein	2.47	-1.58
lpg2123	-	cobalt zinc cadmium cation transporter	2.47	-1.92
lpg2941	*waaM*	hypothetical (lipid A biosynthesis lauroyl acyltransferase) (may be fused with subsequent ORF)	2.46	1.39
lpg0157	*map-1*	methionine aminopeptidase	2.46	1.14
lpg0216	-	Hypothetical protein	2.46	-1.02
lpg2801	-	phosphatidylglycerophosphate synthase	2.46	-1.11
lpg0173	*oxyR*	transcriptional regulator, LysR	2.45	-1.02
lpg2341	*djlA*	DNA binding protein DnaJ, heat shock protein	2.45	1.04
lpg2573	-	transposase (resolvase, DNA invertase) (resolvase/integrase)	2.45	1.36
lpg0987	-	membrane protein?	2.44	1.40
lpg1907	-	Hypothetical protein	2.44	1.32
lpg0920	-	Phosphatidylglycerophosphatase B (Pap2)	2.44	-1.51
lpg2699	-	ATPase or kinase	2.44	-1.29
lpg2542	-	Hypothetical protein	2.42	-1.15
lpg2166	*lem19*	hypothetical protein	2.42	-1.51
lpg0867	*recQ*	ATP-dependent DNA helicase RecQ	2.42	-1.21
lpg2600	-	Acyltransferase	2.42	-1.90

lpg0256	-	Conserved domain protein	2.41	1.03
lpg2388	-	amino acid permease (transporter) (L-asparagine permease)	2.41	-1.13
lpg1324	-	multidrug resistance efflux pump	2.41	1.04
lpg1931	-	Hypothetical protein	2.40	1.25
lpg1460	-	Hypothetical protein	2.39	-1.60
lpg1531	-	phenazine biosynthesis PhzF (oxidoreductase)	2.39	1.20
lpg1807	-	periplasmic protein	2.38	-1.19
lpg0679	-	adenylyl transferase	2.38	-1.83
lpg2167	-	transcription regulator protein, DeoR family	2.38	1.08
lpg0816	*icd*	isocitrate dehydrogenase, NADP-dependent	2.38	-2.22
lpg0734	-	glutamine dependent NAD+ synthetase	2.37	1.17
lpg2034	-	cation efflux family protein	2.37	-1.30
lpg2066	-	acetyltransferase, GNAT family	2.37	-1.14
lpg2863	-	pteridine reductase 1	2.36	-1.18
lpg0929	*pilO*	type IV pilus biogenesis protein PilO	2.36	-1.44
lpg0617	-	major outer membrane protein	2.36	-2.89
lpg0248	-	arsenate reductase	2.35	1.27
lpg0008	-	Hypothetical protein	2.35	-3.23
lpg2947	-	ABC transporter, ATP binding protein	2.35	-2.06
lpg0956	-	hypothetical protein	2.35	-1.40
lpg0764	-	Hypothetical protein	2.34	1.07
lpg0290	-	lipoprotein	2.34	-1.71
lpg1798	-	Hypothetical protein	2.34	-1.27
lpg1389	-	tRNA (5 methylaminomethyl-2-thiouridylate) methyltransferase (tRNA methyltransferase)	2.34	-1.10
lpg1765	*lolA*	outer membrane lipoprotein carrier protein	2.33	-1.52
lpg1081	-	reverse transcriptase	2.33	1.16
lpg2506	-	sensor histidine kinase/response regulator LuxN	2.33	-1.56
lpg2991	-	hemolysin, lipoprotein	2.33	-1.44
lpg2272	-	transmembrane protein	2.33	1.01
lpg1562	*merA1*	mercuric reductase	2.33	-1.16
lpg1254	*virB4*	LvhB4 (type IV secretion system protein B4)	2.32	-1.03
lpg0373	-	components of sensory transduction system	2.32	1.08
lpg2679	-	D-isomer specific 2-hydroxyacid dehydrogenase (glycerate dehydrogenase)	2.32	-2.50
lpg0621	*sidA*	SidA	2.32	1.30
lpg1886	*acyP*	acylphosphatase	2.31	1.09
lpg1579	-	glycine cleavage T protein (aminomethyl transferase)	2.31	-1.38
lpg1240	-	Hypothetical protein	2.30	1.09
lpg0727	*nusB*	transcription termination factor NusB	2.29	-2.25
lpg2270	-	oxidoreductase (NAD-dependent epimerase/dehydratase)	2.28	1.03
lpg0925	*ponA*	penicillin binding protein 1A (transpeptidase) (peptidoglycan synthetase)	2.28	-1.93
lpg1120	*lem6*	hypothetical protein	2.28	1.17
lpg2478	-	glycosyltransferase, group 2 family protein (glycan biosynthesis)	2.27	-1.15

lpg0458	*icmF*	IcmF (Dot/Icm substrate)	2.27	-2.27
lpg0055	-	transcriptional regulator, LysR family	2.27	1.18
lpg1647	-	hypothetical (exported protein)	2.26	1.35
lpg1652	-	myo-inositol-2-dehydrogenase (oxidoreductase, NAD binding)	2.26	-2.53
lpg2032	-	transporter, permease (integral membrane protein)	2.26	-1.09
lpg0168	-	hypothetical protein	2.25	-1.14
lpg2806	-	Hypothetical protein	2.25	1.13
lpg2090	-	putative conjugative transfer protein TraK	2.24	1.11
lpg1988	-	dihydrofolate reductase	2.24	-1.24
lpg1975	-	Hypothetical protein	2.24	1.03
lpg2404	-	Hypothetical protein	2.24	-1.24
lpg2631	*pepA*	aminopeptidase A/I (leucine aminopeptidase)	2.23	-1.49
lpg2286	-	pirin (chromosome condensation) protein	2.23	-1.10
lpg2588	-	acid sphingomyelinase-like phosphodiesterase	2.23	-1.06
lpg0375	-	Hypothetical protein	2.22	1.05
lpg1795	-	oxidoreductase, short chain dehydrogenase/reductase family	2.22	1.11
lpg1296	-	protein involved in catabolism of external DNA	2.22	-1.43
lpg0123	*dsbA*	thiol:disulfide interchange protein DsbA (disulfide isomerase)	2.22	-1.54
lpg1772	-	hypothetical (lipoprotein?)	2.20	-1.22
lpg0654	*dam*	DNA adenine methylase (DNA-adenine methyltransferase) Dam	2.20	-1.74
lpg1261	-	Hypothetical protein	2.20	1.16
lpg2135	-	chemiosmotic efflux system protein B (cation efflux system)	2.20	1.09
lpg0040	-	integral membrane protein (YhfP-like protein)	2.19	-1.22
lpg0492	*yqiY*	amino acid (glutamine) ABC transporter, permease	2.19	-1.03
lpg1103	-	hypothetical (esterase)	2.19	-1.63
lpg0194	*katG2*	catalase/(hydro)peroxidase KatG	2.18	-2.64
lpg2484	-	ribosomal protein HAM1 (xanthosine triphosphate pyrophosphatase)	2.17	-1.15
lpg2314	-	dihydropicolinate synthase	2.17	-2.25
lpg0111	*fdfT*	squalene and phytoene synthases	2.16	-1.62
lpg2663	-	hypothetical protein	2.16	-1.25
lpg1309	-	Hypothetical protein	2.16	1.12
lpg0131	*dapB*	dihydropicolinate reductase	2.16	1.00
lpg2378	-	Hypothetical protein	2.15	-1.06
lpg1867	-	site specific recombinase, phage integrase	2.15	1.03
lpg2911	-	serine carboxypeptidase	2.15	1.07
lpg1697	-	conserved hypothetical protein	2.14	1.02
lpg1970	-	glutathione S-transferase	2.13	1.11
lpg0110	-	Hypothetical protein	2.12	-1.65
lpg1475	*bioD*	ATP-dependent dethiobiotin synthetase	2.12	-1.16
lpg2409	-	Hypothetical protein	2.12	1.01
lpg1479	-	potassium efflux system KefA (integral membrane protein)	2.12	-1.09

lpg0186	-	ABC sugar transporter, permease	2.11	-1.12
lpg0974	-	Hypothetical protein	2.11	1.19
lpg2436	-	Hypothetical protein	2.11	-1.22
lpg2299	*hepA*	ATP-dependent RNA helicase (RNA polymerase associated) HepA	2.11	-1.79
lpg0128	-	3-hydroxyisobutyrate dehydrogenase	2.11	-2.08
lpg1874	-	general secretion pathway protein L	2.11	1.11
lpg0562	-	Hypothetical protein	2.11	-1.22
lpg0235	-	Hypothetical protein	2.10	-1.14
lpg0900	-	Hypothetical protein	2.10	-1.54
lpg1319	-	type II secretory pathway protein E (ATPase EpsE)	2.09	-1.94
lpg1038	-	VrrB (contains histidine/glycine rich portion)	2.09	-1.78
lpg1513	-	type I secretion system LssZ	2.09	1.05
lpg2877	-	Hypothetical protein	2.09	1.15
lpg1585	-	Hypothetical protein	2.08	-3.12
lpg2514	-	outer membrane efflux protein	2.08	-1.24
lpg0211	*tspO*	tryptophan rich sensory protein TspO	2.08	-1.19
lpg2273	*ugpB*	glycerol-3-phosphate binding periplasmic protein	2.07	-1.62
lpg2925	-	Outer membrane efflux protein	2.07	1.13
lpg0661	-	ABC transporter permease protein	2.07	1.02
lpg0886	-	sodium:dicarboxylate symporter	2.05	-1.03
lpg0789	-	alginate O-acetyltransferase AlgI	2.04	-1.41
lpg1138	-	spermidine/putrescine-binding periplasmic protein PotD	2.03	-1.92
lpg1028	-	chemiosmotic efflux system C protein B	2.03	1.09
lpg1198	*hisC*	histidinol-phosphate aminotransferase	2.02	-1.21
lpg1033	-	Hypothetical protein	2.02	1.09
lpg2745	-	Hypothetical protein	2.01	-2.43
lpg2072	-	Hypothetical protein	2.01	-1.03
lpg0204	-	2-deoxy-D-gluconate-3-dehydrogenase	2.01	-1.03
lpg0212	*phrB*	deoxyribodipyrimidine photolyase (DNA photolyase)	2.01	-2.04
lpg0899	-	A/G specific adenine glycosylase	2.00	-1.63
lpg1883	-	transmembrane protein	2.00	-1.08

[a] Data were obtained from Faucher, S. et al. (2011). *Legionella pneumophila* transcriptome during intracellular multiplication in human macrophages. Front Microbiol 2: 1-18. T_{18}: 18 hours after infection, T_0: infection at zero time.

[b] Data were obtained from Bruggemann, H., et al. (2006). Virulence strategies for infecting phagocytes deduced from the *in vivo* transcriptional program of *Legionella pneumophila*. Cell Microbiol 8: 1228-1240. T_{14}: 14 hours after infection, T_8: 8 hours after infection.

Appendix III. Copyright permission

JOHN WILEY AND SONS LICENSE TERMS AND CONDITIONS

Nov 21, 2013

This is a License Agreement between Hany Abdelhady ("You") and John Wiley and Sons ("John Wiley and Sons") provided by Copyright Clearance Center ("CCC"). The license consists of your order details, the terms and conditions provided by John Wiley and Sons, and the payment terms and conditions.

All payments must be made in full to CCC. For payment instructions, please see information listed at the bottom of this form.

License Number	3273961395930
License date	Nov 21, 2013
Licensed content publisher	John Wiley and Sons
Licensed content publication	Cellular Microbiology
Licensed content title	Virulence strategies for infecting phagocytes deduced from the in vivo transcriptional program of Legionella pneumophila
Licensed copyright line	Copyright © 2006, John Wiley and Sons
Licensed content author	Holger Brüggemann,Arne Hagman,Matthieu Jules,Odile Sismeiro,Marie-Agnès Dillies,Catherine Gouyette,Frank Kunst,Michael Steinert,Klaus Heuner,Jean-Yves Coppée,Carmen Buchrieser
Licensed content date	Mar 3, 2006
Start page	1228
End page	1240
Type of use	Dissertation/Thesis
Requestor type	University/Academic
Format	Print and electronic
Portion	Figure/table
Number of figures/tables	2
Original Wiley figure/table number(s)	Figure 2
Will you be translating?	No
Total	0.00 USD

This is a License Agreement between Hany Abdelhady ("You") and John Wiley and Sons ("John Wiley and Sons") provided by Copyright Clearance Center ("CCC"). The license consists of your order details, the terms and conditions provided by John Wiley and Sons, and the payment terms and conditions.

All payments must be made in full to CCC. For payment instructions, please see information listed at the bottom of this form.

License Number	3273970778028
License date	Nov 21, 2013
Licensed content publisher	John Wiley and Sons
Licensed content publication	Molecular Microbiology
Licensed content title	Two small ncRNAs jointly govern virulence and transmission in Legionella pneumophila
Licensed copyright line	Â© 2009 The Authors. Journal compilation Â© 2009 Blackwell Publishing Ltd
Licensed content author	Tobias Sahr,Holger BrÃ¼ggemann,Matthieu Jules,Mariella Lomma,Christiane Albert-Weissenberger,Christel Cazalet,Carmen Buchrieser
Licensed content date	Mar 30, 2009
Start page	741
End page	762
Type of use	Dissertation/Thesis
Requestor type	University/Academic
Format	Print and electronic
Portion	Figure/table
Number of figures/tables	1
Original Wiley figure/table number(s)	Figure 9
Will you be translating?	No
Total	0.00 USD

This is a License Agreement between Hany Abdelhady ("You") and John Wiley and Sons ("John Wiley and Sons") provided by Copyright Clearance Center ("CCC"). The license consists of your order details, the terms and conditions provided by John Wiley and Sons, and the payment terms and conditions.

All payments must be made in full to CCC. For payment instructions, please see information listed at the bottom of this form.

License Number	3273971064542
License date	Nov 21, 2013
Licensed content publisher	John Wiley and Sons
Licensed content publication	Molecular Microbiology
Licensed content title	Legionella pneumophila couples fatty acid flux to microbial differentiation and virulence
Licensed copyright line	© 2009 The Authors. Journal compilation © 2009 Blackwell Publishing Ltd
Licensed content author	Rachel L. Edwards,Zachary D. Dalebroux,Michele S. Swanson
Licensed content date	Jan 16, 2009
Start page	1190
End page	1204
Type of use	Dissertation/Thesis
Requestor type	University/Academic
Format	Print and electronic
Portion	Figure/table
Number of figures/tables	1
Original Wiley figure/table number(s)	Figure 8
Will you be translating?	No
Total	0.00 USD

This is a License Agreement between Hany Abdelhady ("You") and John Wiley and Sons ("John Wiley and Sons") provided by Copyright Clearance Center ("CCC"). The license consists of your order details, the terms and conditions provided by John Wiley and Sons, and the payment terms and conditions.

All payments must be made in full to CCC. For payment instructions, please see information listed at the bottom of this form.

License Number	3273971318967
License date	Nov 21, 2013
Licensed content publisher	John Wiley and Sons
Licensed content publication	FEMS Microbiology Letters
Licensed content title	The progeny of Legionella pneumophila in human macrophages shows unique developmental traits
Licensed copyright line	Â© 2013 Federation of European Microbiological Societies. Published by John Wiley & Sons Ltd. All rights reserved
Licensed content author	Hany Abdelhady,Rafael A. GarduÃ±o
Licensed content date	Nov 11, 2013
Start page	99
End page	107
Type of use	Dissertation/Thesis
Requestor type	Author of this Wiley article
Format	Print and electronic
Portion	Figure/table
Number of figures/tables	1
Original Wiley figure/table number(s)	Figure 1
Will you be translating?	No
Total	0.0 USD

This is a License Agreement between Hany Abdelhady ("You") and John Wiley and Sons ("John Wiley and Sons") provided by Copyright Clearance Center ("CCC"). The license consists of your order details, the terms and conditions provided by John Wiley and Sons, and the payment terms and conditions.

All payments must be made in full to CCC. For payment instructions, please see information listed at the bottom of this form.

License Number	3315441485099
License date	Jan 24, 2014
Licensed content publisher	John Wiley and Sons
Licensed content publication	FEMS Microbiology Letters
Licensed content title	The progeny of Legionella pneumophila in human macrophages shows unique developmental traits
Licensed copyright line	© 2013 Federation of European Microbiological Societies. Published by John Wiley & Sons Ltd. All rights reserved
Licensed content author	Hany Abdelhady,Rafael A. Garduño
Licensed content date	Nov 11, 2013
Start page	99
End page	107
Type of use	Dissertation/Thesis
Requestor type	Author of this Wiley article
Format	Print and electronic
Portion	Full article
Will you be translating?	No
Total	0.00 USD

TERMS AND CONDITIONS

trade name, service mark or other branding ("Marks") of WILEY or its licensors is granted hereunder, and you agree that you shall not assert any such right, license or interest with respect thereto.

5. NEITHER WILEY NOR ITS LICENSORS MAKES ANY WARRANTY OR REPRESENTATION OF ANY KIND TO YOU OR ANY THIRD PARTY, EXPRESS, IMPLIED OR STATUTORY, WITH RESPECT TO THE MATERIALS OR THE ACCURACY OF ANY INFORMATION CONTAINED IN THE MATERIALS, INCLUDING, WITHOUT LIMITATION, ANY IMPLIED WARRANTY OF MERCHANTABILITY, ACCURACY, SATISFACTORY QUALITY, FITNESS FOR A PARTICULAR PURPOSE, USABILITY, INTEGRATION OR NON-INFRINGEMENT AND ALL SUCH WARRANTIES ARE HEREBY EXCLUDED BY WILEY AND ITS LICENSORS AND WAIVED BY YOU.

6. WILEY shall have the right to terminate this Agreement immediately upon breach of this Agreement by you.

7. You shall indemnify, defend and hold harmless WILEY, its Licensors and their respective directors, officers, agents and employees, from and against any actual or threatened claims, demands, causes of action or proceedings arising from any breach of this Agreement by you.

8. IN NO EVENT SHALL WILEY OR ITS LICENSORS BE LIABLE TO YOU OR ANY OTHER PARTY OR ANY OTHER PERSON OR ENTITY FOR ANY SPECIAL, CONSEQUENTIAL, INCIDENTAL, INDIRECT, EXEMPLARY OR PUNITIVE DAMAGES, HOWEVER CAUSED, ARISING OUT OF OR IN CONNECTION WITH THE DOWNLOADING, PROVISIONING, VIEWING OR USE OF THE MATERIALS REGARDLESS OF THE FORM OF ACTION, WHETHER FOR BREACH OF CONTRACT, BREACH OF WARRANTY, TORT, NEGLIGENCE, INFRINGEMENT OR OTHERWISE (INCLUDING, WITHOUT LIMITATION, DAMAGES BASED ON LOSS OF PROFITS, DATA, FILES, USE, BUSINESS OPPORTUNITY OR CLAIMS OF THIRD PARTIES), AND WHETHER OR NOT THE PARTY HAS BEEN ADVISED OF THE POSSIBILITY OF SUCH DAMAGES. THIS LIMITATION SHALL APPLY NOTWITHSTANDING ANY FAILURE OF ESSENTIAL PURPOSE OF ANY LIMITED REMEDY PROVIDED HEREIN.

9. Should any provision of this Agreement be held by a court of competent jurisdiction to be illegal, invalid, or unenforceable, that provision shall be deemed amended to achieve as nearly as possible the same economic effect as the original provision, and the legality, validity and enforceability of the remaining provisions of this Agreement shall not be affected or impaired thereby.

10. The failure of either party to enforce any term or condition of this Agreement shall not constitute a waiver of either party's right to enforce each and every term and condition of this Agreement. No breach under this agreement shall be deemed waived or excused by either party unless such waiver or consent is in writing signed by the party granting such

waiver or consent. The waiver by or consent of a party to a breach of any provision of this Agreement shall not operate or be construed as a waiver of or consent to any other or subsequent breach by such other party.

11. This Agreement may not be assigned (including by operation of law or otherwise) by you without WILEY's prior written consent.

12. Any fee required for this permission shall be non-refundable after thirty (30) days from receipt

13. These terms and conditions together with CCC's Billing and Payment terms and conditions (which are incorporated herein) form the entire agreement between you and WILEY concerning this licensing transaction and (in the absence of fraud) supersedes all prior agreements and representations of the parties, oral or written. This Agreement may not be amended except in writing signed by both parties. This Agreement shall be binding upon and inure to the benefit of the parties' successors, legal representatives, and authorized assigns.

14. In the event of any conflict between your obligations established by these terms and conditions and those established by CCC's Billing and Payment terms and conditions, these terms and conditions shall prevail.

15. WILEY expressly reserves all rights not specifically granted in the combination of (i) the license details provided by you and accepted in the course of this licensing transaction, (ii) these terms and conditions and (iii) CCC's Billing and Payment terms and conditions.

16. This Agreement will be void if the Type of Use, Format, Circulation, or Requestor Type was misrepresented during the licensing process.

17. This Agreement shall be governed by and construed in accordance with the laws of the State of New York, USA, without regards to such state's conflict of law rules. Any legal action, suit or proceeding arising out of or relating to these Terms and Conditions or the breach thereof shall be instituted in a court of competent jurisdiction in New York County in the State of New York in the United States of America and each party hereby consents and submits to the personal jurisdiction of such court, waives any objection to venue in such court and consents to service of process by registered or certified mail, return receipt requested, at the last known address of such party.

Wiley Open Access Terms and Conditions

Wiley publishes Open Access articles in both its Wiley Open Access Journals program [http://www.wileyopenaccess.com/view/index.html] and as Online Open articles in its subscription journals. The majority of Wiley Open Access Journals have adopted the Creative Commons Attribution License (CC BY) which permits the unrestricted use, distribution, reproduction, adaptation and commercial exploitation of the article in any medium. No permission is required to use the article in this way provided that the article is

Conditions applicable to non-commercial licenses (CC BY-NC and CC BY-NC-ND)

For non-commercial and non-promotional purposes individual non-commercial users may access, download, copy, display and redistribute to colleagues Wiley Open Access articles. In addition, articles adopting the CC BY-NC may be adapted, translated, and text- and data-mined subject to the conditions above.

Use by commercial "for-profit" organizations

Use of non-commercial Wiley Open Access articles for commercial, promotional, or marketing purposes requires further explicit permission from Wiley and will be subject to a fee. Commercial purposes include:

- Copying or downloading of articles, or linking to such articles for further redistribution, sale or licensing;
- Copying, downloading or posting by a site or service that incorporates advertising with such content;
- The inclusion or incorporation of article content in other works or services (other than normal quotations with an appropriate citation) that is then available for sale or licensing, for a fee (for example, a compilation produced for marketing purposes, inclusion in a sales pack)
- Use of article content (other than normal quotations with appropriate citation) by for-profit organizations for promotional purposes
- Linking to article content in e-mails redistributed for promotional, marketing or educational purposes;
- Use for the purposes of monetary reward by means of sale, resale, license, loan, transfer or other form of commercial exploitation such as marketing products
- Print reprints of Wiley Open Access articles can be purchased from: corporatesales@wiley.com

  The modification or adaptation for any purpose of an article referencing the CC BY-NC-ND License requires consent which can be requested from RightsLink@wiley.com .

  Other Terms and Conditions:

  BY CLICKING ON THE "I AGREE..." BOX, YOU ACKNOWLEDGE THAT YOU HAVE READ AND FULLY UNDERSTAND EACH OF THE SECTIONS OF AND PROVISIONS SET FORTH IN THIS AGREEMENT AND THAT YOU ARE IN AGREEMENT WITH AND ARE WILLING TO ACCEPT ALL OF YOUR OBLIGATIONS AS SET FORTH IN THIS AGREEMENT.

v1.8

If you would like to pay for this license now, please remit this license along with your payment made payable to "COPYRIGHT CLEARANCE CENTER" otherwise you will be invoiced within 48 hours of the license date. Payment should be in the form of a check or money order referencing your account number and this invoice number RLNK501165349.
Once you receive your invoice for this order, you may pay your invoice by credit card. Please follow instructions provided at that time.

Make Payment To:
Copyright Clearance Center
Dept 001
P.O. Box 843006
Boston, MA 02284-3006

For suggestions or comments regarding this order, contact RightsLink Customer Support: customercare@copyright.com or +1-877-622-5543 (toll free in the US) or +1-978-646-2777.

Gratis licenses (referencing $0 in the Total field) are free. Please retain this printable license for your reference. No payment is required.